UNIVERSITÀ
DEGLI STUDI
DI PADOVA

Head Office: Università degli Studi di Padova

Department of GEOSCIENCES

Ph.D. COURSE IN: EARTH SCIENCES
SERIES: XXXI

ESTIMATE OF BED MATERIAL TRANSPORT IN LARGE GRAVEL-BED RIVERS USING THE VIRTUAL VELOCITY APPROACH AND THE MORPHOLOGICAL METHOD

Coordinator: Prof. Claudia AGNINI
Supervisor: Prof. Nicola SURIAN
Co-Supervisor: Prof. Luca MAO

Ph.D. student: Andrea BRENNA

“Il viaggio non finisce mai. Solo i viaggiatori finiscono. E anche loro possono prolungarsi in memoria, in ricordo, in narrazione.

Quando il viaggiatore si è seduto sulla sabbia della spiaggia e ha detto: "Non c'è altro da vedere", sapeva che non era vero. La fine di un viaggio è solo l'inizio di un altro. Bisogna vedere quel che non si è visto, vedere di nuovo quel che si è già visto, vedere in primavera quel che si è visto in estate, vedere di giorno quel che si è visto di notte, con il sole dove la prima volta pioveva, vedere le messi verdi, il frutto maturo, la pietra che ha cambiato posto, l'ombra che non c'era. Bisogna ritornare sui passi già fatti, per ripeterli, e per tracciarvi a fianco nuovi cammini.

Bisogna ricominciare il viaggio. Sempre. Il viaggiatore ritorna subito.”

“The journey is never over. Only travellers come to an end. But even then they can prolong their voyage in their memories, in recollections, in stories.

When the traveller sat in the sand and declared: “There’s nothing more to see” he knew it wasn’t true. The end of one journey is simply the start of another. You have to see what you’ve missed the missed the first time, see again what you already saw, see in the springtime what you saw in the summer, in daylight what you saw at night, see the sun shining where you saw the rain falling, see the crops growing, the fruits ripen, the stone which has moved, the shadow that was not there before. You have to go back to the footsteps already taken, to go over again or add fresh ones alongside them.

You have to start the journey anew. Always. The traveller sets out once more.”

Viaggio in Portogallo

Journey to Portugal

José Saramago

CONTENTS

ABSTRACT

The bed material transport, defined as the mobilization of the coarse sediment forming the channel bed and the lower banks, is one of the key factors controlling gravel-bed rivers morphodynamics. In large gravel-bed rivers, the high spatial and temporal variability of intermittent bed material load makes its quantification extremely challenging since the use of transport formulas often provides incongruent results while the field techniques (e.g. samplers, traps, geophones) are more suitable for small streams. Among the alternatives to achieve estimates of such key process in wide-rivers, (i) the morphological method and (ii) the use of data provided by tracers to calculate the flux starting from the virtual velocity of the moved grains represent two viable possibilities. The morphological method has a long application history and provides robust transport estimates but, currently, in order to convert the channel volume changes in bed material fluxes by the diffused sediment budgeting procedure, it requires to include in the study area a section where the transport is known, estimable or negligible. For this reason, it is independently applicable only under specific boundary conditions as the presence of a zero-flux coarse sediment boundary (e.g. dam, lake or distal gravel-sand transition). The application of the "virtual velocity approach" has been less explored in literature, although some theoretical frameworks allow to carry out transport estimates addressing a dedicated field monitoring potentially applicable in a wide range of large gravel-bed rivers. This research project aims (i) to improve the application of the virtual velocity approach and (ii) to validate the estimates provided by such method comparing them with the results obtained at the same site and for the same period by an independent and reliable approach as the morphological sediment-budgeting procedure.

For achieving those aims, the study focuses on a 4-km long study sector of the Parma River, a North-Apennines stream (Italy) with a catchment area of 815 km^2, total river length of 92 km and torrential hydrological regime led by winter and spring rainfalls. Within the study sector, upstream bounded by the Marano dam representing a zero-flux coarse sediment boundary since its closure in 2005, three reaches have been identified. The four cross-sections considered for the monitoring activities and calculations are located within the middle reach (reach 2: mean width= 84 m; single-thread configuration; D_{50} surface sediments= 63 mm; high streambed armoring) and the downstream reach (reach 3: mean width= 109 m; wandering configuration; D_{50} surface sediments= 50 mm; moderate streambed armoring).

The virtual velocity approach (i.e. the first method adopted in this research) is a hybrid estimation technique based on a theoretical framework and substantial field-data collection allowing the calculation of the coarse component of the bed material transport. We collected data in the study sector jointly employing two tracer types (painted clasts and Passive Integrated Transponders tags) and scour chains and performing several grain size analysis over the period January 2016 - May 2017, obtaining reach-specific empirical relations between the tractive forces induced by the water flow on the streambed and the parameters involved in the transport estimation. Those data, combined with equations for the fractional transport calculation included in the theoretical framework of the approach and with the grain-size distribution curves of the bed materials, permitted to relate the calculated dimensionless shear stress (τ^*) with the instantaneous-local bed material flux. Finally the bed material loads at the four considered cross-sections during each of the nine competent events that occurred over the study period were estimated integrating the instantaneous-local fluxes ($m^3\ m^{-1}\ s^{-1}$) over the time (i.e. event hydrograph) and space (i.e. cross-section extension) and using data input configurations taking into account for the sensitivity of the method to different application factors.

For independently estimating the sediment regime in the study sector applying a morphological method (i.e. the second approach adopted in this research) using the sediment budgeting procedure, we calculated the volumetric variations along the river-sector during three periods following the dam closure (2005) employing LiDAR and photogrammetric Digital Elevation Models (DEM). Errors have been assessed considering type and quality of data and the different channel features. The Geomorphic Change Detection software has been adopted for deriving three study-sector DEMs of Difference (DoD). Exploiting the zero-flux coarse sediment boundary of the Marano dam, we converted the volumetric changes into mean coarse sediment transport ($m^3\ yr^{-1}$) at the four study-sections during the periods 2006-2008, 2008-2016 and April 2016 - April 2017.

For the period April 2016 - April 2017 (i.e. the “comparison period”) at the four cross-sections, both the adopted calculation approaches provided independent transport estimates. In particular, we considered the sum of the sediment fluxes estimated by the virtual velocity approach at each section during the four competent events that occurred during the comparison period and the estimates provided by the morphological method for the most recent DoD time interval. In order to add another comparison term, three transport formulas have been applied for addressing the same calculation. The virtual velocity approach and the morphological method provided remarkably similar estimates

along the whole study sector. Transport values provided by both methods are extremely low at the high impacted reach 2 (at sections 1 and 2 yearly bed material fluxes range between 120 m^3 and 315 m^3 during the comparison period), increasing up to 1600 m^3 at sections 3 and 4 located within reach 3. Formulas, being less sensitive to the mobility parameters which affect the channel sediments dynamics at local scale, provided less congruent results and small longitudinal changes of bed material load.

Considering the overall results of the research, we derived some conclusions about the sediment dynamics and channel evolution in a typical example of gravel-bed river impacted by human interventions: (i) the considered study sector has been highly altered by the dam closure which, interrupting the longitudinal continuity of the coarse sediment transfer, influenced its evolution in terms of morphology, bed material characteristics, sediment mobility and bed material transport rates; (ii) the sediment transport increases moving away from the dam but a general decreasing trend affecting the bed material load has been observed over the time since dam closure in 2005. Applying the two independent estimation approaches, from a methodological point of view the main outcomes of this research are: (i) some crucial methodological improvements (e.g. use of multiple tracers types and development of adequate data input configurations) made the virtual velocity approach a suitable method for estimating the bed material load in large gravel-bed rivers; (ii) since the virtual velocity approach estimates are remarkably similar with those obtained by the robust morphological method, it is possible to conclude that the virtual velocity approach provides reliable estimates of the coarse fraction of the bed material load.

Due to the difficulties for obtaining bed material load estimates in the contexts of large gravel-bed rivers but considering the key role played by this variable in determining their morphodynamics, and several practical implications, the virtual velocity approach represents a viable alternative for improving our skills in estimating this important fluvial process.

RIASSUNTO

Il trasporto del materiale grossolano costituente il letto dei corsi d'acqua ghiaiosi rappresenta uno dei fattori più importanti che determinano la morfodinamica di tali sistemi alluvionali. Nei corsi d'acqua ad alveo ghiaioso di grandi dimensioni, l'ampia variabilità spaziale e temporale che caratterizza tale processo di trasporto rende la sua quantificazione estremamente complessa in quanto l'utilizzo di diverse formule di trasporto spesso fornisce risultati incongruenti mentre le tecniche di stima in campo (campionatori, trappole, geofoni) risultano efficacemente applicabili solo nell'ambito di corsi d'acqua di ridotte dimensioni. Fra le possibili alternative per affrontare la stima di tale processo nei corsi d'acqua ghiaiosi ad alveo ampio si distinguono, (i) il metodo morfologico e (ii) l'utilizzo di dati forniti dai traccianti al fine di calcolare il flusso di sedimenti a partire dal concetto di velocità virtuale dei clasti mobilizzati durante i processi di trasporto. Il metodo morfologico è stato utilizzato nell'ambito di numerose applicazioni fornendo stime affidabili del trasporto di materiale d'alveo grossolano, ma, allo stato attuale, al fine di convertire le variazioni volumetriche misurate lungo un settore studio in stime di flusso di sedimento mediante la diffusa tecnica del bilancio di sedimento, esso richiede di includere nel settore analizzato almeno una sezione trasversale in corrispondenza della quale il trasporto sia noto, stimabile o nullo. Per questa ragione il metodo morfologico risulta essere applicabile in modo indipendente solo quando sussistano alcune condizioni al contorno, ad esempio in presenza di una sezione dove il trasporto di materiale grossolano risulti pari a zero (a valle di una diga, di un lago o alla transizione distale fra ghiaie e sabbie). Il metodo della "velocità virtuale" è stato limitatamente applicato il letteratura ma alcuni approcci teorici potenzialmente applicabili in un'ampia gamma di corsi d'acqua ghiaiosi sono stati sviluppati al fine di convertire i dati di campo raccolti tramite i traccianti in stime del trasporto. Questo progetto di ricerca è volto quindi a (i) implementare le procedure di applicazione dell'approccio della velocità virtuale e (ii) a validare le stime di trasporto ottenute mediante tale procedura confrontandole con quelle fornite lungo il medesimo tratto e per lo stesso intervallo temporale da una tecnica indipendente e affidabile quale il metodo morfologico applicato attraverso la procedura del bilancio dei sedimenti.

Al fine di raggiungere tali scopi, lo studio si è focalizzato su un settore esteso per 4 km del Torrente Parma, un corso d'acqua dell'Appennino settentrionale con un bacino idrologico di 815 km^2, una lunghezza complessiva di 92 km e caratterizzato da un regime delle portate di tipo torrentizio dominato da precipitazioni invernali e primaverili. Il

settore-studio è delimitato a monte dal manufatto regolatore di una cassa di espansione (cassa di Marano) che fin dalla sua ultimazione nel 2005 costituisce una sezione a trasporto nullo in relazione alla componente grossolana del materiale d'alveo. All'interno del settore studio sono stati riconosciuti tre tratti distinti. Le quattro sezioni trasversali considerate nelle attività di monitoraggio e di calcolo sono collocate in corrispondenza del tratto mediano (tratto 2: larghezza media= 84 m; configurazione planimetrica a canale singolo; D_{50} sedimenti superficiali= 63 mm e elevato grado di corazzamento) e del tratto di valle (tratto 3: larghezza media= 109 m; configurazione planimetrica a canali multipli; D_{50} sedimenti superficiali= 50 mm e moderato grado di corazzamento).

L'approccio della velocità virtuale è un metodo di stima ibrido basato su un quadro teorico di equazioni popolate attraverso relazioni empiriche derivanti da dati raccolti in campo che permettono il calcolo frazionale della componente grossolana costituente il trasporto di materiale d'alveo. Durante il monitoraggio eseguito nel settore studio sono stati utilizzati due tipi di traccianti passivi (clasti colorati e *Passive Integrated Transponders tags*), catene per la misura dello spessore di sedimento mobilizzato e sono state eseguite numerose analisi granulometriche del materiale d'alveo nel periodo gennaio 2016 - maggio 2017. A partire dai dati di campo raccolti sono state determinate delle relazioni empiriche tratto-specifiche fra le forze trattive indotte dal flusso dell'acqua al fondo e i parametri di calcolo richiesi dalla procedura di stima. Tali dati di partenza, combinati con le equazioni per il calcolo frazionale del trasporto e con le curve granulometriche stabilite, hanno permesso di derivare delle relazioni fra lo sforzo di taglio adimensionale e il trasporto istantaneo e unitario ($m^3\ m^{-1}\ s^{-1}$) indotto al fondo. Infine, il trasporto grossolano avvenuto alle quattro sezioni considerate durante ciascuno dei nove eventi di piena competenti verificatisi durante il periodo di calcolo è stato determinato integrando il trasporto istantaneo e unitario nel tempo (considerando l'idrogramma dell'evento) e nello spazio (considerando l'estensione della sezione) attraverso diverse configurazioni che considerano la sensitività del metodo in risposta ad alcuni fattori di calcolo.

Per applicare in modo indipendente il secondo metodo di stima del regime del trasporto grossolano (il metodo morfologico) attraverso la procedura del bilancio di sedimenti, sono state determinate le variazioni volumetriche verificatesi lungo il settore-studio durante tre periodi di tempo distinti successivi alla chiusura della diga (2005) utilizzando modelli digitali del terreno (DEM) derivati da procedura fotogrammetrica o mediante LiDAR. Gli errori sono stati considerati differentemente in funzione delle caratteristiche del dato spaziale utilizzato e mediante il *Geomorphic Change Detection software* sono state calcolate

le variazioni volumetriche derivando tre DEMs of Difference (DoD) del settore-studio. Sfruttando la sezione a trasporto nullo della diga di Marano, le variazioni volumetriche ottenute sono state convertite in stime del trasporto medio ($m^3\ yr^{-1}$) avvenuto alle sezioni trasversali considerate anche per l'applicazione del metodo della velocità virtuale durante i periodi 2006-2008, 2008-2016 e aprile 2016 - aprile 2017.

Durante il periodo aprile 2016 - aprile 2017 entrambi gli approcci applicati in questa ricerca hanno quindi fornito le stime di trasporto alle quattro sezioni-studio. Nel dettaglio, per quanto concerne l'approccio della velocità virtuale sono state sommate le stime di trasporto ottenute alle sezioni durante quattro eventi di piena competenti verificatisi nel periodo di confronto mentre relativamente al metodo morfologico ci si è riferiti alla stima derivata dal DoD eseguito per l'intervallo di tempo più recente. Al fine di aggiungere un ulteriore termine di confronto sono state inoltre applicate tre formule di stima del trasporto per affrontare il medesimo calcolo. I due metodi testati in questa ricerca hanno fornito stime significativamente simili lungo l'intero settore-studio evidenziando valori di trasporto al fondo estremamente bassi in corrispondenza delle sezioni collocate nel tratto 2 fortemente impattato dalla presenza della diga (alle sezioni 1 e 2 i valori annuali di trasporto ottenuti si attestano fra i 120 m^3 e i 315 m^3 per il periodo aprile 2016 - aprile 2017) per poi incrementare fino a 1600 m^3 in corrispondenza delle sezioni 3 e 4 collocate nel tratto 3 dove la disponibilità di sedimento è maggiore. Le formule di trasporto applicate, essendo meno sensibili ai parametri di mobilità che controllano la dinamica dei sedimenti d'alveo alla scala locale, generalmente hanno fornito risultati incongruenti e variazioni longitudinali del trasporto molto meno marcate.

Considerando i risultati della presente ricerca, le principali conclusioni ottenute in merito alla dinamica dei sedimenti e all'evoluzione di un alveo interessato da impatto antropico dovuto alla disconnessione longitudinale nel trasferimento di materiale d'alveo grossolano sono: (i) il settore-studio indagato è stato fortemente impattato dalla costruzione della diga la quale ha significativamente influenzato la sua evoluzione determinandone lo sviluppo morfologico, le caratteristiche del materiale d'alveo, la mobilità dei sedimenti grossolani e i tassi di trasporto nel tempo; (ii) il trasporto stimato di sedimento grossolano aumenta nello spazio allontanandosi dalla diga ma un decremento generale del trasporto è avvenuto nel tempo a partire dalla chiusura del manufatto regolatore della cassa di espansione avvenuta nel 2005. Applicando i due metodi di stima selezionati, da un punto di vista metodologico le principali conclusioni ottenute possono essere riassunte come segue: (i) alcune importanti migliorie metodologiche ottenute

(utilizzo di traccianti multipli, sviluppo di configurazioni di calcolo adeguate alla complessità dei sistemi fluviali naturali) hanno reso l'approccio della velocità virtuale un'alternativa praticabile per la stima del trasporto del materiale d'alveo grossolano in corsi d'acqua ghiaiosi di grandi dimensioni; (ii) poiché le stime ottenute mediante l'approccio della velocità virtuale risultano essere significativamente simili a quelle fornite da un metodo indipendente e robusto quale il metodo morfologico, si può affermare che l'approccio della velocità virtuale sia in grado di fornire stime affidabili del trasporto.

Viste le note difficoltà nell'ottenere stime del trasporto del materiale d'alveo grossolano in corsi d'acqua ghiaiosi di grandi dimensioni, ma considerata la cruciale importanza di tale fenomeno nel determinarne la morfodinamica e le numerose ricadute connesse sia di carattere applicativo che scientifico, l'approccio della velocità virtuale sviluppato in questa ricerca risulta essere un valido contributo all'avanzamento delle conoscenze necessarie per lo studio di questo processo fluviale.

1. INTRODUCTION

Sediment transport and morphologies of gravel-bed rivers

In alluvial rivers, channels are formed in clastic material that they have directly transported and deposited (i.e. channels are "self-formed" as stated by Church (2006)). For that reason, sediment dynamics and transport processes represent two key controlling factors on alluvial system morphodynamics, determining channel morphology, streambed material characteristics and their evolution over the time (Bridge, 2003; Church, 2006). Several rivers classifications exist based on channel morphology (e.g. Leopold and Wolman, 1957; Rosgen, 1994; Fuller et al., 2013), but, focusing on transport processes, in this research we adopted a classification of alluvial channels that considers the type of sediment and the main transport regime as proposed by Schumm (1963; 1977; 1985) and developed by Church (1992; 2006). The considered classification highlights the relations existing between sediment dynamics and channel morphologies.

Among the different channel classes recognized, the gravel-bed rivers are fluvial types where the coarse material (i.e. from gravel to boulders) dominates the characters of the bed and lower bank deposits, eventually associated to a percentage of finer material (i.e. sand and silt) located in the interstices of the gravel or on the top of the banks (Church, 2010). Gravel-bed rivers are widespread, from upland valleys to mountain forelands, assuming variable features in function of the relief energy, clastic material availability and streambed sediments characteristics (e.g. grain size). Within the "gravel-bed rivers" category, different sub-types dominated by typical channel materials and transport mechanisms can be recognized. In mountain areas, where terrain is steep (i.e. > 0.05), gravel-bed streams are characterized by very coarse streambed material (cobble or boulder), narrow channels and morphologies varying from continuous cascade to step–pool cascade (Figure 1a) (Montgomery and Buffington, 1997). According to Church's classification (2006), in those "jammed channels" sediments are episodically purged by high magnitude events occurring also as debris flows. Progressively moving downstream along the landscape, the stream gradients declines (< 0.05). Streambed sediments become dominated by gravel and cobble episodically mobilized by the water-flow tractive forces. In those "threshold channels", often characterized by single-thread or eventually wandering morphologies, appear the first elementary riffle–pool sequences (Figure 1b) (Montgomery and Buffington, 1997). Finally, in lowland areas, where gradients are below 0.02, gravel-bed rivers typically express well-developed riffle-pool-bar triplets (Figure 1c), consisting of sandy-gravel to

cobble-gravel deposits mobilized and deposited by the shear stress induced by the water flow during competent events. Channel morphologies vary from single-thread to braided configurations due to the possible lateral accretion of bar complexes leading the develop of large systems characterized by active channels wider than some tens of meters (e.g. from 20-30 m, defined by Church (1992) as the lower threshold of the channel width for identifying a "large river") to some hundreds of meters. Such fluvial systems can be defined as "large gravel-bed rivers" (Church, 2010). The sequence of morphologies, streambed sediment features and transport mechanisms briefly synthesized above according to Church (2002) and Church (2006) typically occurs along several gravel-bed rivers as described by Grant et al. (1990) and by Montgomery and Buffington (1997).

Figure 1. Characteristic morphologies of some gravel-bed river types: (a) step-pool cascade in a mountain "jammed-channel" stream, Torrente Ventra, North-Apennines (Piacenza, Italy); (b) riffle-pool sequence in a mountain "threshold channels" stream, Rio Grande, North-Apennines (Piacenza, Italy); (c) pool–riffle–bar structure in a lowland "large gravel-bed river", Torrente Parma, North-Apennines (Parma, Italy).

Differently from systems dominated by fine material, the geometry, morphology and streambed characteristics of gravel-bed channels are direct consequences of the mobilization of the coarse material forming the bed, defined by Church (2006) as "bed material transport". The bed material transport, under the control of the tractive forces induced by the water flow, shapes the morphological units (e.g. bars) which self-form the channel. Since in gravel-bed rivers the streambed material is mainly coarse, the bed material transport usually occurs by the bedload mechanism (i.e. coarse material moved in contact with the bed by rolling, sliding and bouncing (Gomez, 1991)) but it can occurs also as intermittently suspended load depending by the grain size of the whole material forming the river bed (Church, 2006). In this work we mainly refer to the coarse component of the bed material transport (i.e. classified in terms of sediment source) mobilized by bedload mechanism (i.e. classified in terms of mode of transport) called "coarse-bed material transport" or "gravel-bed material transport" (Figure 2). In systems characterized by strong

predominance of coarse material forming the channel, the coarse-bed material transport is very similar to the total bed material load due to the relatively poor presence of fine material in the bed.

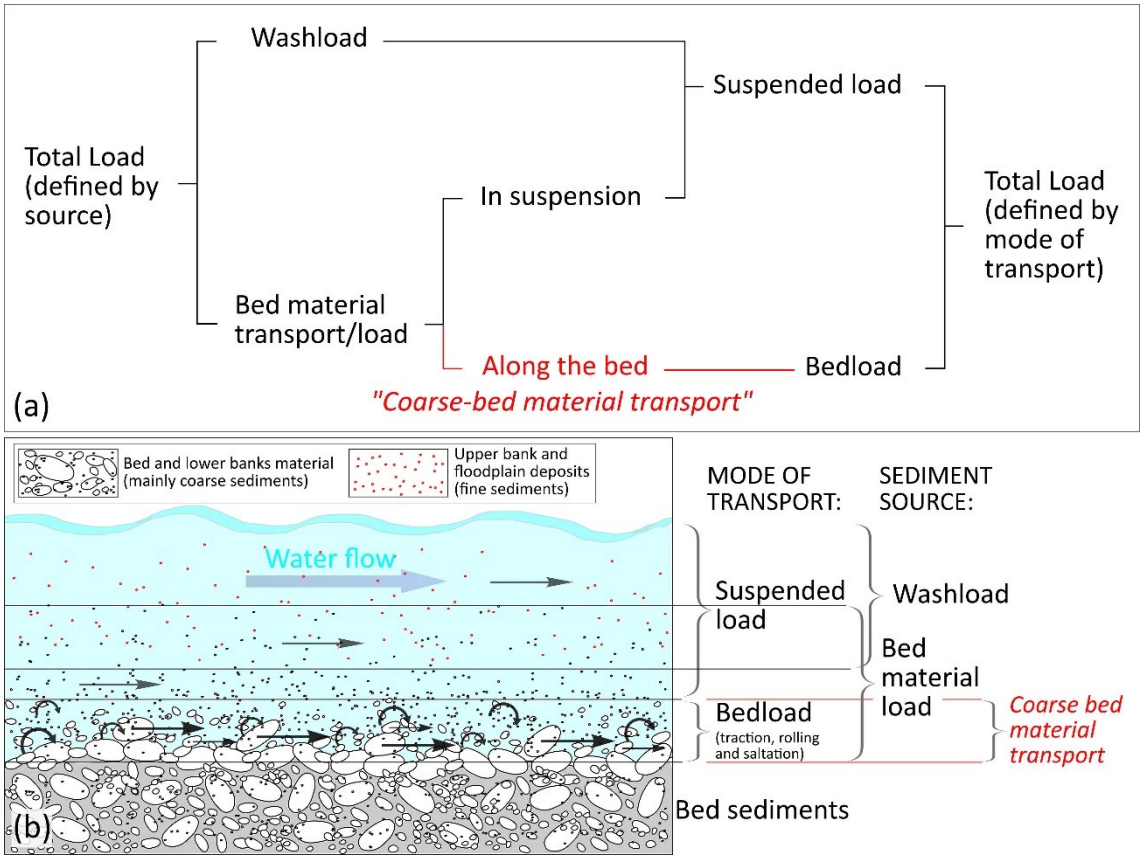

Figure 2. Breakdown of total stream sediment load in terms of sediment source and mode of transport (a). The transport process investigated in this work is highlighted in red (modified from Hicks and Gomez (2016)). The reported sketch (b) refers to the gravel-bed rivers where the bed material load is mainly composed by coarse grains move in contact with the streambed by bedload mechanism.

Estimate of bed material transport in large gravel-bed rivers

Several models describing the river evolution mechanisms identify the sediment regime as one of the key parameters controlling their morphodynamic. For instance, the classical Lane's balance (1955) conceptualizes fluvial systems as the result of the physical relationship between sediment supply and energy able to mobilize the in-channel material (i.e. water discharge). Similarly, the Thorne's model (1997) considers the water and sediment regimes as the two control factors which, in concurrence with some boundary conditions (i.e. slope, sediment type and vegetation), determine channel forms and

processes. If the water discharge regime is an input variable relatively simple to be determined (see Whiting (2016) for a complete review), the solid transport quantification represents a more challenging task in the majority of fluvial systems. In rivers dominated by suspended transport the fine sediment regime estimation is successfully addressed employing field techniques based on the spatially distributed measurement of both sediment concentration and water velocity (see Hicks and Gomez (2016) for a complete review).

In gravel-bed rivers, where the episodic mobilization of the coarse streambed material plays a dominant role (Church, 2006; Church and Ferguson, 2015), the bed material load estimation currently represents an issue without simple solutions. Anyhow, being the coarse material transport a crucial parameter for understanding the morphodynamic of rivers with relevant fallout for several scientific and practical questions (e.g. infrastructure management, sediment mining, flood hazard), different solutions have been developed for dealing this challenge depending from the gravel-bed river-type and channel features. Improvements on the challenge to achieve reliable quantifications of the bed material transport is needed by river engineers, ecologists, geomorphologists and land-use planners.

One of the most common approach for addressing this issue is through theoretically-based formulas, which are able to predict the bed material load rates under given flow conditions. Despite several formulas have been developed for specific fluvial types and temporal scales (e.g. Recking et al., 2012), often the application of different relations proposed for a given context provides strongly incongruent estimates (e.g. Gomez and Church, 1989; Martin and Ham, 2005; Lopez et al., 2014). To overcome this issue, direct measure techniques as portable traps and samplers (e.g. Helley and Smith, 1971; Emmett, 1979; Bunte et al., 2004) and indirect acoustic methods like geophones and hydrophones (e.g. Rickenmann, 2017) are commonly used in small streams where their installation and human presence during a competent flood does not represent a problem in term of safety. Furthermore, despite some recent works are investigating the possibility of employing acoustic-measure techniques resistant to large floods and sensitive to grain motion not only locally but also over distances of some meters (e.g. hydrophones adopted by Geay et al. (2017)), the data provided by direct and indirect field techniques usually are referred to punctual measures. Alternatively, Acoustic Doppler profiling (e.g. Rennie et al., 2017) is used to get an estimate of the distributions of the bed velocity during competent events, obtaining a velocity map that is transformed to bed material transport using site-specific calibrations. Due to the high spatial and temporal variability affecting the bed material

transport in large gravel-bed rivers (Clayton and Pitlick, 2007; Ryan and Dixon, 2007), direct and indirect monitoring-techniques data must be used just like inputs or constraints for other theoretically-based approaches in order to obtain transport estimations in that contexts (e.g. Wilcock, 2001). For those reasons, generally field measurement techniques are more suitable for transport quantification in small gravel-bed streams (i.e. channels typical of high-gradient mountain areas described in the above section) (Ferguson, 2007) but less for investigations in large gravel-bed rivers which are likely to represent the most challenging context for achieving reliable estimates of bed material transport (Ferguson, 2007; Wohl et al., 2015). After several decades of studies, Ferguson (2007) synthetized that, among the reliable possibilities for achieving estimates of such key process, the (i) morphological method (Lane et al., 1995; Ashmore and Church, 1998, Vericat et al., 2017) and the (ii) use of approaches based on the grains virtual velocity calculation (Hassan and Church, 1992; Wilcock, 1997; Haschenburger and Church, 1998) starting from data collected through tracer clasts represent two most promising approaches for large gravel-bed rivers.

Motivations of this work

The morphological method is an inverse solution to calculate the rates of sediment transport using observations on channel morphology and change in form though time, based on the continuity principle applied to river sediment and involving the quantification of sediment inputs (Q_b^{in}), outputs (Q_b^{out}) and storage changes (ΔV) over the time along a river sector (Ashmore and Church, 1998). Due to the solidity of its theoretical paradigm (Ashmore and Church, 1998), its several applications (e.g. Griffiths, 1979; Martin and Church, 1995; McLean and Church, 1999; Eaton and Lapointe, 2001) and improvements in the employed topographical-data quality and elaborations (e.g. Passalacqua et al., 2015; Vericat et al., 2017), there is a consensus about the reliability of the transport estimates provided by the morphological method. Despite some improvements have been achieved in the challenge of making the method independent from specific boundary conditions (e.g. Vericat et al., 2017), in order to convert the volumetric changes into transport values using the diffuse sediment budgeting procedure ($\Delta V = Q_b^{in} - Q_b^{out}$), the morphological approach requires to include within the study sector a section where the transport is known (e.g. Merz et al., 2006). This condition implies that the method can be independently applied only under particular boundary conditions, for instance including into the study area a section where the coarse-sediment flux is equal to zero as a dam, a lake (e.g. Ham and Church, 2000) or the distal gravel-sand transition (e.g. Surian and Cisotto, 2007). Alternatively, it requires

to be applied coupled with a technique (e.g. direct continuous measurements of flux across one boundary as in Grams et al. (2013) or theoretically-based transport model as in Anderson and Pitlick (2014)) able to provide a local bed material flux boundary constraint (i.e. transport estimate at a selected section) taking in account for the possible errors involved, which could eventually undermine the reliability of the overall approach.

In order to allow the bed material transport estimation in a wider range of large gravel-bed river sectors it is required to adopt and develop methods which do not require particular boundary conditions for their application. Considering the conclusions reached by Ferguson (2007) and the long application history of tracing techniques for sediment dynamics monitoring using tracer clasts (see Hassan and Roy (2016) and Vázquez-Tarrío et al. (2018) for a complete review), we identified the approaches based on the grains virtual velocity calculation as a suitable way to provide a contribution to this issue. Those techniques are called "virtual velocity approaches" since employ data collected in the field by tracers for calculating the virtual velocity (i.e. defined as the mean velocity characterizing the clasts movement during the period for which particles might be in motion during a flood (Haschenburger and Church, 1998)) of the grains entrained from the river bed during competent events. Some theoretical frameworks and application protocols have been proposed (Wilcock, 1997; Haschenburger and Church, 1998; Liébault and Laronne, 2008; Mao et al., 2017) for calculating the coarse sediment transport starting from virtual velocity data. The virtual velocity approach is then a "hybrid approach", that is a method based on a theoretical framework but requiring several input data acquired by field monitoring (i.e. “real data”). Since the virtual velocity approach does not represent a direct measure technique of transport, it is subjected both to some simplifications imposed by the adopted theoretical framework and to field-monitoring data uncertainties. Furthermore, this approach has been rarely applied in the context of large gravel-bed rivers, leading to a relatively poor methodological development and evaluation of its performance.

Considering (i) the crucial importance of the coarse material transport in the morphodynamics of gravel-bed rivers, (ii) the difficulties in quantifying this process in large gravel-bed rivers and (iii) the state of the art of the methods currently available for these fluvial types (referring in particular to the characteristics and limitations of the morphological and virtual velocity approaches), this work aims to provide a contribution for obtaining reliable bed material transport estimates in large gravel-bed rivers using a technique suitable for a broad spectrum of study sector. The promising, although poorly explored, virtual velocity approach based on the theoretical framework developed by

Wilcock (1997) represents the selected methodology. The specific objectives of the research are (i) to improve the application of the virtual velocity approach assessing its strengths and limitations, evaluating the significance of each factor feeding in the calculation and developing the methodology in terms of data collection, processing and use in the estimation and (ii) to validate the estimates provided by such approach comparing such estimates with the results obtained at the same study sector by an independent and robust approach as the morphological method in order to assess its performance in large gravel-bed rivers.

Selected case study

In order to address the bed material transport estimation using the two methods and to compare the results at the same river sector, it was necessary to select a gravel-bed river where it was possible to independently apply the virtual velocity approach and the morphological method. The virtual velocity approach requires the presence of bars within the active channel to allow the installation of tracers but for applying the morphological method using the budgeting segregation procedure it is needed to include in the study sector a section where the transport is known (often equal to zero).

Due to its physiographic setting, geological characteristics and rainfall regime, the northern slope of the Apennines (Italy) is characterized by the presence of several gravel-bed rivers transporting coarse sediment from the mountain chain to the Po-plain lowland. The Parma River, a North-Apennines tributary of the Po River (Italy), was selected as case study. Main characteristics of the Parma River are: basin extension of 815 km^2; length of the whole river of 92 km (Figure 3a); torrential hydrological regime led by winter and spring rainfalls. The middle part of the Parma River course, flowing through the high plain, is characterized by coarse bed-sediment and active channel larger than some tens of meters (up to 350 m) (Figure 3b). In particular, the data acquisition and the transport regime calculations focused on a 4-km long study sector located immediately downstream from a retention basin dam (Marano dam) that, since its closure in 2005, represents a zero-flux coarse sediment boundary (Figure 3c). The study sector, besides being suitable for the independent application of both methods, has been remarkably affected by human activities. This condition allowed us to analyze the coarse sediment dynamics, the transport regimes, the morphological evolution and the relations existing between these aspects, carrying out new insights about the complex morphodynamic response of a large gravel-

bed river to the human-alteration of the sediment longitudinal transfer. This point represents the third aim of our research.

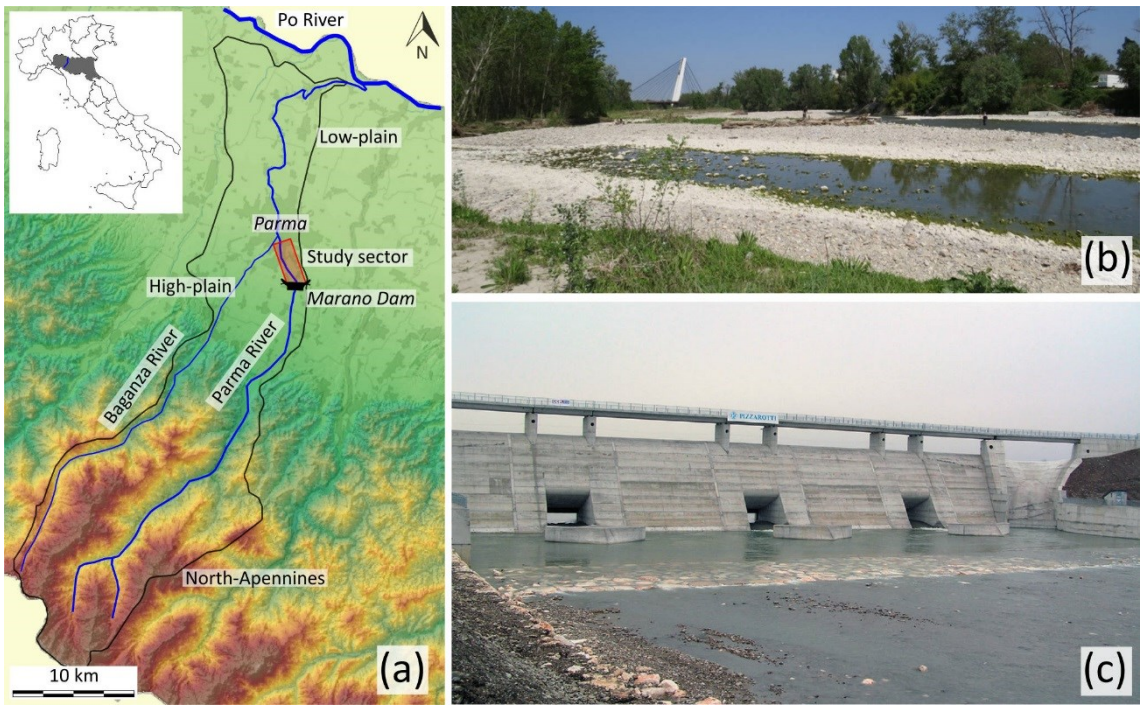

Figure 3. General setting of the Parma River catchment and the study area: (a) river catchment and location of the study sector; (b) the active channel of the Parma River within the study sector; (c) the Marano dam (from AIPO).

Research questions

Considering the premises introduced in the previous sections, the primary goals of this research are to improve the application of the virtual velocity approach as a promising alternative for estimating the bed material transport in large gravel-bed rivers (objective (1)) and to validate the virtual velocity approach by comparing its transport estimates with those provided by an independent morphological method (objective (2)). In complement to this, thanks to the characteristics of the selected study sector impacted by the closure of a dam, it is possible to analyze the effects induced on a gravel-bed river by human regulation in terms of morphological evolution, alteration of streambed-material features and transport regime modifications (objective (3)).

Starting from the reported objectives, this work seeks to address three key research questions. The first two questions regard the methodological objectives ((1) and (2)) introduced above, which have never been addressed in detail before:

a) Considering that the virtual velocity approach is based on a theoretical framework which requires several input data acquired by field monitoring, how is it possible to improve its application and which factors have to be considered for obtaining reliable bed material transport estimates in different large gravel-bed river contexts?

b) How reliable and accurate are the transport estimates provided by the virtual velocity approach, considering different gravel-bed river contexts and time scales of analysis (e.g. instantaneous, single flood, annual)?

The last research question refers to the objective (3), being focused on the impacts induced by human regulation on the fluvial system. Since the majority of previous works focus mainly on the morphological effects induced by dams on fluvial systems (e.g. Grant, 2012) and since in this work we use and develop approaches aimed at estimating the bed material transport in large gravel-bed rivers, the third question is:

c) To what extent is a dam able to impact on sediment mobility and transport regime of a large gravel-bed river and which relations exist between sediment transport and other key factors of river morphodynamics (i.e. channel morphology and streambed material features)?

Thesis structure

This work deals with the challenge of improving and assessing the reliability of the virtual velocity approach for estimating the bed material transport in large gravel-bed rivers. For achieving these aims, the virtual velocity approach and a reliable morphological method have been applied on the same study sector of the Parma River impacted by the presence of a dam representing a zero coarse-sediment flux boundary for independently estimating the coarse-transport regime during a period of 17 months at four cross-sections.

The thesis mainly consists of a collection of papers submitted (or "to be submitted") to scientific journals and it is structured in six chapters. Figure 4 summarizes the thesis structure indicating the chapters, their main objectives and the relations existing between the different parts of the work. Each chapter focuses on a specific research objective and question, but, on the other hand, several connections relate the different parts of the thesis, which can share employed data and methodology (i.e. chapters 2 and 3), objective (i.e. chapters 3 and 4) or results (i.e. chapters 3, 4 and 5).

The first chapter represents the research introduction where the general context of the work is presented with some preliminary considerations on sediment transport and

channel morphology, and the explanation of the wider research aim and the specific objectives and questions that the thesis seeks to deal with.

The second chapter (*Water Recourses Research*, in revision) includes the field data collected during the monitoring carried out along the Parma River in order to apply the virtual velocity approach for the transport estimation. Considering the role of some key input factors (i.e. streambed grain size, water stage, section topography) and the reach-specific empirical relations between the shear stress and the calculation parameters derived for the study sector, an application framework including several methodological improvements has been developed for calculating the bed material transport in different large gravel-bed rivers. The main goal of this chapter is to address the research objective 1.

Using the empirical relations obtained for the specific study sector and following the methodological issues addressed in chapter two, in chapter three (*Earth Surface Processes and Landforms*, submitted) we calculated the bed material transport at four study sections during nine competent events between January 2016 and May 2017. The presence of the dam allowed us also to analyze the effects induced by river regulation on the streambed material dynamics (e.g. sediment mobility at different morphological units and occurrence of partial and full transport).

Considering the river morphological evolution over the last 160 years, chapter four (to be submitted to *Geomorphology*) deals with the alterations induced by the human activities (e.g. sediment mining, dam and retention basin construction) on the study sector focusing on the transport regime variations that occurred since the dam closure in 2005. Employing a morphological method based on the sediment budgeting procedure, the coarse material transport downstream from the Marano retention basin has been calculated for three periods including a time interval coincident with the period considered by the virtual velocity approach estimation. Both chapters three and four allow us to deal with the research objective (3) considering the impact of the human regulation on the morphodynamics of the studied fluvial system using different methods, taking into account different temporal scales of analysis and focusing on different specific aspects induced by the human alteration.

Considering the results obtained in chapters three and four, the chapter five (paper in preparation) addresses a comparison between the transport estimates provided by the two independent approaches at the same locations during a 12-months period. Starting from the good agreement between the results provided by the two adopted approaches, the

reliability of the virtual velocity approach estimates has been analyzed in comparison with some adopted theoretically-based transport formulas dealing with the second methodological research objective (objective (2)).

The two sections reported in the last chapter (Discussion and Conclusions, Chapter six) consider the main outcomes of the previous chapters, seeking to answer the three research questions stated above. Some wider final remarks are also reported for reflecting about the possible applications, wider implications and future perspectives of the tested approaches.

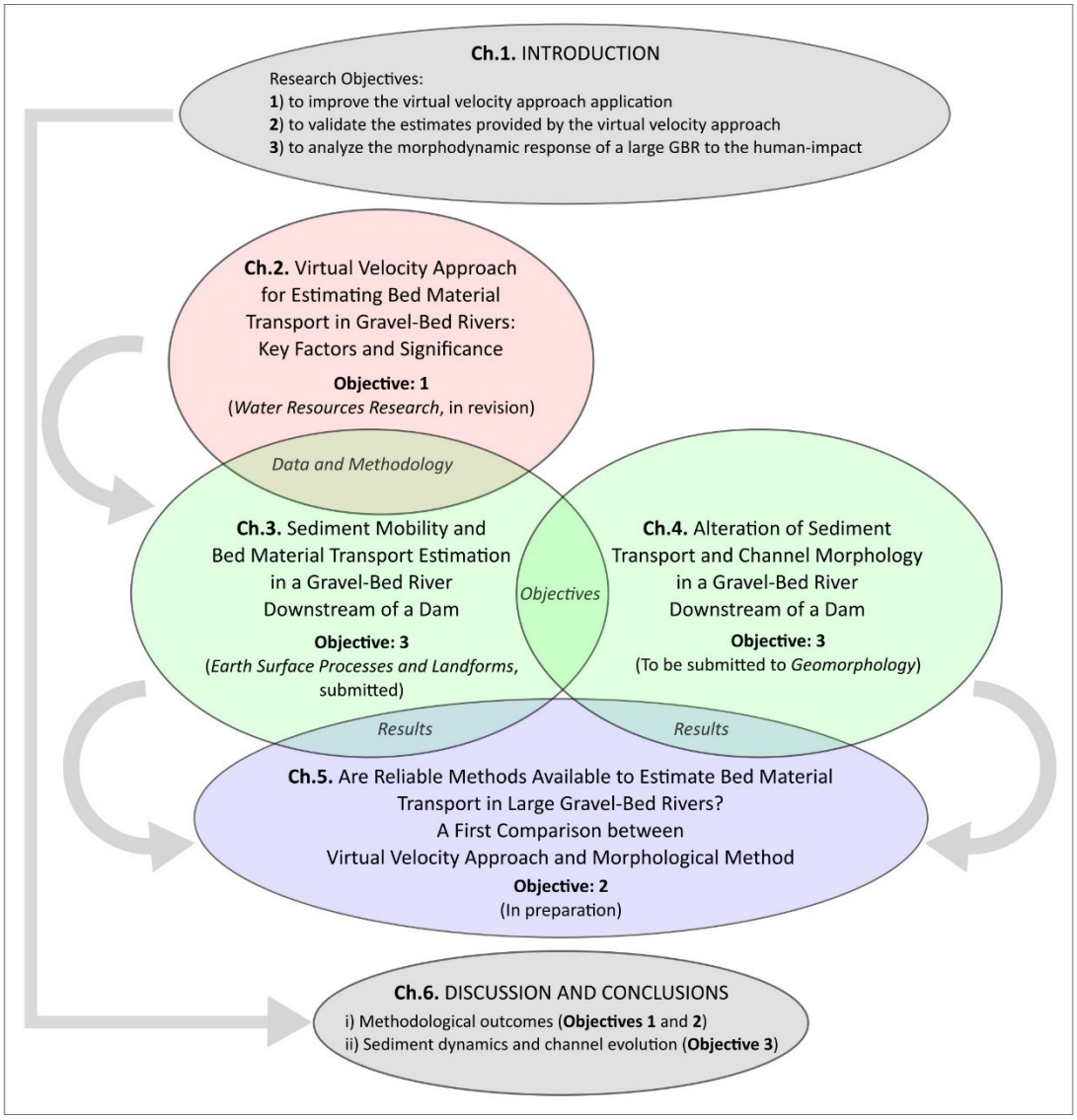

Figure 4. Structure of the thesis. Each circle represents a chapter. The circles superimpose based on their interrelations which are specified in the figure. The scientific journal where each chapter has been submitted and the current stage of revision are plotted as well.

References

Anderson, S., & Pitlick, J. (2014). Using repeat lidar to estimate sediment transport in a steep stream. *Journal of Geophysical Research: Earth Surface*, *119*(3), 621-643. https://doi.org/10.1002/2013JF002933

Ashmore, P. E., & Church, M. (1998). Sediment transport and river morphology: a paradigm for study. In P. C. Klingeman, R. L. Beschta, P. D. Komar, J. B. Bradley (Eds.), *Gravel-Bed Rivers in the Environment* (pp. 115-148). Highlands Ranch, CO: Water Resources Publications LLC

Bridge, J. S. (2009). *Rivers and floodplains: forms, processes, and sedimentary record*. Hoboken, NJ: John Wiley & Sons

Bunte, K., Abt, S. R., Potyondy, J. P., & Ryan, S. E. (2004). Measurement of coarse gravel and cobble transport using portable bedload traps. *Journal of Hydraulic Engineering*, *130*(9), 879-893. https://doi.org/10.1061/(ASCE)0733-9429(2004)130:9(879)

Church M. (1992). Channel Morphology and Typology. In: P. Callow, G.E. Petts (Eds.), *The Rivers Handbook* (pp. 126-143). Oxford, UK: Blackwell Publishing Ltd

Church, M. (2002). Geomorphic thresholds in riverine landscapes. *Freshwater biology*, *47*(4), 541-557. https://doi.org/10.1046/j.1365-2427.2002.00919.x

Church, M. (2006). Bed material transport and the morphology of alluvial river channels. *Annu. Rev. Earth Planet. Sci*., 34, 325-354. https://doi.org/10.1146/annurev.earth.33.092203.122721

Church, M. (2010). Gravel-Bed Rivers. In T. P. Burt, R. J. Allison (Eds.), *Sediment Cascades: An Integrated Approach* (pp. 241-269). Hoboken, NJ: John Wiley & Sons

Church, M., & Ferguson, R. I. (2015). Morphodynamics: Rivers beyond steady state. *Water Resources Research*, 51(4), 1883-1897. https://doi.org/10.1002/2014WR016862

Clayton, J. A., & Pitlick, J. (2007). Spatial and temporal variations in bed load transport intensity in a gravel bed river bend. *Water Resources Research*, 43(2). https://doi.org/10.1029/2006WR005253

Eaton, B. C., & Lapointe, M. F. (2001). Effects of large floods on sediment transport and reach morphology in the cobble-bed Sainte Marguerite River. *Geomorphology*, *40*(3-4), 291-309. https://doi.org/10.1016/S0169-555X(01)00056-3

Emmett, W. W. (1979). A field calibration of the sediment-trapping characteristics of the Helley-Smith bedload sampler (Vol. 1139). Washington, DC: US Government Printing Office

Ferguson, R. (2007). Gravel-bed rivers at the reach scale. In H. Habersack, H. Piégay, M. Rinaldi (Eds.), *Gravel-bed Rivers VI: from process understanding to river restoration* (pp. 33-60). Amsterdam, Netherlands: Elsevier.

Fuller, I. C., Reid, H. E., & Brierley, G. J. (2013). Methods in Geomorphology: Investigating River Channel Form. In J. F. Shroder (Ed.), *Treatise on Geomorphology*, *Vol. 14* (pp. 73-91). Amsterdam, Netherlands: Elsevier.

Geay, T., Belleudy, P., Gervaise, C., Habersack, H., Aigner, J., Kreisler, A., ... & Laronne, J. B. (2017). Passive acoustic monitoring of bed load discharge in a large gravel bed river. *Journal of Geophysical Research: Earth Surface*, *122*(2), 528-545. https://doi.org/10.1002/2016JF004112

Gomez, B. (1991). Bedload transport. *Earth-Science Reviews*, *31*(2), 89-132. https://doi.org/10.1016/0012-8252(91)90017-A

Gomez, B., & Church, M. (1989). An assessment of bed load sediment transport formulae for gravel bed rivers. *Water Resources Research*, *25*(6), 1161-1186. https://doi.org/10.1029/WR025i006p01161

Grams, P. E., Topping, D. J., Schmidt, J. C., Hazel, J. E., & Kaplinski, M. (2013). Linking morphodynamic response with sediment mass balance on the Colorado River in Marble Canyon: issues of scale, geomorphic setting, and sampling design. *Journal of Geophysical Research: Earth Surface*, *118*(2), 361-381. https://doi.org/10.1002/jgrf.20050

Grant, G. E. (2012). The geomorphic response of gravel-bed rivers to dams: perspectives and prospects. In M. Church, P. M. Biron, A. G. Roy (Eds.), *Gravel-bed Rivers: Processes, Tools, Environments* (pp. 165-181). Hoboken, NJ: John Wiley & Sons

Grant, G. E., Swanson, F. J., & Wolman, M. G. (1990). Pattern and origin of stepped-bed morphology in high-gradient streams, Western Cascades, Oregon. *Geological Society of America Bulletin*, *102*(3), 340-352. https://doi.org/10.1130/0016-7606(1990)102<0340:PAOOSB>2.3.CO;2

Griffiths, G. A. (1979). Recent sedimentation history of the Waimakariri River, New Zealand. *Journal of Hydrology (new zealand)*, 6-28.

Haschenburger, J. K., & Church, M. (1998). Bed material transport estimated from the virtual velocity of sediment. *Earth Surface Processes and Landforms*, *23*(9), 791-808. https://doi.org/10.1002/(SICI)1096-9837(199809)23:9<791::AID-ESP888>3.0.CO;2-X

Ham, D. G., & Church, M. (2000). Bed-material transport estimated from channel morphodynamics: Chilliwack River, British Columbia. *Earth Surface Processes and Landforms*, *25*(10), 1123-1142. https://doi.org/10.1002/1096-9837(200009)25:10<1123::AID-ESP122>3.0.CO;2-9

Hassan, M. A., & Church, M. (1992). The movement of individual grains on the streambed. In P. Billi, R. D. Hey, C. R. Thorne, P. Tacconi (Eds.), *Dynamics of gravel-bed rivers* (pp. 159-175). Hoboken, NJ: John Wiley & Sons. https://doi.org/10.1002/esp.3290180510

Hassan, M. A., & Roy, A. G. (2016). Coarse particle tracing in fluvial geomorphology. In G.M. Kondolf, H. Piégay (Eds.), *Tools in fluvial geomorphology* (pp. 306-323). Hoboken, NJ: John Wiley & Sons. https://doi.org/10.1002/9781118648551.ch14

Helley, E. J., & Smith, W. (1971). Development and calibration of a pressure-difference bedload sampler. Open-File Report (No. 73-108). Menlo Park, CA: Water Resour. Div., U. S. Geol. Surv. https://doi.org/10.3133/ofr73108

Hicks, D. M., & Gomez, B. (2016). Sediment transport. In G.M. Kondolf, H. Piégay (Eds.), *Tools in fluvial geomorphology* (pp. 324-356). Hoboken, NJ: John Wiley & Sons. https://doi.org/10.1002/9781118648551.ch15

Lane, E. W. (1955). Importance of fluvial morphology in hydraulic engineering. *Proceedings (American Society of Civil Engineers); v. 81, paper no. 745*.

Lane, S. N., Richards, K. S., & Chandler, J. H. (1995). Morphological Estimation of the Time-Integrated Bed Load Transport Rate. *Water Resources Research*, *31*(3), 761-772. https://doi.org/10.1029/94WR01726

Leopold, L. B., & Wolman, M. G. (1957). River channel patterns: braided, meandering, and straight. Washington, DC: US Government Printing Office

Liébault, F., & Laronne, J. B. (2008). Evaluation of bedload yield in gravel-bed rivers using scour chains and painted tracers: the case of the Esconavette Torrent (Southern French Prealps). *Geodinamica Acta*, *21*(1-2), 23-34. https://doi.org/10.3166/ga.21.23-34

López, R., Vericat, D., & Batalla, R. J. (2014). Evaluation of bed load transport formulae in a large regulated gravel bed river: The lower Ebro (NE Iberian Peninsula). *Journal of hydrology*, *510*, 164-181. https://doi.org/10.1016/j.jhydrol.2013.12.014

Mao, L., Picco, L., Lenzi, M. A., & Surian, N. (2017). Bed material transport estimate in large gravel-bed rivers using the virtual velocity approach. *Earth Surface Processes and Landforms*, *42*(4), 595-611. https://doi.org/10.1002/esp.4000

Martin, Y., & Church, M. (1995). Bed-material transport estimated from channel surveys: Vedder River, British Columbia. *Earth Surface Processes and Landforms*, *20*(4), 347-361. https://doi.org/10.1002/esp.3290200405

Martin, Y., & Ham, D. (2005). Testing bedload transport formulae using morphologic transport estimates and field data: lower Fraser River, British Columbia. *Earth Surface Processes and Landforms*, *30*(10), 1265-1282. https://doi.org/10.1002/esp.1200

McLean, D. G., & Church, M. (1999). Sediment transport along lower Fraser River: 2. Estimates based on the long-term gravel budget. *Water Resources Research*, *35*(8), 2549-2559. https://doi.org/10.1029/1999WR900102

Merz, J. E., Pasternack, G. B., & Wheaton, J. M. (2006). Sediment budget for salmonid spawning habitat rehabilitation in a regulated river. *Geomorphology*, *76*(1), 207-228. https://doi.org/10.1016/j.geomorph.2005.11.004

Montgomery, D. R., & Buffington, J. M. (1997). Channel-reach morphology in mountain drainage basins. *Geological Society of America Bulletin*, *109*(5), 596-611. https://doi.org/10.1130/0016-7606(1997)109<0596:CRMIMD>2.3.CO;2

Passalacqua, P., Belmont, P., Staley, D. M., Simley, J. D., Arrowsmith, J. R., Bode, C. A., ... & Wheaton, J. M. (2015). Analyzing high resolution topography for advancing the understanding of mass and energy transfer through landscapes: A review. *Earth-Science Reviews*, *148*, 174-193. https://doi.org/10.1016/j.earscirev.2015.05.012

Recking, A., Liébault, F., Peteuil, C., & Jolimet, T. (2012). Testing bedload transport equations with consideration of time scales. *Earth Surface Processes and Landforms*, *37*(7), 774-789. https://doi.org/10.1002/esp.3213

Rennie, C. D., Vericat, D., Williams, R. D., Brasington, J., & Hicks, M. (2017). Calibration of acoustic doppler current profiler apparent bedload velocity to bedload transport rate. In D. Tsutsumi, J. B. Laronne (Eds.), *Gravel-Bed Rivers: Processes and Disasters* (pp. 209-233). Hoboken, NJ: John Wiley & Sons

Rickenmann, D. (2017). Bedload transport measurements with geophones, hydrophones, and underwater microphones (passive acoustic methods). In D. Tsutsumi, J. B. Laronne (Eds.), *Gravel-Bed Rivers: Processes and Disasters* (pp. 185-208). Hoboken, NJ: John Wiley & Sons

Rosgen, D. L. (1994). A classification of natural rivers. *Catena*, *22*(3), 169-199. https://doi.org/10.1016/0341-8162(94)90001-9

Ryan, S. E., & Dixon, M. K. (2007). 15 Spatial and temporal variability in stream sediment loads using examples from the Gros Ventre Range, Wyoming, USA. In H. Habersack, H. Piégay, M. Rinaldi (Eds.), *Gravel-Bed Rivers VI: From Process Understanding to River Restoration* (pp. 387-407). Amsterdam, Netherlands: Elsevier.

Schumm, S. A. (1963). *A tentative classification of alluvial river channels an examination of similarities and differences among some Great Plains rivers*. Circ. No. 477 US Geological Survey

Schumm, S. A. (1977). *The fluvial system* (Vol. 338). Hoboken, NJ: John Wiley & Sons

Schumm, S. A. (1985). Patterns of alluvial rivers. *Annual Review of Earth and Planetary Sciences*, *13*(1), 5-27. https://doi.org/10.1146/annurev.ea.13.050185.000253

Surian, N., & Cisotto, A. (2007). Channel adjustments, bedload transport and sediment sources in a gravel-bed river, Brenta River, Italy. *Earth Surface Processes and Landforms*, *32*(11), 1641-1656. https://doi.org/10.1002/esp.1591

Thorne C.R. (1997). Channel types and morphological classification. In: C.R. Thorne, R.D. Hey, M.D. Newson (Eds.), *Applied Fluvial Geomorphology for River Engineering and Management* (pp. 175-222). Hoboken, NJ: John Wiley & Sons

Vázquez-Tarrío, D., Recking, A., Liébault, F., Tal, M., & Menéndez-Duarte, R (2018). Particle transport in gravel-bed rivers: revisiting passive tracer data. *Earth Surface Processes and Landforms*. https://doi.org/10.1002/esp.4484

Vericat, D., Wheaton, J. M., & Brasington, J. (2017). Revisiting the Morphological Approach: Opportunities and Challenges with Repeat High-Resolution Topography. In D. Tsutsumi, J. B. Laronne (Eds.), *Gravel-Bed Rivers: Processes and Disasters* (pp. 121-158). Hoboken, NJ: John Wiley & Sons

Whiting, P. J. (2016). Flow measurement and characterization. In G.M. Kondolf, H. Piégay (Eds.), *Tools in fluvial geomorphology* (pp. 260-277). Hoboken, NJ: John Wiley & Sons. https://doi.org/10.1002/9781118648551.ch12

Wilcock, P. R. (1997). Entrainment, displacement and transport of tracer gravels. *Earth Surface Processes and Landforms*, *22*(12), 1125-1138. https://doi.org/10.1002/(SICI)1096-9837(199712)22:12<1125::AID-ESP811>3.0.CO;2-V

Wilcock, P. R. (2001). Toward a practical method for estimating sediment-transport rates in gravel-bed rivers. *Earth Surface Processes and Landforms*, *26*(13), 1395-1408. https://doi.org/10.1002/esp.301

Wohl, E., Bledsoe, B. P., Jacobson, R. B., Poff, N. L., Rathburn, S. L., Walters, D. M., & Wilcox, A. C. (2015). The natural sediment regime in rivers: Broadening the foundation for ecosystem management. *BioScience*, 65(4), 358-371. https://doi.org/10.1093/biosci/biv002

2. VIRTUAL VELOCITY APPROACH FOR ESTIMATING BED MATERIAL TRANSPORT IN GRAVEL-BED RIVERS: KEY FACTORS AND SIGNIFICANCE

Andrea Brenna[1], Nicola Surian[1], and Luca Mao[2]

[1] *Department of Geosciences, University of Padova, Padova, Italy.*

[2] *School of Geography, University of Lincoln, Lincoln, UK.*

Water Resources Research, in revision.

Abstract

In large gravel-bed rivers bed material transport estimation is a challenging task since theoretically-based formulas often fail to predict sediment fluxes, and it is difficult to carry out field measurements. A viable alternative to direct measurement is provided by the virtual velocity approach representing a hybrid solution to calculate the bed material transport based on a theoretical framework and use of tracers. This work aims to improve the methodology and to assess the role of input factors through a case-study application carried out in the Parma River (Italy). Two tracer types and scour chains were deployed at four sections. Data on water level, transport processes, particle travel distances and active layers were collected over 17 months and 6 events. The transport that occurred during two different events was calculated applying different configurations taking in account for several input factors (i.e. grain size, water stage, topography). Applying simple or more complex configurations lead to significant differences in estimate: in relation to channel morphodynamics, different factors (e.g. variability of water level within the cross-section in multi-thread channels) play a key-role on transport processes. Results indicate that it is crucial to collect and process field data developing reach-specific transport rating-curves and to combine different type of tracers for monitoring the clasts displacement lengths. Based on the methodological improvements and sensitivity analysis addressed in this study, we developed a decision tree in order to design future applications of the virtual velocity approach for estimating the bed material load in different gravel-bed river contexts.

1. Introduction

In the context of alluvial rivers characterized by coarse streambed material, episodic bed material transport is the most significant factor controlling a river evolution and morphodynamic processes (Church, 2006; Ferguson, 2007; Ashmore, 2013; Church and Ferguson, 2015). A reliable estimation of bed material transport is a key issue to address several questions but it is notoriously hard to achieve (Ferguson, 2007; Haschenburger, 2013). One of the most used solutions to address this issue is through theoretically-based

formulas (e.g. Recking et al., 2012) but often the application of different relations proposed for a given context provides strongly incongruent estimates (Gomez and Church, 1989; Martin and Ham, 2005; Lopez et al., 2014). To overcome this issue, traps and portable samplers (Bunte et al., 2004, 2007) and indirect passive acoustic methods, like geophones, hydrophones (Rickenmann, 2017) and Acoustic Doppler profiling (Rennie et al., 2004a), have been successfully applied in different contexts (Rennie et al., 2004b, 2017; Rickenmann et al., 2014; Wyss et al., 2016). For defining the instantaneous flux, field measurements need to be carried out during transporting events, implying several issues in term of human safety and instrument installation during a flood in the context of wide rivers. Furthermore obtained results, referred to punctual and instantaneous measures, are affected by sources of errors (Vericat et al., 2006; Bunte et al., 2008) due to the high sediment transport spatial variability along a section in large rivers (Clayton and Pitlick, 2007; Ryan and Dixon, 2007; Williams et al., 2015) and temporal variation during fluctuating hydrographs (Hoey, 1992). Bed material load field-measurement techniques are suitable for small streams and the most appropriate methods depend on the specific time-scale of interest.

A robust alternative for estimating bed material rate in large rivers is represented by the morphological methods (Lane et al., 1995; Ashmore and Church, 1998) which provide reasonable estimates integrated in time and space, taking in account for errors and uncertainties (McLean and Church, 1999; Brasington et al., 2003; Wheaton et al., 2010) based on volumetric differencing techniques. Some improvements have been achieved in the challenge of making the method independent from specific boundary conditions, using surrogate estimates of particle path lengths (Pyrce and Ashmore, 2003a; Kasprak et al., 2015; Vericat et al., 2017) based on local morpho-types (e.g. dominant particles travel distances tie to the length scale of the bar topography) or directly employing tracer-particle travel distances (e.g. Ashmore and Church, 1998; Pyrce and Ashmore, 2003b; Papangelakis and Hassan, 2016;). However, the specification of transport rate from volumetric change (ΔV) using the diffuse sediment budgeting approach ($\Delta V = Q_b^{in} - Q_b^{out}$) requires knowledge of a reference river section where the transport is known, estimable or negligible (Merz et al., 2006; Surian and Cisotto, 2007) in order to reduce the equation unknowns from two (reach transport in- (Q_b^{in}) and out- (Q_b^{out})) to one. This condition implies that the morphological approach often requires to be applied coupled with a method able to provide a local bed material flux boundary constraint (see Vericat et al. (2017)).

The use of tracers represents a technique applied for a long time in fluvial geomorphology, providing information about transport processes and their relations with the water flow. Two types of tracer exist (see Hassan and Roy (2016)): passive tracers, which must be seen or sensed by an observer or a detector, and active tracers, which emit waves or rays detected by a spectrometer or receiver. Active tracers (e.g. radio transmitters) are very powerful but, on the other hand, are expensive and installable only on large grains (e.g. cobble). Passive tracers (e.g. painted clasts and Passive Integrated Transponders tags) have been extensively used for sediment dynamics monitoring in several field studies (e.g. Petit, 1987; Church and Hassan, 1992; Sear, 1996; Thompson and Wohl, 2009; Bradley and Tucker, 2012; Haschenburger, 2013b; Hassan and Bradley, 2017) since they are cheap and easy to apply. One of the most promising application concerning tracer data is the development of calculation procedures to estimate bed material transport involving the particles displacement lengths and the definition of the bed mobile surface layer thickness. An important parameter obtainable from tracers is the virtual velocity of the entrained grains. The virtual rate of travel was firstly calculated by Hassan et al. (1992) starting from the concept of path length (Einstein, 1937) and then the virtual velocity was defined as the mean velocity characterizing the clasts movement during the period for which particles might be in motion during a flood (i.e. considering travel distances and competence period as in Ferguson and Wathen (1998), Haschenburger and Church (1998) and Liébault et al. (2012)). Virtual velocity is different from the actual instantaneous-velocity since, also during a "competent period", the coarse grains are characterized by short periods of quick movement interspersed with intervals of rest (Haschenburger and Church, 1998). Considering the field-determined virtual velocity of moved grains, some researches (e.g. Haschenburger and Church, 1998; Liébault and Laronne, 2008) assessed the bed material transport in small streams. The adopted methods assumed uniform sediment transport for the whole section. In large gravel-bed rivers the active sediment transport mechanisms can change in time, at different river sections but also considering different locations at the same section, due to the relation between topography, water flux and local sediment characteristics (Haschenburger and Wilcock, 2003; Surian et al., 2009). A useful theoretical framework, able to take in account these aspects, was developed by Wilcock (1997). Such framework allows to calculate the bed material transport rate over a unit portion of the channel taking into account the tractive forces induced on the river bed by the water flow (i.e. shear stress) which determine the local mobility condition of the sediment. Mao et al. (2017) applied for the first time the Wilcock's framework to estimate

the bed material transport occurring in two north-Italian large gravel-bed rivers at some cross-sections during different transport events.

Due to the difficult in carrying out transport estimates at the "competent-event" time scale in large gravel-bed rivers using the approaches described above, we identified the virtual velocity approach as a suitable way to provide a contribution about this issue (i.e. determination of the bed material load occurring during a whole event), giving connections between grain motion, transfer processes and river morphodynamic. In particular, the theoretical framework proposed by Wilcock (1997) seems appropriate to address the transport estimate in wide rivers. Since the Wilcock's framework (1997) was applied in few field case-studies, several methodological questions have not yet been addressed. This work applies the virtual velocity framework proposed by Wilcock (1997) through a tracer-based approach in order to estimate bed material transport in large gravel-bed rivers. We collected data through a two-year monitoring program in a sector of a north-Apennine river using different types of tracers. The research aims to assess the approach strengths and limitations, in particular evaluating for the first time the significance of each factor that feed in the calculation through a simplified sensitivity analysis, in terms of data collection, processing and use in the estimation. The specific research objectives are (i) to define a spatial scale (e.g. segment, reach, sub-reach) for field data collection and processing appropriate for the local river characteristics; (ii) to assess which tracer types are more suitable to provide reliable travel distances and to test the accordance of data collected from different tracer types; (iii) to assess how each input factor (e.g. sediment grain size, water stage, section topography) affects transport estimates and if such estimates vary significantly using different input factor configurations.

2. Materials and Methods

2.1 Study site and monitored events

The study was carried out in a sector of the Parma River (Northern Apennines, Italy) (Figure 1). Its drainage basin has a total area of 815 km^2 and the length of the whole river is 92 km. The middle sector of the river is characterized by coarse bed-sediment (i.e. gravel, pebbles and eventually cobbles). The selected study area is located upstream from the city of Parma and it is bounded at its upstream end by the closure dam of the Marano retention basin, which retains all coarse sediments, representing a zero-flux coarse sediment boundary. As a result, the channel pattern changes notably upstream and downstream from the dam, being respectively braided (average width = 340 m; braiding index = 2.5 - 3) and

single-thread with alternate bars or wandering (average width = 60-160 m; braiding index = 1.1 - 1.2). Along the 4 km-long study sector, we selected four monitoring cross-sections: sections 1 and 2 (slope = 0.0051; width = 90-110 m), located respectively 1950 m and 2200 m downstream from Marano dam, and sections 3 and 4 (slope = 0.0051; width = 120-140 m), located respectively 3250 m and 3400 m downstream from the dam (Figure 1). The study sector features (width, sediments characteristics, morphology) vary moving downstream from the dam, making possible to recognize at least two different reaches (Figure 1) characterized by internal variability at the morphological unit spatial scale.

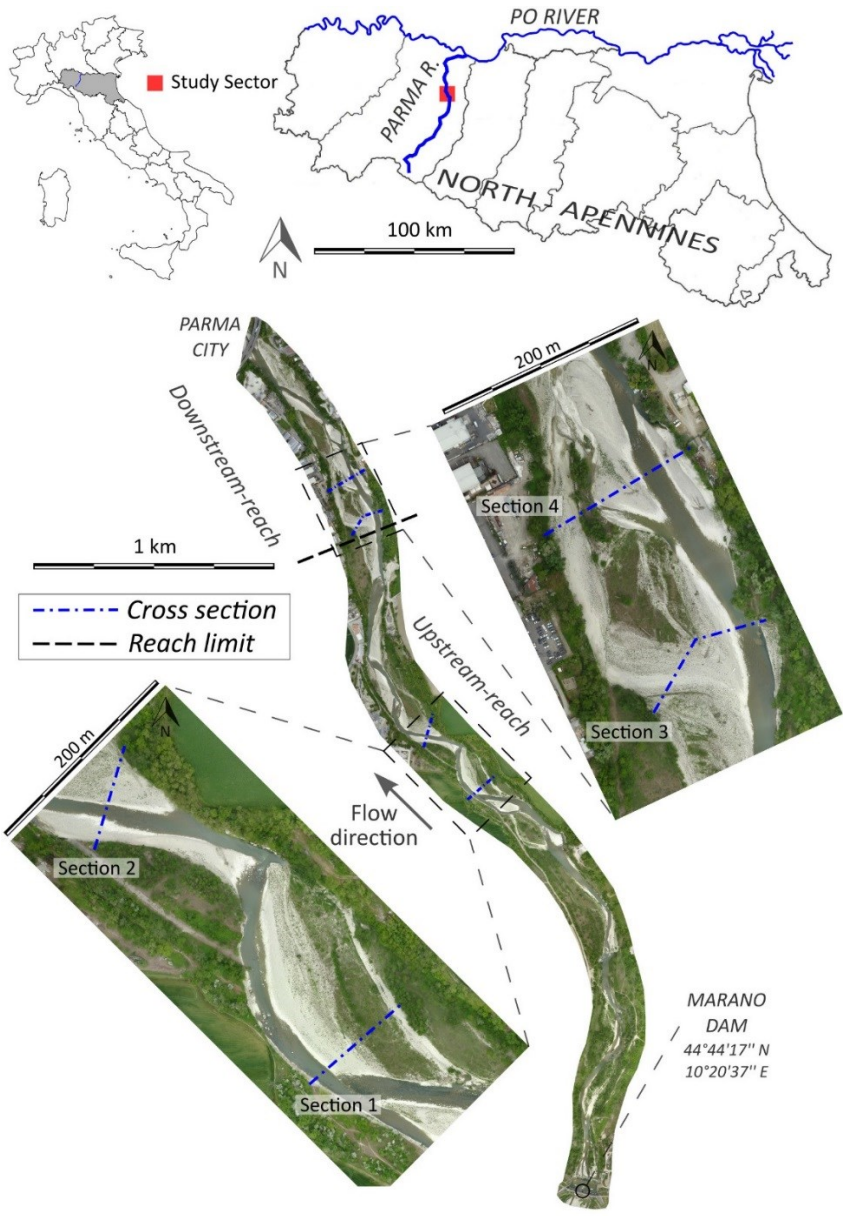

Figure 1. Location of the Parma River and monitored cross-sections positions within the study sector.

The river is characterized by a hydrological regime led by seasonal rainfall with most of the precipitation occurring between November and April (Figure 2a).

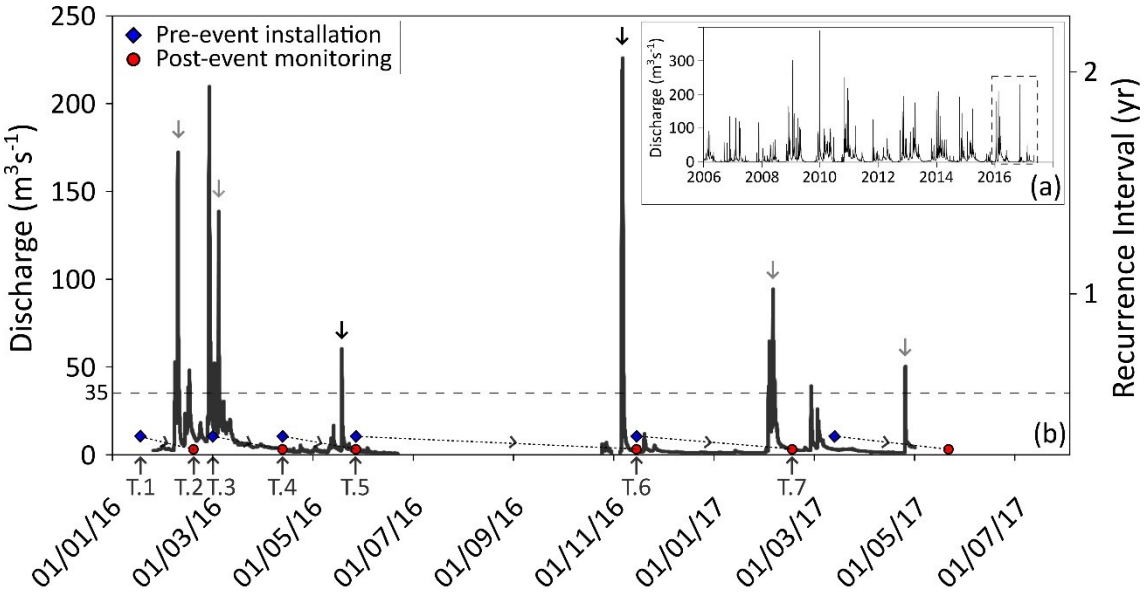

Figure 2. Hydrographs during the last 11 years (a) and during the monitoring period (January 2016 – May 2017) (b). In (b), the vertical arrows point out the six monitored events; the two black arrows point out the transport events that were considered for bed material load estimate. The timing of the acquired cross-sections topographies, the pre-event installations (e.g. painting of patches, seeding of PIT tags, scour chains installation) and the post-event monitoring (e.g. survey of tracers in terms of transport processes, lengths of movement, etc.) are plotted in (b). The discharge threshold of 35 m^3 s^{-1} is plotted as well.

Not knowing a priori the water discharge required to induce a competent bed material transporting event at the considered sections, we calibrated the monitoring implementation based on the fieldwork experience. The first field-observations (e.g. direct observations of minor morphological changes or sediment mobilization after a flood) allowed us to define a discharge threshold approximately equal to 35 m^3 s^{-1} in order to identify a monitoring-significant (i.e. transporting) event. Over the 17 months of monitoring (January 2016 - May 2017), nine events occurred, the largest one with a recurrence interval of 2.1 years (Figure 2b). Due to logistic issues (e.g. not sufficient time between two events), pre-event installation and field monitoring, each one covering a single flood, were carried out for six events.

2.2 Estimating bed material transport through the virtual velocity approach

Wilcock's (1997) approach allows the bed material transport calculation defining the mass and size distribution of material entrained and transported by flow from a unit channel area during a defined period. Bed sediments in a specific unit area can be in three different mobility conditions: no motion, partial mobility and full mobility. Partial mobility is the condition in which only a fraction of the surface particles of a certain grain size are mobilized over a time interval (Wilcock and McArdell, 1997). The mass of material of the *i*-size entrained from a defined surface area, M_i (in kg m^{-2}) is given by:

$$M_i^{PT} = \frac{m_i F_i Y_i}{D_i^2} \qquad (1)$$

where m_i is the mass of a single particle of size *i* (in kg), F_i is the proportion of fraction *i* in the surface grain distribution, D_i is the diameter of fraction *i* grains (in m) and Y_i is the proportion of surface particles of the fraction *i* transported in the event. The mass of a single grain of fraction *i* is calculated using the spherical approximation as $m_i=((\pi/6)\rho_s D_i^3)$ where ρ_s is the density of the grain material (in kg m^{-3}). When the tractive forces overcome a certain threshold such that Y_i becomes 1, full mobility occurs. In this case, all surface particles of a certain size are removed (Wilcock and McArdell, 1997) and subsurface grains could be transported up to the thickness of a certain active layer (Wilcock, 1997). Equation (1) then becomes:

$$M_i^{FT} = \frac{m_i F_i d_s}{D_i^3} \qquad (2)$$

where d_s is the active layer thickness (in m) and F_i is now referring to the active layer.

When M_i is known, to obtain the unit mass fractional transport rate (q_i^u, in kg m^{-1} s^{-1}) it is necessary to multiply the mass of entrained sediment (M_i, in kg m^{-2}) by the virtual velocity characterizing the *i*-size particles movement (V_i, in m h^{-1}):

$$q_i^u = M_i V_i \qquad (3)$$

The main opportunity provided by Wilcock's (1997) framework is to allow the calculation of q_i^u, referring to a definable portion of channel.

Mobility conditions are determined by the intensity of the tractive forces locally induced by the flow on the streambed, expressed by the shear stress (τ in N m^{-2}). To calculate this parameter we used the depth-slope approach (Wilcock, 1993; Mueller et al., 2005) through

the formula: $\tau = \rho_w g h_w S$ where ρ_w is the water density (in kg m^{-3}), g is the gravity acceleration (in m s^{-2}), h_w is the water depth (in m, defined for each 1-m wide portion of cross-section), and S is the local streambed slope (in our case, it was averaged considering 200 m upstream and downstream from each section to represent the mean slope of the entire section bearing in mind the features of the channel along the study sector). To make τ independent from the sediment grain size, we used the conventional dimensionless formulation of shear stress (τ^*) considering the local median grain size (D_{50}) applying equation (4):

$$\tau^* = \frac{\tau}{(\rho_s - \rho_w) g D_{50}} \qquad (4)$$

We assumed a ρ_s= 2600 kg m^{-3} and used the surface D_{50} as done in several previous works (e.g. Parker, 1990; Mueller et al., 2005).

As proposed by Mao et al. (2017), we simplified the equation (1) as follow:

$$M_i^{PT} = \frac{m_i F_i Y}{D_i^2} \qquad (5)$$

where Y is the percentage of mobilized streambed for a defined bed area and it is a proxy of the partial transport intensity defined like a condition of sediment mobility in which some surface grains remain immobile over the duration of a transport event, indicating the active portion of all grains on the bed surface (Haschenburger and Wilcock, 2003). Through the equations (2), (3) and (5) we calculated values referred to a single *i* grain size fraction. To obtain the whole entrained and moved material as a function of shear stress, it is required to calculate the mass of entrained sediment and the fractional mass transport rate for each grain size class and then to sum all fractional results:

$$q^u = \sum q_i^u \qquad (6)$$

where q^u is the total unit mass transport rate (in kg m^{-1} s^{-1}) for the transported channel sediment.

2.3 Field monitoring procedures and data processing

2.3.1 Topographic surveys, bed material grain size and tracers

The four cross-sections were surveyed before and after each monitored event (Figure 2b) using a differential global positioning system (dGPS, Leica GS14, vertical accuracy equal to ±0.02 m). Employing aerial-photographs, sediments-vegetation field observations and elevation data, using types and criteria reported in Mao and Surian (2010) morphological

units (or fluvial landforms) recognizable along the sections were classified in: main channel, secondary channels, low and high bars, islands, floodplains and terraces (Figure 3). For each pre-event installation (Figure 2b), we selected between two and eight sites along each section (Figure 3) representative of each morphological unit surface sediments suitable for image grain size analysis and tracer installation (e.g. lack of fine sediments and herbaceous vegetation). Using an aluminum frame, we were able to define rectangular areas of 0.8 m * 0.6 m (respectively cross-stream and downstream) which were orthogonally photographed using a 16 megapixel digital camera. The photos were processed by the Digital Gravelometer software (Graham et al., 2005a, 2005b, 2010) deriving the surface grain-size distribution characterizing each site. Due to the camera resolution, we applied a lower truncation of 6 mm, comparable with that commonly used in the manual pebble count (Wolman, 1954; Bunte and Abt, 2001). Using the same procedure, we acquired and elaborated six photographs of vertical exposures visible in correspondence of incised bars margins along the study sector (channel bank, figure 3), deriving values about the subsurface grain-size distribution (Storz-Peretz and Laronne, 2013). Considering the percentage of the area excluded from the grain-size calculation by the Digital Gravelometer software since composed by material finer than the imposed analysis-threshold (6 mm), it was possible to conclude that fine material (< 6 mm) in average accounts for about 20% of sediment volume in the study reach for both surface and subsurface sediment. Field observations about the streambed material fabric and structuring were carried out, focusing on sediment armoring evidences (e.g. imbrication and grain sorting).

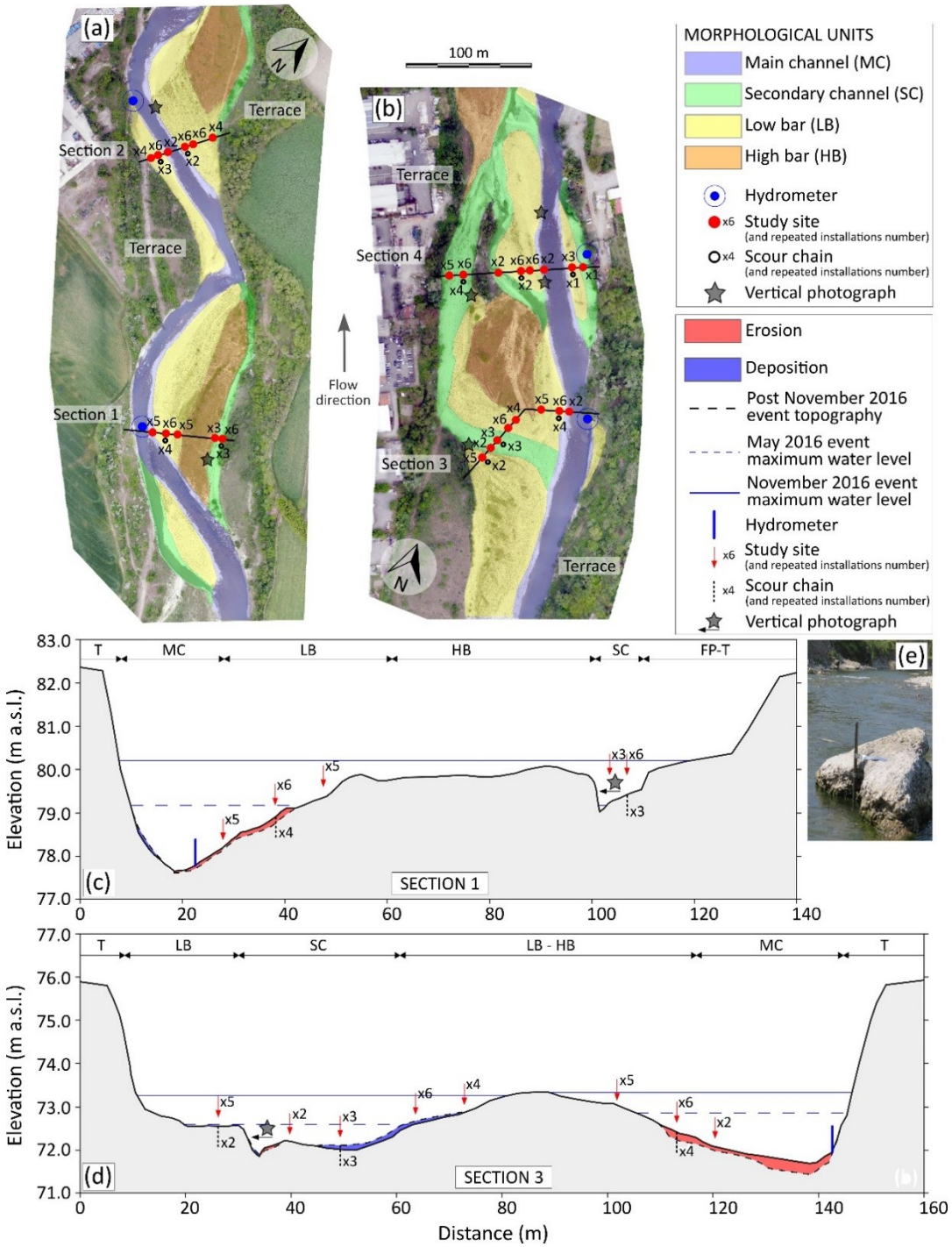

Figure 3. Aerial photographs (April 2016) of the study sections areas and the two cross-sections (section 1 (a); section 3 (b)) considered for the transport calculations. Morphological units are shown (MC: main channel; SC: secondary channel; LB: low bar; HB: high bar; FP: floodplain; T: terrace). Cross-sections (section 1 (c); section 3 (d)): black continuous lines identify the May-event and the November pre-event topography while dotted lines refer to the post-November 2016 event topography. Hydrometers (installation image example is provided (e)), study sites (i.e. painted areas), scour chains and vertical photographs positions are plotted as well both in plans and sections.

After the photographic procedure, the surface of the patches (area 0.8 m * 0.6 m) was painted using a fluorescent spray paint, i.e. each clast in the surface became a painted tracer (overall, 117 painted areas and about 38,000 painted clasts coarser than 6 mm were colored). This procedure avoids disturbing the surface bed material or modifying the natural sediment structure, and easily marks a large number of clasts without grain size limitations. The elevation (m a.s.l.) of each installed painted area were determined using the dGPS. To maximize the recovery rate we coupled painted areas with Passive Integrated Transponders tags (PIT tags). Each PIT is detectable using an antenna if buried up to a maximum of 0.3-0.4 m (Lamarre et al., 2005). 23-mm long PITs (Texas Instruments, LF Glass Transponder) were inserted inside drilled individual-clast previously measured (b-axes). For each pre-flood installation, we seeded between six and ten PITs for each painted area (898 PITs were employed during the whole monitoring with, on average, 150 PITs seeded during each event, similar to Chapuis et al. (2015)), choosing clasts with sizes comparable with the coarser component of the local bed material (ranging from 28 to 180 mm). PIT tagged clasts were placed close to the painted areas replacing existing clasts with similar size and shape, avoiding protrusion from the bed, in order to mimic the interlocking of natural surface particles forming the streambed (Chapuis et al., 2015).

2.3.2 Section-specific water flow

Information about water level are required to calculate tractive forces (equation 4). To obtain section-specific hydrographs, we used two techniques: local pressure transducers and field evidences. One pressure hydrometers (Solinst Levelogger 3001, accuracy ±0.005 m) was installed in correspondence of the main channel at each study sections (the positions of the four hydrometers are reported in Figure 3), anchoring them at stable supports (i.e. boulders, trees or levees) in hollow metal casings (Figure 3). Knowing the pressure transducers elevation, the water level above it and using a barometric compensation (atmospheric data collected by a Solinst Barologger 3001 installed near to the study sector) it was possible to obtain a simple hydrograph referred to the specific river location with a precision of ±0.02 m and temporal resolution of 30 minutes. Field evidence of the maximum level reached by water during a flood (i.e. trash lines) in different portions of the channel (main channel and secondary channel banks or related bar surfaces) have been collected using a dGPS after each monitored event at each section. Finally, data from local hydrometers and field evidences have been related with the corresponding discharges provided by the Marano dam gauging station (time resolution of 30 minutes) through simple regression analysis (i.e. polynomial relationships).

2.3.3 Sediment mobility

The sections were surveyed immediately after the transport events. The painted areas were orthogonally photographed again and using the approach applied by Mao and Surian (2010) and Mao et al. (2017), we described the effects of the transport. Areas could be: located above the maximum water stage (AWS), under no-motion (NM), partial transport (PT) (when some surface grains entrained and others remained immobile, independently of their size considering the bed as a whole, as defined by Haschenburger and Wilcock, 2003) or full transport (FT) conditions (referred to painted areas interested by a complete particle removal). After each monitored event, we searched and collected all the tracer grains that moved downstream from the installed and activated study sites. For the painted particles the survey was limited to the visible grains on the bed surface whereas using an antenna, it was possible to recover also buried PITs (collected and stored for the following installations). Particle size (b-axes) and travelled distance from the center of the origin study site of each recovered tracer-grain were individually measured using a caliber and a tape, respectively.

2.3.4 Proportion of the bed mobilized and Active layer

Partial transport processes reflect on the equation (5) through the *Y* parameter which refers to the percentage of mobilized bed material for a defined area, varying from 0 (no motion) to 1 (full transport). To quantify the extent of partial transport over the study sites we used the photographs collected after the events analyzing them as described by Mao et al. (2017). The painted residue pixels represent the percentage of not mobilized streambed surface, and *Y* (a proxy for the extent of partial transport (sensu Haschenburger and Wilcock, 2003) at the painted area scale) is equal to one minus that value.

Where locally full mobility occurs, the subsurface sediment can be mobilized due to the establishment of a mobile surface layer (Church and Haschenburger, 2017), considered in equation (2). In order to collect field evidence about active layer thickness (erosion and sedimentation) we used scour chains and topographic surveys. Scour chains are able to record the event-based maximum depth of scour or deposition (event active layer, as defined by Church and Haschenburger, 2017), taking in account also two-phases processes (Carling, 1987; Liebault and Laronne, 2008; Houbrechts et al., 2012). Following the approach used by Laronne et al. (1994), for four of the six monitored-events, we installed from one to three chains at each section in correspondence of some selected painted areas, using during the entire study period 28 chains in correspondence of painted sites (12 at

sections 1-2 and 16 at sections 3-4) (Figure 3). In order to extend the active layer dataset, we also employed topographical data measuring the post-event bed elevation in correspondence of each painted area where transport occurred, determining the variation in comparison with the pre-event elevation. Painted area elevation changes can just provide the sum of scour and fill at the considered point (i.e. punctual net variation), possibly leading to underestimation of the actual event active layer thickness in case of two-phases erosion-deposition processes, when compensation can occur (Lindsay and Ashmore, 2002).

2.3.5 Sediment transport calculation

Considering section topographies, event hydrographs and the local bed-material D_{50} (in function of morphological unit distribution characterizing the sections during the specific event), we were able to calculate the dimensionless shear stress (τ^*, equation (4)) active on the river bed for each 1 m-wide portion of cross-sections (local τ^*) with a time interval of 30 minutes (instantaneous τ^*). Monitored parameters (mobility conditions, Y and d_s) collected from all flooded painted areas were coupled with the maximum dimensionless shear stress (τ^*_{max}) active at the event peak on the specific study site, since collected data are considered as the results of the maximum acting tractive forces. The grain size specific virtual velocity (V_i, as defined by Wilcock, 1997) was calculated dividing the mean i-size fraction travel distance by the duration of transport determined considering the period for which the τ^* locally active on the streambed was adequate to induce particle movement. Through regression analysis between the field monitored (Y and d_s) or computed (mobility conditions, V_i) parameters and the τ^*_{max}, we defined empirical relations able to determine the parameters values in function of local and instantaneous τ^* active on the streambed. These relations (d_s=f(τ^*) and Y=f(τ^*)) allowed to deal with the fractional transport equations (Equations (2) and (5)) and to calculate the unit fractional sediment transport rate (q_i^u, Equation (3)) introducing the virtual velocity empirical relations V_i=f(τ^*, D_i). Considering the local sediment grain size distribution, the total unit mass transport rate (q^u) were calculated using equation (6) on each 1 m-wide portion of the sections with a temporal resolution of 30 minutes. Integrating the single calculated total unit mass transport rates (q^u) over space (the cross-section extension) and time (the duration of the transport event), we estimated the bed material transport occurring for a specific section during a single transport event.

2.3.6 Calculation factors and sensitivity analysis

We calculated the bed material load for all channel material consisting of clasts larger than 6 mm (b-axes). In order to apply the described calculation procedure it is necessary to consider some factors influencing the data input choices and possibly leading to relevant differences in the estimation results. Using the obtained empirical relations and the associated uncertainties, we tested the method sensitivity considering four application factors, selected on the base of their hypothesized importance and the feasibility and efforts required to measure such factors during the fieldwork. Calculations were carried out through seven data input configurations (Table 1).

Input factors configuration	*Spatial variable (in-section) water level*	*Morpho-unit specific D_{50} for τ^* calculation*	*Morpho-unit specific grain size curve for q^u- τ^* relations*	*Changing section topography during a transport event*
Configuration 1	No	No	No	No
Configuration 2	**Yes**	No	No	No
Configuration 3	No	**Yes**	No	No
Configuration 4	No	No	No	**Yes**
Configuration 5	**Yes**	**Yes**	No	No
Configuration 6	**Yes**	**Yes**	**Yes**	No
Configuration 7	**Yes**	**Yes**	**Yes**	**Yes**

Table 1. The seven input factors configurations adopted for the bed material load estimation.

The simplest setting (configuration 1) considers a single section D_{50} for τ^* calculation and an average water stage for the whole section, fixed cross-section topography during a transport event (i.e. the pre-event section topography) and a single section-sediment grain size distribution for the fractional transport calculation. We progressively introduced application factors taking into account some aspects related to the natural complexity of the system: using (i) spatial variable water level along a single section (configuration 2) we tested the importance of the water flux at specific channel locations; considering (ii) local streambed D_{50} (configuration 3) and (iii) morpho-unit specific grain-size curves (configuration 6) we evaluated the impact of the sediment characteristics on the tractive forces effectiveness and the importance of the fractional calculation; employing (iv) variable section topographies (i.e. pre-event topography which progressively changes into post-event topography during a single event calculation when full transport occurs) (configuration 4), we looked for the effect of the section-morphology evolution during a

competent event. Configurations 5, 6 and 7 (which takes in account all considered factors), allowed us to obtain new insights about the combined effects of different factors on the sediment flux estimates. The significance of the differences in estimates provided by different factors configurations have been evaluated considering the calculation uncertainties also in relation with the natural variability of sediment flux intensity at a given flow in a given section (Ashmore, 2013). This variability was estimated starting from the field-monitoring data collected from several study-sites experiencing different mobility conditions due to local and specific morphological-unit and sedimentological features.

3. Results

3.1 Field observations

3.1.1 Grain size and bed armoring

Overall, 105 surface bed sediment and 6 vertical incised bar margins (Figure 3) photographs (each photograph contains from 100 to 500 grains coarser than 6 mm) were collected. Obtained grain size curves, divided in 11 half-psi classes (i.e. psi= -phi; phi= $-\log_2 D$; D= grain size in mm), show a broad variability. Mean D_{50} and D_{84} were derived accordingly to different groupings: finally 6 different mean curves (Figure 4a) and characteristic parameters (Figure 4b) were considered in order to describe the average surface grain size distribution according to section location (i.e. sections 1-2 and 3-4) and morphological unit (main channel, secondary channel and bar). Those curves show a decreasing trend in the grain size moving from upstream to downstream sections with main channel characterized by coarser material and secondary channels by finer material (Figure 4b). No temporal trends in grain sizes have been identified during the data-collecting period (January 2016 - May 2017). Similar subsurface grain-size distribution along the entire study sector were obtained from the vertical photographs analysis, determining mean D_{50} and D_{84} respectively equal to 36 and 79 mm (Figure 4b). Field observations allowed us to recognize surficial grain sorting, imbrication and presence of coarser surficial grains in the upstream sections: these evidences of streambed armoring tend to decrease moving downstream from the dam. The calculated armor ratios (as $D_{50}^{surf}/D_{50}^{subsurf}$) confirm field evidences: armor ratio ranges from 1.56 to 2.86 (mean 1.75) in sections 1 and 2, whereas it ranges from 1.20 to 2.46 (mean 1.47) in sections 3 and 4. In accordance with Hassan et al. (2006), values higher and lower than 1.50 have been respectively considered as indicative of high and moderate bed armoring for intermittent rivers.

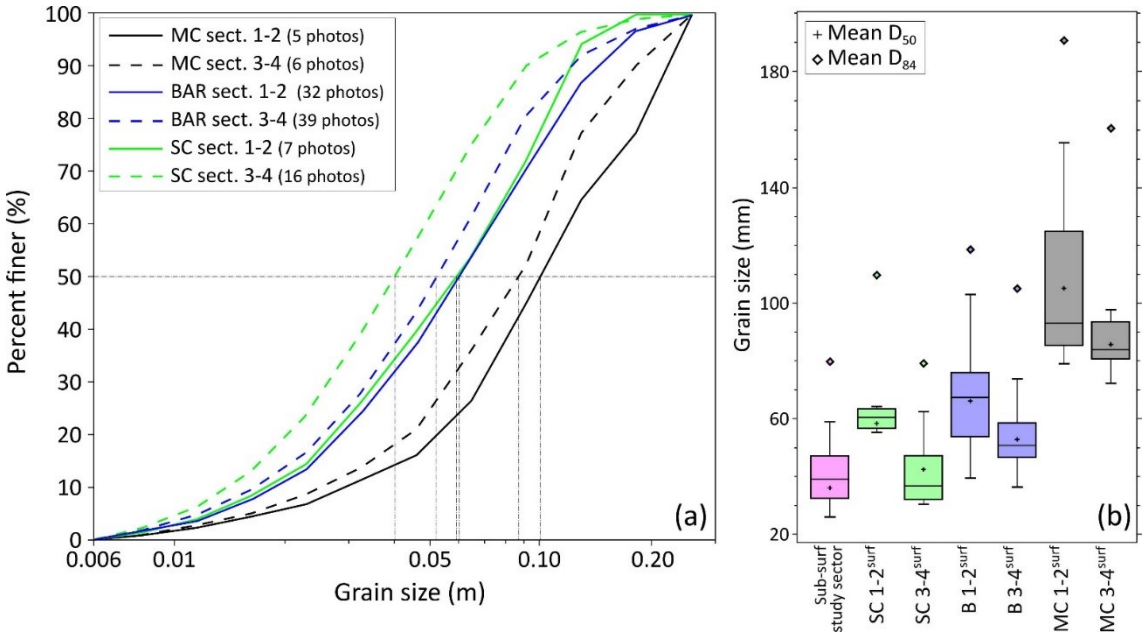

Figure 4. The surface grain size distribution curves truncated at 6 mm (a) and the study sites D_{50} and D_{84} box plot (b) of the channel surface and subsurface sediments. Surface sediments were divided in six groups according to location and morphological unit (MC: main channel; SC: secondary channel; B: bar). In the plot (b), boxes ends represent the 25th and 75th percentiles, whiskers ends are the 10th and 90th percentiles, crosses and lines respectively indicate the mean and the median D_{50} values, diamonds indicates the mean D_{84} values.

3.1.2 Water depth and flow intensity

Comparing hydrometer data and field evidences (i.e. trash line) some discrepancies in the maximum water stages reached at the flood peak at a specific section were observed (Figure 5). Furthermore, data collected by hydrometers referred only to the main channel. Downstream sections are characterized by wandering morphology: the maximum water levels reached in the secondary channel for section 3 (Figure 5), show that water level is not uniform within the section, being lower in the secondary channel during all the monitored events. Due to the reliability of the numerous collected field evidences, in order to define the final section hydrographs for the entire study period we used the hydrometers data exclusively for low water discharge conditions ($q_w < 30$ m^3 s^{-1}). For higher flow conditions, we used the location-specific empirical relationships derived between local water-stages evidence (i.e. maximum levels obtained by trash-lines) and corresponding discharge data at Marano dam through simple regression analysis (Figure 5). Based on local water levels (time resolution= 30 minutes) and grain size distribution, the local instantaneous τ^* shows a broad variability, being higher at locations were sediments are finer (i.e. secondary

channel and bar) and lower were bed material is coarser (i.e. main channel) (Figure 6a, b, c).

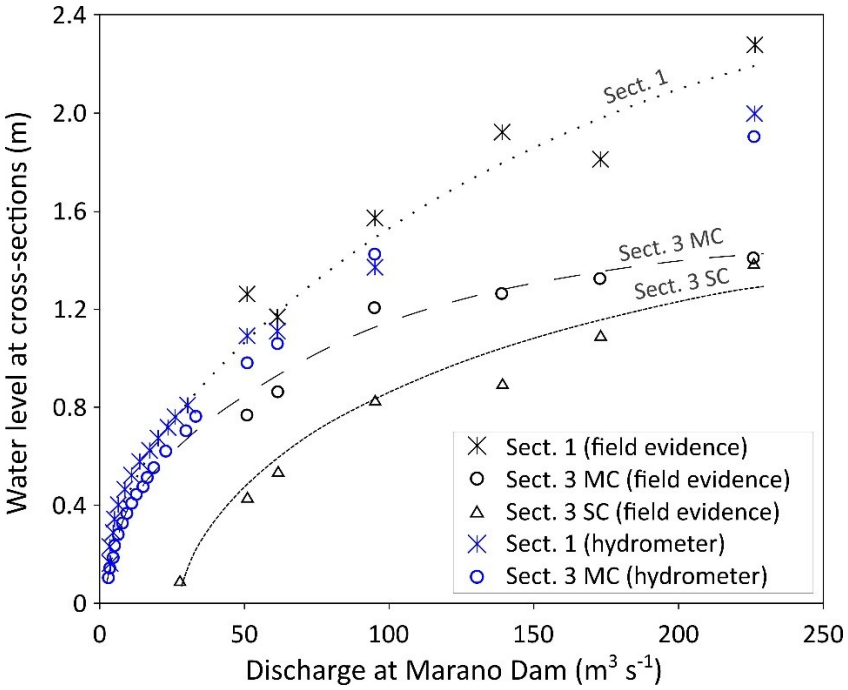

Figure 5. The maximum water level (i.e. water stage at the deepest point of the considered section or section-part. MC: main channel; SC: secondary channel) as a function of discharge at different locations. Data are distinct based on location (section 1 and section 3) and measuring method (hydrometers data and field evidences). The three final relationships ($h_w^{sect.1}$= -0.00003$(q_w)^2$+0.0156(q_w)+0.30, R^2= 0.89; $h_w^{sect.3MC}$= -0.00002$(q_w)^2$+0.0095(q_w)+0.40, R^2= 0.94; $h_w^{sect.3SC}$= 0.00457(q_w)+0.32, R^2= 0.92) adopted to determine the instantaneous local water stages from water discharge data (q_w) are plotted as well. Trash line elevations have an error of ±0.02 m due to instrumental accuracy.

3.1.3 Assessment of the proportion of the bed entrained

Considering the data derived from the painted areas under partial transport conditions, we related through simple regressions the calculated fraction of mobilized streambed material (Y) with the τ^*_{max} experienced by the study site during the event. Y tends to increase with the tractive forces active on the bed. Separately considering data collected from sections 1-2 and 3-4, the best-fit regressions, characterized by different trends (Figure 7a), give logarithmic equations:

$$Y^{1\text{-}2} = 4.10+1.04\log(\tau^*) \qquad (R^2= 0.93, \text{Conf. Limit}= 0.08) \qquad (7)$$

$$Y^{3\text{-}4} = 4.16+0.97\log(\tau^*) \qquad (R^2= 0.82, \text{Conf. Limit}= 0.11) \qquad (8)$$

Equations (7) and (8), respectively referring to upstream and downstream sections, have been employed to calculate the local and instantaneous percentage of activated streambed at section locations experiencing partial transport condition (Figure 6d). Confidence limit refers to the 95% limit on the regression slope.

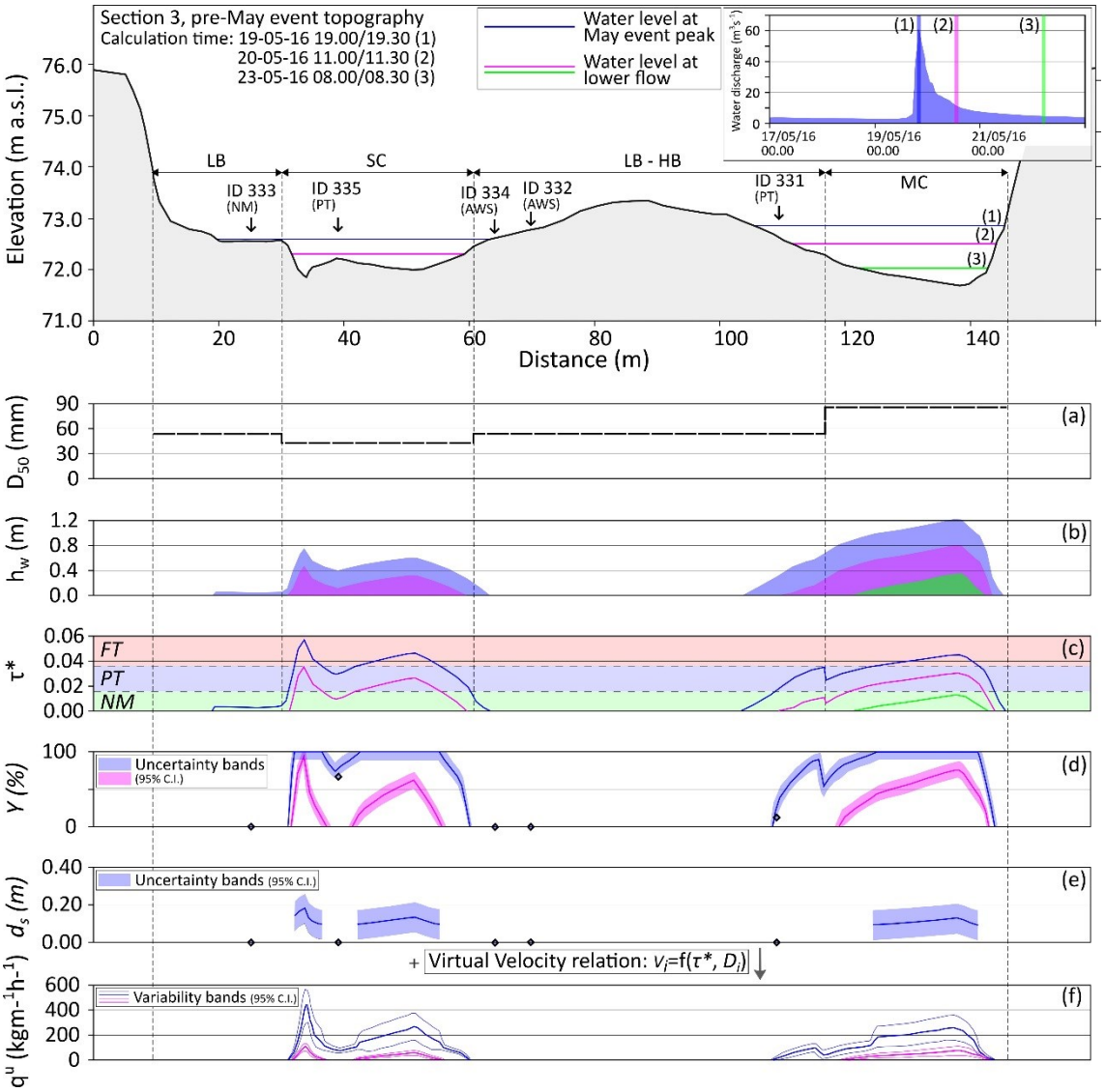

Figure 6. Example of input data (section topography, a, b), instantaneous and local calculation of parameters involved in the estimation (c, d, e) (uncertainty bands in (d) and (e) derive from the confidence intervals reported in Figure 7 and relative equations) and instantaneous-local and section estimated transport (f). Three time intervals of the May event at section 3 are considered. Lines in lower plots refer to values calculated from the derived empirical relations applying configuration 6. Pre-event topography is considered: the five study sites (i.e. painted areas with PIT tags and scour chains) installed along section 3 before this event are plotted in the section scheme and the punctual field monitored parameters (Y, d_s) are indicated with diamonds.

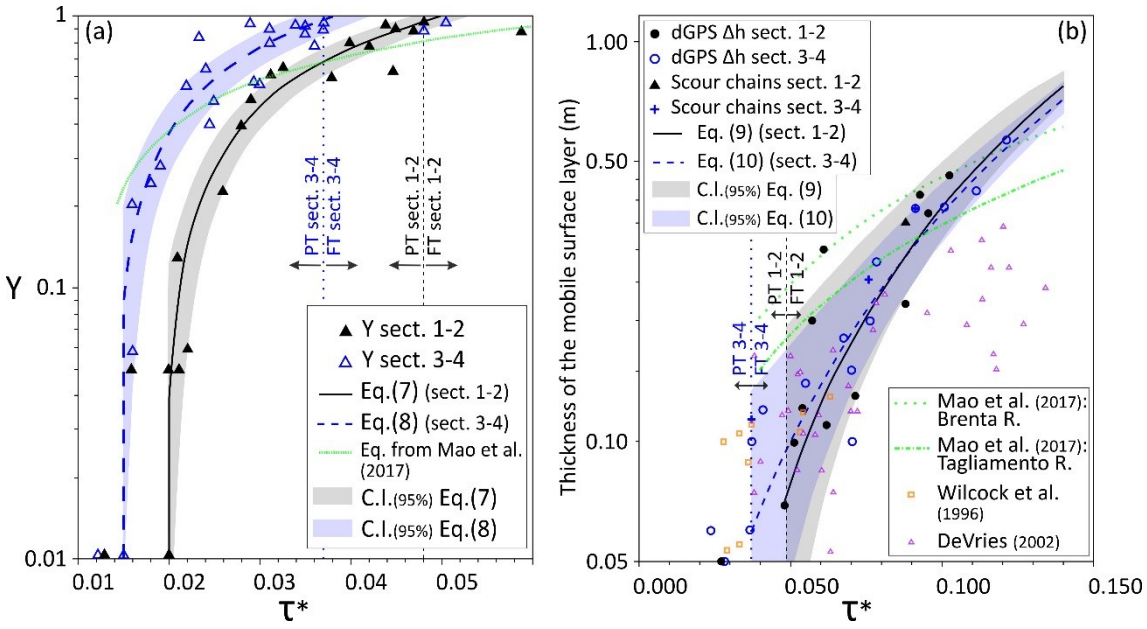

Figure 7. Measured percentage of mobilized streambed (a) and mobile surface layer thickness (b) as a function of dimensionless shear stress. Data are divided on the base of location (sections 1-2 in black and 3-4 in blue) and type of survey (i.e. topographic survey and scour chains). Obtained regression relations are plotted with their confidence limits. For comparison, in (a) the relation between percentage of mobilized streambed and dimensionless shear stress obtained by Mao et al. (2017) considering their whole dataset is plotted as well. In (b) the relations between mobile surface layer thickness and dimensionless shear stress obtained by Mao et al. (2017) for Brenta and Tagliamento rivers and the data collected by Wilcock et al. (1996) and by DeVries (2002) are plotted as well.

3.1.4 Estimate of the active layer thickness

The event active layer thickness is the maximum depth of sediment mobilized during an event (Church and Haschenburger, 2017). We related through simple regressions the maximum measurable erosion or deposition thickness (also in case of two-phase process) with the τ^*_{max}. Only 4 out of 28 installed event-scour chains provided reliable estimate of the active layer thickness due to some technical issues (e.g. complete chain removal caused by lateral erosion or tear). Plotting chains data with those collected by topographic surveys (27 measurements) it turned out that the two techniques provided quite comparable results (Figure 7b). For this reason, we decided to fit jointly chains and elevation changes data, elaborating separately data collected from sections 1-2 and 3-4. The best-fit regressions follow the squared-x models:

$$d_s^{1\text{-}2} = -0.021+40.3(\tau^*)^2 \qquad (R^2= 0.74, \text{Conf. Limit}= 0.09 \text{ m}) \qquad (9)$$

$$d_s^{3\text{-}4} = 0.011+35.7(\tau^*)^2 \qquad (R^2= 0.83, \text{Conf. Limit}= 0.06 \text{ m}) \qquad (10)$$

Equation (9) and equation (10), respectively referring to upstream and downstream sections, have been employed to calculate the local and instantaneous mobile surface layer thickness (Church and Haschenburger, 2017) at section locations experiencing full transport condition (Figure 6e). Confidence limit refers to the 95% limit on the regression slope.

3.1.5 Estimate of travel distances

Our travel distance data refer to "unconstrained-stone conditions" since we considered the first displacements after tracer seeding for both employed tracers types which start from the bed surface. Painted clasts mobilized from study ranged from 2 to 170 mm in size (but we considered only particles coarser than 6 mm), while those with PITs ranged from 28 to 165 mm. We analyzed the collected data in terms of travelled distances, grain size, τ^*_{max} active on the source study site and tracer type (Figure 8). For low to medium τ^*_{max} (<0.04), painted particles displacement lengths do not show statistically significant differences with those provided by PITs (Figure 8a, b, c). For high τ^*_{max} values, leading to full transport condition, the number of collected painted clasts decreases. Where some clasts were found (Figure 8d), PITs based distances seem to be about 35% higher. For very high values of τ^*_{max} the collected data came almost exclusively from PITs (Figure 8e, f). The number of tracers collected in relation to moderate transport conditions is around 100-300 clasts for study site (with a maximum of 494 for one study site) predominantly coming from painted clasts, while for high τ^* values the recovered tracers range between 6 and 40. Overall 4991 moved painted particles were collected. Considering the number of clasts colored at each painted area and the calculated study sites Y, we estimated a total value of about 18,000 moved painted particles from the 77 study sites interested by transport (47% of the 38,000 colored grains). The average painted clasts recovery rate is about 28%, but, referring to the single study sites, it varies from 0 (intense transport, e.g. site 441, figure 8f) to about 100% (low transport, e.g. site 242, figure 8a). Overall 467 PIT tagged clasts were entrained (52% of the 898 seeded PITs) and 401 were recovered both at the surface or buried (71 PITs, at a depth variable between few centimeters and 0.45 m, in agreement with the estimate of the active layer thickness). The PITs recovery rate after a single displacement is close to 100% for partial transport conditions and commonly more than 80% for very intense full transport conditions.

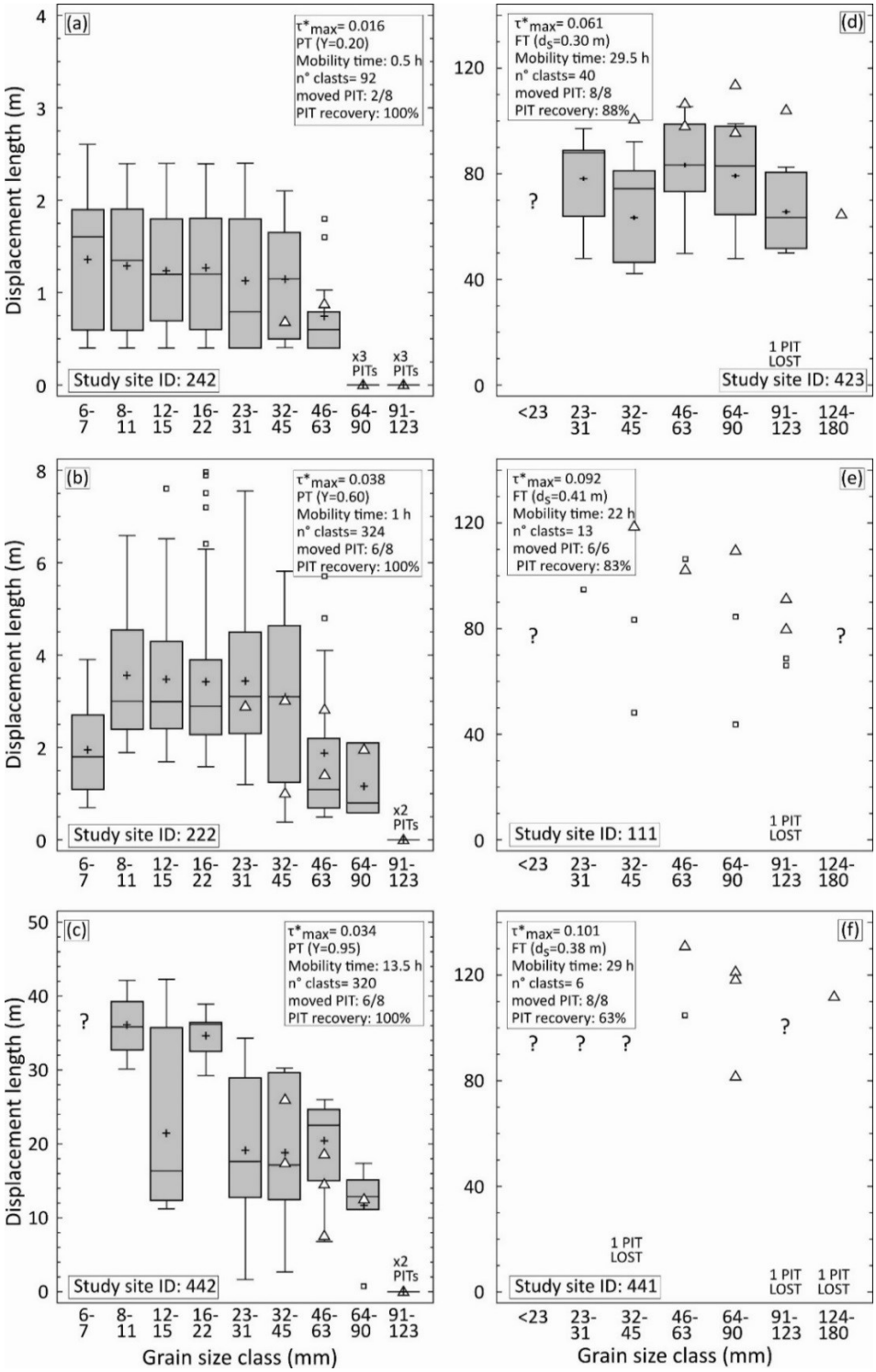

Figure 8. Ranges of tracers displacement lengths. Six study sites characterized by different maximum dimensionless shear stress and mobility conditions are shown. Data are divided in grain size classes. Boxes and small squares refer to painted clasts while triangles to PITs. Question marks mean that no tracers were found for a specific size class. Knowing the exact number of PIT tags installed and entrained at each site, it is possible also to indicate the number of PITs moved but not recovered (i.e. PIT lost).

3.2 Computation of parameters

3.2.1 Sediment mobility: defining thresholds between mobility conditions

Considering the 117 sites installed along the four cross-sections (Figure 3), 15% of the sites were at elevations that were not flooded by the monitored events, 19% experienced no motion conditions, 43% and 23% were in partial and full transport conditions, respectively. The collected data were analyzed considering the τ^*_{max} experienced by a painted area through one-way analysis of variance (ANOVA), to define thresholds in terms of τ^* between mobility conditions. As a first step the whole dataset was considered, showing that the three mobility classes were statistically different (ANOVA, p-value <0.002), but characterized by a significant overlap (Figure 9a).

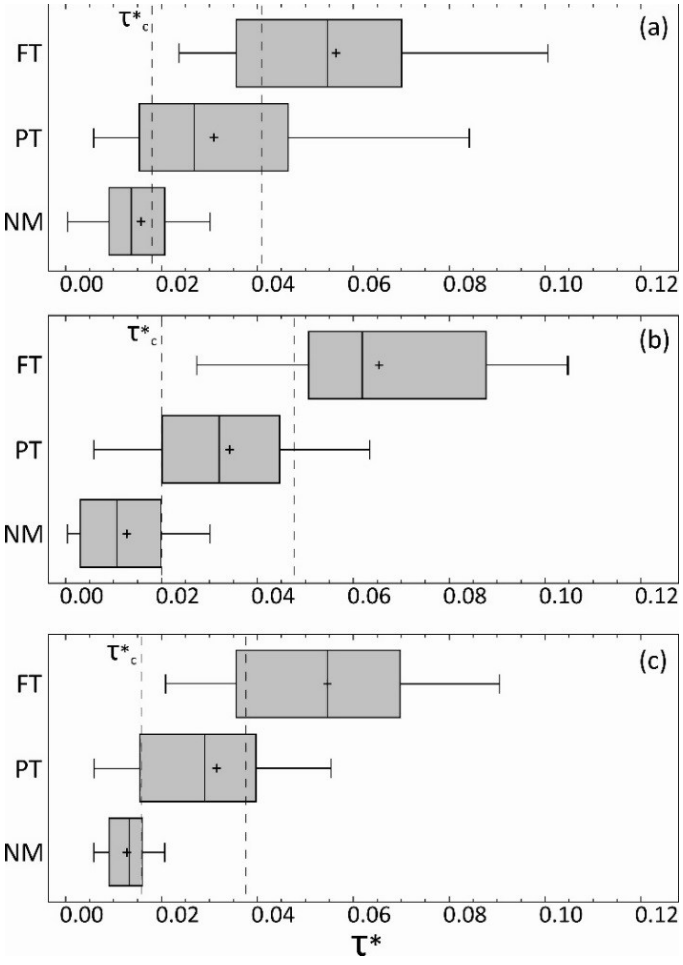

Figure 9. Ranges of the maximum dimensionless shear stress acting over the painted areas inducing different sediment mobility conditions (NM: no motion; PT: partial transport; FT: full transport). Boxes ends represent the 25th and 75th percentiles while whiskers ends are the 10th and 90th percentiles. Crosses indicate the mean values and lines indicate the median values. Plot (a) refers to the whole dataset, plot (b) to sections 1-2 and plot (c) to sections 3-4. The thresholds between

different mobility conditions (indicated by dashed lines) vary considering the three analyzed datasets. Critical shear stress (τ^*_c) refers to the passage from NM to PT condition.

Then, considering two subsets, with data collected respectively at sections 1 and 2 (Figure 9b) and sections 3 and 4 (Figure 9c), we obtained strongly different classes (ANOVA, p-values <0.001 in both analyses). Being the probability density functions of mobility classes symmetrical and characterized by the same shape, to define the local thresholds of τ^* able to induce different mobility conditions we decided to use the median value between the 75th percentile of the lower mobility class and the 25th percentile of the upper mobility class distributions. Using the two subsets, local thresholds were defined: full transport occurs at τ^* higher than 0.048 and 0.037, respectively for upstream and downstream sections; partial transport occurs at τ^* between 0.020 (τ^*_c) and 0.048 and 0.015 (τ^*_c) and 0.037, respectively for 1-2 and 3-4 sections. Local mobility thresholds have been employed in order to determine the processes active along sections in function of the local and instantaneous τ^* (Figure 6c).

3.2.2 Virtual velocity

Using the 30 minutes bed-acting τ^* data and the defined local mobility-thresholds, we were able to calculate the time of movement for each study site (in hours). We used a combination of painted and PIT-tagged clasts displacement-length data in order to calculate mean travel distances (in m) for each of the defined 11 particles size-classes for each site during a competent event. Virtual velocity (in mh^{-1}) was derived dividing the mean displacement length by the mobility duration, determined as the total time for which the τ^* active on the study site was larger than that needed to initiate clast movement (i.e. $\tau^* > \tau^*_c$) (local competent flow duration during a flood, e.g. as in Haschenburger and Church (1998)). Considering 77 sites and 11 size-classes, we would potentially have had a total of 847 data relating virtual velocity to grain size and τ^*_{max}. Actually, for several size-classes we did not have displacement lengths: we used 268 inputs (127 and 141 respectively from sections 1-2 and 3-4) in order to apply multiple regression analysis between V_i, D_i and τ^*_{max} distinguishing upstream and downstream sections data (S.E. is the Standard Error of the regressions):

$$V_i^{1\text{-}2} = 0.64 - 15.07 D_i + 44.98 \tau^* \quad (R^2 = 0.49, \text{estimate S.E.} = 1.27 \text{ m h}^{-1}, \text{p-value} < 0.05) \quad (11)$$

$$V_i^{3\text{-}4} = 1.76 - 16.65 D_i + 32.23 \tau^* \quad (R^2 = 0.48, \text{estimate S.E.} = 0.78 \text{ m h}^{-1}, \text{p-value} < 0.05) \quad (12)$$

Empirical equations (11) and (12), showing that virtual velocity (in mh^{-1}) has direct and inverse relations with τ^* and grains size (D_i) respectively, have been employed to calculated the specific virtual velocity of each grain-size class moved during a transport event at a specific channel location and time interval.

3.3 Bed material fluxes

3.3.1 Temporal and spatial flux variability

Considering the derived local empirical relations between τ^* and the parameters, we used Wilcock's equations (1997) to determine bed material transport rating curves. Using the six local surface grain size curves (Figure 4a) we applied equation (3) and then equation (6) to obtain six rating curves for the three considered morphological units (MC, B, SC), in the upstream (1-2) and downstream (3-4) sections (Figure 10).

The rating curves τ^*-q^u provide an estimation of local unit bed material transport (in kg $m^{-1}\,h^{-1}$) as a function of the local τ^* active on the bed. The six curves start in correspondence of the τ^*_c and are characterized by two sub-trends referring to partial transport and, above the PT-FT thresholds, to full transport conditions. Since the measured depth of the mobilized surface layer (Figure 7b) is commonly thinner than the observed armored surface depth (about 0.3-0.4 m) and due to the results obtained about the persistence of the armor layer during competent flows (Wilcock and DeTemple, 2005), we considered the surface grain size distributions also for the elaboration of the full transport range rating-curves. Considering local and instantaneous τ^* active on the bed (Figure 6c), we determined the instantaneous-section bed material load as the sum of the unit bed material transports (1 m-wide, 30 minutes) along the whole section, determined using τ^*-q^u specific for section and morpho-unit (Figure 6f). The event-section bed material load was determined as the sum of the instantaneous-section bed material loads calculated for the entire duration of the transport event.

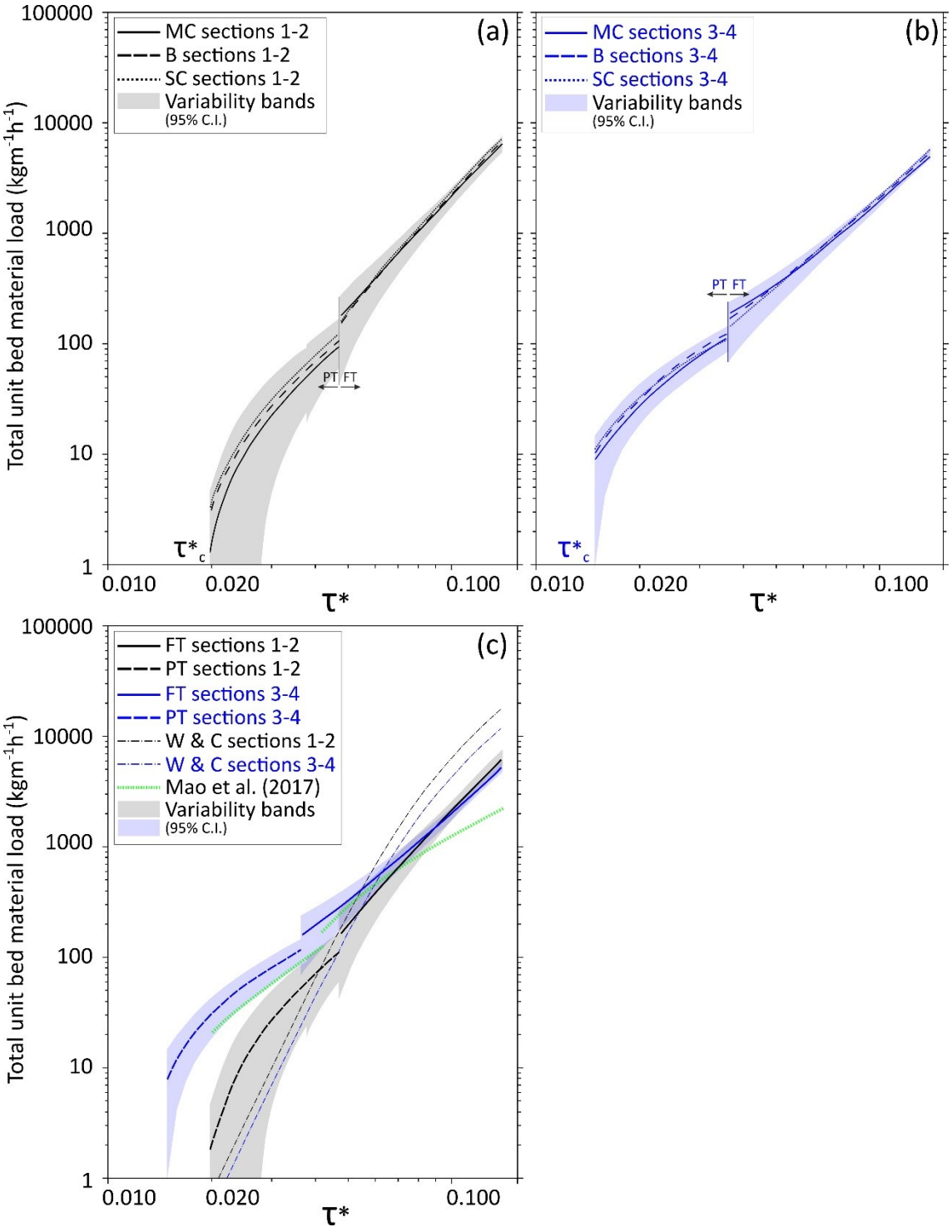

Figure 10. Section and morphological-unit specific sediment transport rating-curves obtained from virtual velocity approach application as a function of the dimensionless shear stress. Black lines in (a) refer to sections 1-2 and blue lines in (b) refer to sections 3-4, and each line-type refer to a specific morphological unit (MC: main channel; SC: secondary channel; B: bar). Each curve has its variability band (95% of confidence intervals) but for graphical reasons they are shown together for sections 1-2 and 3-4 curves. In (c) are reported the two mean τ^*-q^u relations for both sites (derived considering

one average grain size distribution curve for sections 1-2 and for sections 3-4) differentiating the parts of curves in partial transport (PT) and in full transport (FT). Rating curves resulting from Wilcock and Crowe (2003) formula (W&C) (i.e. considering a specific mean grain size distribution curve for sections 1-2 and for sections 3-4) and rating curve obtained by Mao et al., (2017) using a virtual velocity approach from Brenta and Tagliamento data are plotted as well in (c).

3.3.2 Uncertainties and natural variability in sediment transport

Due to several sedimentological (e.g. surface material packing and structure) and morphodynamic (e.g. sediment supply, fluvial-unit dynamics) reasons, local-unit bed material load can be very different responding to a given τ^* (Cudden and Hoey, 2003). The τ^*-q^u curves were developed starting from empirical relations based on field data (Y, d_s, V_i) collected from study sites located at different morphological units, under different morphodynamic transport conditions and subjected to the natural variability of local sediments mobilization mechanisms which ultimately produced data scattering. For these reasons, empirical equations are coupled with uncertainty bands determined using the confidence limits of regressions (Figures 6d, 6e, 7 and 8). Propagating the three sources of uncertainty (i.e. Y, d_s, V_i) through the general rule for multiplied quantities (i.e. adding in quadrature Y confidence limit and V_i standard error for partial transport; d_s confidence limit and V_i standard error for full transport) for each τ^* value, we determined the variability bands of the τ^*-q^u curves (Figure 10). Using the τ^*-q^u curves and the variability bands, for each local and instantaneous τ^* value considered in our calculations, we determined the mean, the maximum and the minimum associated q^u (Figure 6f). Integrating those values on the whole section, the corresponding instantaneous-section transport values were determined. The same operation allowed the calculation of the mean, maximum and minimum event-section transport values integrating the instantaneous-section fluxes (mean, maximum and minimum) over the hydrograph trend and finally to determine the variability (i.e. ±) associated with each estimate.

3.3.3 Transport estimate using different data input configurations

We tested the virtual velocity approach at two morphologically different sections (sections 1, sinuous with alternate bars, and 3, wandering; see figure 3) and for two events of different magnitude (May 2016 - RI< 1 year and November 2016 - RI= 2.1 year; see figure 2b). All calculations were carried out using rating curves derived for specific locations (i.e. considering separately data collected from sections 1-2 and 3-4 and relative empirical relations) but they can be applied to a sediment transport calculation according to different

input factors configurations. The estimates have been performed considering seven configurations (tables 1 and 2). Through configuration 1 we applied the virtual velocity bed material load calculation adopting the simplest setting. Configurations 2, 3, 4 introduce improving factors one at a time. Configuration 2 considers different water stages along the cross-section, which may have significant implications if there are secondary channels (Figure 5). Configuration 3 introduces different D_{50} to calculate the τ^* active on different morphological units within the same section (Figures 6a and 6c). Configuration 4 includes possible section topographical variations taking place during the flood event (Figure 3). Configuration 5 is a combination of settings 2 and 3. The first five input settings use only two mean τ^*-q^u rating curves derived considering one average grain size distribution curve for sections 1-2 and sections 3-4 (Figure 10c), whereas configuration 6 considers the six τ^*-q^u rating curves derived for specific morphological units (Figures 10a and 10b). Finally, configuration 7 incorporates the four factors considered for this sensitivity analysis (Table 1). Configuration settings were designed in order to evaluate the impact of single selected factors and the effects of some of their possible combinations.

Event bed material transport estimates are presented as volume of moved material through a section during a competent flux with an uncertainty determined through the variability estimation procedure applied for each calculation and configuration. In order to convert the original results calculated in kg to sediment volume (in m^3), we considered sediment porosity equal to 0.25 (not defined in the field due to the measure difficulties) as suggested for alluvial gravels by Carling and Reader (1982) and adopted in previous studies carried out for similar channel material (e.g. Martin and Church, 1995; Surian and Cisotto, 2007). At section 1 transport estimates vary from 64±44 m^3 (configuration 1) to 3±3 m^3 (configuration 7) and from 614±158 m^3 (configuration 1) to 158±74 m^3 (configuration 7) respectively for May and November 2016 events (Table 2).

Input factors configuration			*May 2016 event*		*November 2016 event*	
			Section		*Section*	
			1	*3*	*1*	*3*
Conf. 1	Water level: section averaged Grain size: averaged Event-section topography: constant	q_{bed}^{tot} (m^3) Uncertainty % PT	64 ±44 72%	533 ±189 59%	614 ±158 6%	1479 ±339 10%
Conf. 2	Water level: spatial variable in section Grain size: averaged Event-section topography: constant	q_{bed}^{tot} (m^3) Uncertainty % PT	64 ±44 72%	449 ±157 59%	614 ±158 6%	1154 ±266 10%
Conf. 3	Water level: section averaged Grain size: variable ($D_{50}^{unit} \rightarrow \tau^*$) Event-section topography: constant	q_{bed}^{tot} (m^3) Uncertainty % PT	<u>4</u> <u>±3</u> <u>100%</u>	256 ±96 65%	<u>160</u> <u>±72</u> <u>14%</u>	1130 ±267 10%
Conf. 4	Water level: section averaged Grain size: averaged Event-section topography: changing in time	q_{bed}^{tot} (m^3) Uncertainty % PT	64 ±44 72%	No Data	617 ±160 5%	1761 ±448 8%
Conf. 5	Water level: spatial variable in section Grain size: variable ($D_{50}^{unit} \rightarrow \tau^*$) Event-section topography: constant	q_{bed}^{tot} (m^3) Uncertainty % PT	4 ±3 100%	<u>114</u> <u>±45</u> <u>85%</u>	160 ±72 14%	650 ±178 13%
Conf. 6	Water level: spatial variable in section Grain size: variable ($D_{50}^{unit} \rightarrow \tau^*$; q^u- τ^*) Event-section topography: constant	q_{bed}^{tot} (m^3) Uncertainty % PT	3 ±3 100%	**107** **±54** **84%**	156 ±73 13%	653 ±186 13%
Conf. 7	Water level: spatial variable in section Grain size: variable ($D_{50}^{unit} \rightarrow \tau^*$; q^u- τ^*) Event-section topography: changing in time	q_{bed}^{tot} (m^3) Uncertainty % PT	**3** **±3** **100%**	No Data	**158** **±74** **13%**	**<u>746</u>** **<u>±230</u>** **<u>19%</u>**

Table 2. Bed material flux estimates obtained using seven configurations of the virtual velocity approach. Estimate variability and partial transport contribution are reported. Bold numbers refer to the most complete configurations applicable for the specific calculation, whereas underlined numbers refer to the simplest configurations that could be appropriate to estimate the transport for the specific section and event (see also figure 12).

At section 3, configuration 1 transport estimates (533±193 m^3 and 1479±339 m^3 respectively for May and November events) decrease significantly considering variable water level and grain sizes (configurations 2 and 3). Due to prevailing erosion during

November event at this section, estimate of sediment flux increases using configuration 4. Conversely, configurations 5 and 6 provide almost identical estimations which are notably lower than the previous ones. Using configuration 7, estimates are equal to 107±54 m^3 and 746±230 m^3 respectively for May and November events. Finally, we were able to distinguish the contribution of partial transport and full transport to the total bed material load estimates (Table 2). Ratio PT/FT depends on the event intensity (lower ratios for more intense events) and section morphology (lower for section 3 were the mobility thresholds are in general lower) but also by the adopted configuration. It is possible to observe a decrease of FT contribution moving from the simplest to the more complex configurations. The estimates variability vary depending on the predominant transport condition that occurred during the considered event. For events characterized by predominant full transport contribution (PT/FT<50%), uncertainty ranges around 25-40% (considering all configurations), whereas increasing up to 50% for calculation characterized by predominant partial transport contribution.

Configurations results, also considering the variability ranges, turn out to be significantly different, at least considering the simplest (i.e. configuration 1) and the most complete input factors settings (i.e. configurations 6 and 7) with values differ by factors between 2 (November event, section 3) and 20 (May event, section 1). These significant differences can be recognized from the section bed material load curves and their variability bands (Figure 11). The estimates obtained for section 3 were analyzed considering also the time distribution of transport along the whole section (i.e. instantaneous-section transport, Figures 11a and 11c). Focusing on the decreasing event tails (Figures 11b and 11d), configuration 1 provides the longest active transport estimation. For the November event, competent flow duration of configuration 7 is longer than that of configuration 6, due to channel incision, although both are shorter than configuration 1. The "actual instantaneous-section transport" is likely to be high variable (Ashmore, 1985, 2013) but since it should fluctuate around the estimate curves (Figure 11b), the transport estimates at event time-scale (i.e. the section-event transport) should not be affected by such fluctuations.

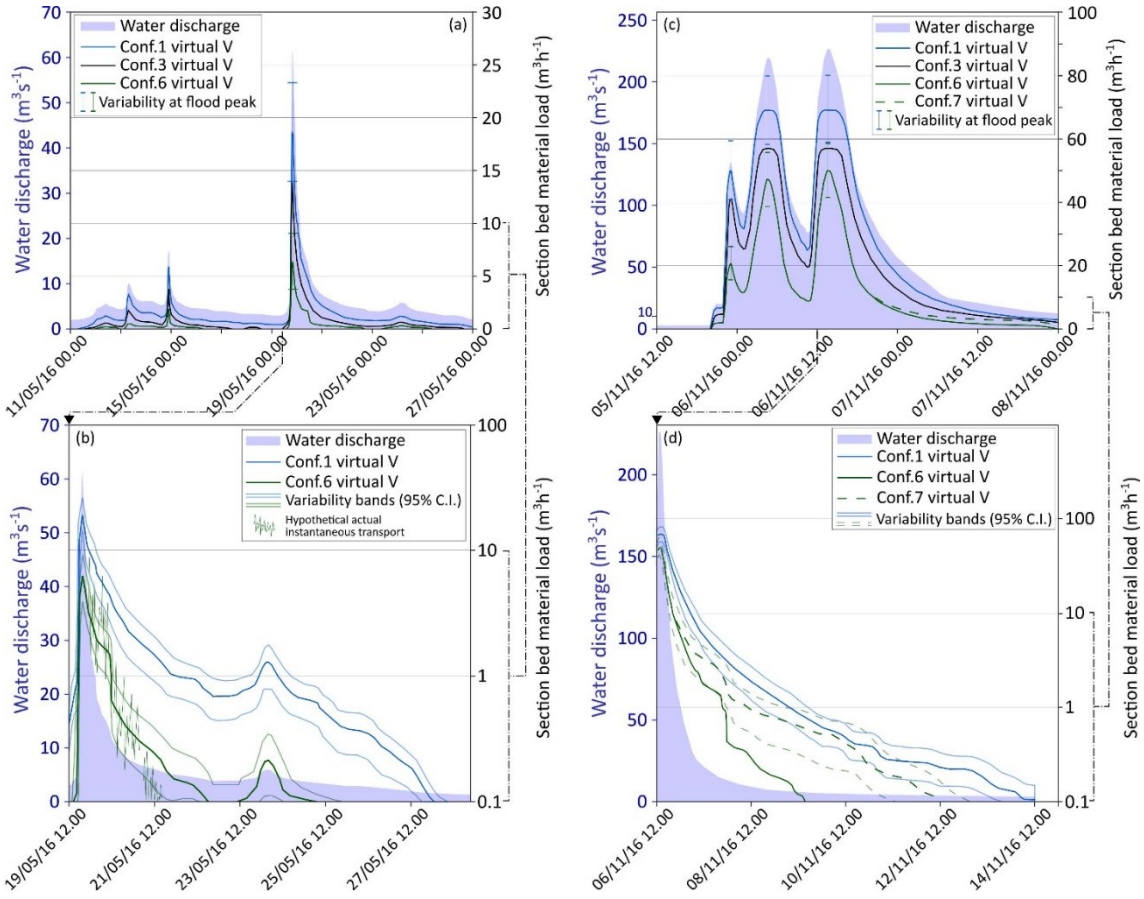

Figure 11. The timing of bed material load in function of water flow at section 3. The curves refer to the bed material transport occurring within the whole section considering different configurations. Plots (a) and (c) refer to the entire May and November events while plots (b) and (d) focus on the event tails. Significant differences about section-transports over the time are obtained applying alternative configurations ((a) and (c)). The water fluxes become competent about at the same time but, due to the low decreasing gradient of the flood tail, strong differences in the end of transport process occur among different configurations ((b) and (d)).

4. Discussion

4.1 Methodological improvements

The virtual velocity approach is a "hybrid estimation method" based on a theoretical framework and substantial field-data collection. Bed material load is characterized by high variations in rate at local spatial scale (Clayton and Pitlick, 2007; Ryan and Dixon, 2007) due to differences in channel material characteristics (e.g. armoring, structure etc.) and sediment supply. For this reason, identifying an appropriate spatial scale for collecting and analyzing field-data represents a crucial point to apply this approach. Considering data from the Parma River, it is worth noting that all the field-collected parameters are characterized

by non-uniformity at the study area scale (i.e. significant differences between field-parameters determined for sections 1-2 and sections 3-4, see Figures (7), (9) and (10)). τ^* processes thresholds are different considering the whole dataset or sub-datasets and statistically different empirical relations have been obtained distinguishing data collected from upstream and downstream sections. The two couples of cross-sections are located within two distinct reaches (sensu Brierley and Fryirs, 2013), different in terms of morphology, width and channel sediments (Figure 1). Our results suggest that the reach, which is homogeneous in terms of morphology and hydraulic characteristics (Grabowski et. al, 2014), should represent the best scale for field-data processing (i.e. definition of the empirical relations between τ^* and the calculation parameters). Differently from Mao et al. (2017), which elaborated jointly data collected at different locations (two rivers and four reaches), empirical relations and rating curves derived in this study could be considered as "reach-specific relations". We observed uniformity within subset of data collected from sections 1-2 (upstream reach) and sections 3-4 (downstream reach) with a variable internal data-scattering (e.g. Figures (7) and (8)) due to the variability of sediment transport mechanisms at local scale. Considering this internal variability (described also by Ferguson (2003)), we were able to define uncertainties bands for empirical relations and rating curves and, ultimately, determining variability of transport estimates. The calculated unit bed material loads and section-fluxes can differ from the actual instantaneous transport (Figure 11b), characterized by variability also under constant water discharge (Ashmore, 1988, 2013), but our estimates and associated uncertainties represent the mean transport values under determined conditions, having been derived from study sites experiencing various morphodynamic processes, providing reliable transport values at the section spatial-scale and transport event time-scale.

For the virtual velocity empirical relations, it is crucial to determine the particle displacement lengths. Collecting reliable grain travel distances is in turn crucial for achieving sound transport estimates. Most of the previous studies aimed at estimating the bed material transport using a virtual velocity approach employed one tracer type at time (e.g. Liebault and Laronne (2008), Milan (2013) and Mao et al. (2017) seeded only painted clasts; Haschenburger and Church (1998) seeded magnetically tagged stones). Few studies (e.g. Vázquez-Tarrío and Menéndez-Duarte, 2014) combined magnetic and painted tracers for estimating the transport rate coarse bed streams. As previously done by Lobera et al. (2017) aiming at assessing different bed mobility patterns in gravel-bed rivers, for the first time we used in combination data provided by painted clasts and PIT tags for defining the

relations between τ^*, grain size and the virtual velocity. Our results confirm that PITs recovery rates are high (>80%) for all mobility conditions (Chapuis et al., 2014), whereas painted clasts recovery is broadly variable (i.e. from 0% to 100%) in relation with transport magnitude (in accordance with Hassan and Church (1992) and Hassan and Roy (2016)). PIT data, although less in number if compared with those obtained from painted clasts, can be assumed to represent the real distances traveled by grains due to their excellent technical performances allowing to recover also tagged clasts which, starting from the bed surface, are buried during the first displacement. As shown in figure 8, for low mobility condition painted clasts and PITs gave similar travel distances, whereas for high mobility (i.e. intense full transport as in figure 8e and 8f) only PITs provided data. From these observations it is possible to conclude that jointly processing displacement length data collected using the two tracer types (considering only tracers which start from the bed surface) does not lead to errors since data are homogeneous when both tracers are present or come mainly from a single type (PITs) in response to intense transport. Painted clast tracers are able to provide a large amount of data regarding all grain sizes in response to low-moderate transport conditions whereas PIT tags provide data, limited in number and in grain size by installation constraints, for all transport conditions giving key information about intense transport processes and validating painted clasts data. In order to perform a sound surface-grain travel distances monitoring, we suggest to jointly employ painted clasts and PIT tags considering data homogeneity and complementary information provided by the two tracer types.

4.2 Calculation parameters: comparisons with previous field studies

For evaluating the reliability of the derived empirical relations between the calculation-parameters (i.e. mobility conditions, Y, d_s and V_i) and the τ^*, we compared our data with those collected in other gravel-bed rivers using similar field techniques. The lack of independent data to control the quality of our estimates makes this comparison particularly useful for supporting the following results carried out by the virtual velocity approach. Relations between τ^* and Y (equations (7) and (8)) are in the same range of the equation obtained by Mao et al. (2017) (Figure 7a). The thickness of the active layer (equations (9) and (10)) is comparable with that observed in other studies (see Figure 7b), although at high τ^* (>0.11) our relations suggest the establishment of a thicker active layer. Finally, the unit bed material load curves show a weaker increase with τ^* than the Wilcock and Crowe (2003) equation whereas the rate of increase appears to be somewhat larger than in the study by Mao et al. (2017) for higher dimensionless shear stresses (>0.08) (Figure 10c). The

steepness of transport rating curves can be quite variable for different field sites (Schneider et al., 2015): in our case at high τ^* the active layer is quite thick, and this could explain the high unit-transport when the tractive forces acting on the bed became stronger. Considering that site-specific characteristics (e.g. sediments structure, armoring, fabric) control the local mobility of the streambed material, these comparisons support the reliability of our empirical relations and transport estimates.

4.3 Data configurations and role of different factors

In order to apply the virtual velocity approach at our real case study several factors have been considered through a series of input factor configurations (Table 1). As reported in Table 2, starting from the simplest model setting, estimated bed material transport tended to decrease progressively including factors leading to a more realistic description of channel processes. Comparing the simplest and the most complete configuration results, the obtained variations are significant also considering the natural variability of the transport processes expressed by the estimated uncertainties. This suggests that including some key factors is crucial in order to achieve reliable estimates. The variability of the estimates induced by the adoption of different configurations at specific sections and for specific events (from factor of 2 to factor of 20) is due to the local characteristics of the channel and to the effects induced by each application factor for different competent floods. Mao et al. (2017), using only a single configuration, did not analyze the importance of the application factors and the sensitivity of the method in response to them.

Focusing on the single factors and considering the estimated variations obtained for different configurations, insights on the role played by different application factors in the virtual velocity approach calculation have been obtained for the first time through a preliminary sensitivity analysis. Adopting water stages distinctly defined for specific channel units produced significant estimate variations (up to -22%) only for section 3, located in the wandering downstream reach. Section 1 estimates were not affected by this factor due to the local single-thread channel morphology (see figure 3). As confirmed from our water stage monitoring results (Figure 6), the assumption of a section-averaged water level represents a simplification, as water levels at a given discharge often differ between adjacent anabranches in multi-thread channels (e.g. Zolezzi et al., 2006). Increasing channel morphology complexity the in-section water stage variability becomes a crucial parameter in order to obtain reliable estimates of τ^*. Similar results about the impact of using width-

averaged or local calculation parameters (i.e. definition of the shear stress induced by the water flow) on the transport estimate results were also reported by Ferguson (2003).

The significant variations (between -24% and -94%) obtained introducing local morphological unit specific D_{50} to calculate the τ^* active on the streambed lead to consider sediments grain size as the most important factor influencing the approach application. Fernández and Garcia (2017) achieved similar results addressing a theoretical sensitivity assessment for two sediment transport relations and concluding that an accurate knowledge of sediment size has more impact on transport predictions than other input variables. The local grain size represents in fact a fundamental variable in the τ^* calculation (equation 4), determining the transport intensity induced by the water flow (see figure (10)). Section 1 estimates are strongly affected by this factor (variations up to -94%), in comparison to section 3 (variation up to -50%). This different response may be due to the higher armoring occurring in the main channel in the middle-upstream part of the study sector (section 1), suggesting that high grain size variations at cross-section scale (e.g. between main channel and bars) can strongly influence transport intensity and its estimation. Considering the high variability characterizing both longitudinally (Mosley and Tindale, 1985; Rice and Church, 1998; Surian, 2002) and transversally (Rice and Church, 2010) the streambed material grain sizes in gravel-bed rivers and the occurrence of armoring conditions (Hassan et al., 2006), an accurate description of this variable is strongly demanded. Combining water stages distinctly defined for channel zones and morphological unit specific D_{50} (see configuration 5 in Table 2), the obtained estimate variations (between -56% and - 94%) confirm the crucial role of these factors.

The last factor considered in this work are topographic variations occurring at a given cross-section during a transporting event. When only partial transport occurred, section topography did not experience elevation changes and, therefore, estimates were not influenced by this factor. For events inducing full transport, the influence of this factor is strictly controlled by the elevation changes that occurred within the section and its positive or negative impact on estimates depends by the predominant erosional or depositional processes. During the November 2016 event both sections experienced intense full transport, but section 1 was in equilibrium (no change in mean section elevation, max erosion= -130 mm, max deposition= +85 mm) whereas section 3 underwent some incision (mean section elevation variation= -6 mm, max erosion= -280 mm, max deposition= +155 mm). Cross-section variations led to a small estimate increase for section 1 (+0.5%) and to a more significant variation (+19%) for section 3. Such results suggest that topographic

variations can affect estimates only for intense transport event and in reaches featuring disequilibrium conditions in sediment transport leading to erosion or aggradation of channel bed (Kondolf, 1997; Grant, 2012).

4.4 Limitations, wider implications and future perspectives for the virtual velocity approach

Reliable field data are essential for applying the virtual velocity approach but some methodological issues persist in data collection. One of the most difficult variables to monitor remains the active layer thickness: scour chains can provide few data and topographic surveys can lead to underestimation of the thickness due to scour and fill compensation over a single hydrograph (see Figure 7b). For these reasons, it would be desirable to test alternative solutions: some promising attempts were carried out by Nawa and Frissell (1993) using sliding-ball monitors and by DeVries et al. (2001) and Gendaszek et al. (2013) employing buried accelerometers. Haschenburger (1996, 2011) used the burial depth of tracers to describe the gravel vertical mixing, suggesting that some improvements in the active layer thickness parametrization could be achieved considering the buried PITs recovering depths.

Tractive forces active on the streambed lead most of the transport processes considered through this approach. Instead of just considering local hydrographs and cross-section topography, more sophisticated τ^* calculation could be applied using numerical hydraulic models (e.g. Booker et al., 2001; Bockelmann et al., 2004). To allow this calculation, digital terrain models and reliable hydrological data are required (Formann et al., 2007; Aggett and Wilson, 2009; Teng et al., 2017), coupled with detailed local grain size information. Considering the results recently achieved about the importance of the larger clasts in determining the mobility of the streambed material (MacKenzie at al., 2018), it could be useful to explore the use of different grain sizes instead of the commonly adopted D_{50} for τ^* calculation.

The clasts mobility-data considered in our work derive mainly from study sites installed in correspondence of bars and secondary channels due to the difficulties in installation and recovery of passive tracers within channel portions submerged during low-flow conditions (in fact 11 out of 117 study sites were installed within the main channel). It is likely that our empirical relations could be improved obtaining a better description of sediment dynamics within the main channel. This could be achieved by employing active tracers as in Cassel et al. (2017). From our water stage monitoring, some differences exist between hydrometers data and field water-level evidences (Figure 6). In order to obtain local hygrographs directly

using hydrometers data, monitoring techniques should be improved, for instance adopting non-intrusive sensors (e.g. down-looking sensors) which do not disturb the flow and do not require barometric compensation which represents a possible source of errors.

Other limitations affect the virtual velocity approach, being it a simplified hybrid estimation method. From our uncertainty analysis we partially considered the different morphodynamic processes active in the channel, but the bed morphology complexity, typical of large gravel-bed rivers, leads to non-uniformity of particle mobility dynamics (Marti and Bezzola, 2006; Recking et al., 2016). Calculating instantaneous and local τ^* some improvements have been achieved, but several issues persist, for instance in the calculation of the local competent flow duration as the above-critical τ^* period (e.g. as done by Haschenburger and Church (1998)), considering that the grains mobility can be influenced by the complex bed topography during the event (Church, 2006). Improvements could be achieved adopting the procedure recently developed by Klösch and Habersack (2018) to calculate unsteady virtual velocity from repeated surveys of tracer positions. Another virtual velocity calculation weakness is due to the exclusive use of tracers starting at the bed surface, which move more easily than the average grains in the active layer mobilized during full transport (Vázquez-Tarrío et al., 2018). As explained by Ferguson and Hoey (2002), if tracers are not fully mixed into the bed the calculated virtual velocity can be overestimated leading to full transport flux over-estimate with effects in particular for bed material load estimates of high-magnitude competent events. Some improvements will be possible considering long term tracers dispersion (e.g. Haschenburger, 2013b) and relation between morphology and tracers mobility (e.g. Papangelakis and Hassan, 2016; Vázquez-Tarrío et al., 2018).

This study has shown some strengths of the virtual velocity approach: it does not require data collection during transport events and it can be applied to wide rivers where alternatives are currently poorly available. The approach is applicable through the proposed transport calculation procedure to a broad spectrum of large gravel-bed rivers, adaptable to specific case-study features using both reach-specific empirical relations and case-specific application factors. The estimate variability obtained from different configurations suggest that the approach (i.e. field monitoring, data processing and transport estimate) requires to be designed according to case-specific aspects, because its sensitivity to different factors varies depending upon river reach features. Some methodological procedures (e.g. reach-specific relations and multiple tracers) remain valid for all contexts, whereas other methodological aspects should be designed according to

specific reach morphology, channel sediments and section stability over the time. With this in mind, we propose a decision tree describing the field measures and elaborations required to deal with the application factors which have an impact on transport estimate (Figure 12).

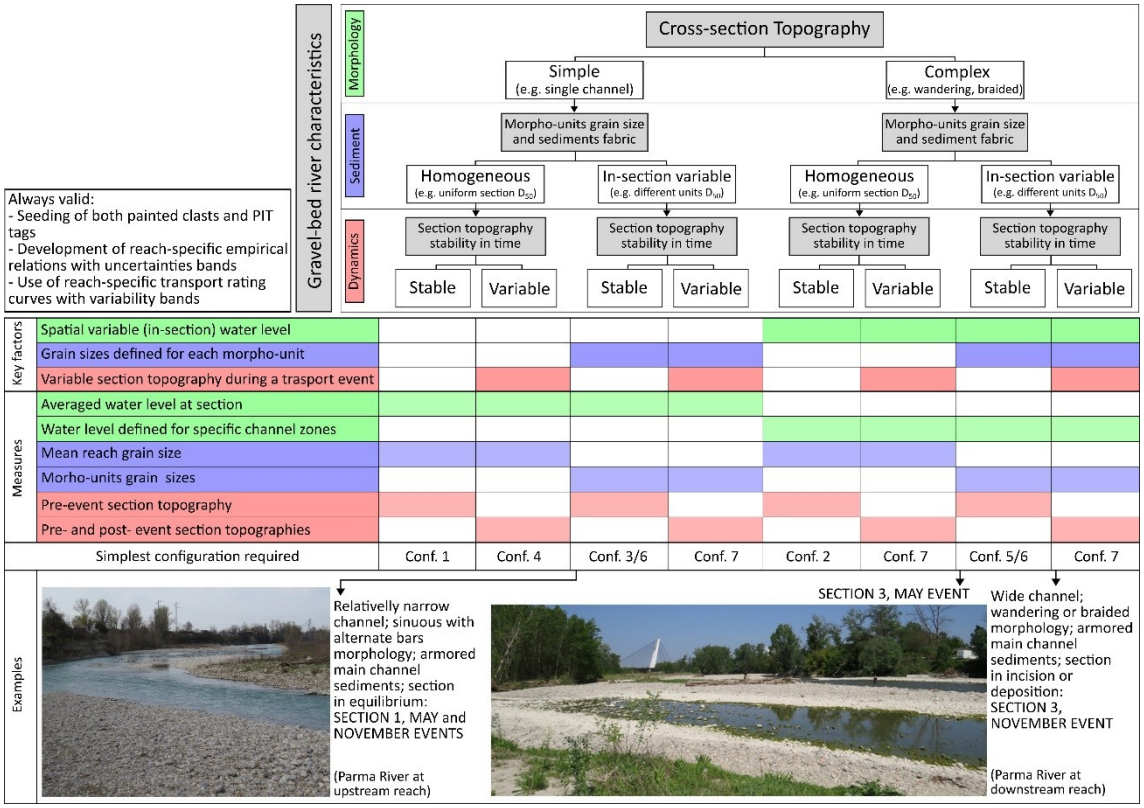

Figure 12. Decision tree for using the virtual velocity approach in different gravel-bed river contexts. Reach morphology and sediment characteristics usually can be assumed constant for the entire study-period, while section topography dynamics depends by both the reach equilibrium conditions and the intensity of the specific competent event. Most influencing application factors, required measures and simplest adequate configurations are reported for specific cases. Examples from this work are shown as well.

Looking at the different configurations estimates for the different sections and events (Table 2), it is possible to observe that in some cases, considering also the uncertainties, it is not essential to adopt the most complete configuration, but the required configuration in order to take in account for all the case-specific key factors can be a simpler one. For instance, at section 1, characterized by single-thread morphology and stable topography, only the in-section variable D_{50} represents a key factor (Figure 12): in fact, configurations 3 and 7 give very similar results (Table 2). On the contrary, all the factors (configuration 7) need to be included for a sound assessment of sediment transport at section 3 during the November 2017 event (Figure 12). The field monitoring and data elaboration efforts

strongly depend by the adopted input factor configuration. For this reason in figure 12 we reported the simplest required configuration to be adopted for some considered river contexts. Finally, we recognize that future applications should try expand the sensitivity analysis carried out in this work.

5. Conclusions

The work aimed to assess the virtual velocity approach strengths and limitations, in particular evaluating for the first time the significance of each factor that feed in the bed material transport calculation through a simplified sensitivity analysis. The main conclusions from this study are as follow.

(i) It is widely accepted that using theoretically-based formulas for estimating bed material transport can led to calculation errors (e.g. Barry et al, 2004; Fernández and Garcia, 2017) and other techniques are not currently used for large gravel-bed rivers (the morphological approach represents the only exception, although its application has some constrains). The virtual velocity approach provides an alternative to trapping techniques (difficult to employ in wide complex rivers) that incorporates some key factors of channel morphology and processes and it is strongly based on field data.

(ii) This work highlights some crucial issues of the monitoring activity in order to derive sound relationships between a set of calculation parameters and the leading variables. Adopting appropriate spatial scales for data collection and processing (i.e. reaches for empirical relationships and morphological units for grain size definition) and the jointly use of painted particles and PITs are two fundamental monitoring strategies for achieving reliable estimates of bed material transport.

(iii) Using simple data input configurations or more complex ones may lead to significant differences in transport estimates. On the other hand, in relation to channel morphodynamics, different factors (e.g. spatial variability of grain size; variability of water level within the cross-section; bed-level changes) play a key-role on transport processes. The proposed “decision tree” can be considered as a first attempt towards a more effective use of the virtual velocity approach to estimate bed material load in a broad spectrum of large gravel-bed rivers.

(iv) In this work we considered the natural transport processes variability evaluating the estimate uncertainties from field-data distributions. Future efforts should be addressed to consider more in detail the complex morphodynamics of large gravel-bed rivers, including a more realistic unsteady virtual velocity calculation and the influence of local morphology on tracers mobility.

Acknowledgements

The authors would like to thank: Silvano Pecora, Mauro Del Longo, Monica Branchi and Paolo Leoni from "Servizio Idro-Meteo-Clima" of Arpae Emilia-Romagna for providing hydrological and meteorological data and for their crucial support throughout the whole monitoring activity; Maria Laura Trento and Pietro Brenna for field assistance. The authors thank the associate editor and three reviewers of *Water Resources Research* for their comments and very helpful suggestions. Data supporting figures, relations and elaborations reported in this work can be found in the Supporting Information (Appendix 1).

References

Aggett, G. R., & Wilson, J. P. (2009). Creating and coupling a high-resolution DTM with a 1-D hydraulic model in a GIS for scenario-based assessment of avulsion hazard in a gravel-bed river. *Geomorphology, 113*(1), 21-34. https://doi.org/10.1016/j.geomorph.2009.06.034

Ashmore, P. E. (1985). Process and form in gravel braided streams: laboratory modelling and field observations, (Doctoral dissertation). Edmonton, Canada: University of Alberta.

Ashmore, P. E. (1988). Bed load transport in braided gravel-bed stream models. *Earth Surface Processes and Landforms*, *13*(8), 677-695. https://doi.org/10.1002/esp.3290130803

Ashmore, P. E. (2013). Morphology and dynamics of braided rivers. In J. F. Shroder (Ed.), *Treatise on Geomorphology*, *Vol. 9* (pp. 289-312). Amsterdam, Netherlands: Elsevier.

Ashmore, P. E., & Church, M. (1998). Sediment transport and river morphology: a paradigm for study. In P. C. Klingeman, R. L. Beschta, P. D. Komar, J. B. Bradley (Eds.), *Gravel-Bed Rivers in the Environment* (pp. 115-148). Highlands Ranch, CO: Water Resources Publications LLC

Barry, J. J., Buffington, J. M., & King, J. G. (2004). A general power equation for predicting bed load transport rates in gravel bed rivers. *Water Resources Research*, *40*(10). https://doi.org/10.1029/2004WR003190

Bockelmann, B. N., Fenrich, E. K., Lin, B., & Falconer, R. A. (2004). Development of an ecohydraulics model for stream and river restoration. *Ecological Engineering*, *22*(4), 227-235. https://doi.org/10.1016/j.ecoleng.2004.04.003

Booker, D. J., Sear, D. A., & Payne, A. J. (2001). Modelling three-dimensional flow structures and patterns of boundary shear stress in a natural pool–riffle sequence. *Earth Surface Processes and Landforms*, *26*(5), 553- https://doi.org/576. 10.1002/esp.210

Bradley, D. N., & Tucker, G. E. (2012). Measuring gravel transport and dispersion in a mountain river using passive radio tracers. *Earth Surface Processes and Landforms*, *37*(10), 1034-1045. https://doi.org/10.1002/esp.3223

Brasington, J., Langham, J., & Rumsby, B. (2003). Methodological sensitivity of morphometric estimates of coarse fluvial sediment transport. *Geomorphology*, *53*(3), 299-316. https://doi.org/10.1016/S0169-555X(02)00320-3

Brierley, G. J., & Fryirs, K. A. (2013). Geomorphology and river management: applications of the river styles framework. Hoboken, NJ: John Wiley & Sons

Bunte, K., & Abt, S. R. (2001). Sampling surface and subsurface particle-size distributions in wadable gravel-and cobble-bed streams for analyses in sediment transport, hydraulics, and streambed

monitoring. Gen. Tech. Rep. RMRS-GTR-74. Fort Collins, CO: U.S. Department of Agriculture, Forest Service, Rocky Mountain Research Station. https://doi.org/10.2737/RMRS-GTR-74

Bunte, K., Abt, S. R., Potyondy, J. P., & Ryan, S. E. (2004). Measurement of coarse gravel and cobble transport using portable bedload traps. *Journal of Hydraulic Engineering*, *130*(9), 879-893. https://doi.org/10.1061/(ASCE)0733-9429(2004)130:9(879)

Bunte, K., Swingle, K. W., & Abt, S. R. (2007). Guidelines for using bedload traps in coarse-bedded mountain streams: construction, installation, operation, and sample processing. Gen. Tech. Rep. RMRS-GTR-191. Fort Collins, CO: U.S. Department of Agriculture, Forest Service, Rocky Mountain Research Station. https://doi.org/10.2737/RMRS-GTR-191

Bunte, K., Abt, S. R., Potyondy, J. P., & Swingle, K. W. (2008). A comparison of coarse bedload transport measured with bedload traps and Helley-Smith samplers. *Geodinamica Acta*, *21*(1-2), 53-66. https://doi.org/10.3166/ga.21.53-66

Carling, P.A. (1987). Bed stability in gravel streams, with reference to stream regulation and ecology. In K.S. Richards (Ed.), *Rivers, from and process in alluvial channels* (pp. 321-347). London, UK: Methuen.

Carling, P. A., & Reader, N. A. (1982). Structure, composition and bulk properties of upland stream gravels. *Earth Surface Processes and Landforms*, *7*(4), 349-365. https://doi.org/10.1002/esp.3290070407

Cassel, M., Dépret, T., & Piégay, H. (2017). Assessment of a new solution for tracking pebbles in rivers based on active RFID. *Earth Surface Processes and Landforms*, *42*(13), 1938-1951. https://doi.org/10.1002/esp.4152

Chapuis, M., Bright, C. J., Hufnagel, J., & MacVicar, B. (2014). Detection ranges and uncertainty of passive Radio Frequency Identification (RFID) transponders for sediment tracking in gravel rivers and coastal environments. *Earth Surface Processes and Landforms*, *39*(15), https://doi.org/2109-2120. 10.1002/esp.3620

Chapuis, M., Dufour, S., Provansal, M., Couvert, B., & De Linares, M. (2015). Coupling channel evolution monitoring and RFID tracking in a large, wandering, gravel-bed river: Insights into sediment routing on geomorphic continuity through a riffle–pool sequence. *Geomorphology*, *231*, 258-269. https://doi.org/10.1016/j.geomorph.2014.12.013

Church, M. (2006). Bed material transport and the morphology of alluvial river channels. *Annu. Rev. Earth Planet. Sci.*, *34*, 325-354. https://doi.org/10.1146/annurev.earth.33.092203.122721

Church, M., & Ferguson, R. I. (2015). Morphodynamics: Rivers beyond steady state. Water Resources Research, 51(4), 1883-1897. https://doi.org/10.1002/2014WR016862

Church, M., & Hassan, M. A. (1992). Size and distance of travel of unconstrained clasts on a streambed. *Water Resources Research*, *28*(1), 299-303. https://doi.org/10.1029/91WR02523

Church, M., & Haschenburger, J. K. (2017). What is the "active layer"?. *Water Resources Research*, *53*(1), 5-10. https://doi.org/10.1002/2016WR019675

Clayton, J. A., & Pitlick, J. (2007). Spatial and temporal variations in bed load transport intensity in a gravel bed river bend. *Water Resources Research*, *43*(2). https://doi.org/10.1029/2006WR005253

Cudden, J. R., & Hoey, T. B. (2003). The causes of bedload pulses in a gravel channel: The implications of bedload grain-size distributions. *Earth Surface Processes and Landforms*, *28*(13), 1411-1428. https://doi.org/10.1002/esp.521

DeVries, P. (2002). Bedload layer thickness and disturbance depth in gravel bed streams. *Journal of Hydraulic Engineering*, *128*(11), 983-991. https://doi.org/10.1061/(ASCE)0733-9429(2002)128:11(983)

DeVries, P., Burges, S. J., Daigneau, J., & Stearns, D. (2001). Measurement of the temporal progression of scour in a pool-riffle sequence in a gravel bed stream using an electronic scour monitor. *Water Resources Research*, *37*(11), 2805-2816. https://doi.org/10.1029/2001WR000357

Einstein, H. A. (1937). Bedload transport as a probability problem. In H.W. Shen (Ed.), *Sedimentation and contaminant criteria for watershed planning and management (reprinted in 1972).* Fort Collins, CO: Water Resources Publications.

Ferguson, R. I. (2003). The missing dimension: effects of lateral variation on 1-D calculations of fluvial bedload transport. *Geomorphology*, *56*(1-2), 1-14. https://doi.org/10.1016/S0169-555X(03)00042-4

Ferguson, R. I. (2007). Gravel-bed rivers at the reach scale. In H. Habersack, H. Piégay, M. Rinaldi (Eds.), *Gravel-bed Rivers VI: from process understanding to river restoration* (pp. 33-60). Amsterdam, Netherlands: Elsevier.

Ferguson, R. I., & Hoey, T. B. (2002). Long-term slowdown of river tracer pebbles: Generic models and implications for interpreting short-term tracer studies. *Water Resources Research*, *38*(8). https://doi.org/10.1029/2001WR000637

Ferguson, R. I., & Wathen, S. J. (1998). Tracer-pebble movement along a concave river profile: Virtual velocity in relation to grain size and shear stress. *Water Resources Research*, *34*(8), 2031-2038. https://doi.org/10.1029/98WR01283

Fernández, R., & Garcia, M.H. (2017). Input-variable sensitivity assessment for sediment transport relations. *Water Resources Research*, 53. https://doi.org/10.1002/2016WR020249.

Formann, E., & Habersack, H. M. (2007). Morphodynamic river processes and techniques for assessment of channel evolution in Alpine gravel bed rivers. *Geomorphology*, *90*(3), 340-355. https://doi.org/10.1016/j.geomorph.2006.10.029

Gendaszek, A. S., Magirl, C. S., Czuba, C. R., & Konrad, C. P. (2013). The timing of scour and fill in a gravel-bedded river measured with buried accelerometers. *Journal of Hydrology*, *495*, 186-196. https://doi.org/10.1016/j.jhydrol.2013.05.012

Grabowski, R. C., Surian, N., & Gurnell, A. M. (2014). Characterizing geomorphological change to support sustainable river restoration and management. *Wiley Interdisciplinary Reviews: Water*, *1*(5), 483-512. https://doi.org/10.1002/wat2.1037

Gomez, B., & Church, M. (1989). An assessment of bed load sediment transport formulae for gravel bed rivers. *Water Resources Research*, *25*(6), 1161-1186. https://doi.org/10.1029/WR025i006p01161

Graham, D. J., Reid, I., & Rice, S. P. (2005a). Automated sizing of coarse-grained sediments: image-processing procedures. *Mathematical Geology*, *37*(1), 1-28. https://doi.org/10.1007/s11004-005-8745-x

Graham, D. J., Rice, S. P., & Reid, I. (2005b). A transferable method for the automated grain sizing of river gravels. *Water Resources Research*, *41*(7). https://doi.org/10.1029/2004WR003868

Graham, D. J., Rollet, A. J., Piégay, H., & Rice, S. P. (2010). Maximizing the accuracy of image-based surface sediment sampling techniques. *Water Resources Research*, *46*(2). https://doi.org/10.1029/2008WR006940

Grant, G. E. (2012). The geomorphic response of gravel-bed rivers to dams: perspectives and prospects. In M. Church, P. M. Biron, A. G. Roy (Eds.), *Gravel-bed Rivers: Processes, Tools, Environments* (pp. 165-181). Hoboken, NJ: John Wiley & Sons

Haschenburger, J. K. (1996). Scour and fill in a gravel-bed channel: observations and stochastic models, (Doctoral dissertation). Retrieved from https://open.library.ubc.ca/. Vancouver, Canada: University of British Columbia

Haschenburger, J. K. (2011). Vertical mixing of gravel over a long flood series. Earth Surface Processes and Landforms, 36(8), 1044-1058. https://doi.org/10.1002/esp.2130

Haschenburger, J. K. (2013a). Bedload kinematics and fluxes. In J. F. Shroder (Ed.), *Treatise on Geomorphology*, *Vol. 9* (pp. 103-123). Amsterdam, Netherlands: Elsevier.

Haschenburger, J. K. (2013b). Tracing river gravels: Insights into dispersion from a long-term field experiment. *Geomorphology*, *200*, 121-131. https://doi.org/10.1016/j.geomorph.2013.03.033

Haschenburger, J. K., & Church, M. (1998). Bed material transport estimated from the virtual velocity of sediment. *Earth Surface Processes and Landforms*, *23*(9), 791-808. https://doi.org/10.1002/(SICI)1096-9837(199809)23:9<791::AID-ESP888>3.0.CO;2-X

Haschenburger, J. K., & Wilcock, P. R. (2003). Partial transport in a natural gravel bed channel. *Water Resources Research*, *39*(1). https://doi.org/10.1029/2002WR001532

Hassan, M. A., & Bradley, D. N. (2017). Geomorphic Controls on Tracer Particle Dispersion in Gravel-Bed Rivers. *In D. Tsutsumi, J. B. Laronne (Eds.), Gravel-Bed Rivers: Processes and Disasters (pp. 209-233). Hoboken, NJ: John Wiley & Sons*

Hassan, M. A., & Church, M. (1992). The movement of individual grains on the streambed. In P. Billi, R. D. Hey, C. R. Thorne, P. Tacconi (Eds.), *Dynamics of gravel-bed rivers* (pp. 159-175). Hoboken, NJ: John Wiley & Sons. https://doi.org/10.1002/esp.3290180510

Hassan, M. A., Church, M., & Ashworth, P. J. (1992). Virtual rate and mean distance of travel of individual clasts in gravel-bed channels. *Earth Surface Processes and Landforms*, *17*(6), 617-627. https://doi.org/10.1002/esp.3290170607

Hassan, M. A., Egozi, R., & Parker, G. (2006). Experiments on the effect of hydrograph characteristics on vertical grain sorting in gravel bed rivers. *Water Resources Research*, *42*(9). https://doi.org/10.1029/2005WR004707

Hassan, M. A., & Roy, A. G. (2016). Coarse particle tracing in fluvial geomorphology. In G.M. Kondolf, H. Piégay (Eds.), *Tools in fluvial geomorphology* (pp. 306-323). Hoboken, NJ: John Wiley & Sons. https://doi.org/10.1002/9781118648551.ch14

Hoey, T. (1992). Temporal variations in bedload transport rates and sediment storage in gravel-bed rivers. *Progress in physical geography*, *16*(3), 319-338. https://doi.org/10.1177/030913339201600303

Houbrechts, G., Van Campenhout, J., Levecq, Y., Hallot, E., Peeters, A., & Petit, F. (2012). Comparison of methods for quantifying active layer dynamics and bedload discharge in armoured gravel-bed rivers. *Earth Surface Processes and Landforms*, *37*(14), 1501-1517. https://doi.org/10.1002/esp.3258

Kasprak, A., Wheaton, J. M., Ashmore, P. E., Hensleigh, J. W., & Peirce, S. (2015). The relationship between particle travel distance and channel morphology: Results from physical models of braided rivers. *Journal of Geophysical Research: Earth Surface*, *120*(1), 55-74. https://doi.org/10.1002/2014JF003310

Klösch, M., & Habersack, H. (2018). Deriving formulas for an unsteady virtual velocity of bedload tracers. *Earth Surface Processes and Landforms*, *43*, 1529-1541. https://doi.org/10.1002/esp.4326

Kondolf, G. M. (1997). Hungry water: effects of dams and gravel mining on river channels. *Environmental management, 21*(4), 533-551. https://doi.org/10.1007/s002679900048

Lamarre, H., MacVicar, B., & Roy, A. G. (2005). Using passive integrated transponder (PIT) tags to investigate sediment transport in gravel-bed rivers. *Journal of Sedimentary Research*, *75*(4), 736-741. https://doi.org/10.2110/jsr.2005.059

Lane, S. N., Richards, K. S., & Chandler, J. H. (1995). Morphological Estimation of the Time-Integrated Bed Load Transport Rate. *Water Resources Research*, *31*(3), 761-772. https://doi.org/10.1029/94WR01726

Laronne, J. B., Outhet, D. N., Carling, P. A., & McCabe, T. J. (1994). Scour chain employment in gravel bed rivers. *Catena*, *22*(4), 299-306. https://doi.org/10.1016/0341-8162(94)90040-X

Liébault, F., Bellot, H., Chapuis, M., Klotz, S., & Deschâtres, M. (2012). Bedload tracing in a high-sediment-load mountain stream. *Earth Surface Processes and Landforms*, *37*(4), 385-399. https://doi.org/10.1002/esp.2245

Liébault, F., & Laronne, J. B. (2008). Evaluation of bedload yield in gravel-bed rivers using scour chains and painted tracers: the case of the Esconavette Torrent (Southern French Prealps). *Geodinamica Acta*, *21*(1-2), 23-34. https://doi.org/10.3166/ga.21.23-34

Lindsay, J. B., & Ashmore, P. E. (2002). The effects of survey frequency on estimates of scour and fill in a braided river model. Earth Surface Processes and Landforms, 27(1), 27-43. https://doi.org/10.1002/esp.282

Lobera, G., Andrés-Domenech, I., López-Tarazón, J. A., Millán-Romero, P., Vallés, F., Vericat, D., & Batalla, R. J. (2017). Bed disturbance below dams: observations from two Mediterranean rivers. *Land Degradation & Development*, *28*(8), 2493-2512. https://doi.org/10.1002/ldr.2785

López, R., Vericat, D., & Batalla, R. J. (2014). Evaluation of bed load transport formulae in a large regulated gravel bed river: The lower Ebro (NE Iberian Peninsula). *Journal of hydrology*, *510*, 164-181. https://doi.org/10.1016/j.jhydrol.2013.12.014

MacKenzie, L. G., Eaton, B. C., & Church, M (2018). Breaking from the average: Why large grains matter in gravel-bed streams. *Earth Surface Processes and Landforms*. https://doi.org/10.1002/esp.4465

Mao, L., & Surian, N. (2010). Observations on sediment mobility in a large gravel-bed river. *Geomorphology*, *114*(3), 326-337. https://doi.org/10.1016/j.geomorph.2009.07.015

Mao, L., Picco, L., Lenzi, M. A., & Surian, N. (2017). Bed material transport estimate in large gravel-bed rivers using the virtual velocity approach. *Earth Surface Processes and Landforms*, *42*(4), 595-611. https://doi.org/10.1002/esp.4000

Marti, C., & Bezzola, G. R. (2006). Bed load transport in braided gravel-bed rivers. *In G.H. Sambrook Smith, J.L. Best, C.S. Bristow, G.E. Petts (Eds.), Braided rivers: Processes, Deposits, Ecology and Management (pp. 199-215).* Oxford, UK: Blackwell Publishing Ltd

Martin, Y., & Church, M. (1995). Bed-material transport estimated from channel surveys: Vedder River, British Columbia. *Earth Surface Processes and Landforms*, *20*(4), 347-361. https://doi.org/10.1002/esp.3290200405

Martin, Y., & Ham, D. (2005). Testing bedload transport formulae using morphologic transport estimates and field data: lower Fraser River, British Columbia. *Earth Surface Processes and Landforms*, *30*(10), 1265-1282. https://doi.org/10.1002/esp.1200

McLean, D. G., & Church, M. (1999). Sediment transport along lower Fraser River: 2. Estimates based on the long-term gravel budget. *Water Resources Research*, *35*(8), 2549-2559. https://doi.org/10.1029/1999WR900102

Merz, J. E., Pasternack, G. B., & Wheaton, J. M. (2006). Sediment budget for salmonid spawning habitat rehabilitation in a regulated river. *Geomorphology*, *76*(1), 207-228. https://doi.org/10.1016/j.geomorph.2005.11.004

Milan, D. J. (2013). Virtual velocity of tracers in a gravel-bed river using size-based competence duration. *Geomorphology*, *198*, 107-114. https://doi.org/10.1016/j.geomorph.2013.05.018

Mosley, M. P., & Tindale, D. S. (1985). Sediment variability and bed material sampling in gravel-bed rivers. *Earth Surface Processes and Landforms*, *10*(5), https://doi.org/465-482. 10.1002/esp.3290100506

Mueller, E. R., Pitlick, J., & Nelson, J. M. (2005). Variation in the reference Shields stress for bed load transport in gravel-bed streams and rivers. *Water Resources Research*, *41*(4). https://doi.org/10.1029/2004WR003692

Nawa, R. K., & Frissell, C. A. (1993). Measuring scour and fill of gravel streambeds with scour chains and sliding-bead monitors. *North American Journal of Fisheries Management*, *13*(3), 634-639. http://dx.doi.org/10.1577/1548-8675(1993)013<0634:MSAFOG>2.3.CO;2

Papangelakis, E., & Hassan, M. A. (2016). The role of channel morphology on the mobility and dispersion of bed sediment in a small gravel-bed stream. Earth Surface Processes and Landforms, 41(15), 2191-2206. https://doi.org/10.1002/esp.3980

Parker, G. (1990). Surface-based bedload transport relation for gravel rivers. *Journal of hydraulic research*, *28*(4), 417-436. https://doi.org/10.1080/00221689009499058

Petit, F. (1987). The relationship between shear stress and the shaping of the bed of a pebble-loaded river La Rulles—Ardenne. *Catena*, *14*(5), 453-468. https://doi.org/10.1016/0341-8162(87)90015-4

Pyrce, R. S., & Ashmore, P. E. (2003a). Particle path length distributions in meandering gravel-bed streams: Results from physical models. *Earth Surface Processes and Landforms*, *28*(9), 951-966. https://doi.org/10.1002/esp.498

Pyrce, R. S., & Ashmore, P. E. (2003b). The relation between particle path length distributions and channel morphology in gravel-bed streams: a synthesis. *Geomorphology*, *56*(1-2), 167-187. https://doi.org/10.1016/S0169-555X(03)00077-1

Recking, A., Liébault, F., Peteuil, C., & Jolimet, T. (2012). Testing bedload transport equations with consideration of time scales. *Earth Surface Processes and Landforms*, *37*(7), 774-789. https://doi.org/10.1002/esp.3213

Recking, A., Piton, G., Vazquez-Tarrio, D., & Parker, G. (2016). Quantifying the morphological print of bedload transport. *Earth Surface Processes and Landforms*, *41*(6), 809-822. https://doi.org/10.1002/esp.3869

Rennie, C. D., & Villard, P. V. (2004a). Site specificity of bed load measurement using an acoustic Doppler current profiler. *Journal of Geophysical Research: Earth Surface*, *109*(F3). https://doi.org/10.1029/2003JF000106

Rennie, C. D., & Millar, R. G. (2004b). Measurement of the spatial distribution of fluvial bedload transport velocity in both sand and gravel. *Earth Surface Processes and Landforms*, *29*(10), 1173-1193. https://doi.org/10.1002/esp.1074

Rennie, C. D., Vericat, D., Williams, R. D., Brasington, J., & Hicks, M. (2017). Calibration of acoustic doppler current profiler apparent bedload velocity to bedload transport rate. In D. Tsutsumi, J. B. Laronne (Eds.), *Gravel-Bed Rivers: Processes and Disasters* (pp. 209-233). Hoboken, NJ: John Wiley & Sons

Rice, S., & Church, M. (1998). Grain size along two gravel-bed rivers: statistical variation, spatial pattern and sedimentary links. *Earth Surface Processes and Landforms*, *23*(4), 345-363. https://doi.org/10.1002/(SICI)1096-9837(199804)23:4<345::AID-ESP850>3.0.CO;2-B

Rice, S. P., & Church, M. (2010). Grain-size sorting within river bars in relation to downstream fining along a wandering channel. *Sedimentology*, *57*(1), 232-251. https://doi.org/232-251. 10.1111/j.1365-3091.2009.01108.x

Rickenmann, D. (2017). Bedload transport measurements with geophones, hydrophones, and underwater microphones (passive acoustic methods). In D. Tsutsumi, J. B. Laronne (Eds.), *Gravel-Bed Rivers: Processes and Disasters* (pp. 185-208). Hoboken, NJ: John Wiley & Sons

Rickenmann, D., Turowski, J. M., Fritschi, B., Wyss, C., Laronne, J., Barzilai, R., ... & Habersack, H. (2014). Bedload transport measurements with impact plate geophones: comparison of sensor calibration in different gravel-bed streams. *Earth Surface Processes and Landforms*, *39*(7), 928-942. https://doi.org/10.1002/esp.3499

Ryan, S. E., & Dixon, M. K. (2007). 15 Spatial and temporal variability in stream sediment loads using examples from the Gros Ventre Range, Wyoming, USA. In H. Habersack, H. Piégay, M. Rinaldi (Eds.), *Gravel-Bed Rivers VI: From Process Understanding to River Restoration* (pp. 387-407). Amsterdam, Netherlands: Elsevier.

Sear, D. A. (1996). Sediment transport processes in pool–riffle sequences. *Earth Surface Processes and Landforms*, *21*(3), 241-262. https://doi.org/10.1002/(SICI)1096-9837(199603)21:3<241::AID-ESP623>3.0.CO;2-1

Schneider, J. M., Rickenmann, D., Turowski, J. M., Bunte, K., & Kirchner, J. W. (2015). Applicability of bed load transport models for mixed-size sediments in steep streams considering macro-roughness. *Water Resources Research*, *51*(7), 5260-5283. https://doi.org/10.1002/2014WR016417

Storz-Peretz, Y., & Laronne, J. B. (2013). Automatic grain sizing of vertical exposures of gravelly deposits. *Sedimentary Geology*, *294*, 13-26. https://doi.org/10.1016/j.sedgeo.2013.05.004

Surian, N. (2002). Downstream variation in grain size along an Alpine river: analysis of controls and processes. *Geomorphology*, *43*(1), 137-149. https://doi.org/10.1016/S0169-555X(01)00127-1

Surian, N., & Cisotto, A. (2007). Channel adjustments, bedload transport and sediment sources in a gravel-bed river, Brenta River, Italy. *Earth Surface Processes and Landforms*, *32*(11), 1641-1656. https://doi.org/10.1002/esp.1591

Surian, N., Mao, L., Giacomin, M., & Ziliani, L. (2009). Morphological effects of different channel-forming discharges in a gravel-bed river. *Earth Surface Processes and Landforms*, *34*(8), 1093-1107. https://doi.org/10.1002/esp.1798

Teng, J., Jakeman, A. J., Vaze, J., Croke, B. F., Dutta, D., & Kim, S. (2017). Flood inundation modelling: A review of methods, recent advances and uncertainty analysis. *Environmental Modelling & Software*, *90*, 201-216. https://doi.org/10.1016/j.envsoft.2017.01.006

Thompson, D. M., & Wohl, E. E. (2009). The linkage between velocity patterns and sediment entrainment in a forced-pool and riffle unit. *Earth Surface Processes and Landforms*, *34*(2), 177-192. https://doi.org/10.1002/esp.1698

Vázquez-Tarrío, D., & Menéndez-Duarte, R. (2014). Bedload transport rates for coarse-bed streams in an Atlantic Region (Narcea River, NW Iberian Peninsula). *Geomorphology*, *217*, 1-14. https://doi.org/10.1016/j.geomorph.2014.04.015

Vázquez-Tarrío, D., Recking, A., Liébault, F., Tal, M., & Menéndez-Duarte, R (2018). Particle transport in gravel-bed rivers: revisiting passive tracer data. *Earth Surface Processes and Landforms*. https://doi.org/10.1002/esp.4484

Vericat, D., Church, M., & Batalla, R. J. (2006). Bed load bias: Comparison of measurements obtained using two (76 and 152 mm) Helley-Smith samplers in a gravel bed river. *Water Resources Research*, *42*(1). https://doi.org/10.1029/2005WR004025

Vericat, D., Wheaton, J. M., & Brasington, J. (2017). Revisiting the Morphological Approach: Opportunities and Challenges with Repeat High-Resolution Topography. In D. Tsutsumi, J. B. Laronne (Eds.), *Gravel-Bed Rivers: Processes and Disasters* (pp. 121-158). Hoboken, NJ: John Wiley & Sons

Wheaton, J. M., Brasington, J., Darby, S. E., & Sear, D. A. (2010). Accounting for uncertainty in DEMs from repeat topographic surveys: improved sediment budgets. *Earth Surface Processes and Landforms*, *35*(2), 136-156. https://doi.org/10.1002/esp.1886

Wilcock, P. R. (1993). Critical shear stress of natural sediments. *Journal of Hydraulic Engineering*, *119*(4), 491-505. https://doi.org/10.1061/(ASCE)0733-9429(1993)119:4(491)

Wilcock, P. R. (1997). Entrainment, displacement and transport of tracer gravels. *Earth Surface Processes and Landforms*, *22*(12), 1125-1138. https://doi.org/10.1002/(SICI)1096-9837(199712)22:12<1125::AID-ESP811>3.0.CO;2-V

Wilcock, P. R., Barta, A. F., Shea, C. C., Kondolf, G. M., Matthews, W. V., & Pitlick, J. (1996). Observations of flow and sediment entrainment on a large gravel-bed river. *Water Resources Research*, *32*(9), 2897-2909. https://doi.org/10.1029/96WR01628

Wilcock, P. R., & DeTemple, B. T. (2005). Persistence of armor layers in gravel-bed streams. *Geophysical Research Letters*, *32*(8). https://doi.org/10.1029/2004GL021772

Wilcock, P. R., & McArdell, B. W. (1997). Partial transport of a sand/gravel sediment. *Water Resources Research*, *33*(1), 235-245. https://doi.org/10.1029/96WR02672

Wilcock, P. R., & Crowe, J. C. (2003). Surface-based transport model for mixed-size sediment. *Journal of Hydraulic Engineering*, *129*(2), 120-128. https://doi.org/10.1061/(ASCE)0733-9429(2003)129:2(120)

Williams, R. D., Rennie, C. D., Brasington, J., Hicks, D. M., & Vericat, D. (2015). Linking the spatial distribution of bed load transport to morphological change during high-flow events in a shallow braided river. *Journal of Geophysical Research: Earth Surface*, *120*(3), 604-622. https://doi.org/10.1002/2014JF003346

Wolman, M. G. (1954). A method of sampling coarse river-bed material. *EOS, Transactions American Geophysical Union*, *35*(6), 951-956. https://doi.org/10.1029/TR035i006p00951

Wyss, C. R., Rickenmann, D., Fritschi, B., Turowski, J. M., Weitbrecht, V., & Boes, R. M. (2016). Measuring bed load transport rates by grain-size fraction using the Swiss plate geophone signal at the Erlenbach. *Journal of Hydraulic Engineering*, *142*(5), 04016003. https://doi.org/10.1061/(ASCE)HY.1943-7900.0001090

Zolezzi, G., Bertoldi, W., & Tubino, M. (2006). Morphological analysis and prediction of river bifurcations. In G.H. Sambrook Smith, J.L. Best, C.S. Bristow, G.E. Petts (Eds.), *Braided rivers: Processes, Deposits, Ecology and Management* (pp. 233-256). Oxford, UK: Blackwell Publishing Ltd

3. SEDIMENT MOBILITY AND BED MATERIAL TRANSPORT ESTIMATION IN A GRAVEL-BED RIVER DOWNSTREAM OF A DAM

Andrea Brenna[1], Nicola Surian[1], and Luca Mao[2]

[1] *Department of Geosciences, University of Padova, Padova, Italy.*

[2] *School of Geography, University of Lincoln, Lincoln, UK.*

Submitted to *Earth Surface Processes and Landforms*.

Abstract

The impacts induced by dam on large gravel-bed rivers are studied from long time considering the morphological and bed alteration responses, but relatively poor knowledge exists about the modifications occurring in terms of coarse transport regime. Using data collected by a tracers-based monitoring program carried out in a 4-km long study-sector of the Parma River (Italy) located downstream from a dam, we applied a virtual velocity approach for estimating the bed material load at four cross-sections. Monitoring and calculation results provided new insights about the impacts of the dam on gravel-bed river material mobility and sediment regime over the 17-months calculation period. A longitudinal gradient of the effects have been recognized along the study sector. Sections located closer to the dam are characterized by more evident impacts due to deficit of coarse sediment input from upstream. Sediment mobility is strongly altered, especially in the high armored main channel, and the overall bed material load is extremely low (ranging between 0.4 and $1*10^3$ m^3 during the calculation period). A partial recovery of sediment dynamics was recognized at the sections located further from the dam where both partial and full transport occur at different water discharges and estimates provide higher sediment yield (about $4*10^3$ m^3 during the calculation period). The presence of a zero-flux sediment boundary was able to induce significant alterations also in terms of partial transport contribution, relations between bed material flux and hydrological characteristics of the competent event, contribution of different morphological units to the total coarse transport of a section and sediment transport regimes.

1. Introduction

Bed material transport represents one of the key processes in gravel-bed river (GBR) dynamics, determining the feedback between water flow, sediment availability and channel morphology (Church, 2006; Ferguson, 2007; Church and Ferguson, 2015). However, being high variable in time and space (e.g. Lisle et al., 2000), it is very difficult to obtain reliable estimates of this process in large GBRs (Ferguson, 2007; Haschenburger, 2013a; Wohl et al.,

2015). Besides, coarse sediment transport can be heavily affected by human disturbances and interventions at a variety of spatial and temporal scales. Dams and reservoirs represent the most impactful human alteration on sediment dynamics in alluvial channel, as they interrupt the downstream flux of coarse material (Grant, 2012; Kondolf et al., 2014). For better understanding the impact of dams on fluvial systems it is necessary to achieve new insights about the sediment mobility and to derive reliable estimates of coarse material load in dam-impacted fluvial sectors.

An effective approach for quantifying coarse sediment dynamics is represented by the use of tracers (see Hassan and Roy, 2016) which provides information about sediment dynamics in terms of travel distances (e.g. Church and Hassan, 1992; Pyrce and Ashmore, 2003), transport processes thresholds (e.g. Mao and Surian, 2010) and particles motion over large timescales (e.g. Ferguson and Wathen, 1998; Ferguson et al., 2002). Data provided by tracers give also essential information for calculating the bed material fluxes by different estimation approaches (e.g. Wilcock, 1997; Haschenburger and Church, 1998; Liébault and Laronne, 2008) that rely on the virtual velocity of the moved grains.

Following the definition of Haschenburger and Wilcock (2003), if during a certain flow condition all the surface sediments are in motion, the transport is locally at full transport conditions. However, if there is a portion of the channel where some grains remain immobile (regardless of their size), the mobility is occurring in partial transport conditions in that channel portion. Partial transport has been observed by several field-monitoring studies involving tracers (e.g. Carling, 1987; Ashworth and Ferguson, 1989; Church and Hassan, 2002; Mao and Surian, 2010). In particular, for frequent low-recurrence interval events (i.e. RI< 2 yr), approximately 25-50% of river bed remains in a state of partial transport and only for event with high recurrence interval the whole section experiences full transport (Haschenburger and Wilcock, 2003). Applying the virtual velocity approach based on Wilcock's framework (1997) to estimate the bed material transport in two Italian large gravel-bed rivers, Mao et al. (2017) found that the contribution of partial transport to the overall transport volume is around 50-70% for discharges that are approximately a third of bankfull discharge and it decreases to 20-30% for near-bankfull discharges. Limited knowledge still exists about the relation between partial transport and the river local-characteristics in terms of channel geometry and bed sediments features (e.g. grain-size, armoring).

The use of tracers combined with morphological observations allowed also to identify the propensity of different morphological units to be activated by specific water discharges (e.g. Surian et al., 2009; Bertoldi et al., 2010; Mao and Surian, 2010; Surian et al., 2015). Nevertheless, no detailed data are available about the contribution of different morphological units to the total river-section transport. Some tracers-based monitoring were performed also in gravel-bed river reaches below dams in order to examine the mobility of surface particles in impacted channels, revealing the modification of the channel sediments characteristics (i.e. coarsening and armoring) and the progressive reduction of grains entrainment and movement (e.g. Vericat et al., 2006, 2008; Lobera et al., 2017). Instead, the dams impact on coarse-sediment regime quantification has received relatively little emphasis in literature, leading to very few attempts of estimating the bed material load in regulated rivers, mainly using direct-measure field techniques (e.g. Vericat and Batalla, 2005, 2006).

During a two-years monitoring program carried out in a 4-km long study-sector of the Parma River (Italy) bonded upstream by a retention basin dam, Brenna et al. (2018) collected the set of data required to calculate the bed material load through the virtual velocity approach based on the Wilcock's framework (1997). Following the first attempt performed by Mao et al. (2017) to apply this calculation in a real case-study, Brenna et al. (2018) improved the methodology developing an application framework which defines some criteria for data collection, processing and transport estimates, and also takes into account uncertainties, approach sensitivity and specific reach characteristics. Using such application framework, we calculated the bed material transport that occurred at four cross-sections during nine competent events that took place over the monitoring period (January 2016 - May 2017). This work aims to improve the current knowledge about the coarse sediment transport dynamics in a river reach downstream of a dam, using the information provided by tracers and the coarse transport estimates obtained through the virtual velocity approach. The specific objectives of the research are (i) to quantify the bed material fluxes at the scale of event, (ii) to assess the partial transport contribution to the overall bed material load volume (iii) to analyze the contribution of each morphological unit to the total section transport in relation to hydrological characteristics of the competent events (e.g. water discharge at flood-peak and effective run-off) and channel-section features (e.g. geometry, morphology, sediment grain-size and structure), and finally (iv) to investigate the longitudinal variations in sediment dynamics and transport caused by the presence of the dam.

2. Study Area

Data employed in this work have been collected in a sector of the Parma River, a Northern Apennines stream (Italy) with a catchment of 815 km^2 and total length of 92 km (Figure 1). The four sections selected for the field-monitoring and transport calculation are located in the middle part of the river course, between 1950 and 3400 m downstream of the Marano retention basin. The construction of the basin started in 1988 and was completed with the closure of the dam, representing a zero coarse-sediments flux boundary, in 2005. As a consequence of the dam closure, the river downstream of the retention basin is narrower (60 to 160 m wide; single-thread to wandering morphology) than upstream (mean width= 350 m; braided configuration). Downstream of the dam the river displays significant longitudinal variability in terms of channel width, morphology and sediment characteristics, making possible to recognize three different reaches (sensu Brierley and Fryirs (2013)) within the 4-km long study sector: reach 1, reach 2 (containing sections 1 and 2) and reach 3 (containing sections 3 and 4) (Figure 1).

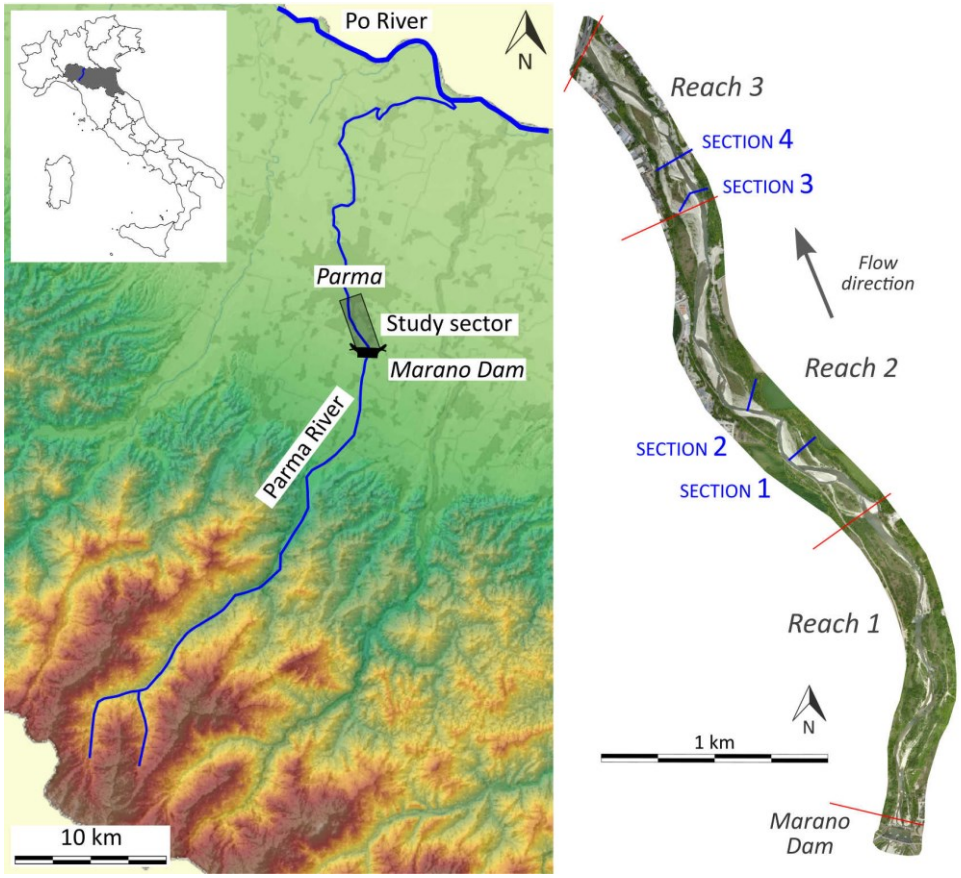

Figure 1. General setting of the Parma River catchment within the North-Apennines and the study sector.

The Parma River hydrological regime is dominated by rainfall and is characterized by high seasonality with most of precipitations occurring between November and April. The mean annual flow calculated immediately downstream from the study-sector is estimated to be about 11 m^3s^{-1}, but during the rainfall periods major floods typically occur while summers are characterized by long dry periods (Figure 2a). Despite the seasonal-torrential regime characterizing the river, over the long time scale (i.e. the last 11 years) a homogenous hydrological annual-regime is recognizable (Figure 2a). Due to its flood mitigation purposes, the dam (closed in 2005) may have influenced the river discharge during major floods (e.g. December 2009 event), but it never operated over the 17-months of monitoring and transport calculation considered in the present study (Figure 2b).

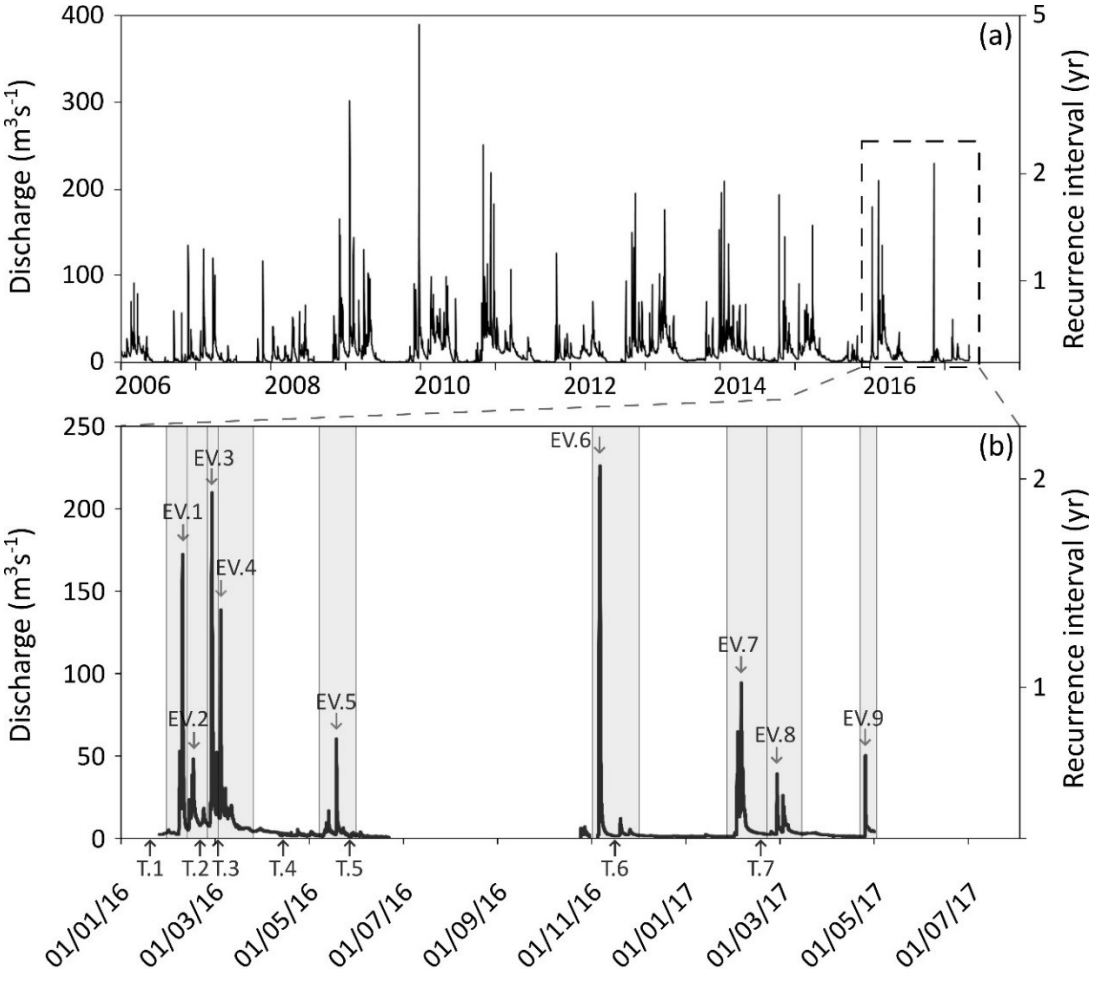

Figure 2. Hydrographs since the dam closure (completed in 2005) (a) and during the calculation period (January 2016 – May 2017) (b). In (b) the vertical arrows point out the nine competent events considered in the calculations. Temporal extension of each calculation event is reported with grey vertical bands and arrows and relative name (e.g. T.1, T.2 etc.) indicate the timing of the seven cross-sections topographies acquired in the field and used in this work.

3. Materials and methods

3.1 Virtual velocity approach for estimating the bed material transport

Due to the difficulty in carrying out direct measurements of bed material load in large gravel-bed rivers (Ferguson, 2007), the virtual velocity approach represents a viable tool to achieve reliable transport estimates (Ferguson, 2007; Mao et al., 2017) in those contexts. In this work we adopted the framework proposed by Wilcock (1997) because it is able to take into account several crucial aspects controlling the transport processes and it allows to distinguish between the partial and the full transport contributions at the local scale. Wilcock's framework (1997) requires to determine some calculation parameters (i.e. sediment mobility thresholds between no motion, partial and full transport conditions; Y: the percentage of mobilized streambed surface; d_s: the thickness of the bed mobile surface layer; V_i: the virtual velocity characterizing the i-size particles movement; M_i: the mass of entrained sediment) in function of the dimensionless shear stress (τ^*) induced by the water flow on the streambed. Brenna et al. (2018) defined the empirical relations between the parameters (i.e. mobility thresholds, Y, d_s and V_i) and the τ^* for two reaches of the Parma River (reaches 2 and 3, see Figure 1) monitoring the required data in the field (installation of 117 painted area, 38,000 painted clasts-tracers, 898 passive integrated transponders and 28 scour chains during the monitoring period) and calculating the instantaneous-local τ^* as a function of the water discharge adopting the depth-slope approach (Wilcock, 1993; Mueller et al., 2005). Taking into account for errors and processes variability, they applied the equation for the fractional sediment transport calculation (Wilcock, 1997) and the derived reach-specific empirical relations to determine the total unit mass transport rate (q^u) occurring for a specific τ^* (time resolution of 30 minutes) on a defined cross-section unit (spatial resolution of 1 m). Integrating the unit mass transport rates over the whole cross-section it was possible to calculate the instantaneous section transport (q^{sect}). Furthermore, integrating those data over the transport event duration, it was possible to estimate the bed material load, and the relative uncertainties, occurring at the section during the entire competent flood (q^{event}).

In order to achieve reliable transport estimates it is crucial to consider some application factors in function of the specific reach characteristics for calculating the τ^* and then determining the bed sediment loads. For this reason, Brenna et al. (2018) tested seven different data input configurations concluding that, depending on the specific river context, relevant estimates differences may be obtained. In this work we applied the method using

the most complete configuration, which considers the following aspects: (i) spatial variable water level over the time along a single section (defined for specific channel units), (ii) morpho-unit specific sediments grain sizes for τ^* calculation, and (iii) cross-section topographies variable over the time (i.e. use of both pre-flood and post-flood topographies for calculations).

3.2 Flood events and study reaches

In order to apply the transport estimate through the most complete configuration, it is necessary to use both the pre- and post-event cross-sections topographies. For this reason, we estimated the bed material load at the four cross-sections adopted for the field monitoring (Figure 3), during the nine competent events that occurred over the study period (Figure 2b) for which the two topographies were mostly available, obtaining 36 estimates of section-event transport.

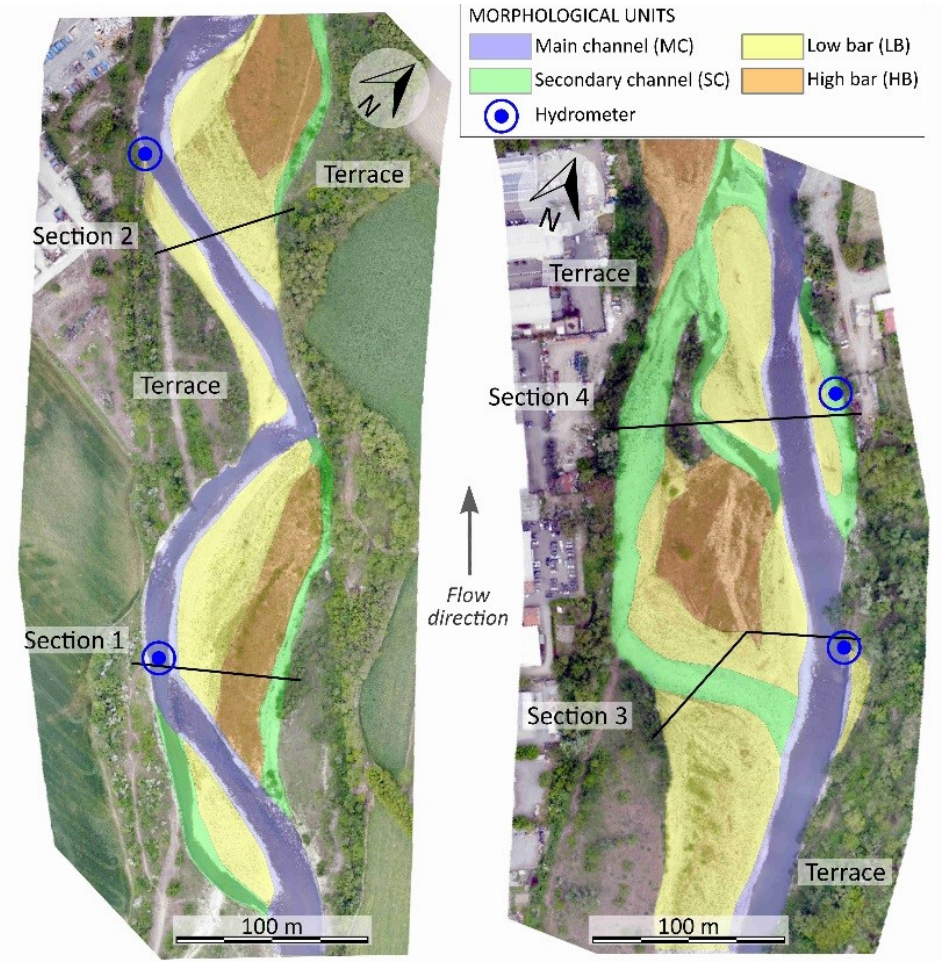

Figure 3. Drone photographs (April 2016) of the study areas and the four cross-sections considered for the transport estimates. Morphological units and hydrometers installation positions are shown.

The nine events have been identified above a minimum flood peak of about 35 $m^3 s^{-1}$, preliminary defined from field observations as the threshold for a possible competent event in the study sector. The events were cut in their falling limb depending on the hydrograph shape (i.e. deviation from the base flow) and then fixed the estimate periods based on the competence of the water flow. In other words, each competent event begins and ends with the active bed material load in the channel provided by our calculation. Using the discharge data provided by the Marano gauging station, for each event we defined the maximum water discharge at the event peak, the effective runoff of the competent flow (i.e. the hydrograph volume above the threshold of flow required for inducing sediment mobilization in the channel) and the recurrence interval (Table 1).

	Peak Data	Q_w^{max} ($m^3 s^{-1}$)	ER (m^3)	RI (yr)
Event 1	10 February 2016	173	4258	1.5
Event 2	17 February 2016	49	4749	<1
Event 3	29 February 2016	210	5845	1.8
Event 4	05 March 2016	139	6756	1.2
Event 5	19 May 2016	61	2343	<1
Event 6	06 November 2016	227	4839	2.1
Event 7	06 February 2017	95	5792	1
Event 8	01 March 2017	40	2954	<1
Event 9	27 April 2017	51	1062	<1

Table 1. Characteristics of the nine flood events monitored in the Parma River and considered in our estimates. Q_w^{max} is the maximum water discharge at the event peak, ER is the effective runoff of the competent flow and RI is the recurrence interval.

The four sections are located within reach 2 (sections 1 and 2) and reach 3 (section 3 and 4). The reach definition was addressed using remote sensing data (i.e. mean channel width, slope and morphological configuration defined from drone photographs and digital elevation models) and information collected in the field focusing on the definition of the surface and sub-surface sediment grain size through photographs analysis procedure (see Storz-Peretz and Laronne (2013) and Mao et al. (2017) for the method description) of 111 sample areas located along the study sector. Collected data are characterized by marked longitudinal variability along the study sector (Table 2). Reach 1 is high impacted by dam disturbance, showing a narrow active channel, single-thread configuration and bed armoring. Moving to the downstream portions of the study sector the mean width increases, there is a progressive recovery of the morphological complexity (wandering morphology in reach 3) and decrease of mean grain size and armoring evidences.

	Mean width (m)	Mean slope (m/m)	Morphology	Grain size (mm)	Armoring (*)
Reach 1	46	0.0053	SAB	-	High
Reach 2	84	0.0055	SAB	D_{50}= 63	High
Reach 3	109	0.0048	W	D_{50}= 50	Moderate

Table 2. Characteristics of the three reaches identified within the selected study sector in terms of morphology and channel sediments. SAB: "sinuous with alternate bars morphology"; W: "wandering morphology". (*): see Table (3) for quantitative information about armor ratio.

3.3 Calculations addressed in this work

The whole channel (following types and criteria reported in Mao and Surian (2010)) has been classified in different morphological units (main and secondary channels, bars and islands; see Figure 3) based on topographical and sediment features (i.e. bed grain size). Based on water discharges and data collected in the field (i.e. trash lines) or provided by local hydrometers installed in correspondence of the study-sections (Figure 3), we defined the water depth for each meter of cross-sections with a time resolution of 30 minutes during the whole study period. Local water depth over time and grain size are the two data required for calculating the τ^* and then q^u (total unit mass transport rate), q^{sect} (instantaneous-section transport) and finally q^{event} (event-section transport) applying the reach-specific empirical relations, the framework equations of the fractional sediment transport (Wilcock, 1997) and the selected input factors configuration (Brenna et al., 2018). For our calculations we used 28 cross-section topographies acquired by dGPS during the monitoring (from T1 to T7 at sections 1, 2, 3 and 4; see Figure 2b) in order to estimate the section-event transport at the study sections (Figure 4).

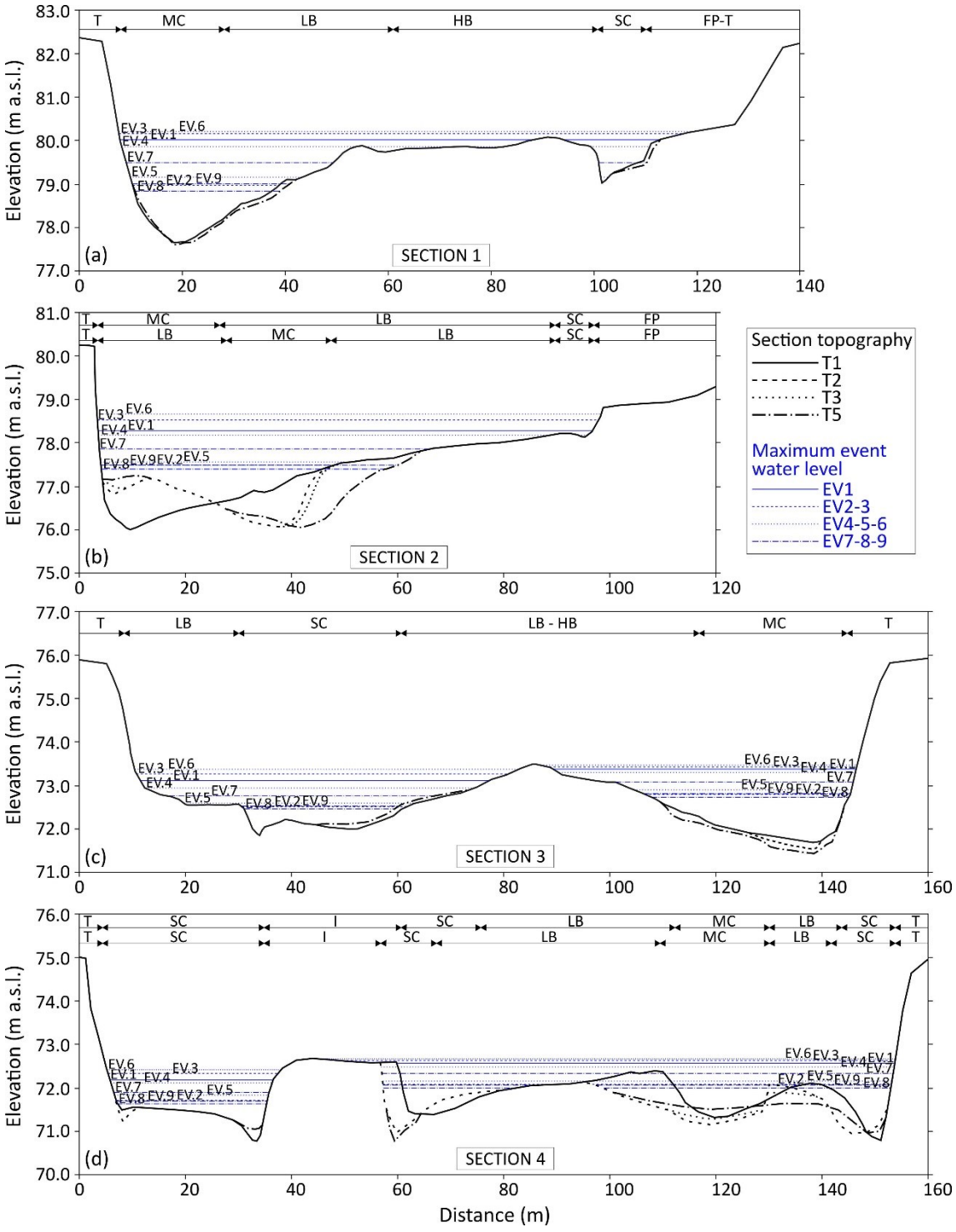

Figure 4. Topographies of the calculation cross-sections. For each section some representative topographies acquired over the study period are plotted, allowing to observe erosion and deposition processes. Horizontal blue lines refer to the maximum levels reached by the water at the peaks of the flood events. At sections 3 (c) and 4 (d) different maximum water levels were reached in the main and secondary channels during the same flood event.

For each of the 36 estimations we calculated the total volume (converting the original results obtained in kg to m^3 considering a porosity of 0.25 as suggested by Carling and Reader (1982)) of bed material transported through a cross-section over the duration of the competent event (i.e. q^{event}) and the relative uncertainty (i.e. errors). The adopted procedure allowed us to distinctly determine the transport contribution provided by partial and full mobility conditions. Discretizing the section in different morphological units, the volume of sediment transported by each morpho-unit (grouped in "channels" and "bars") was defined applying the estimate procedure to limited portions of the channel.

It is worth noting that our transport estimates are based on τ^* calculations carried out along cross-sections, so the obtained values derive from the volume of material entrained from the streambed (i.e. surface and mobile layer thickness) crossed by the section. Considering that those sediments, arrived from upstream in a previous period, is part of the bed and it is moving downstream along the channel, it represents the bed material load that is passing through a section for a specific competent event or period.

4. Results

4.1 Cross-sections geometry and bed sediment structure

Sections 1 and 2 (located within reach 2, respectively 1857 m and 2199 m downstream from the dam) are characterized by single-thread configuration, widths of 106 m and 88 m and hydraulic radius (R_h, calculated at the water level reached at the event 6 peak, the maximum discharge that occurred during the study period) of 2.33 m and 2.73 m, respectively (Figure 4a, b). From the results obtained comparing the 111 available surface and sub-surface grain sizes (Brenna et al., 2018) (Table 3), the streambed is highly armored (calculated as $D_{50}^{surf}/D_{50}^{subsurf}$ and interpreted in accordance with Hassan et al., 2006) in all the morphological units. Sections 3 and 4 (located within reach 3, respectively 3152 m and 3294 m downstream from the dam) have wandering morphology, widths of 138 m and 129 m and hydraulic radius of 1.80 m and 2.20 m, respectively (Figure 4c, d). Bed armoring ranges from moderate to high since secondary channels and bars sediments are significantly finer than sediments in the main channel (Table 3).

	Sub-surface		All section surface			Main channel			Secondary channel			Bar		
	D_{50}	D_{84}	D_{50}	D_{84}	Ar	D_{50}	D_{84}	Ar	D_{50}	D_{84}	Ar	D_{50}	D_{84}	Ar
S1	36	79	70	122	1.94	107	192	2.97	58	110	1.61	63	118	1.75
S2			72	135	2.00									
S3			56	110	1.55	86	161	2.39	42	79	1.17	53	104	1.47
S4			54	106	1.50									

Table 3. Grain size and armor ratio (Ar= $D_{50}^{surf}/D_{50}^{subsurf}$) of channel sediments obtained through different grouping criteria (S= section).

Each event reached a certain maximum stage at each cross-section (Figure 4), being events 8 and 6 the smaller and higher in terms of water height, respectively (see Table 1). At the peak of the largest event (event 6, with a recurrence interval of 2.1 yr) the water covered almost the whole channel area at all the sections, but it did not reach the adjacent floodplain and terraces being the river incised along the entire study sector.

4.2 Relationships between transport estimates and hydrological characteristics of competent events

Each event-section (q^{event}) transport estimate carried out by the virtual velocity approach refers to a specific cross-section and event. We described the events by two hydrological parameters: the discharge at the peak (Q_w^{max}, in $m^3 s^{-1}$) and the effective runoff (ER, in m^3) calculated as the volume of water flowing during the whole competent event. Bed material transport at sections 1 and 2 is always much lower (about -75%, in the range of the studied events) than the values estimated at sections 3 and 4 (Figure 5).

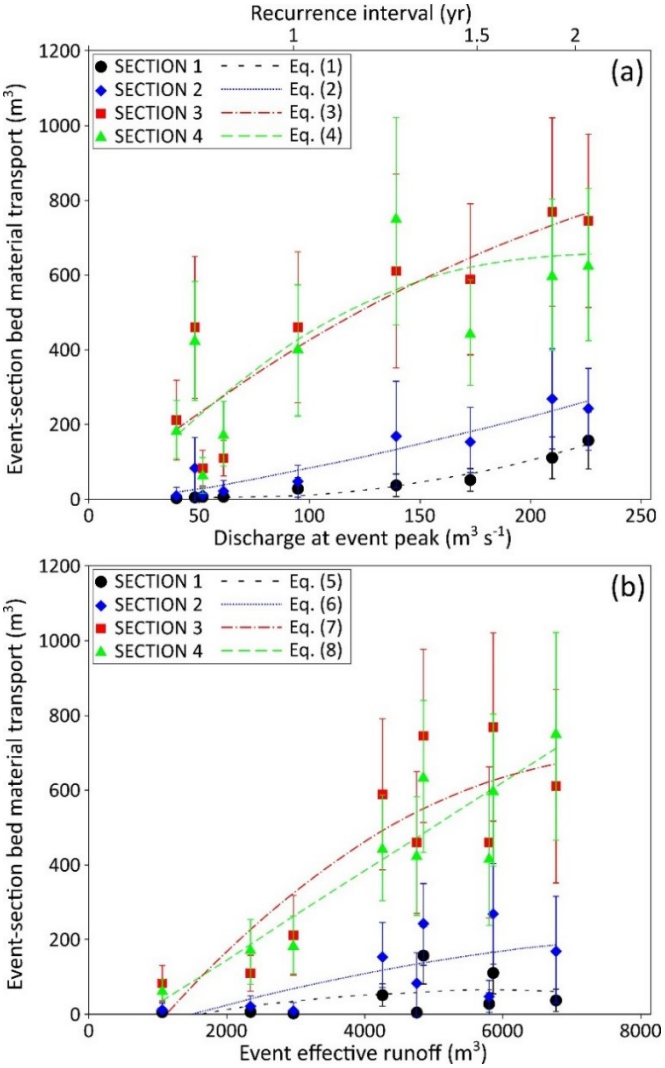

Figure 5. Bed sediments load volumes calculated for all analyzed events at the four cross-sections plotted in function of two different hydrological parameters (maximum water discharge at the event peaks (a) and event effective runoffs (b)) of the competent floods. Lines refer to equations from (1) to (8) reported in the text.

In order to find a relation between the hydrological features of the events and the transport estimates, simple and multiple regression analysis have been performed between Q_w^{max}, ER and q^{event} data.

The best relations obtained by simple regressions between q^{event} estimates and Q_w^{max} (Figure 5a) are:

$$\text{Section 1 } q^{event} = 0.0047(Q_w^{max})^2 - 0.499Q_w^{max} + 14.74 \ (R^2 = 0.98) \quad (1)$$

$$\text{Section 2 } q^{event} = 0.0018(Q_w^{max})^2 + 0.823Q_w^{max} - 18.20 \ (R^2 = 0.89) \quad (2)$$

$$\text{Section 3 } q^{event} = -0.0067(Q_w^{max})^2+4.892Q_w^{max}+3.09 \ (R^2= 0.78) \quad (3)$$

$$\text{Section 4 } q^{event} = -0.0167(Q_w^{max})^2+6.913Q_w^{max}-80.19 \ (R^2= 0.67) \quad (4)$$

The best relations obtained by simple regressions between q^{event} estimates and ER (Figure 5b) are:

$$\text{Section 1 } q^{event} = -4*10^{-6}(ER)^2+0.042ER-57.46 \ (R^2= 0.25) \quad (5)$$

$$\text{Section 2 } q^{event} = -3*10^{-6}(ER)^2+0.060ER-82.97 \ (R^2= 0.46) \quad (6)$$

$$\text{Section 3 } q^{event} = -2*10^{-5}(ER)^2+0.238ER-246.78 \ (R^2= 0.74) \quad (7)$$

$$\text{Section 4 } q^{event} = -5*10^{-7}(ER)^2+0.123ER-97.85 \ (R^2= 0.82) \quad (8)$$

The coefficients of determinations of the regressions obtained for sections 1 and 2 event transport are higher when the peak discharge is considered (Eqs. 1 and 2), whereas for section 3 and 4 transport estimate is well explained also by the effective runoff, particularly in section 4.

The best relations obtained by multiple regressions between q^{event} estimates, Q_w^{max} and ER are (S.E. is the Standard Error of the regressions):

$$\text{Section 1 } q^{event} = -27.78+0.75Q_w^{max}+0.001ER \ (R^2= 0.88, \text{S.E.}= 21.90) \quad (9)$$

$$\text{Section 2 } q^{event} = -67.79+1.14Q_w^{max}+0.011ER \ (R^2= 0.92, \text{S.E.}= 33.48) \quad (10)$$

$$\text{Section 3 } q^{event} = -102.44+2.12Q_w^{max}+0.071ER \ (R^2= 0.94, \text{S.E.}= 71.37) \quad (11)$$

$$\text{Section 4 } q^{event} = -115.89+1.30Q_w^{max}+0.089ER \ (R^2= 0.93, \text{S.E.}= 73.43) \quad (12)$$

The coefficients of determinations of the multiple regressions are remarkably higher in comparison with the simple regressions R^2 at sections 3 and 4 while at sections 1 and 2 they are similar with those obtained considering only the Q_w^{max}.

4.3 Partial transport: assessing its role in relation to magnitude event and cross-section characteristics

For each section-event transport estimate we calculated the percentage of total bed material load (q^{event}) entrained and transported from the streambed under partial transport condition. Distinguishing between the estimates obtained for different sections, the contribution of partial transport to total bed material load (%PT) has been related with the

magnitude of the competent event expressed in terms of discharge at the event peak (or recurrence interval) and effective runoff (Figure 6a, b).

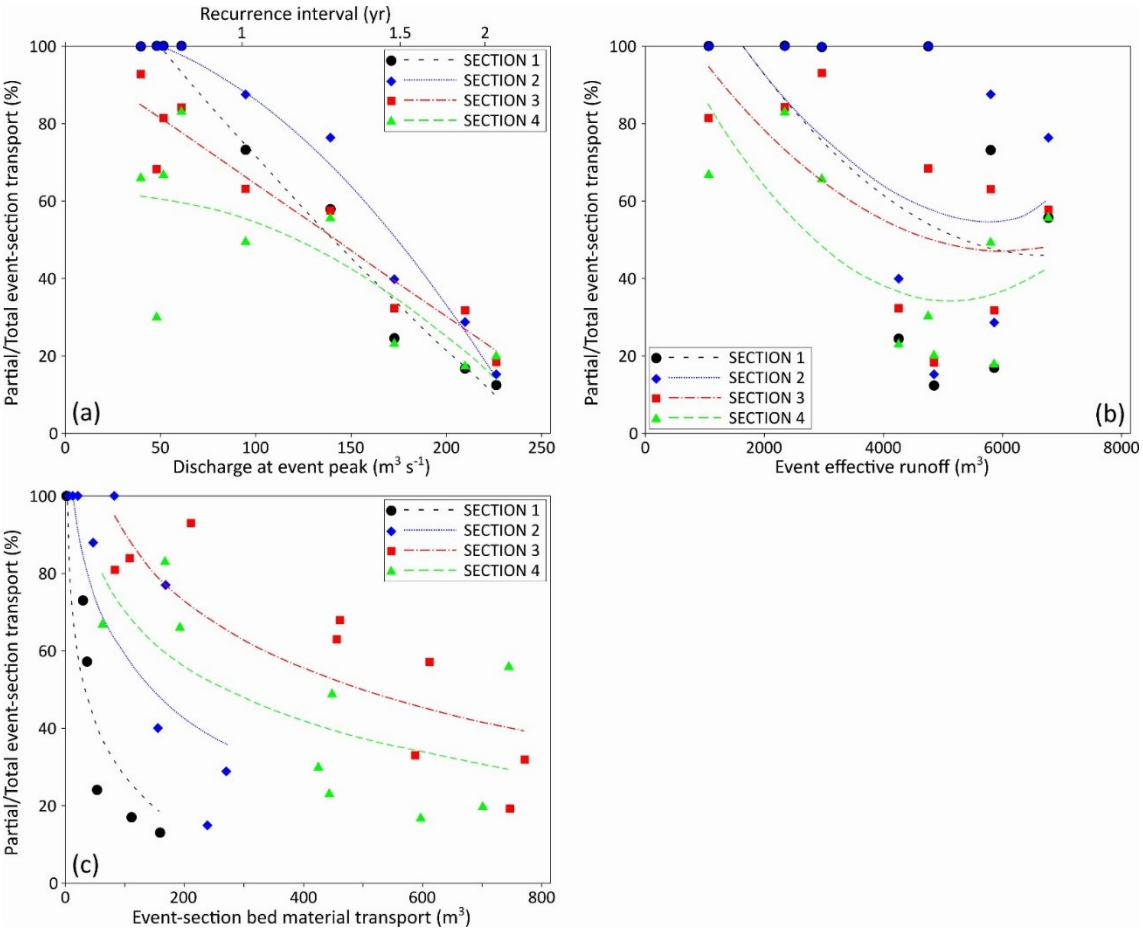

Figure 6. Relative contribution of partial transport to the total bed material load at the four considered cross-sections during the nine analyzed events as a function of two hydrological parameters describing the competent floods ((a) and (b)) and of the total bed material transport estimated at each section for each event (c).

Evidences show that at higher magnitude events the relative contribution of the partial transport decreases substantially for all considered sections. The %PT contribution varies from 66-100% for event 8 (the lowest one, RI<1 yr) to 13-20% for event 6 (the highest one, RI=2.1 yr). Since the use of the RI (based on the event Q_w^{max}) could be misleading in evaluating the flood magnitude, the %PT have been related also with the event effective runoff (Figure 6b). Despite a higher data dispersion, a general decrease of the partial transport contribution increasing the event ER is still recognizable, with a slight increase for events with very high ER. Conforming to this general trend, each section is characterized by different propensity to partial transport, expressed in figures 6a and 6b as the data

dispersion at a fixed water discharge. To better visualize that differences, the event-section contribution of partial transport have been related with the total q^{event}, distinguishing between estimates carried out at the four sections (Figure 6c). At sections 1 and 2, for low values of transport the partial mobility represents the only active mechanism (%PT=100%) whereas, increasing the mobilized volume of bed material, the partial transport contribution decreases rapidly (about 10-25%). Sections 3 and 4 show a different behavior, since full transport occurs (%PT= 65-90%) even at low total q^{event}, whereas increasing the bed material load the partial transport contribution remains relevant (%PT=20-60%).

4.4 Morphological units contribution to the total bed material load

By discretizing the cross-sections based on the morphological units identified within the channel (Figures 3 and 4), it was possible to determine for each event the transport contribution provided by specific morphological features such as "channels" (i.e. main and secondary channels units) and "bars" (i.e. low and high bars units). Summing the bed material load estimates for the nine considered events, we calculated the contribution provided by channels and bars to the total bed material load at the four sections during the entire study period (i.e. 17 months). Considering the values of transport estimated for the different morpho-units (Figure 7a), the bars contribute with comparable volumes at the four sections (ranging from 172 m^3 at section 1 to 566 m^3 at section 3), whereas the channels provide extremely different sediment fluxes with bed material load varying between 226 m^3 at section 1 to 3463 m^3 at section 3.

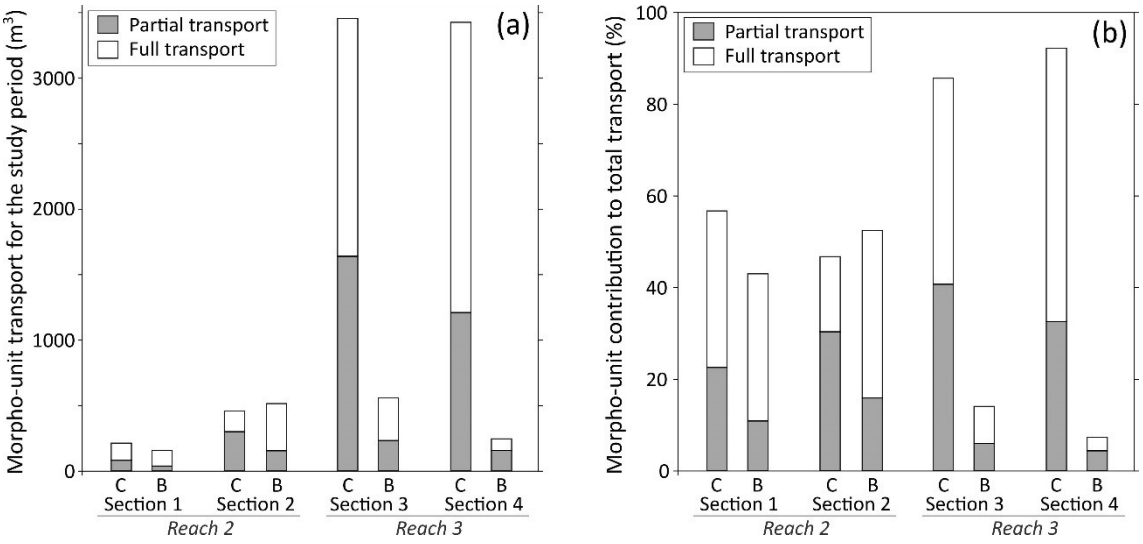

Figure 7. Bed material load calculated at the four cross-sections for different morphological units (C: channels; B: bars) during the entire study period. In plot (a) values are reported as total volume of

mobilized material from each section while in plot (b) are expressed the percentages of transport mobilized from each morpho-unit.

At sections 1 and 2 the contributions of channels and bars are similar, with a prevalence of material moved from the channels at section 1 (57% of the total bed material load) and a slight prevalence of sediments entrained from bars at section 2 (53%) (Figure 7b). Processes are very different at sections 3 and 4 (reach 3) where almost all transport takes place within the channels (86% at section 3 and 93% at section 4) and bars slightly contribute to sediment mobilization (Figure 7b).

4.5 Longitudinal variability of bed material load and transport processes

As anticipated by figures 5 and 7a, the estimated q^{event} and the total values of transport obtained for the study period show an increasing trend moving from upstream (i.e. 1 and 2, located within reach 2) to downstream sections (i.e. 3 and 4, located within reach 3). Plotting all the estimates results as a function of the distances between the sections and the dam zero-flux boundary (Figure 8a), for all competent events, regardless of flood magnitude, it appears that transport significantly increases moving away from the dam, reaching the maximum at section 3 and then slightly decreasing at section 4. Considering the event magnitudes (here expressed as Q_w^{max} or RI) it was possible also to analyze the longitudinal variability of the partial transport contribution (Figure 8b). High magnitude events (in particular events 3 and 6 with RI of about 2 yr, inducing higher transport for all sections) show a slightly increase of %PT moving downstream along the study sector while during low magnitude events the %PT are higher at section 1 and 2 and lower at sections 3 and 4.

Total bed material load (i.e. full plus partial transport) at the four cross-sections during the entire study period (i.e. calculated adding at each section the estimates obtained for the nine competent events) (Figure 9) strongly increases moving from sections located within reach 2 (397±217 m^3 at section 1 and 994±603 m^3 at section 2) to sections located within reach 3 (4030±1520 m^3 at section 3 and 3626±1280 m^3 at section 4). The total volume of material moved under partial transport conditions is equal to 107 m^3, 463 m^3, 1882 m^3 and 1327 m^3 for sections 1, 2, 3 and 4, respectively.

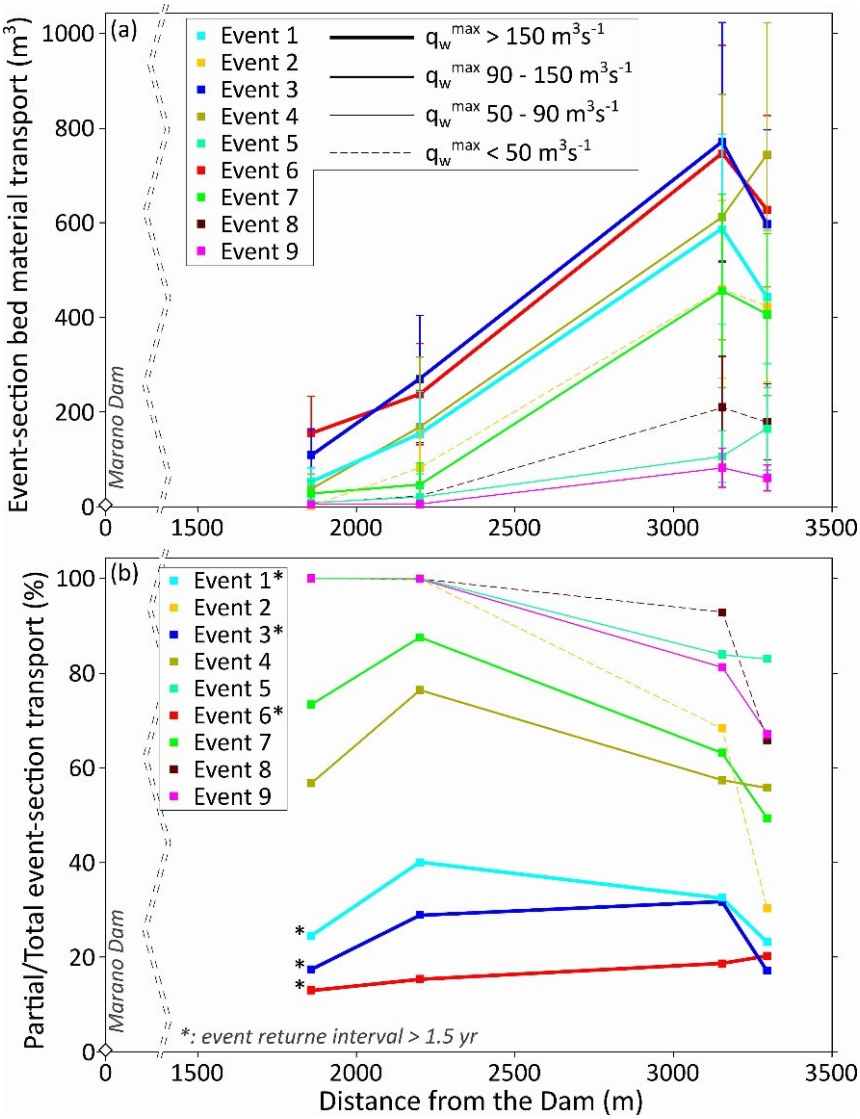

Figure 8. Bed material load (a) and partial transport contribution (b) estimated for each analyzed event at the four considered sections, plotted in function of the distance from the zero-flux boundary (i.e. Marano dam). Lines from thin to thick indicate events with increasing magnitude.

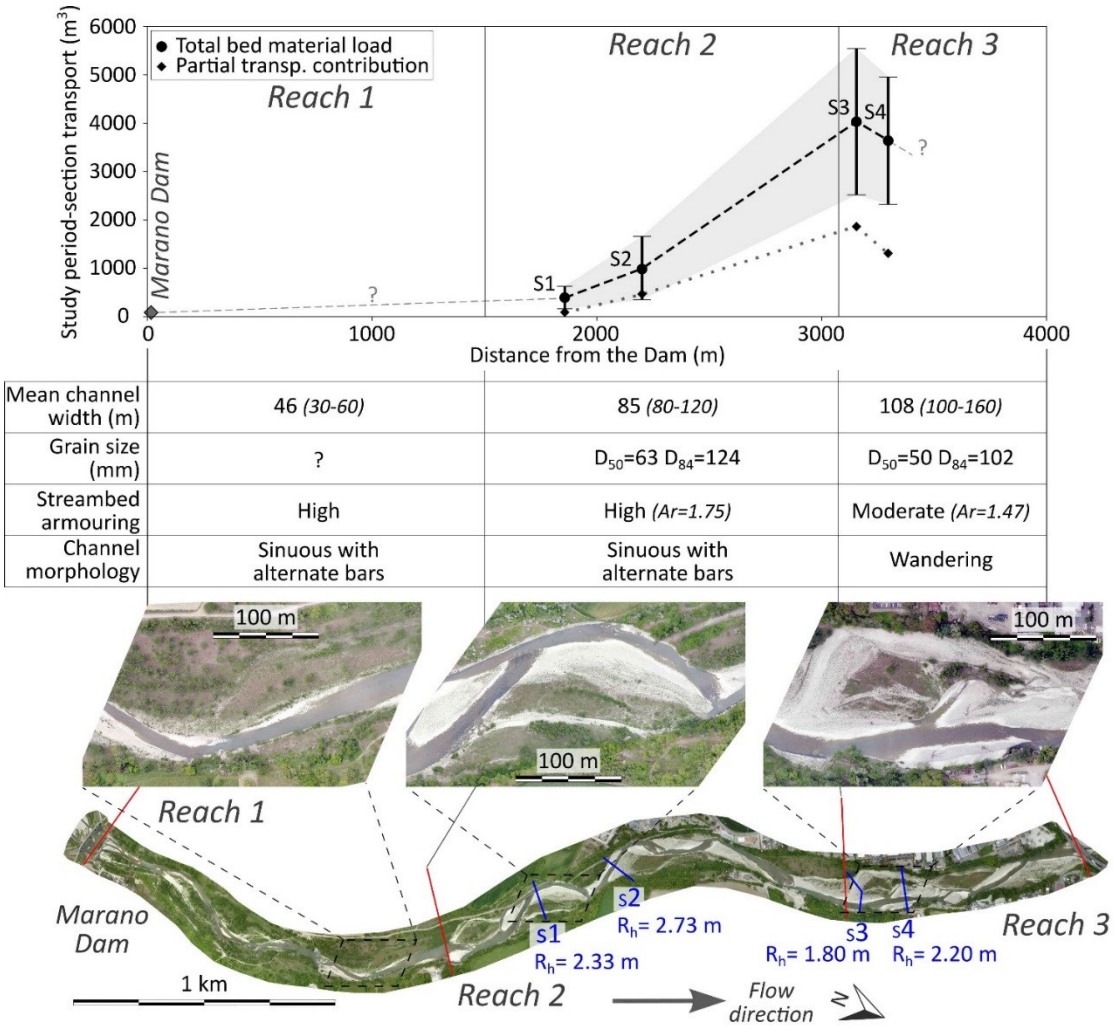

Figure 9. Total bed material load estimated at the four cross-sections during the calculation period (January 2016 – May 2017) and detail of the partial transport contribution related with the characteristics of the study sector. For each reach some morphological and bed sediment features are reported coupled with example images obtained from drone photographs.

Being the sections topographies different for each flood due to local erosion and deposition processes, the discharge thresholds required for inducing transport at each section are not steady in time. Our calculations show that for sections 1 and 2 the minimum discharge required to identify a competent water flow (i.e. inducing local τ^* sufficient to trigger at least partial transport in a 1-m wide portion of cross-section) is about 20 $m^3 s^{-1}$, while at sections 3 and 4 considerably lower values (between 7 and 13 $m^3 s^{-1}$) are sufficient. The thresholds required for local (i.e. 1-m of section) full transport range between 80 and 90 $m^3 s^{-1}$ and around of 25 $m^3 s^{-1}$, in sections 1 - 2 and sections 3 – 4, respectively. According to such thresholds, sediment mobility varies widely along the study sector. Considering the hourly water discharge, sections 1 and 2 experienced respectively 50 and 99 days of partial

transport and 3 and 4 days of local full mobility during the entire calculation period (463 days between January 2016 and May 2017). Local partial transport took place at sections 3 and 4 respectively for 117 and 119 days, while full transport was locally active for 32 and 46 days.

5. Discussion

5.1 Which hydrological parameters better explains bed material load?

Being the adopted estimation method based on the evaluation of the tractive stress induced by the water flow on the streambed during a competent flood, it is reasonable to expect significant relation between the hydrological characteristics of the event and the estimated bed material load. However, the question is still: which hydrological parameters predicts better bed material load? Considering the R^2 coefficients of the simple regressions, sections 1 and 2 event transport-estimates better fit with the magnitude of the competent events expressed in terms of Q_w^{max} (as in Schneider et al. (2014)), section 3 estimates have a similar relation with Q_w^{max} and ER, while section 4 estimates seems to be better explained by the ER of the events (as in Haschenburger (2013b) and Phillips et al. (2013)). At sections 1 and 2 sediments are coarser and structured, and only high water discharges are able to induce adequately τ^* for inducing bed material mobility. Sediment mobility generally occurs only close at the event peaks, when also full transport can locally occur for short intervals (i.e. few hours). For this reason, the discharge at the flood peak (Q_w^{max}) seems to represent a good predictor for describing the bed material load at sections where streambed is high armored. At sections 3 and 4 the streambed sediments are more mobile being finer and less structured. Transport processes are active for longer periods during competent events with significant partial transport occurring also during the rising and falling limbs of the flood. In those contexts, the Q_w^{max} is not sufficient for describing the entire flood characteristics (i.e. the variable hydrograph shape, as observed by Reid at al. (1998) and Powell et al. (2001)) and the event effective runoff (ER) becomes a significant parameter or the most important one (e.g. at section 4) to explain bed sediment transport. Therefore, at sections where sediments have a fairly good mobility, multiple regressions considering both the Q_w^{max} and the ER of an event provide a better prediction of event-section bed material load. Our observations confirm that the hydraulic forcing of sediment transport is superimposed by the sedimentological control (as recently highlighted by Vázquez-Tarrío et al. (2018)) related with the local characteristics of the streambed material.

5.2 The role of partial transport in gravel-bed rivers

In the study sector the Parma River is notably incised (i.e. incision is about 4 m), and thus it seems more appropriate to refer to "bar-full" conditions which occurred during some of the monitored events (i.e. events 1, 3 and 6) rather than "bankfull" conditions. Bar-full conditions comply with some of the criteria adopted in literature to identify the channel forming discharge (e.g. Williams, 1978; Leopold, 1994; Petit and Pauquet, 1997). In agreement with results obtained by Haschenburger and Wilcock (2003) and Mao et al. (2017), our estimates confirm that partial transport plays an important role especially during low magnitude events, while for higher magnitude floods (i.e. bar-full events) full transport becomes the dominant mechanism of sediment mobilization (Figure 6).

Some differences have been observed about the importance of partial transport contribution and its relations with the event magnitude between the four sections. At sections 1 and 2 for low magnitude events, all bed material load occurs in partial transport conditions, while for high magnitude events the full transport becomes the very dominant process. Sections 3 and 4 have a more smooth behavior characterized by full transport also for low magnitude events (although partial transport is dominant) which becomes the main mechanism for high magnitude events during which partial transport still maintains a significant role. These differences can be interpreted in terms of channel geometry and sediment characteristics. Sections 1 and 2 have higher hydraulic radius and high streambed armoring while sections 3 and 4 have lower hydraulic radius and lower armoring. These characteristics would suggest that the high armoring at sections 1 and 2 inhibits the full transport onset for low magnitude events, despite the high hydraulic radius promoting higher shear stress. On the other hand, when the flood becomes as competent as necessary to mobilize the armored layer (e.g. breakup of armor layer, see Vericat et al. (2006)) almost all transport takes place in full mobility conditions. Where the sediments are less structured (i.e. sections 3 and 4) partial and full transport mechanisms are less discrete, being locally active at the same time for a wide range of flood conditions. In accordance with some of the results carried out by Vericat et al. (2008), the streambed sediments conditions (e.g. grain size, armoring, structure) appear to be the most important control factor on the activation of different transport mechanisms and so on the importance of the partial transport contribution for specific locations and events.

5.3 What is the role of different morphological units to total bed material load?

The bed material load that moved on the bars over the whole calculation period is similar at the four considered sections. However, the transport within the channels is one order of magnitude higher at the sections 3 and 4 than at sections 1 and 2. Therefore, channels and bars similarly contribute to the total section-transport at reach 2, whereas the majority of sediment flux moves within the channels at the reach 3 (Figure 7). Observations at reach 3 comply with those of previous studies in terms of morphological units mobility (e.g. Harvey et al., 1979; Haschenburger and Wilcock, 2003; Surian et al., 2009; Bertoldi et al., 2010; Surian et al., 2015). Indeed, channels experienced sediment transport (potentially also full mobility) during floods within the range of considered events (also for event with RI lower than 1 year) while bars are activated during floods with higher magnitude, but still relatively frequent (i.e. floods with RI lower than 1.5-2.5 years) (e.g. Surian et al., 2015). In reach 2 the river bed is highly armored and the main channel shows an extremely developed armor layer able to partially inhibit the streambed material entrainment and transport (e.g. Reid and Laronne, 1995; Pitlick et al., 2008). Besides, channel configuration is single-thread, without secondary channels. For those reasons, the transport contribution of channels significantly decreases along reach 2, becoming comparable with contribution from the bars, and leading to a low total bed material load.

The relations adopted in this work for the transport estimation derive from the field data collected by Brenna et al. (2018) which installed passive tracers mainly on bars and secondary channels. Due to the importance of the transport occurring within the main channel (as observed also by Liébault et al., 2012), it is advisable to collect in the future more information about the sediment dynamics in this morphological unit. Since the passive tracers require to be installed in zones only periodically flooded for allowing their recovery (e.g. bars and secondary channels), the combined use of active tracers (see Hassan and Roy, 2016) seeded in the main channel (e.g. McNamara and Borden, 2004; Cassel et al., 2017) could represent an improvement for monitoring sediment mobility of the whole channel bed.

5.4 Longitudinal transport variability and effects induced by the dam

Our bed material load estimations show a significant increasing trend moving away from the zero-flux boundary represented by the Marano Dam (Figure 9). In addition, the description of the transport processes at the different sections (in terms of partial transport dynamics, contribution provided by different morphological units and sediment mobility at

different flow stages) confirms a progressive trend from section 1 to section 4 according with the longitudinal gradients of the study sector characteristics. In accordance with results provided by several works focusing on gravel-bed rivers responses to dam closure in terms of channel morphology (e.g. Petts, 1979; Andrews, 1986; Sear, 1995; Kondolf, 1997; Grant et al., 2003; Graf, 2006; Curtis et al. 2010) and bed sediments (e.g. Vericat et al., 2006, 2008; Lobera et al., 2017), the current channel features observed downstream from the Marano dam reflect the impact induced on the study sector by the interventions carried out between 1988 and 2005. Indeed, the channel upstream from the dam is on average 300 m wide and characterized by braided morphology and median surface grain size of 45 mm with little armor evidences (unpublished field observations). Instead, downstream of the dam, the channel is narrower and morphologically less complex, and the bed is less armored moving from reach 1 (i.e. the closest to the dam) to reach 3 (Figure 9). Being the sediment transport a key control factor on the morphodynamics of an alluvial channel (Church, 2006), interrupting the longitudinal transfer of coarse material by the dam induced the observed disturbance on transport processes, channel morphology and bed-channel structure.

Sections located within reach 2 are strongly impacted by the dam, although higher disturbance may be expected in reach 1 which was not analyzed in this study. High water discharges are required to activate the sediment mobility (especially full transport) since the overall sections armoring is high. In particular, the main channel armoring, likely generated by progressive selective erosion as described by Parker and Sutherland (1990), inhibits the grain entrainment causing a decrease of the overall bed material load (in accordance with the observation carried out by Dietrich et al., 1989). Sections at reach 3 (i.e. 3 and 4, further from the dam) maintain sediment dynamics more close to those observed in un-impacted river contexts. Bed material is more mobile and transport occurs within a range of water discharges comply with those described in literature in different morpho-units (e.g. Surian et al., 2015).

Over the entire calculation period (17 months between January 2016 - May 2017, a period characterized by an average hydrological trend) at reach 2 the estimated total bed material transport ranges from $0.4*10^3$ m^3 to $1*10^3$ m^3, while about $4*10^3$ m^3 of bed material load occurred at reach 3. Previous sediment regime estimates carried out using different methods in similar contexts (i.e. gravel-bed rivers characterized by draining areas of about 1000 km^2, channel width ≈ 100 m, channel slope ≈ 0.005 m/m) not impacted by dam, provide remarkable different results. For instance, Mao et al. (2017) obtained through a virtual velocity approach an annual sediment yield between $11*10^3$ and $32*10^3$ m^3 yr^{-1} at

similar sections located along the Brenta River (Italy). Also considering the downstream part of Parma River study sector (i.e. reach 3), our estimates remain much lower than such results. The impact on sediment transport induced by the retention basin dam affects the sediment regime in the study sector some kilometers downstream from the zero-flux boundary. In the Chilliwack River (British Columbia), a gravel-bed river draining 1230 km^2, Ham and Church (2000) calculated by an inverse approach the annual sediment yield of a study sector located downstream of a natural lake which impacts the river in a way similar to a dam, interrupting the coarse sediment transfer from upstream. Their estimates are similar with those obtained in this work, being 4-8*10^3 m^3 yr^{-1} some kilometers downstream from the lake.

As conceptualized in the models proposed by Petts and Greenwood (1985) and Petts and Gurnell (2005), channels respond to upstream impoundment moving from a "pre-dam quasi-equilibrium state" to a new "post-dam quasi-equilibrium state" through a relaxation time (i.e. transient state) which can occur over a time scale from tens to hundreds of years. During this period river morphology, streambed-sediment features and transport regime change responding to the human-alteration. The impacts (e.g. channel degradation) progressively migrate downstream from the dam with variable rates (Malhotra, 1951; Petts, 1984). Based on the different evidences collected moving away from the dam in terms of sediment characteristics (i.e. grain-size and armoring), mobility (i.e. occurrence of partial and full transport) and estimated bed material fluxes, reach 2 is more impacted than reach 3. Considering also that the fist interventions for the construction of the retention basin started thirty years ago (1988), it is reasonable to hypothesize that reach 2 is currently in an advanced phase of its relaxation period, perhaps having already reached its new equilibrium. Reach 3 is probably experiencing its transient adjustment to the post-dam quasi-equilibrium, in fact it still maintains more natural (i.e. un-impacted) characteristics. To address this topic in more detail it is necessary to extend the time-scale of our analysis and to consider also the morphological response of the study sector. In this perspective it would also be possible to assess the effective current-state of each reach and to discuss the future trends of the river sector in terms of morphodynamic response.

6. Conclusions

Considering data collected in the field by a tracers monitoring and applying a virtual velocity approach for estimating the bed material load that occurred in a river sector located downstream from a zero coarse-sediments flux boundary, this work gives new insights

about the impacts of a dam on a large gravel-bed river in terms of sediment dynamics and transport regime alterations. The main outcomes can be summarized as follow.

(i) Relations between the hydrological characteristics of the competent flood and the estimated sediment transport are not straightforward. Considering the events Q_w^{max} and ER, the features of the streambed plays an important role in determining how they can explain the estimated sediment transport. Where the streambed is highly armored, the discharge at the flood peak represents a good predictor for describing the event bed material load while in less bed-structured reaches both the Q_w^{max} and the ER are required for explaining the transport. Such differences are due to the different modes of entraining and transporting the channel material during a flood under the control of the streambed characteristics.

(ii) The partial transport plays an important role during low magnitude events, while full transport becomes the dominant mechanism of sediment mobilization for higher magnitude floods. Despite this general observation, the ratio between partial and full transport contribution to total bed material load is not constant along the whole study sector, varying in function of the streambed features. Where the armoring is higher, full mobility occurs only when the water flow becomes as competent as necessary to induce the breakup of the armor layer, leading almost the total of the sediment mobilization. Where the armoring is lower, partial and full mobility occur at the same time for a wide range of discharge conditions and moderate flows can induce transport since the sediment mobility is not inhibited by the streambed structure.

(iii) Under un-disturbed conditions, the sediment transport flowing through a channel section is more easily activated within the main channel where the tractive forces of the water flow are higher. At reach 3, the local transport estimates confirm this assertion since the majority of the sediment load occurred within the main and secondary channels. Instead, where the main channel is characterized by high armoring and single-tread configuration (i.e. reach 2), channel and bars similarly contribute to the total section-transport.

(iv) All the considered mobility parameters and effects are not constant along the three reaches recognized within the study sector, showing a decreasing trend of the impacts moving away from the dam (i.e. from reach 1 to reach 3). The increase of the bed material transport calculated moving away from the dam (i.e. partial

recovery of the natural sediment mobility) represents the synthetic expression of this longitudinal trend. Among the investigated parameters, the characteristics of the channel material (e.g. grain size, armoring and structure) seems to play a key role in the control of the sediment dynamics.

Our results highlights the impacts that dams can induce on coarse material dynamics and sediment regime in large gravel-bed rivers, which are the primary control factors on the following morphodynamic response in terms of channel reorganization (e.g. morphology) and streambed features alteration (e.g. grain size, structure) (Church, 2006; Church and Ferguson, 2015). Being gravel-bed rivers widespread in several physiographic contexts around the world (Church, 2010) and considering the high number of dams regulating their courses (Oud, 2002; Grant, 2012), the observations carried out in the selected case-study could be useful for understanding the dynamics of other large rivers impacted by dams. The new insights achieved about the coarse sediments dynamics in terms of partial transport contribution, relations between bed material flux and hydrological characteristics of the competent event, and estimates of sediment regimes are likely to be applicable to many other rivers experiencing degradation evolution due to the interruption of longitudinal sediment transfer.

Acknowledgements

This research was supported by funds from the University of Padova (DOR funds). The authors would like to thank: Silvano Pecora, Mauro Del Longo and Monica Branchi from "Servizio Idro-Meteo-Clima" of Arpae Emilia-Romagna for providing hydrological data. Supplementary materials about employed data and numerical results of our calculations are available in the Supporting Information (Appendix 2).

References

Andrews, E. D. (1986). Downstream effects of flaming gorge reservoir on the Green River, Colorado and Utah. *Geological Society of America Bulletin*, *97*(8), 1012-1023. https://doi.org/10.1130/0016-7606(1986)97

Ashworth, P. J., & Ferguson, R. I. (1989). Size-selective entrainment of bed load in gravel bed streams. *Water Resources Research*, *25*(4), 627-634. https://doi.org/10.1029/WR025i004p00627

Bertoldi, W., Zanoni, L., & Tubino, M. (2010). Assessment of morphological changes induced by flow and flood pulses in a gravel bed braided river: The Tagliamento River (Italy). *Geomorphology*, *114*(3), 348-360. https://doi.org/10.1016/j.geomorph.2009.07.017

Brenna, A., Surian, N., & Mao, L. (2018). Virtual Velocity Approach for Estimating Bed Material Transport in Gravel-Bed Rivers: Key Factors and Significance. *Water Resources Research* (under review)

Brierley, G. J., & Fryirs, K. A. (2013). Geomorphology and river management: applications of the river styles framework. Hoboken, NJ: John Wiley & Sons

Carling, P.A. (1987). Bed stability in gravel streams, with reference to stream regulation and ecology. In K.S. Richards (Ed.), *River channels: environment and process* (pp. 321-347). London, UK: Methuen.

Carling, P. A., & Reader, N. A. (1982). Structure, composition and bulk properties of upland stream gravels. *Earth Surface Processes and Landforms*, 7(4), 349-365. https://doi.org/10.1002/esp.3290070407

Cassel, M., Dépret, T., & Piégay, H. (2017). Assessment of a new solution for tracking pebbles in rivers based on active RFID. *Earth Surface Processes and Landforms*, *42*(13), 1938-1951. https://doi.org/10.1002/esp.4152

Church, M. (2006). Bed material transport and the morphology of alluvial river channels. *Annu. Rev. Earth Planet. Sci.*, *34*, 325-354. https://doi.org/10.1146/annurev.earth.33.092203.122721

Church, M. (2010). Gravel-Bed Rivers. In T. P. Burt, R. J. Allison (Eds.), *Sediment Cascades: An Integrated Approach* (pp. 241-269). Hoboken, NJ: John Wiley & Sons

Church, M., & Ferguson, R. I. (2015). Morphodynamics: Rivers beyond steady state. *Water Resources Research*, 51(4), 1883-1897. https://doi.org/10.1002/2014WR016862

Church, M., & Hassan, M. A. (1992). Size and distance of travel of unconstrained clasts on a streambed. *Water Resources Research*, *28*(1), 299-303. https://doi.org/10.1029/91WR02523

Church, M., & Hassan, M. A. (2002). Mobility of bed material in Harris Creek. *Water Resources Research*, *38*(11). https://doi.org/10.1029/2001WR000753

Curtis, K. E., Renshaw, C. E., Magilligan, F. J., & Dade, W. B. (2010). Temporal and spatial scales of geomorphic adjustments to reduced competency following flow regulation in bedload-dominated systems. *Geomorphology*, *118*(1-2), 105-117. https://doi.org/10.1016/j.geomorph.2009.12.012

Dietrich, W. E., Kirchner, J. W., Ikeda, H., & Iseya, F. (1989). Sediment supply and the development of the coarse surface layer in gravel-bedded rivers. *Nature*, 340(6230), 215. https://doi.org/10.1038/340215a0

Ferguson, R. (2007). Gravel-bed rivers at the reach scale. In H. Habersack, H. Piégay, M. Rinaldi (Eds.), *Gravel-bed Rivers VI: from process understanding to river restoration* (pp. 33-60). Amsterdam, Netherlands: Elsevier.

Ferguson, R. I., Bloomer, D. J., Hoey, T. B., & Werritty, A. (2002). Mobility of river tracer pebbles over different timescales. *Water Resources Research*, *38*(5). https://doi.org/10.1029/2001WR000254

Ferguson, R. I., & Wathen, S. J. (1998). Tracer-pebble movement along a concave river profile: Virtual velocity in relation to grain size and shear stress. *Water Resources Research*, *34*(8), 2031-2038. https://doi.org/10.1029/98WR01283

Graf, W. L. (2006). Downstream hydrologic and geomorphic effects of large dams on American rivers. *Geomorphology*, *79*(3-4), 336-360. https://doi.org/10.1016/j.geomorph.2006.06.022

Grant, G. E. (2012). The geomorphic response of gravel-bed rivers to dams: perspectives and prospects. In M. Church, P. M. Biron, A. G. Roy (Eds.), *Gravel-bed Rivers: Processes, Tools, Environments* (pp. 165-181). Hoboken, NJ: John Wiley & Sons

Grant, G. E., Schmidt, J. C., & Lewis, S. L. (2003). A geological framework for interpreting downstream effects of dams on rivers. In J. E. O'Connor, G. E. Grant (Eds.), *A peculiar river* (pp. 203-219). Washington, DC: American Geophysical Union.

Ham, D. G., & Church, M. (2000). Bed-material transport estimated from channel morphodynamics: Chilliwack River, British Columbia. *Earth Surface Processes and Landforms*, *25*(10), 1123-1142. https://doi.org/10.1002/1096-9837(200009)25:10<1123::AID-ESP122>3.0.CO;2-9

Harvey, A. M., Hitchcock, D. H., & Hughes, D. J. (1979). Event frequency and morphological adjustment of fluvial systems in upland Britain. In D.D. Rhodes, G. P. Williams (Eds.), *Adjustments of the fluvial system* (pp. 139-167). Dubuque, IA: Kendall/Hunt Publication

Haschenburger, J. K. (2013a). Bedload kinematics and fluxes. In J. F. Shroder (Ed.), *Treatise on Geomorphology*, *Vol. 9* (pp. 103-123). Amsterdam, Netherlands: Elsevier.

Haschenburger, J. K. (2013b). Tracing river gravels: Insights into dispersion from a long-term field experiment. *Geomorphology*, 200, 121-131. https://doi.org/10.1016/j.geomorph.2013.03.033

Haschenburger, J. K., & Church, M. (1998). Bed material transport estimated from the virtual velocity of sediment. *Earth Surface Processes and Landforms*, *23*(9), 791-808. https://doi.org/10.1002/(SICI)1096-9837(199809)23:9<791::AID-ESP888>3.0.CO;2-X

Haschenburger, J. K., & Wilcock, P. R. (2003). Partial transport in a natural gravel bed channel. *Water Resources Research*, *39*(1). https://doi.org/10.1029/2002WR001532

Hassan, M. A., & Roy, A. G. (2016). Coarse particle tracing in fluvial geomorphology. In G.M. Kondolf, H. Piégay (Eds.), *Tools in fluvial geomorphology* (pp. 306-323). Hoboken, NJ: John Wiley & Sons. https://doi.org/10.1002/9781118648551.ch14

Hassan, M. A., Egozi, R., & Parker, G. (2006). Experiments on the effect of hydrograph characteristics on vertical grain sorting in gravel bed rivers. *Water Resources Research*, *42*(9). https://doi.org/10.1029/2005WR004707

Kondolf, G. M. (1997). Hungry water: effects of dams and gravel mining on river channels. *Environmental management, 21*(4), 533-551. https://doi.org/10.1007/s002679900048

Kondolf, G. M., Gao, Y., Annandale, G. W., Morris, G. L., Jiang, E., Zhang, J., ... & Hotchkiss, R. (2014). Sustainable sediment management in reservoirs and regulated rivers: Experiences from five continents. *Earth's Future*, *2*(5), 256-280. https://doi.org/10.1002/2013EF000184

Leopold, L. B. (1994). A View of the River. Cambridge, MA: Harvard University Press.

Liébault, F., Bellot, H., Chapuis, M., Klotz, S., & Deschâtres, M. (2012). Bedload tracing in a high-sediment-load mountain stream. *Earth Surface Processes and Landforms*, *37*(4), 385-399. https://doi.org/10.1002/esp.2245

Liébault, F., & Laronne, J. B. (2008). Evaluation of bedload yield in gravel-bed rivers using scour chains and painted tracers: the case of the Esconavette Torrent (Southern French Prealps). *Geodinamica Acta*, *21*(1-2), 23-34. https://doi.org/10.3166/ga.21.23-34

Lisle, T. E., Nelson, J. M., Pitlick, J., Madej, M. A., & Barkett, B. L. (2000). Variability of bed mobility in natural, gravel-bed channels and adjustments to sediment load at local and reach scales. *Water Resources Research*, *36*(12), 3743-3755. https://doi.org/10.1029/2000WR900238

Lobera, G., Andrés-Domenech, I., López-Tarazón, J. A., Millán-Romero, P., Vallés, F., Vericat, D., & Batalla, R. J. (2017). Bed disturbance below dams: observations from two Mediterranean rivers. *Land Degradation & Development*, *28*(8), 2493-2512. https://doi.org/10.1002/ldr.2785

Malhotra, S. L. (1951). Effects of barrages and weirs on the regime of rivers. In *Proceedings of the International Association of Hydrological Sciences, 4th Meeting* (pp. 335-347).

Mao, L., Picco, L., Lenzi, M. A., & Surian, N. (2017). Bed material transport estimate in large gravel-bed rivers using the virtual velocity approach. *Earth Surface Processes and Landforms*, *42*(4), 595-611. https://doi.org/10.1002/esp.4000

Mao, L., & Surian, N. (2010). Observations on sediment mobility in a large gravel-bed river. *Geomorphology*, *114*(3), 326-337. https://doi.org/10.1016/j.geomorph.2009.07.015

McNamara, J. P., & Borden, C. (2004). Observations on the movement of coarse gravel using implanted motion-sensing radio transmitters. *Hydrological Processes*, *18*(10), 1871-1884. https://doi.org/10.1002/hyp.1453

Mueller, E. R., Pitlick, J., & Nelson, J. M. (2005). Variation in the reference Shields stress for bed load transport in gravel-bed streams and rivers. *Water Resources Research*, *41*(4). https://doi.org/10.1029/2004WR003692

Oud, E. (2002). The evolving context for hydropower development. *Energy Policy*, *30*(14), 1215-1223. https://doi.org/10.1016/S0301-4215(02)00082-4

Parker, G., & Sutherland, A. J. (1990). Fluvial armor. *Journal of Hydraulic Research*, *28*(5), 529-544. https://doi.org/10.1080/00221689009499044

Petit, F., & Pauquet, A. (1997). Bankfull discharge recurrence interval in gravel-bed rivers. *Earth Surface Processes and Landforms*, *22*(7), 685-693. https://doi.org/10.1002/(SICI)1096-9837(199707)22:7<685::AID-ESP744>3.0.CO;2-J

Petts, G. E. (1979). Complex response of river channel morphology subsequent to reservoir construction. *Progress in Physical Geography*, 3(3), 329-362.

Petts, G. E. (1984). *Impounded rivers: perspectives for ecological management*. Hoboken, NJ: John Wiley & Sons

Petts, G. E., & Greenwood, M. (1985). Channel changes and invertebrate faunas below Nant-Y-Moch dam, River Rheidol, Wales, UK. *Hydrobiologia*, *122*(1), 65-80.

Petts, G. E., & Gurnell, A. M. (2005). Dams and geomorphology: research progress and future directions. *Geomorphology*, *71*(1-2), 27-47. https://doi.org/10.1016/j.geomorph.2004.02.015

Phillips, C. B., Martin, R. L., & Jerolmack, D. J. (2013). Impulse framework for unsteady flows reveals superdiffusive bed load transport. *Geophysical Research Letters*, *40*(7), 1328-1333. https://doi.org/10.1002/grl.50323

Pitlick, J., Mueller, E. R., Segura, C., Cress, R., & Torizzo, M. (2008). Relation between flow, surface-layer armoring and sediment transport in gravel-bed rivers. *Earth Surface Processes and Landforms*, *33*(8), 1192-1209. https://doi.org/10.1002/esp.1607

Powell, D. M., Reid, I., & Laronne, J. B. (2001). Evolution of bed load grain size distribution with increasing flow strength and the effect of flow duration on the caliber of bed load sediment yield in ephemeral gravel bed rivers. *Water Resources Research*, *37*(5), 1463-1474. https://doi.org/10.1029/2000WR900342

Pyrce, R. S., & Ashmore, P. E. (2003). The relation between particle path length distributions and channel morphology in gravel-bed streams: a synthesis. *Geomorphology*, *56*(1-2), 167-187. https://doi.org/10.1016/S0169-555X(03)00077-1

Reid, I., & Laronne, J. B. (1995). Bed load sediment transport in an ephemeral stream and a comparison with seasonal and perennial counterparts. *Water Resources Research*, *31*(3), 773-781. https://doi.org/10.1029/94WR02233

Reid, I., Laronne, J. B., & Powell, D. M. (1998). Flash-flood and bedload dynamics of desert gravel-bed streams. *Hydrological Processes*, *12*(4), 543-557. https://doi.org/10.1002/(SICI)1099-1085(19980330)12:4<543::AID-HYP593>3.0.CO;2-C

Schneider, J. M., Turowski, J. M., Rickenmann, D., Hegglin, R., Arrigo, S., Mao, L., & Kirchner, J. W. (2014). Scaling relationships between bed load volumes, transport distances, and stream power in steep mountain channels. *Journal of Geophysical Research: Earth Surface*, *119*(3), 533-549. https://doi.org/10.1002/2013JF002874

Sear, D. A. (1995). Morphological and sedimentological changes in a gravel-bed river following 12 years of flow regulation for hydropower. *River Research and Applications*, *10*(2-4), https://doi.org/247-264. 10.1002/rrr.3450100219

Storz-Peretz, Y., & Laronne, J. B. (2013). Automatic grain sizing of vertical exposures of gravelly deposits. *Sedimentary Geology*, *294*, 13-26. https://doi.org/10.1016/j.sedgeo.2013.05.004

Surian, N., & Cisotto, A. (2007). Channel adjustments, bedload transport and sediment sources in a gravel-bed river, Brenta River, Italy. *Earth Surface Processes and Landforms*, *32*(11), 1641-1656. https://doi.org/10.1002/esp.1591

Surian, N., Mao, L., Giacomin, M., & Ziliani, L. (2009). Morphological effects of different channel-forming discharges in a gravel-bed river. *Earth Surface Processes and Landforms*, *34*(8), 1093-1107. https://doi.org/10.1002/esp.1798

Surian, N., Barban, M., Ziliani, L., Monegato, G., Bertoldi, W., & Comiti, F. (2015). Vegetation turnover in a braided river: frequency and effectiveness of floods of different magnitude. *Earth Surface Processes and Landforms*, *40*(4), 542-558. https://doi.org/10.1002/esp.3660

Vázquez-Tarrío, D., Recking, A., Liébault, F., Tal, M., & Menéndez-Duarte, R (2018). Particle transport in gravel-bed rivers: revisiting passive tracer data. *Earth Surface Processes and Landforms*. https://doi.org/10.1002/esp.4484

Vericat, D., & Batalla, R. J. (2005). Sediment transport in a highly regulated fluvial system during two consecutive floods (lower Ebro River, NE Iberian Peninsula). *Earth Surface Processes and Landforms*, *30*(4), 385-402. https://doi.org/10.1002/esp.1145

Vericat, D., & Batalla, R. J. (2006). Sediment transport in a large impounded river: The lower Ebro, NE Iberian Peninsula. *Geomorphology*, *79*(1-2), 72-92. https://doi.org/10.1016/j.geomorph.2005.09.017

Vericat, D., Batalla, R. J., & Garcia, C. (2006). Breakup and reestablishment of the armour layer in a large gravel-bed river below dams: The lower Ebro. *Geomorphology*, *76*(1-2), 122-136. https://doi.org/10.1016/j.geomorph.2005.10.005

Vericat, D., Batalla, R. J., & Garcia, C. (2008). Bed-material mobility in a large river below dams. *Geodinamica Acta*, *21*(1-2), 3-10. https://doi.org/10.3166/ga.21.3-10

Wilcock, P. R. (1997). Entrainment, displacement and transport of tracer gravels. *Earth Surface Processes and Landforms*, 22(12), 1125-1138. https://doi.org/10.1002/(SICI)1096-9837(199712)22:12<1125::AID-ESP811>3.0.CO;2-V

Wilcock, P. R. (1993). Critical shear stress of natural sediments. *Journal of Hydraulic Engineering*, *119*(4), 491-505. https://doi.org/10.1061/(ASCE)0733-9429(1993)119:4(491)

Williams, G. P. (1978). Bank-full discharge of rivers. *Water resources research*, *14*(6), 1141-1154. https://doi.org/10.1029/WR014i006p01141

Wohl, E., Bledsoe, B. P., Jacobson, R. B., Poff, N. L., Rathburn, S. L., Walters, D. M., & Wilcox, A. C. (2015). The natural sediment regime in rivers: Broadening the foundation for ecosystem management. *BioScience*, 65(4), 358-371. https://doi.org/10.1093/biosci/biv002

4. ALTERATION OF SEDIMENT TRANSPORT AND CHANNEL MORPHOLOGY IN A GRAVEL-BED RIVER DOWNSTREAM OF A DAM

Andrea Brenna[1], Nicola Surian[1], Joseph M. Wheaton[2] and Luca Mao[3]

[1] *Department of Geosciences, University of Padova, Padova, Italy.*

[2] *Department of Watershed Sciences, Utah State University, Logan, Utah USA.*

[3] *School of Geography, University of Lincoln, Lincoln, UK.*

To be submitted to *Geomorphology.*

Abstract

Alteration of sediment regime represents one of the key factors controlling the response of gravel-bed river to dam closure. This work aims to estimate the spatial-temporal bed material transport variations induced on a 4-km sector of the Parma River (northern Apennines, Italy) upstream bounded by a retention basin dam, and to assess the relations between material transport alteration and changes in channel morphology and bed material characteristics. Historical, remote sensing and field data allowed us to reconstruct the human impact acting on this river, the morphological evolutionary trajectory of the study sector and to estimate, leveraging on a morphological approach, the variation in sediment regime since the dam closure (2005). Coarse material transport immediately downstream from the dam was already low (2.000 $m^3 yr^{-1}$) just after dam closure (2006-2008), but increasing moving downstream along the study sector up to 14.000 $m^3 yr^{-1}$. The second and third considered periods (2008-2016 and 2016-2017) were characterized by much lower sediment fluxes. Morphological analysis shows a dominant channel degradation style (i.e. narrowing and incision) and coarsening of bed material along the whole river sector. Channel morphodynamic has been explained in terms of flowing of a "mobile sediment-wave tail" under-supplied from upstream sediment contribution. In a decennial time interval the dynamics of sediment regime have been completely altered along distances of few kilometers from the dam. Good relations have been recognized between the evolution of sediment regime, morphological responses in terms of channel width and bed elevation changes and bed armoring. Coarse sediment transport effectively controls the evolution of the gravel-bed river to human regulation, but positive or negative feedbacks exist between morphological and sedimentological responses and transport regime.

1. Introduction

Gravel-bed rivers, as a type of alluvial channels, are systems that change their dynamics and architecture responding to different controlling factors (Grant et al., 2013). For

instance, using the classical "balance" conceptual model (Lane, 1955), alluvial rivers can be described as the result of the physical relationship between sediment supply and energy able to transport sediments. Natural factors can broadly affect river dynamics at long time scales (Blum and Törnqvist, 2000; Macklin and Lewin, 2003) while human disturbances modifying flow and sediment regimes produce a large spectrum of effects on channels acting at remarkable short time scales (Gregory, 2006; Hoffmann et al., 2010). Dams represent one of the most impactful human alteration of this kind, affecting the two river-dynamic controlling factors (i.e. water flow regime alteration and interruption of downstream flux of sediment) and channel form through a discrete perturbation (Grant, 2012; Kondolf et al., 2014). Since channel morphology is a direct consequence of sediment transport (Church, 2006; Church and Ferguson, 2015) and in coarse-bedded rivers the episodic bed material transport represents one of the key process controlling their morphodynamics (Ferguson, 2007; Ashmore, 2013; Hashenburger, 2013), it is of crucial importance to quantify the impact induced by a dam on sediment regime and, specifically, how bed material load may change through time and distance downstream from a dam.

Several studies described the wide spectrum of effects induced by river regulation in different river contexts (e.g. Petts and Greenwood, 1985; Brandt, 2000; Petts and Gurnell, 2005), quantifying the perturbation on fluvial system by empirical analyses (e.g. Williams and Wolman, 1984; Pitlick and Wilcock, 2001) and analytical models (e.g. Schmidt and Wilcock, 2008). Most of the previous studies focused on the morphological effects induced by dams on the river channels (e.g. Petts, 1979; Andrews, 1986; Kondolf, 1997; Grant et al., 2003; Graf, 2006), observing that bedload-dominated systems respond to a competency and sediment input reduction through three different styles of adjustment (Petts, 1984): passive response, degradation and aggradation. Degradation occurs when the water flow is still able to mobilize the bed sediments and channel moves toward a new equilibrium with reduced sediment supply by narrowing, incision and morphological complexity reduction (e.g. Sear, 1995; Curtis et al. 2010). The river channel moves from a “pre-dam quasi-equilibrium state” to a “post-dam quasi-equilibrium state” through a relaxation period composed by a first reaction phase (i.e. the time between dam closure and the initiation of changes) and an adjustment phase (i.e. time in which the changes are produced) (Petts and Greenwood, 1985; Petts and Gurnell, 2005). During this period, that can extend from tens to hundreds of years (Petts, 1979; Curtis et al. 2010; Carley et al., 2012), the river morphodinamics (e.g. channel morphology, streambed-sediment features and transport regime) evolves

responding to the human-alteration with impacts that progressively migrate downstream from the dam with variable rates (e.g. Malhotra, 1951; Petts, 1984).

The dams' impact on sediment transport regime has received relatively little emphasis in literature, with some evidences focusing on the bed material mobility revealing the modification of the channel sediments characteristics (i.e. coarsening and armoring) and progressive reduction of grains entrainment and movement (e.g. Pohl, 2004; Vericat et al., 2006, 2008; Lobera et al., 2017). The main challenge for describing the sediment regime alteration in human-impacted systems is the quantification of bed material fluxes, due to the practical issues in carrying out measurements of bed material transport especially in the context of large gravel-bed rivers (Ferguson, 2007; Haschenburger, 2013; Wohl et al., 2015). Some of the few attempts in this direction have been carried out by Vericat and Batalla (2005; 2006) who estimated the transport upstream and downstream from dams in a highly regulated large gravel-bed river (lower Ebro, Spain) using direct-measure field techniques. They highlighted how the reservoirs trap almost all the upstream sediment input and that, since the floods have been only slightly reduced, the material transported downstream from the dams is frequently entrained from the riverbed causing channel degradation. An alternative to direct measurements of bed material load is the inverse method (i.e. solve for flux) or the morphological approach (Lane et al., 1995; Ashmore and Church, 1998; Vericat et al., 2017), which requires topographical information at different dates, also allowing estimation and comparison of mean sediment fluxes during different time periods. The method, if based on sediment budgeting procedures, requires that sediment transport is known at one, or more, river section (e.g. Merz et al., 2006; Surian and Cisotto, 2007). Such section is often taken downstream of a dam or a lake, since coarse sediment flux can be reasonably assumed negligible (e.g. Ham and Church, 2000). Some recent studies employed the morphological approach based on DEMs of Difference (DoDs; see Williams, 2012) for investigating the effects of the sediment continuity below dams, obtaining different results in terms of sediment yield modifications depending by the specific cumulative societal-impacts to the rivers and characteristics of the fluvial system (e.g. Carley et al., 2012; Heckmann et al., 2017).

The case-study selected for this work is the Parma River, an Italian northern Apennines stream (Emilia Romagna Region). We used historical, field and remote sensing data to analyze the extent to which a sector bounded upstream by a dam, responded to human pressures in terms of channel changes, evolution of bed material characteristics and sediment transport regime alterations. We focused the analysis over the period 2006 - 2017,

that is after dam closure (i.e. 2004 - 2005), but reconstruction of evolutionary trajectory of channel morphology was expanded to a much longer period (i.e. 1853 - 2017) to better contextualize recent channel morphodynamics on a longer-term trajectory taking in account also for the previous human impacts (e.g. gravel mining).

Due to the poor quantitative descriptions about the impact of dams on coarse sediment regime in large gravel-bed rivers, it is not currently possible to relate the geomorphic and channel-material responses with their main controlling factor (i.e. bed material flux) using "real data". This work aims to estimate, for the first time, the spatial-temporal bed material transport variations induced by a dam, leveraging a reliable but relatively poorly-applied approach as the morphological budgeting procedure, and to relate them with channel morphology and bed material alterations. Therefore, we aim to analyze the whole river morphodynamic response of the study river taking in account the three main controlling factors (i.e. sediment flux, morphology and channel material) in order to achieve new insights about their relations. Considering that the study sector has been impacted by multiple human-stressors being the closure of the dam the last one, it is important to define its current state in the evolution from the pre- to the post- impact regimes in order to understand if it has already reached a new equilibrium or it is still evolving through a transient state. Specifically, the research objectives are (i) to reconstruct the history of the multiple human-pressures in the river catchment to put the observations carried out for the most recent period (2006-2017) in an evolution context useful to interpret the current study sector conditions; (ii) to understand how (i.e. space, time, magnitude) the bed material transport regime has changed along the study sector since the dam closure; (iii) to define the evolutionary trajectory of the study sector, relating it with the sediment transport variations; (iv) to analyze the present and former channel material characteristics and their variations with the sediment regime changes; (v) to understand the relations existing between the three morphodinamic driving-factors and, finally, (vi) to define the current state of the study sector within its evolutionary trajectory for allowing some consideration about its future trends in terms of morphological and transport-regime evolution.

2. Study Area

2.1 General setting

The Parma catchment is located in the northern Apennines (northern Italy) and covers a total area of 815 km^2 with an elongated North-South shape. The Parma River is a right tributary of the Po River and has a total length of 92 km (Figure 1).

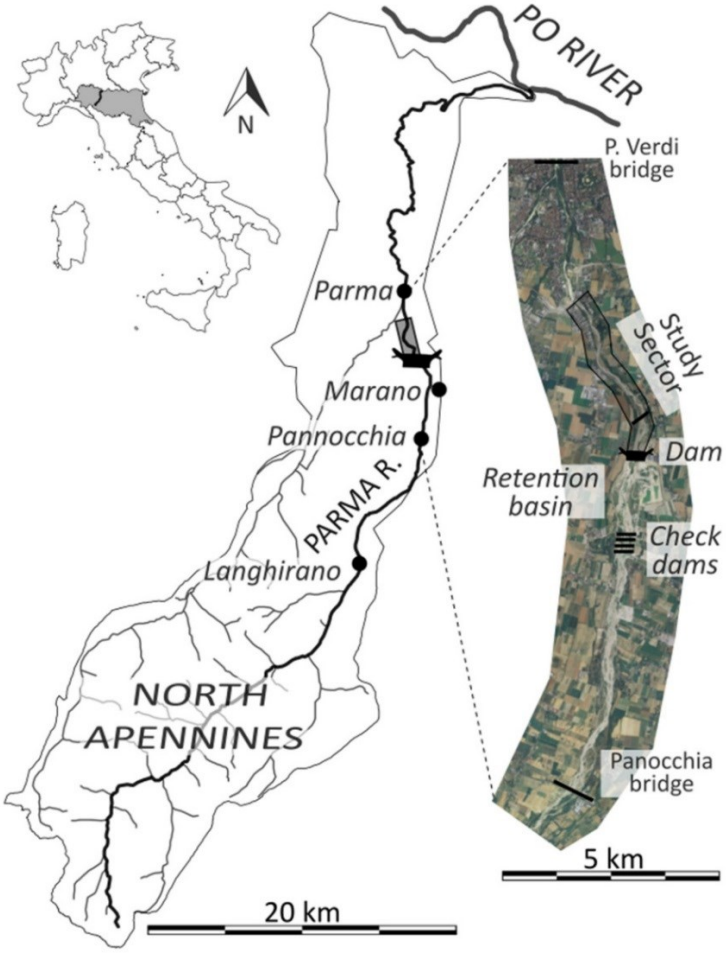

Figure 1. General setting of the Parma River catchment and the study area.

The upper part of the river course is within the Apennines, where outcropping rock (mainly marls, turbidities and limestones) are alternated with glacial and slope deposits. Between Langhirano and Panocchia the landscape is hilly and the river develops a large partially-confined braided configuration. Downstream from Panocchia the river flows into the high plain area, geologically characterized by Quaternary fluvial deposits. River morphology is braided upstream the Marano retention basin and sinuous or wandering between the basin dam and the Parma City. Downstream of the urban segment (where receives the Baganza River contribution), the Parma River displays a meandering morphology, up to the confluence with the Po River (Figure 1).

The catchment climate is characterized by cold winters and dry summers; annual rainfalls vary from 800 to 2000 mm yr^{-1} with most of the precipitation occurring between December and April. Due to the relatively low elevation of the mountain part of the basin, the river hydrological regime is dominated by rainfall. The mean annual discharge

calculated at Parma Ponte Verdi (Parma City) is estimated to be about 11 $m^3 s^{-1}$ but the river regime is very torrential (Figure 2): major floods typically occur during the rainfall period, while discharge is close to zero during the summer months. Analyzing the last 13 years hydrograph (Figure 2) it is possible to observe an homogeneous flow regime: only during the 2009 and 2010 winters, two major floods occurred.

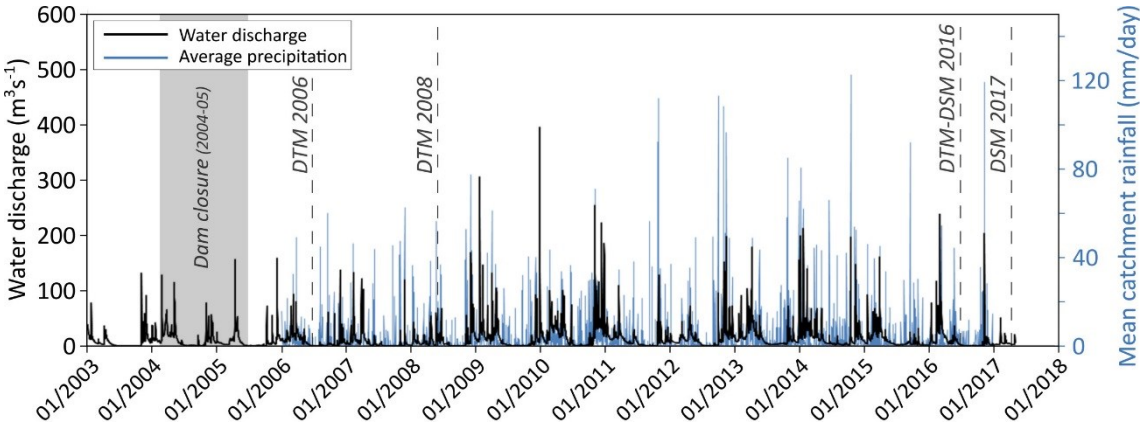

Figure 2. Daily hydrograph and mean precipitations in the Parma River catchment during the period 2004-2017. Dam closure period and employed DEMs data are shown.

2.2 Human impacts

Due to geomorphological and social reasons, during the last century Italian rivers experienced similar evolutionary trends (Surian and Rinaldi, 2003, 2004; Surian et al., 2009a; Scorpio et al., 2015). The North-Apennine rivers experienced a consistent evolutionary trajectory, showing remarkable channel adjustments starting from the end of XIX century in response to a range of human interventions, experiencing channel narrowing, bed incision and evolution from braided to wandering configurations (e.g. Marchetti, 2002; Surian and Rinaldi, 2003; Rinaldi et al., 2005a, 2008; Pellegrini et al., 2008; Bollati et. al, 2014; Clerici et. al, 2015; Gumiero et al., 2015). No previous researches focused to analyze the land use change in the Parma catchment, but in accordance with the results obtained for adjacent Apennine catchments (Duci, 2011; Preciso et al., 2012; Gumiero et al., 2015) and large-scale works (Falcucci et al., 2007; Fuchs et al., 2015), it is likely that the significant reforestation occurred from the end of the XIX century in the upper part of the basins reduced the sediment production. In-channel sediment mining represents the most important human impact on the Parma River. Between the 1920s and the 2000', with maximum rates during the period 1950s – 1980s for the Po Plain infrastructures building (e.g. highways), more than five millions cubic meters of material were extracted by several quarries distribute along the river course. Around 2.330.000 m^3 of in-channel sediments

were mined from the high plain river sector between Panocchia and Parma City (see Figure 1). In order to improve the hydraulic safety of the Parma city and the low plain area, in 1983 local agencies designed a retention basin located upstream of the urban center (near to Marano Village, see Figure 1) to laminate the potentially dangerous flood events. Between 1988 and 1993 basin levees and check dams were built, and in 2004 - 2005 the basin dam was finally closed. Due to his engineering features, the Marano Dam retains all coarse sediments, thus representing a zero coarse-sediments flux boundary. Due to its purposes, the retention basin does not affect the water flow during normal conditions or ordinary floods but, through dam hydraulic maneuvers, it laminates high return time events (RI> 10-15 yr), allowing a maximum discharge of 500 m^3s^{-1}. The dam has never worked between January 2016 and May 2017. Historical discharge data on the Parma River start from 2003 (see Figure 2). For this reason it is not possible to assess to what extent the dam has altered flow regime, but considering the dam characteristics it is very likely that the water discharge recorded over the last 14 years has been impacted to a small degree by the retention basin operations.

2.3 Study sector

We focused our work in a 4 km-long sector located immediately downstream of the Marano dam and closed at the beginning of the urban river segment (Figure 1). This sector was selected because of the presence of the zero-flux sediment boundary, which is essential to estimate the bed material transport using the morphological approach, and because it represents an area potentially impacted by multiple human pressures over the last decades. Three reaches (sensu Brierley and Fryirs (2013) and Rinaldi et al. (2015)) were identified on the basis of the examined features (i.e. channel width, slope and morphology; mean bed material grain size and structuring; presence of bedrock outcropping) (Table 1 and Figure 3).

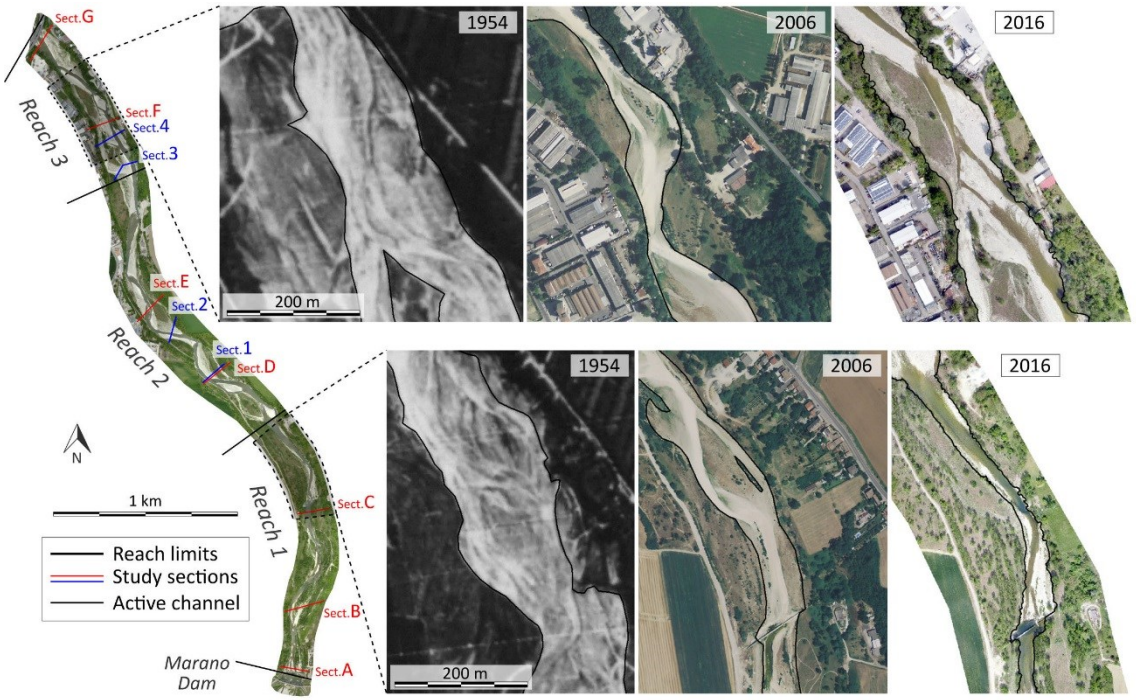

Figure 3. Study sector and extension of the three reaches. Red lines refer to 1972 topographical sections and blue lines identify the positions of the four additional sections considered for the calculation of sediment regimes. The six images on the right show the channel changes at two representative sites over the study period.

	Reach 1 *Length= 1436 m*	***Reach 2*** *Length= 1636 m*	***Reach 3*** *Length= 929 m*
Mean channel width (m)	46	84	109
Mean channel slope (m/m)	0.0053	0.0055	0.0048
Channel morphology	SAB	SAB	W
Mean grain size (mm)	-	D_{50}= 63 mm D_{84}= 124 mm	D_{50}= 50 mm D_{84}= 102 mm
Bed material structuring	High armoring	High armoring	Moderate armoring
Local outcropping of bedrock	Present	Present	Absent

Table 1. Morphological and bed material characteristics of the three reaches identified within the selected study sector (SAB= Sinuous with alternate bars; W= Wandering). See Table (4) for quantitative information about armor ratio.

3. Materials and methods

The multiple analyses conducted in this work, aimed to reconstruct the historical evolution of the channel (i.e. width, morphological configuration and bed elevation) and to estimate the bed material transport by a sediment budgeting procedure, require to use several data types. Table 2 illustrates the main types of data employed in this work whereas in the following paragraphs all specific methods are explained in detail.

Data type	Availability years	Use of data
Historical map	1853	Mapping of channel planform
Aerial/Drone photographs	1954, 1988, 2006, 2008, 2016, 2017	Mapping of channel planform DTM errors estimation
Field topographic cross-sections	1972, 2016, 2017	Channel elevation calculation DTM errors estimation
Digital elevation models	2006, 2008, 2016, 2017	Sediment budget calculation Channel elevation calculation
Field grain-size analysis	2016, 2017	Sediment budget calculation

Table 2. Data types employed in this work.

3.1 Historical channel evolution

3.1.1 Channel planform

An historical map (1853) and six aerial or drone photographs (1954, 1988, 2006, 2008, 2016 and 2017) were used to analyze the channel planform changes over the last 160 years through a multitemporal GIS analysis (Tables 2 and 3). All the material employed for the channel planform analysis was already georectified and it was on-line available from the "Geoportale Nazionale" of Italy and "Geoportale of Emilia-Romagna Region" (historical map and 1954, 1988, 2006 and 2008 photographs) or commissioned by the authors (2016 and 2017 drone photographs). For each of the six considered years, channels were digitized in ArcGIS defining polygons including single channels and bars to derive average active channel width, morphological pattern and related changes over time. Average channel widths were then calculated for the three defined reaches (Figure 3) dividing the channel polygons areas by the reach lengths. Preliminarily we did a coregistration check choosing at least ten stable points along the study sector for the six used surveys. According to previous analyses involving analogous methodologies and data (e.g. Liébault and Piégay, 2001; Surian et al., 2009c; Scorpio and Rosskopf, 2016;), to use historical maps or aerial photographs with a root mean square error (RMSE) ≤ 6 m (1954 photograph) or ≤ 3 m can

lead to errors which are relatively low if compared to the magnitude of channel width modifications.

Year	*Data type*	*Data source*	*Scale*	*Pixel/Cell size (m)*	*Vertical error (m)*	*Use of data*
1853	Historical map	Geoportale E-R	1:50.000	-	-	PM
1954	Aerial photographs (B/W)	Geoportale E-R	1:34.000	1.20	-	PM
1972	Topographic cross-sections	AIPO	-	-	≈ 0.10	EC
1988	Aerial photographs (B/W)	Geoportale Nazionale	-	1.00	-	PM
2006	Aerial photographs (colors)	Geoportale Nazionale	-	0.50	-	PM
	DTM (LiDAR)	AIPO – ARPAE	-	1.00	0.15	MM, EC
2008	Aerial photographs (colors)	Geoportale E-R	-	0.50	-	PM
	DTM (LiDAR)	MATTM	-	1.00	0.15	MM, EC
2016	Drone photographs (colors)	Authors	-	0.04	-	PM, Err
	DTM (LiDAR)	AIPO – ARPAE	-	1.00	0.15	MM, EC
	DSM (Photogrammetry)	Authors	-	1.00	0.08 / 0.15	MM, EC
	Topographic cross-sections (dGPS)	Authors	-	-	< 0.03	Err
2017	Drone photographs (colors)	Authors	-	0.04	-	PM, Err
	DSM (Photogrammetry)	Authors	-	1.00	0.07 / 0.10	MM, EC
	Topographic cross-sections (dGPS)	Authors	-	-	< 0.03	Err

Table 3. Characteristics of employed material. E-R: Emilia-Romagna Region; AIPO: Interregional Agency of the Po River; ARPAE: Local Environmental agency of Emilia-Romagna Region; MATTM: Italian Ministry of the Environment. PM: mapping of channel planform; EC: calculation of channel elevation; MM: application of the morphological method for estimating the bed material fluxes; Err: errors estimation.

Due to the channel type features, the braiding index (Bi) has been used to describe channel morphology at different times. To calculate this parameter we employed the channel-count index proposed by Ashmore (1991). Following the indications of Egozi and Ashmore (2008) and considering the average wetted width of the river**,** an adequate number of sections (e.g. between 10 and 15) were defined for each reach and the number of active channels was counted along the transects deriving then the mean value for each

reach. Despite the possible inaccuracies in the estimation (Surian, 2006) and the variability of the described thresholds (e.g. Rinaldi et al., 2012, 2013, 2016), the braiding index was useful for distinguishing between braided (Bi > 1.5) and other configurations (wandering and sinuous with alternate bars, Bi < 1.5) recognized in this work.

3.1.2 Channel-bed elevation

Bed-channel elevation changes were assessed by comparing seven topographic cross sections acquired in the field by the Interregional Agency of the Po River (AIPO) in 1972 (Figure 3, sections A, B, C, D, E, F, G) with sections extracted using ArcGIS 3D Analyst at the same locations from available DEMs (2006, 2008, 2016 and 2017) (Tables 2 and 3). For each cross section, the mean bed elevation was obtained as the average elevation of all the points of the channel bed starting from the bank toe (Grabowski and Gurnell, 2016). For the 1972 topographic sections, a weighted average elevation taking into account the distance between each pair of points was used (Surian et al., 2009b). Errors in elevation have been accounted considering the different uncertainties associated with the available DEMs (see Table 3). A more detailed explanation of such errors is provided in the next sections.

3.2 Sediment transport estimation

3.2.1 The Morphological Method

As defined by Ashmore and Church (1998), the morphological method is an inverse solution to calculate rates of sediment transport using observations on channel morphology and change in form though time. Several morphological approaches exist, but the fundamental rule is represented by the continuity principle applied to river sediment, involving the quantification of sediment inputs, outputs and storage changes over the time in a defined river sector, expressed as:

$$Q_o = Q_i - (1-p)\delta S/\delta t \qquad (1)$$

where Q_o is the volumetric transport out of the sector per defined time interval (δt), Q_i is the volumetric transport into the sector per defined time, p is the sediment porosity and δS is the change in storage (volumetric variation) occurred over the define time interval in the sector. The method provides robust estimates of the time-averaged (δt, the study period) and space-averaged (the study sector) volume of sediment transport. To define the transport rates at selected locations from explicit channel sediment budgeting (which is a common solution to address the inverse sediment transport estimation, also adopted in this study), it is necessary (i) to measure the erosion and sedimentation volumes and then to

calculate the net change storage for each sector/reach and (ii) to include a known sediment-flux section in the study area (Vericat et al., 2017).

3.2.2 Channel deformation: HRT, terrain models uncertainty and DoDs thresholding

Among the possible ways to determine the net volume change of a reach over the time, we used high resolution topographic (HRT) data involving three LiDAR DTMs (2006, 2008 and 2016) and two photogrammetric DSMs (2016 and 2017) (Table 3) to calculate three DEMs of Difference (DoDs; see Lane at al., 1995, 2003; Brasington et al., 2000; Williams, 2012) of the study sector for the periods 2006-2008, 2008-2016 and 2016-2017. Due to the fact that changes in river bed elevation (i.e. $\Delta z/\Delta t$) are often comparable with the measure techniques errors (Murphy et al., 2008), many studies focused on the uncertainties account (e.g. Brasington et al., 2003; Wheaton, 2008; Wheaton et al., 2010; Milan et al. 2011; Carley et al., 2012). To deal with DEMs uncertainties and their propagation during the DoD derivation procedure (see Passalacqua et al., 2015 and Vericat et al., 2017 for a methodological review), two different strategies were adopted depending on the employed data features.

Referring to 2006, 2008 and 2016 LiDAR DTMs the elaborated terrain models were the only available data (Table 3); no original data and simultaneous aerial photographs or independent check points were available. For this reason, a spatially uniform error distribution was adopted, introducing a constant uncertainty across the surfaces cells equal to ± 0.15 m on the base of typical LiDAR data precision for exposed or mildly vegetated terrains (James et al., 2007) and data-providers indications (Figure 4a). The 2006 and 2008 surveys were acquired during dry periods, so the areas occupied by water are almost equal to zero. For the 2016 survey, the wet part of the channel representing the 8% of the area (where vertical uncertainties are greater) was already removed from the provided DTM.

More sophisticated error modelling was possible for the 2016 and 2017 photogrammetric DSMs obtained by drone (Figure 4b). For those surveys, topographic points measured along the sector by a dGPS during the fieldwork were available (Tables 2 and 3). Elaborating in ArcGIS the original drone photographs, we digitized the 2016 and 2017 channels on the base of the terrain exposure characteristics identifying: well exposed sediments area, poorly vegetated area (e.g. covered by grass), vegetated area (e.g. covered by arboreal vegetation) and wet channels. Overall, 101 and 156 dGPS points measured in the field respectively for the 2016 and 2017 surveys were classified based on their position in the four described classes and the calculated elevation differences between the DSM

surface and the dGPS point altitude at the same position were statistically elaborated to define uncertainties for each terrain class for both surveys. Based on this procedure, two error modellings spatially uniform within specific exposure regions were defined, for each derived DSM surface (Table 4). The two surveys were acquired in May and April, when the vegetated and wet areas occupy a small part of the channel. Furthermore, areas with point density (x,y,z data) equal to zero (e.g. deep water, thick vegetation zones) were automatically excluded from the considered surfaces.

DEM Year	*Vertical uncertainties (m)*				*No points area*
	Exposed sediments	*Poorly vegetated*	*Vegetated*	*Wet*	
2016	± 0.08 (57%)	± 0.15 (19%)	± 1.80 (6%)	± 0.56 (10%)	8%
2017	± 0.07 (53%)	± 0.10 (29%)	± 2.00 (9%)	± 0.21 (5%)	4%

Table 4. Errors and percentage of covered area of each classes adopted for the 2016 and 2017 DEMs uncertainties modelling.

The DEMs and the associated errors surfaces were elaborated using the Geomorphic Change Detection software (GCD) (Wheaton et al., 2010) to derive the three study-sector DoDs (Figure 4). Only for the 2016 both LiDAR DTM and photogrammetric DSM were available (Table 3). We used the DTM for the 2008 - 2016 DoD production and the DSM for the 2016 - 2017 DoD for consistency with the other employed data type (LiDAR DTM and photogrammetric DSM for 2008 and 2017, respectively). The 2006 - 2008 DoD was obtained using LiDAR DTMs for both years. All employed DEMs were concurrent and projected on the same reference system. In order to avoid systematic error of vertical positioning between sequential DEMs that can highly impact on the DoDs calculation procedure (see Lallias-Tacon et al. (2014)), we performed an elevation conformity test conducted comparing elevations of more than ten stable points (e.g. levees, check dams etc.) between each couple of sequential DEMs, which confirmed that the elevation differences were conform with the error range. Uncertainties, associated to each cell by the error surfaces for each DEM, were simply propagated as the sum of the errors of two concurrent DEMs in quadrature. Considering the magnitude of change relative to the propagated error (*t* value) and defining a flexible minimum level of detection (*min*LoD; confidence limit = 95%), the *min*LoD was used to identify DoD cells where the elevation difference is taken to be true. For the 2016-2017 DoD, some additional filters were applied in order to exclude unrealistic variations due to DEMs localized issues (i.e. cell with elevation changes > 5 m; single erosion or deposition area < 2 m^2).

Through the simple equation:

$$\Delta V_{DoD} = \Sigma V_d - \Sigma V_e \qquad (2)$$

where ΣV_d is the total volume of deposition of a sector and ΣV_e is the total volume of erosion of the same sector, both obtained considering only the significant changes of the DoD after the thresholding procedure and multiplying cell-by-cell the $\Delta z/\Delta t$ by the respective cell area (1 m^2), the net sector volumetric changes (ΔV_{DoD}) were calculated. Uncertainties associated with those volumes were estimated by GCG software considering the errors surfaces adopted in the calculations.

3.2.3. Estimate of bed material transport

The three final sector DoDs and calculated ΔV_{DoD} data were elaborated as described above (Figure 4). Seven sections, the three reaches downstream limits and four additional sections located in correspondence to river sites where an independent field bed material load monitoring is in progress (sections 1, 2, 3 and 4, see Figure 3), were defined along the study area, dividing the sector in seven "sub-reaches". ΔV_{DoD} were then spatially splitted out in order to outline the net volume change of each sub-reach using the Budget Segregation procedure provided by GCD software. Imposing the dam like a zero-flux coarse sediment boundary and using the sub-reaches net volume changes, we solved the equation (1) calculating the volume of bed material transport that occurred between two surveys on each of the seven selected sections (q_{out} in m^3). Sediment transport errors were simply obtained adding in quadrature the volumetric changes uncertainties provided by the GCD software. In order to estimate the average annual transport (mean q_{out} in $m^3\ yr^{-1}$), the obtained values (in m^3) were divided by the time between the two DEMs used for the DoD elaboration (2 years for the 2006 - 2008, 8 years for the 2008 - 2016 and 1 year for the 2016 - 2017 DoDs).

For estimating bed material flux (q_{in} and q_{out} in m^3), porosity (p) and a percentage of fine material (i.e. sand and fine gravel) which is not mobilized as bedload need to be calculated. We addressed this issue by acquiring during the fieldwork (January 2016 – May 2017) an adequate number of bed sediments and bank material photographs along the study sector and upstream the Marano retention basin (Table 2). Using surface and vertical exposures photographs, it was possible to estimate the surface and subsurface grain size distributions (Storz-Peretz and Laronne, 2013). The images were processed by the Digital Gravelometer software (Graham et al., 2005a, 2005b, 2010) deriving the mean reaches grain sizes and the

percentage of fine material (< 6 mm, due to the images resolution). The sediment porosity was estimated based on the grain size data. The effective average bed material transport was then calculated considering these two material parameters. The fieldwork allowed us to collect useful additional information about the river-bed setting, describing the sediment fabric and structuring (focusing on armoring evidences, i.e. imbrication and grain sorting) and qualitatively mapping the presence of local bedrock outcroppings along the river channel.

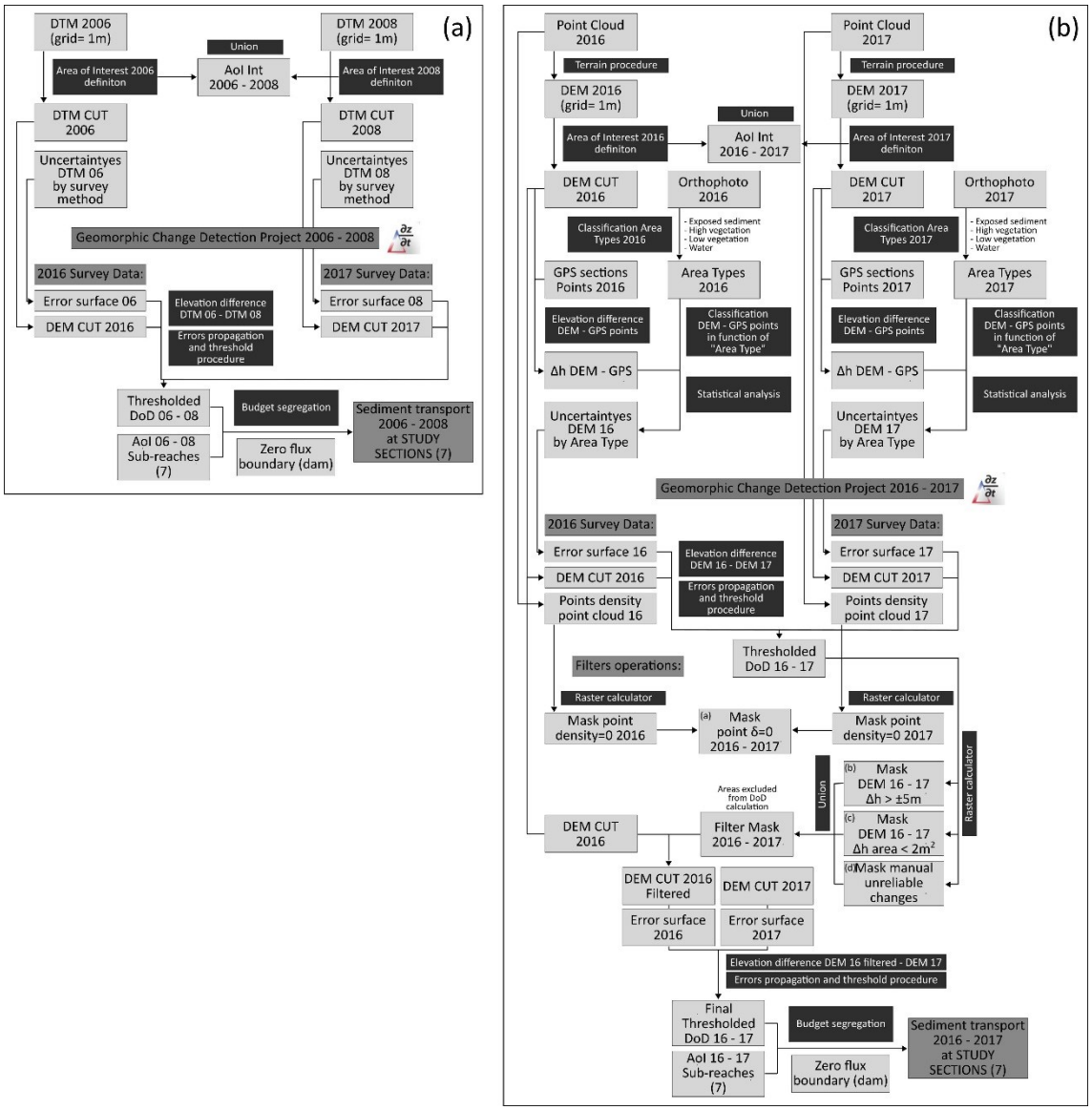

Figure 4. Workflows adopted for the calculation of the sediment transport regimes by the morphological approach for the 2006-2008, 2008-2016 (a) and 2016-2017 (b) periods.

4. Results

4.1. Historical evolutionary trajectory (1853 - 2006)

In order to contextualize present channel processes within the evolutionary trajectory of the river, morphological changes that occurred from the middle of the XIX century to dam closure (2004-2005) were analyzed at the reach scale. The study sector underwent notable channel changes over the last 160 years, specifically channel narrowing and reduction of morphological complexity (Figure 5a and Table 5). From 1853 to 1954 the channel experienced a mean narrowing of 25%, although retaining the original braided configuration. Starting from the '50 an intense sediment exploitation activity superimposed to the changes in land use. Between 1954 and 1988 the river experienced the maximum narrowing rate (mean channel narrowing of 60% at reach 2) and shift from braided to sinuous with alternate bars (at reaches 3). Between 1988 and the dam closure, a homogeneous narrowing process continued and the whole study sector settled on a wandering pattern. The channel evolution can be divided in three phases (1, before 1954; 2, 1954 - 1988; 3, after 1988, see Figure 5a), in accordance with the conclusions obtained for many other Italian rivers (Surian et al., 2009a). The 1972 bed elevation profile is between 2 and 3 m lower than the 1954 surface along the entire study sector. During the period 1972 – 2006, intense incision occurred in reach 1 (up to - 5.50 m at section A) and 2 (up to - 2.40 m at section D), while equilibrium characterized reach 3 (Figure 6).

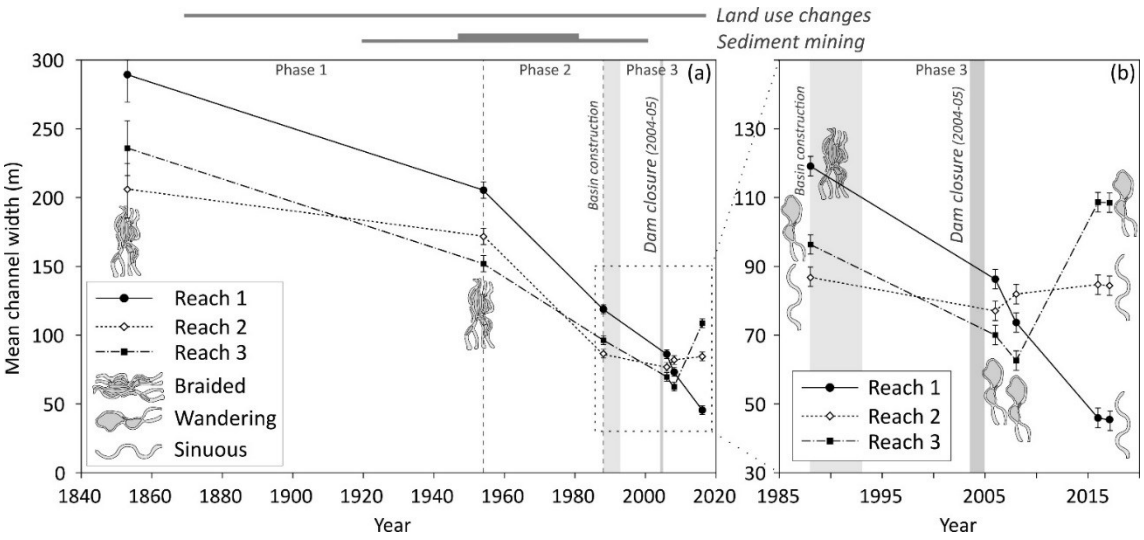

Figure 5. Changes in mean channel width for the three reaches over the long-term (1853-2017) (a) and over the last 30 years (1988-2017) (b). Reaches morphological configurations are plotted as well. Vertical bands identify the basin construction and dam closure periods; horizontal bars indicate temporal interval and relative intensity of the human impacts in the Parma River catchment.

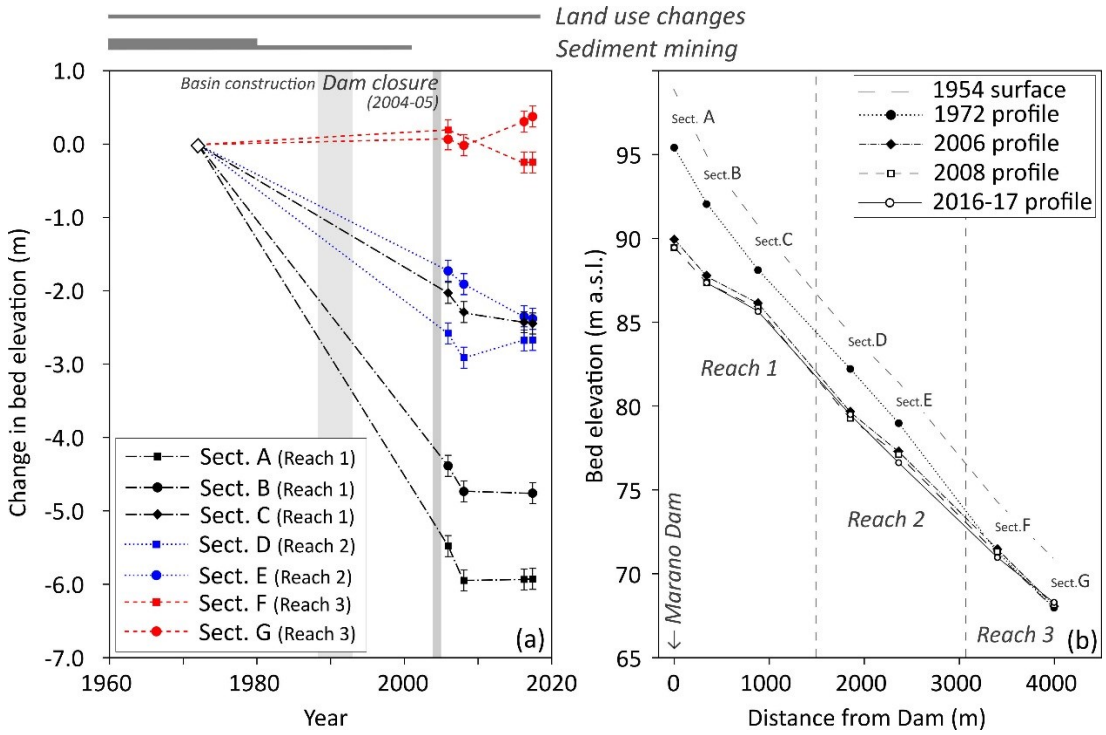

Figure 6. Temporal trends of bed-level changes at the seven cross-sections (a) and changes of the longitudinal bed profiles over the period 1954-2017 (b). In plot (a) vertical bands and horizontal bars indicate time and intensity of human impacts. The 1954 bed surface elevation has been estimated based on the available 1954 aerial photographs for recognizing the active channel position and using the terraces elevation derived from the 2006 DTM.

4.2. Post dam-closure channel changes (2006 - 2017)

An investigation with higher temporal resolution was carried out for the most recent period, i.e. after the dam closure (Figure 5b and Table 5). Reach 1 has undergone the most intense narrowing (-84% from the 1853 width), which is still in progress. Reach 2 has not shown significant changes, while reach 3, after a first narrowing phase (2006 - 2008), started widening again. The 2006 channel pattern did not change until 2008, but during the most recent period (2008 - 2017) only reach 3 has maintained the pre-dam wandering morphology, while the upstream reaches has evolved into a sinuous with alternate bars configuration. In general, a more spatially variable evolution (i.e. reach specific) is recognizable after dam closure, in comparison with the homogeneous behavior of the study sector during the period 1853 - 2006. An accurate reconstruction of bed-elevation changes was possible for the period 2006 - 2017 using the available DEMs (Figure 6 and Table 5). Immediately after the dam closure (i.e. 2006-2008), incision occurred along the entire study sector with decreasing intensity moving downstream from the dam. In reach 1 the incision

was up to -0.55 m at section A, in reach 2 was up to -0.35 m at section D, and reach 3 was in equilibrium (Figure 6a). From the 2008 to the present, reach 1 has not experienced significant changes, reach 2 shows a moderate incision with some locations in aggradation (e.g. section D) and reach 3 is characterized by depositional trend (+ 0.30 m from 2008 to 2017 at section G) but with localized incision zones (e.g. section F) (Figure 6a).

Year	*Data*	*Reach 1*	*Reach 2*	*Reach 3*
1853	Mean Width (m)	290 ± 20	207 ± 20	236 ± 20
	Morphology	Braided	Braided	Braided
1954	Mean Width (m)	206 ± 6	173 ± 6	152 ± 6
	Morphology	Braided	Braided	Braided
1988	Mean Width (m)	119 ± 3	87 ± 3	96 ± 3
	Braiding Index	2.11	1.10	1.33
	Morphology	Braided	SAB	Wandering
2006	Mean Width (m)	86 ± 3	77 ± 3	70 ± 3
	Mean Elevation (m a.s.l.)	86.13	77.66	70.34
	Braiding Index	1.22	1.20	1.50
	Morphology	Wandering	Wandering	Wandering
2008	Mean Width (m)	74 ± 3	82 ± 3	63 ± 3
	Mean Elevation (m a.s.l.)	85.77	77.41	70.29
	Braiding Index	1.44	1.40	1.33
	Morphology	Wandering	Wandering	Wandering
2016	Mean Width (m)	46 ± 3	85 ± 3	108 ± 3
	Mean Elevation (m a.s.l.)	85.72	77.31	70.62
	Braiding Index	1.11	1.20	1.50
	Morphology	SAB	SAB	Wandering
	Grain size surface (mm)	*Hp. D_{50} ≈ 63 ; D_{84} ≈ 124*	D_{50} = 63 ; D_{84} = 124	D_{50} = 50 mm; D_{84} = 102
	Grain size subsurf. (mm)	---------- $D_{50}^{subsurf}$ = 36 ; $D_{84}^{subsurf}$ = 79 ----------		
	Armoring (Armor ratio)	*Hp. + + +*	+ + + (1.75)	+ + (1.47)
2017	Mean Width (m)	46 ± 3	84 ± 3	109 ± 3
	Mean Elevation (m a.s.l.)	85.72	77.29	70.67
	Braiding Index	1.10	1.10	1.20
	Morphology	SAB	SAB	Wandering
	Grain size surface (mm)	*Hp. D_{50}≈ 63 mm; D_{84}≈ 124 mm*	D_{50}= 63 mm; D_{84}= 124 mm	D_{50}= 50 mm; D_{84}= 102 mm
	Grain size subsurf. (mm)	---------- $D_{50}^{subsurf}$ = 36 ; $D_{84}^{subsurf}$ = 79 ----------		
	Armoring (Armor ratio)	*Hp. + + +*	+ + + (1.75)	+ + (1.47)

Table 5. Topographical, morphological and channel material characteristics of the three study reaches at the considered times. "+++" means high armoring and "++" means moderate armoring. SAB= Sinuous with alternate bars.

4.3. Bed material characteristics

Channel material was characterized by using 111 photographs of the bed and incised bar margins (i.e. channel bank) along reach 2 and 3 (see Figure 3) and 36 bed sediments photographs taken upstream the retention basin (near the Panocchia bridge, see Figure 1). From image analysis, the surface study sector sediments are characterized by D_{50} ranging between 63 and 50 mm and D_{84} between 124 and 102 mm, in reach 2 and 3, respectively. No samples are available for reach 1, but field observations make it reasonable to infer that its sediments are similar to reach 2 (Table 5). Similar grain size along the entire study sector was obtained from the vertical photographs analysis, deriving mean D_{50} and D_{84} for the subsurface sediments equal to 36 and 79 mm, respectively. Grains finer than 6 mm in average represent the 20% of volume of sediments in the study reach both for surface and subsurface material. The porosity was calculated using the Carling and Reader (1982) as 0.25 and 0.27 for the surface and subsurface material, respectively. The mean surface grain size obtained for the upstream-dam sampling site (Panocchia bridge: D_{50} = 45 mm, D_{84} = 88 mm) is finer than the study-sector surface distribution but similar to the subsurface one. Field observations allowed us to recognize diffused evidences of bed armoring (i.e. sorting, imbrication, and presence of coarser surface grains), especially along reaches 1 and 2. The obtained armor ratios (calculated as $D_{50}^{surf}/D_{50}^{subsurf}$) confirm field evidences of evident armoring. Indeed, reach 2 has a mean armor ratio of 1.75 (ranging from 1.61 to 2.94), while in reach 3 the mean armor ratio is equal to 1.47 (ranging from 1.17 to 2.39) which are respectively high and moderate values for intermittent rivers (Hassan et al., 2006). Some bedrock outcrops occur along reaches 1 and 2. Such outcrops represent just small portion of the whole channel (less than 1% of channel area) but they do indicate that the alluvial cover is relatively thin in the study sector.

4.4. Estimate of coarse sediment transport

The DEM of Difference (DoD) analysis allowed to identify channel areas that underwent depositional or erosional processes and also to calculate the net volume changes along the whole study sector or its portions (i.e. reaches, sub-reaches) during different time intervals (Figure 7 and Table 6). The 2006 - 2008 DoD highlights predominant erosion along the entire study sector with subordinate volumes of deposition for all reaches. During the second investigated period (2008 - 2016) the three reaches experimented both depositional and erosional processes. The single involved deposited (ΣV_d) or eroded (ΣV_e) volumes are higher than those calculated for 2006 - 2008 DoD but the net reaches volumetric changes

(ΔV_{DoD}) are actually lower and spread over a longer time interval. For the more recent DoD (2016 - 2017), determined over the shortest interval (one year), almost no volumetric variation occurred at reach 1. Both reach 2 and 3 are characterized by limited volumetric changes, respectively by dominant erosion and deposition.

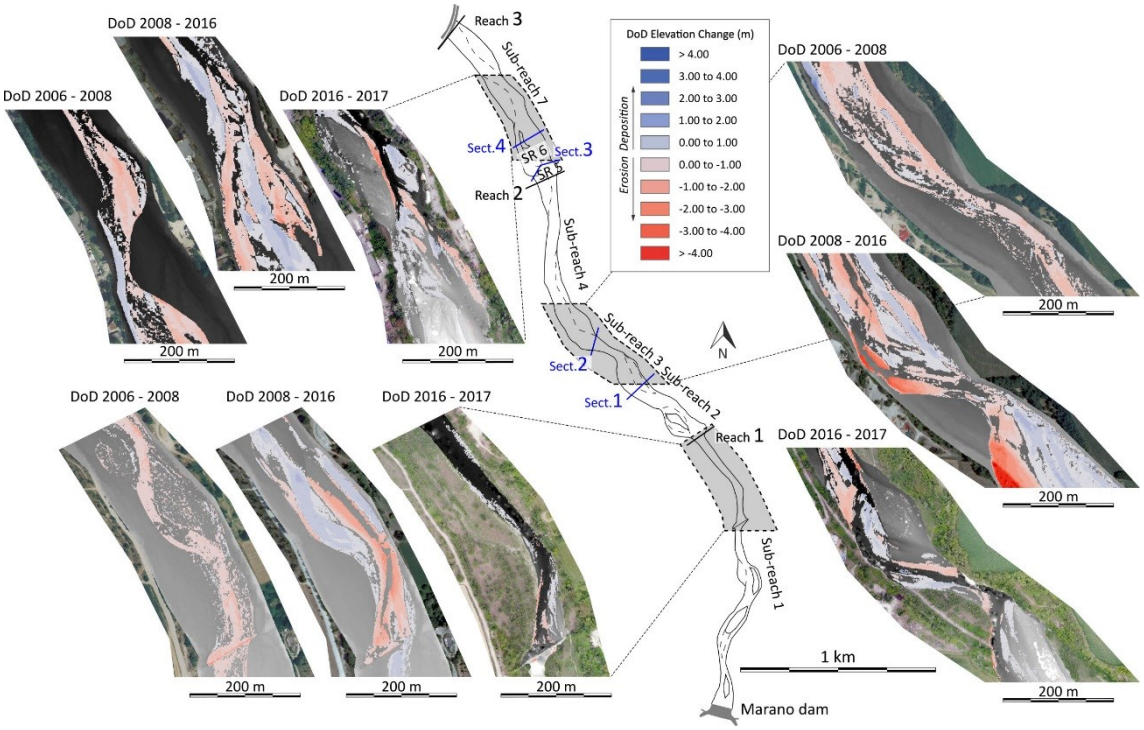

Figure 7. DEM of Difference (DoD) obtained for the three considered time intervals (2006-2008, 2008-2016 and 2016-2017).

Time period	Data	Reach 1	Reach 2			Reach 3		
		Sub-reach 1	*Sub-reach 2*	*Sub-reach 3*	*Sub-reach 4*	*Sub-reach 5*	*Sub-reach 6*	*Sub-reach 7*
		R1 closure	*Section 1*	*Section 2*	*R2 closure*	*Section 3*	*Section 4*	*R3 closure*
2006 - 2008 Δt = 2 yr	ΣV_e (m^3)	12288 ± 4895	14067 ± 4560	8273 ± 2947	38948 ± 11830	3792 ± 1190	8568 ± 2385	22359 ± 7448
	ΣV_d (m^3)	4738 ± 1565	3773 ± 1517	3982 ± 1568	23837 ± 5337	850 ± 327	4608 ± 1447	18327 ± 5347
	ΔV_{DoD} (m^3)	-7550 ± 5138	-10294 ± 4806	-4291 ± 3338	-15111 ± 12978	-2942 ± 1234	-3960 ± 2790	-4032 ± 9166
	V_{in} (m^3)	0	7550 ± 5138	17844 ± 7035	22135 ± 7787	37246 ± 15135	40188 ± 15185	44148 ± 15439
	V_{out} (m^3)	7550 ± 5138	17844 ± 7035	22135 ± 7787	37246 ± 15135	40188 ± 15185	44148 ± 15439	48180 ± 17954
	q_{in} (m^3)	0	4379 ± 2980	10350 ± 4080	12838 ± 4516	21603 ± 8778	23309 ± 8807	25606 ± 8375
	q_{out} (m^3)	4379 ± 2980	10350 ± 4080	12838 ± 4516	21603 ± 8778	23309 ± 8807	25606 ± 8375	27944 ± 10413
	q_{out}^{mean} (m^3 yr^{-1})	**2190 ± 1490**	**5175 ± 2040**	**6419 ± 2258**	**10801 ± 4389**	**11655 ± 4404**	**12803 ± 4187**	**13972 ± 5207**
2008 - 2016 Δt = 8 yr	ΣV_e (m^3)	17029 ± 4165	25771 ± 3263	30192 ± 3188	33240 ± 6758	3755 ± 909	9901 ± 2184	30696 ± 7522
	ΣV_d (m^3)	16143 ± 3870	20981 ± 6328	10533 ± 3420	29632 ± 9070	2489 ± 909	8941 ± 2581	26903 ± 6767
	ΔV_{DoD} (m^3)	-886 ± 5685	-4790 ± 7120	-19659 ± 4675	-3608 ± 11311	-1266 ± 1286	-960 ± 3381	-3793 ± 10118
	V_{in} (m^3)	0	886 ± 5685	5676 ± 9111	25335 ± 10241	28943 ± 15258	30209 ± 15312	31169 ± 15681
	V_{out} (m^3)	886 ± 5685	5676 ± 9111	25335 ± 10241	28943 ± 15258	30209 ± 15312	31169 ± 15681	34962 ± 18662
	q_{in} (m^3)	0	532 ± 3144	3406 ± 5467	15201 ± 6144	17366 ± 9155	18125 ± 9187	18701 ± 9409
	q_{out} (m^3)	532 ± 3144	3406 ± 5467	15201 ± 6144	17366 ± 9155	18125 ± 9187	18701 ± 9409	20977 ± 11197
	q_{out}^{mean} (m^3 yr^{-1})	**66 ± 426**	**426 ± 683**	**1900 ± 768**	**2171 ± 1144**	**2266 ± 1148**	**2338 ± 1176**	**2622 ± 1400**
2016 - 2017 Δt = 1 yr	ΣV_e (m^3)	1833 ± 587	740 ± 152	1251 ± 336	6096 ± 1431	58 ± 30	441 ± 136	4133 ± 1097
	ΣV_d (m^3)	1717 ± 711	652 ± 293	1246 ± 467	3286 ± 1102	336 ± 159	486 ± 238	5019 ± 1596
	ΔV_{DoD} (m^3)	-116 ± 922	-88 ± 330	-5 ± 575	-2810 ± 1806	278 ± 162	45 ± 274	886 ± 1937
	V_{in} (m^3)	0	116 ± 922	204 ± 979	209 ± 1136	3019 ± 2134	2741 ± 2140	2696 ± 2157
	V_{out} (m^3)	116 ± 922	204 ± 973	209 ± 1136	3019 ± 2134	2741 ± 2140	2696 ± 2157	1810 ± 2899
	q_{in} (m^3)	0	70 ± 553	122 ± 588	125 ± 681	1811 ± 1280	1645 ± 1284	1618 ± 1294
	q_{out} (m^3)	70 ± 553	122 ± 588	125 ± 681	1811 ± 1280	1645 ± 1284	1618 ± 1294	1086 ± 1739
	q_{out}^{mean} (m^3 yr^{-1})	**70 ± 553**	**122 ± 588**	**125 ± 681**	**1811 ± 1280**	**1645 ± 1284**	**1618 ± 1294**	**1086 ± 1739**

Table 6. Results obtained from the morphological approach application about sub-reach volumetric variations (ΣV_e: erosion; ΣV_d: deposition; ΔV_{DoD}: net volume change), volume of incoming (V_{in}) and outgoing (V_{out}) material and incoming (q_{in}) and outgoing (q_{out}) bed material load. For each considered periods it is reported also the mean annual transport regime calculated at the sub-reaches closure sections (q_{out}^{mean}). Error associated with each determined value is reported as well. Values in bold are those we used for the discussion about the evolution of sediment regime during the study period.

The bed material transport was calculated at the selected seven sections for the three DoDs periods using the sediment budgeting procedure and starting from the zero gravel-flux boundary represented by the dam for each time interval (similar to Ham and Church (2000) which employed the zero-flux coarse sediment boundary represented by a lake and four calculation periods). ΔV_{DoDs} involved in the calculation were multiplied by the percentage of channel sediment coarser than 6 mm and by 1-*p* in order to convert volumes of material (V_{in} and V_{out} in m^3) into the bed material load (q_{in} and q_{out} in m^3). From observations reported in the previous section, the grain size of surface sediments have likely changed over time. We assumed that the subsurface grain size is representative of the pre-dam conditions, which progressively coarsened afterwards. The percentage of sediments coarser than 6 mm is equal to 80% both for pre-dam and present condition, while we adopted the current surface sediment estimated porosity for the 2008-2016 and 2016-2017 calculations (i.e. 0.8*(1-0.25) = 0.6) and the subsurface sediment estimated porosity for 2006-2008 (i.e. 0.8*(1-0.27) = 0.58). For allowing a proper comparison of sediment fluxes of different periods, the mean annual transport values (q_{out}^{mean} in $m^3\ yr^{-1}$) for each section were calculated. Bed material load budgets for the three time intervals are shown in Figure 8 and numerical values are reported in Table 6.

During the period immediately following the dam closure (2006-2008), reach 1 was characterized by relatively low transport (≈ 2.000 $m^3\ yr^{-1}$). Bed material transport tends to strongly increase along reach 2 (from 5.000 to 10.000 $m^3\ yr^{-1}$) and it is around 14.000 $m^3\ yr^{-1}$ at reach 3 closure. The second study period (2008 - 2016) is the longest one considered, so the obtained transport values represent time-averaged estimates. In this period sediment flux was much lower than in the time span 2006 - 2008: at the downstream section of reach 1 bed material load was almost equal to zero and it was 2000 - 2500 $m^3\ yr^{-1}$ from the middle part of reach 2 (section 2) to the downstream section of the study sector. In 2016 - 2017 the bed material transport was slightly lower than during the previous period. Transport along reach 1 remained very low, increasing in the second part of reach 2 (after section 2) up to 1800 $m^3\ yr^{-1}$. Reach 3 was characterized by depositional processes leading to a decrease of sediment transport.

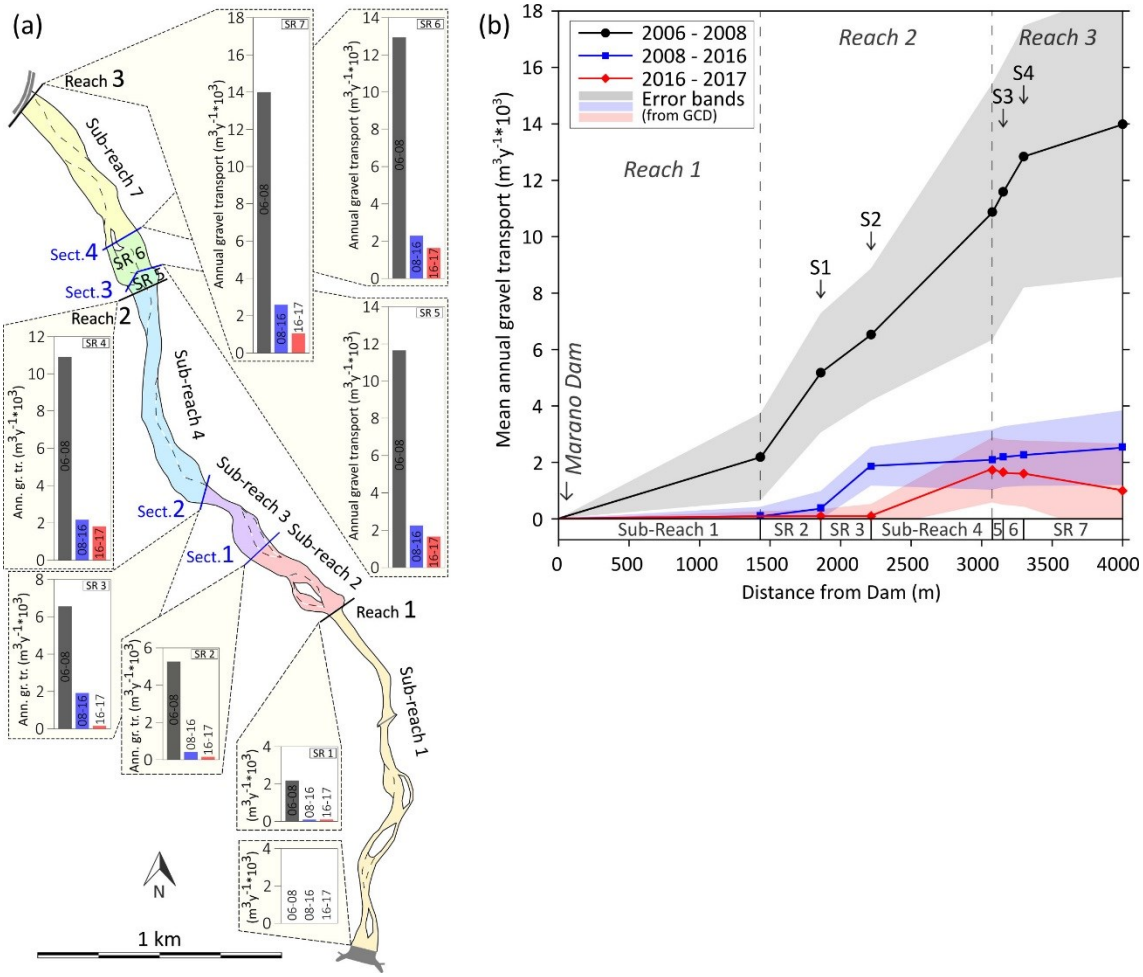

Figure 8. Mean annual bed material transport estimated at the seven sub-reaches closure sections during the three analyzed periods (a) and coarse sediment regime curves plotted considering the distance between the Marano dam (zero-flux boundary) and sub-reaches boundaries (b). In plot (b) calculation error bands are potted as well.

All the transport estimates are affected by uncertainties due to the employed data features and elaborations procedures. Obtained errors are significant (see Table 6; mean error= 44%; minimum error= 32%; low transport estimates have higher errors), but the final coarse sediment calculations from morphological approach can be considered reliable, keeping in mind that the bed material flux estimates, especially in the context of wide coarse-bedded rivers, are always affected by a certain degree of uncertainty (Wilcock, 2001). Estimates reliability is supported by the solidity of the morphological approach (Ashmore and Church, 1998), by a long applications history (e.g. Martin and Church, 1995; McLean and Church, 1999) and finally by the technological improvements in the topographical data quality and uncertainties estimation (e.g. Wheaton et al., 2010; Vericat et al., 2017).

4. Discussion

The reconstruction of the human activities in the Parma River catchment and the analysis of the morphological channel changes allow us to infer that the study sector has been affected by multiple impacts driven by anthropic factors in a similar way to other Apenninic rivers (e.g. Surian et al., 2009a; Bollati et al., 2014). Morphological alteration (in terms of channel width, bed elevation and morphological configuration) has been very intense since the 1950s, showing that the study area was already a "human-impacted river sector" at the time of retention basin (1988 - 1993) and dam construction (2004 - 2005) (Figure 5 and 6).

Using a morphological approach, we estimated the mean sediment transport regimes characterizing the three reaches included in the study sector during three time intervals since the Marano dam closure (Figure 8). The observed general decreasing trend in sediment flux cannot be explained by a water flow decrease or flood reduction as evidenced by hydrograph in Figure 2 showing homogeneous annual discharges over the last 13 years and because no significant variations in annual and formative discharges occurred between pre- and post- dam closure periods. As shown by several studies, dams affect sediment transfer continuity and downstream bed material flux regime (e.g. Grant et al., 2003; Phillips et al., 2005; Vericat and Batalla, 2006). Although sediment yield before the basin construction and dam closure is unknown, some reasonable estimates can be done for the Parma study sector. Since the impacts of dam on sediment transport, similarly to morphological effects, tends to downstream propagate and intensify over a relaxation time period (Petts and Gurnell, 2005), the mean transport value obtained for reach 3 (the farthest from the dam) during the time interval immediately following the dam closure (2006-2008) has been assumed as the best approximation of the sediment yield characterizing the whole sector before the basin and dam construction. Being the study area relatively homogeneous in term of channel width during that period and the impact on upstream sediment supply (i.e. land use change and sediment mining) not localized near to the area of interest, this assumption about longitudinal-steady sediment regime could be assumed reasonable. Figure 9 summarizes the mean transport estimates and relates them with the observed morphological variations in terms of reach mean channel widths and bed elevation.

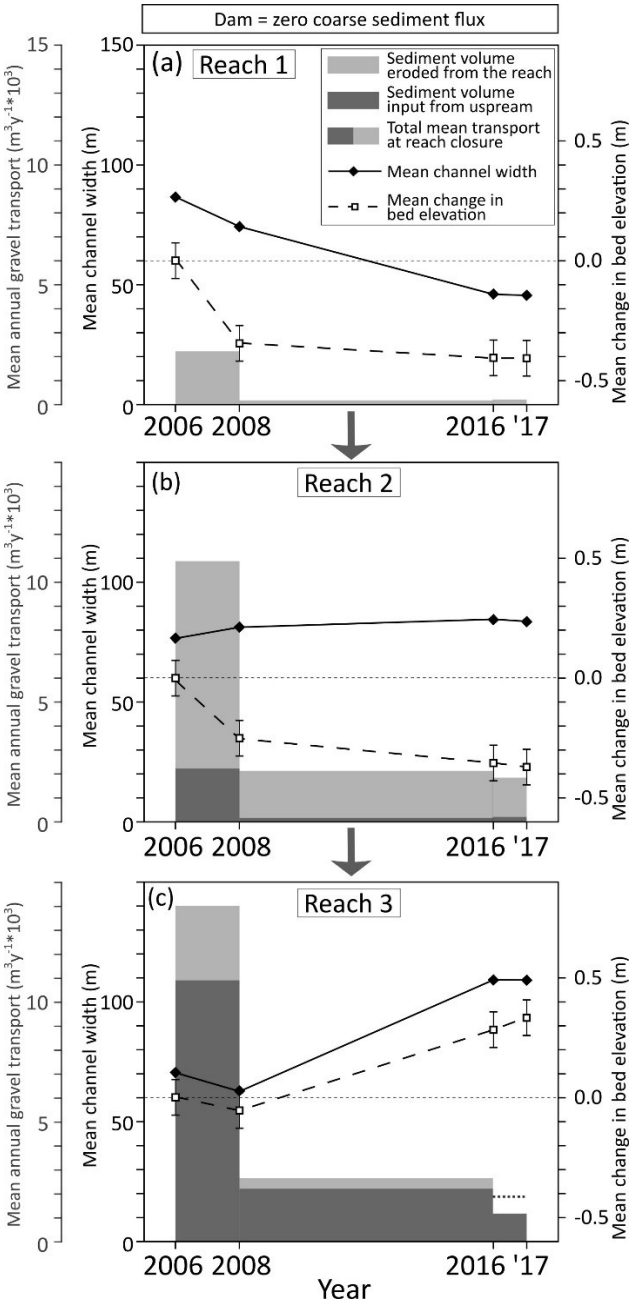

Figure 9. Summary of the morphological changes (i.e. channel width and bed elevation) and respective mean coarse sediment regimes obtained for the three reaches during the three analyzed periods. Moving from top (a) to bottom (b, c) results refers to reaches progressively further from the Marano dam (i.e. reach1, reach 2, reach 3). For each reach and time period it is possible to distinguish between the component of transport estimated at the reach downstream section due to sediment input from upstream (in dark grey) and due to erosion within the reach (light grey).

During the first investigated time interval (2006-2008, immediately after the dam closure) the sediment input from upstream was reduced to zero. The mean coarse transport at the downstream boundary of reach 1 is already low (i.e. 2.000 $m^3 yr^{-1}$), while it increases

up to 14.000 $m^3 yr^{-1}$ at the study sector downstream limit (value adopted as representative of the pre-dam sector annual sediment yield). The entire volume of sediment output from reach 1 was arguably derived from the erosion of material stored within the reach. Indeed, reach 1 underwent moderate narrowing and incision due to bed material evacuation while transport at reach 2 downstream section is partially due to the reach 1 material input and mostly to marked entrainment of material previously stored in reach 2, by channel incision and widening. Sediment evacuation from reach 3 was less significant (i.e. weak incision and narrowing) and the high transport estimate at the downstream reach (i.e. study sector limit) was likely due to a substantial input from upstream reaches. The 2008 - 2016 mean transport is markedly lower in all reaches. The upstream sediment input in the study sector still remained equal to zero but the erosion of material from reach 1 became very low (i.e. bed elevation was quite stable and channel width decreased) leading to negligible sediment yield at reach 1 closure. Some incision along reach 2 was responsible for the mild increase of mean material flux at reach downstream section. Transport at reach 3 end remained similar to the upstream input, since channel widening was coupled with channel aggradation. Finally, a similar behavior to the one described for the period 2008-2016 has been observed for the most recent period (2016 - 2017).

To explain the variations observed in sediment regime (Figure 8) it is worth referring to the concept of sediment slug (or wave) defined as bodies of clastic material associated with disequilibrium in fluvial systems over time periods above the event scale which propagates downstream along the channel through bars or bar assemblage dynamics, inducing major channel change (Griffiths, 1979; Nicholas et al., 1995). The provided definition highlights the relation existing between material flux and channel morphology (i.e. process-form interaction) involving temporal and spatial fluctuations in sediment transport rates and storage volumes (Macklin and Lewin, 1989; Griffiths, 1993; Bertrand and Liébault, 2018). Defining the section average transport estimates, we were able to consider both the upstream input of sediment and material mobilization due to change in reach storage volume. Considering the value of 14.000 $m^3 yr^{-1}$ as representative of the pre-dam mean annual transport regime (referring to hydrological years definable as "normal" in terms of discharge and number of flood events), we would have expected a similar value also at the reach 1 downstream limit for the period immediately following the dam closure (2006-2008), since the reach should have been fed of sediments during the previous period. Actually, the obtained estimate is considerably lower than the expected ($\approx$ 2.000 $m^3 yr^{-1}$) increasing only in the downstream reaches. For this reason, it is likely that the impact on

upstream sediment input started before the dam closure (2004-2005), and in 2006-2008 the reach 1 was already partially depleted of transportable material. As shown in the proposed evolutionary model (Figure 10), the decrease of upstream sediment contribution started since the basin levees and check dams construction (i.e. in 1993) inducing partial interruption of longitudinal transfer of material and evacuation of sediment stored in reach 1 (Figure 10a, b).

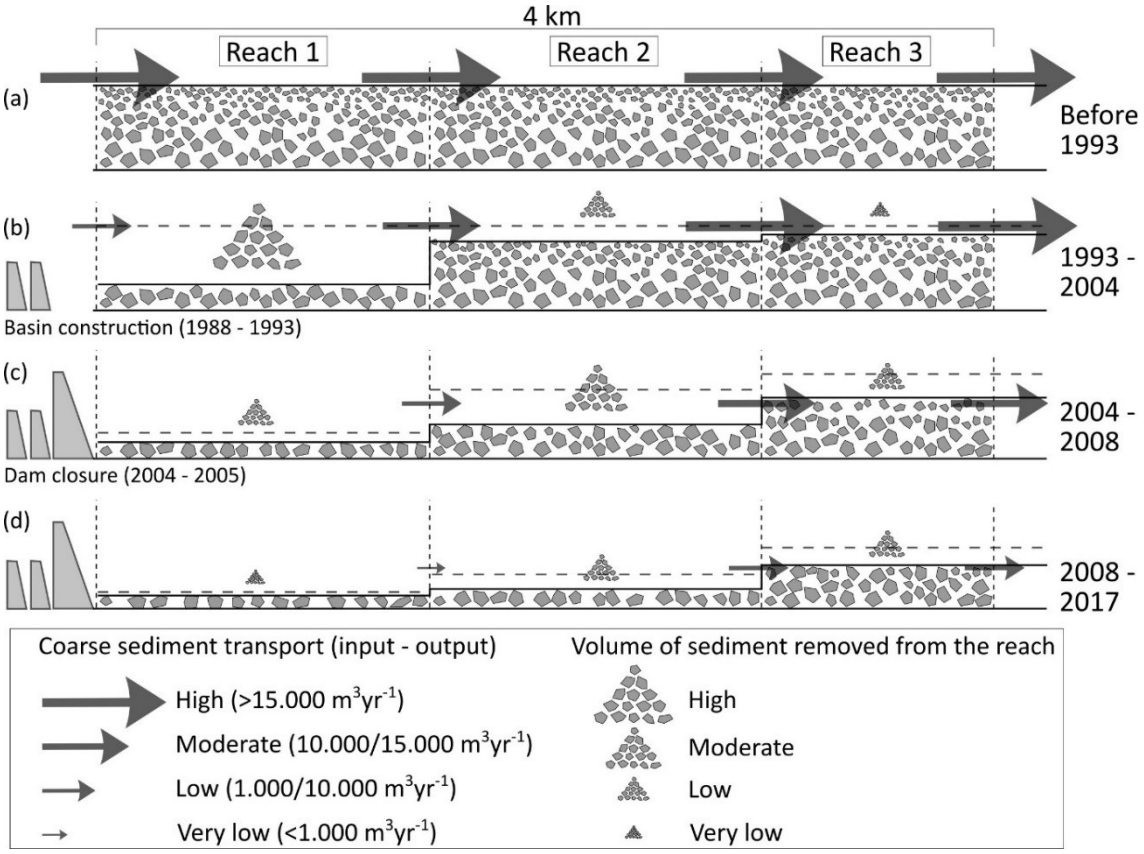

Figure 10. Proposed study sector evolutionary model taking into account human impacts, coarse sediment transport and material evacuated. Each plot (a, b, c, d) refers to a period considered as homogeneous in term of active processes and evolution. Pattern symbolizes the grain size of the clastic material stored in the channel. Data about stages (c) and (d) (calculation periods) derive directly from our estimates, while stages (a) and (b) data have been partially inferred, specifically those concerning sediment transport.

This interpretation is supported by the high incision experienced by the reach 1 between 1972 and 2006 (Figure 6). Slowik et al. (2018) have recently observed similar effects on morphological response of rivers to technical works that precede dam closure. Disequilibrium condition in sediment input increased when the dam was finally closed in 2004-2005 and the upstream sediment contribution became equal to zero. During the

period 2005-2008, weak evacuation took place in reach 1 but the tail of the flowing mobile-sediment wave, undersupplied from upstream, moved into reach 2 and partially into reach 3 (Figure 10c). In the most recent period (2008-present, Figure 10d), the observed sediment flux at reach 1 closure is almost equal to zero because all the mobile material was likely already evacuated in the previous period, causing sediment coarsening and streambed armoring due to selective transport (Dietrich et al., 1989). Such variations in grain size and bed structure are supported by the results obtained from bed material analysis, which confirm a progressive coarsening and armoring affecting channel sediments over the time. In the most recent period, reaches 2 and 3 have maintained a weak active transport, although most of the material have been already evacuated also by those reaches. The reconstructed propagation of mobile-sediment wave is conform to results obtained in a similar context by Madej and Ozaki (1996). They observed the movement of a sediment wave at a rate of 800-1600 m yr^{-1} during period of moderately low flows. According to such rate, it would be reasonable that after 24 years from basin construction and 12 years from dam closure, mobile sediment may have been almost completely removed from the 4-km long study area.

The morphological and sediment transport evolution characterizing the study reaches falls into the "degradation" style of channel adjustment following river regulation (Petts, 1984). Water flow has not been highly impacted by retention basin since it works only during large floods (recurrence interval > 10-15 years), not affecting most frequent formative events (i.e. events with recurrence interval = 2-3 years). On the other hand, sediment input from upstream has been progressively reduced to zero by basin and dam closure (defined as “type 4” in Brandt’s classification (2000)). This implies that flow has remained competent to mobilize large amount of channel material, to produce the flowing of a mobile-sediment wave, and to form an armored channel bed. Such sequence of processes completely developed in reaches 1 and 2, both experiencing incision, sediment coarsening, morphological complexity reduction and narrowing (especially in reach 1). Reach 3 behavior is slightly different: the contribution to study sector sediment output comes mainly from bank erosion, as testified by channel widening (Figure 9). Reach 3 received large amount of sediment from upstream reaches during the whole investigated period. This condition, differently from what happened in reaches 1 and 2, has probably allowed to maintain a more complex channel configuration, with bars and multiple channels, promoting divergence of flow, bank erosion and dissipation of excess flow energy through lateral channel wandering rather than incision (Bridge, 1993, 2009).

From the observations discussed above and considering the proposed evolutionary model (Figure 10), it seems that reaches 1 and 2 are currently in an advanced phase of their relaxation period, perhaps having already reached their new post-dam quasi-equilibrium state through a degradation-evolution path (Petts and Gurnell, 2005). The high armoring developed on channel bed in these reaches will likely continue to inhibit sediment entrainment, also because the retention basin does not allow the occurrence of very high magnitude discharges. The presence of this static armor (Little and Mayer, 1976; Parker and Sutherland, 1990) acts as a block for future morphological changes (e.g. incision). Reach 3 is experiencing its transient adjustment to the post-dam quasi-equilibrium, as suggested by the more dynamic conditions observed also for the most recent investigated period. The streambed material is still mobile (moderate armoring) and its characteristics (e.g. complex configuration with multiple channels) probably lead to a longer relaxation period, suggesting that its evolution will continue for several years in the future.

In order to include in the morphodynamic response analysis also the disturbance of the channel sediments induced by selective erosion, we related this parameter with calculated sediment transport regimes and channel morphological features. As highlighted by several works, the rate of coarse material transport is commonly closely tied to channel width and braiding intensity (e.g. Nicholas, 2000; Ashmore, 2001; Bertoldi et al., 2009; Ashmore et al., 2011; Bertrand and Liébault, 2018; Peirce et al., 2018), but such relationships are not shown in the Parma River downstream of the dam. Figure 11 illustrates the relationships between mean annual gravel transport at the three reach closures with mean channel width and braiding index for three periods.

Considering a specific channel width (Figure 11a) or braiding index (Figure 11b), very different transport values are observed. Reaches 1, 2 and 3 estimates obtained for the period 2016-2017 are supported by field data indicating diffused armoring affecting the channel bed. For previous periods, no data are available about the bed material conditions. However, from the evolutionary model (Figure 10c), reaches 2 and 3 during the first period (2006-2008) were probably the only ones not affected by undersupply of sediment and, therefore, by selective erosion. Reasonably, these two estimates come from reaches characterized by undisturbed bed sediments (i.e. without or with poorly developed armoring), explaining the fact that, for fixed width or braiding index, the obtained mean coarse sediment transports are up to one order of magnitude higher than those corresponding to bed-armoring conditions.

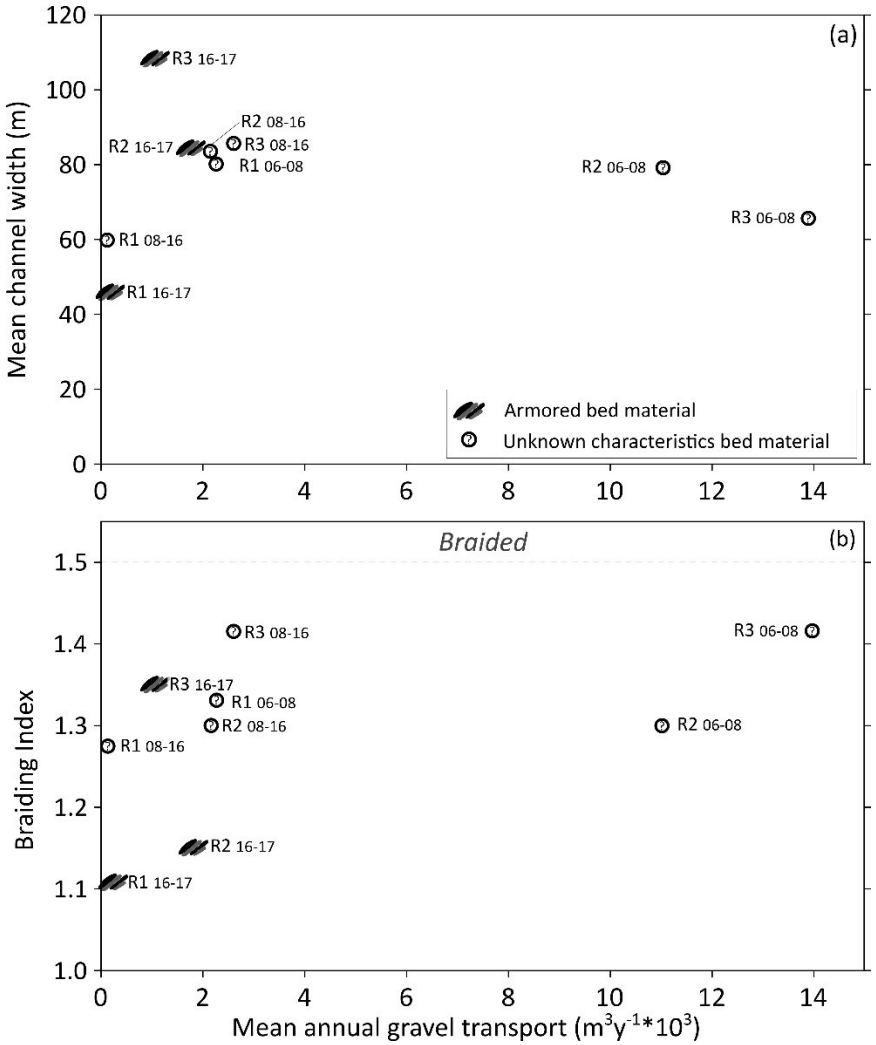

Figure 11. Relationships between mean annual coarse sediment transport, bed material characteristics and mean channel width (a) and braiding index (b). Each point refers to a specific reach for an investigated time period. Mean width and braiding index values were obtained considering the beginning and the end of each period. Transport values refers to the downstream section of each reach.

5. Conclusions

Data about human impacts on fluvial system, sediment regimes, morphological evolution and bed material characteristics allowed us to analyze the complex morphodynamic response of gravel-bed river to the construction of a retention basin closed by a dam. The main results and insights from this study can be summarized as follows.

(i) The Parma River was affected by a long history of human pressure started in the middle of the XIX century (e.g. land use change and sediment mining) able to induce strong channel narrowing (up to 70%), incision (between 3 and 7 meters)

and likely decrease of bed material transport along the study area also before the river regulation. Since the construction of the Marano basin infrastructures in 1988-1993, the evolutionary tendency suggests a significant deficit of sediment imported in the sector from upstream, finally reducing to zero in 2005 by the dam closure.

(ii) Transport regime estimates for the three reaches located downstream from the dam show a marked decreasing trend in the mean annual gravel transport rate affecting the study sector during the last 11 years. The combined impacts of earlier basin construction works and later dam closure have been able to make the annual coarse sediment transport close to zero in a large gravel-bed river over a decennial time scale. After 24 years from basin construction and 12 years from dam closure, transport has decreased from more than 14.000 $m^3 yr^{-1}$ to close to zero for reaches 1 and 2 and has been reduced of about 85% four kilometers downstream from the dam.

(iii) Sediment regime evolution has been interpreted as led by the passage of the tail of a mobile-sediment wave undersupplied from upstream material input. From this point of view, the evolution of channel morphology and the bed material responses are controlled by the dynamics induced by the flowing under-supplied sediment wave and its propagation in space and time. Channel incision and/or widening represent the evacuation of the material previously stored in the river sector not sufficiently replaced by sediments coming from upstream. These processes, inducing morphological channel changes, partially supply sediment to the downstream river reaches, delaying the coarse material transport decrease. Bed material disturbance, which occurs through coarsening and armoring, is another consequence of mobile sediments evacuation. After the passage of the flowing under-supplied sediment wave, the residual bed material is composed by the coarser particles which are entrained and mobilized much less frequently.

(iv) The river regulation (i.e. basin construction and dam closure) induced a response which developed through a channel-degradation path. In particular, reaches 1 and 2 are likely in their new post-dam quasi-equilibrium state and the high streambed armoring inhibits sediment entrainment and so future morphological changes. Reach 3 is still experiencing its transient adjustment from the pre-dam to the post-dam quasi-equilibrium, maintaining coarse sediment mobility and the possibility of future morphological changes.

(v) The analyzed case-study allowed us to evaluate the complex relations existing between the three factors (i.e. sediment regime, morphological setting and bed material characteristics) driving the morphodynamics of a large gravel-bed river experiencing strong deficit of sediment. Sediment regime and its alterations control effectively the channel morphological evolution and the bed sediments disturbance, however morphological variations can in turn influence downstream transport providing material (e.g. channel widening and incision) while bed armoring strongly reduces sediment mobility and, therefore, bedload transport. Therefore, positive or negative feedbacks exist between these two factors and sediment transport.

Conclusions obtained from real river-data considered the whole morphodynamic response of a regulated large-gravel bed river sector experiencing degradation-style evolution. Future research could focalize on different river types, human impacts and evolutionary trends, expanding the knowledge about the interactions happening between the key parameters controlling the morphodynamic response of fluvial systems impacted by human activities, thinking carefully about the quantitative estimation of sediment regime alteration.

References

Andrews, E. D. (1986). Downstream effects of flaming gorge reservoir on the Green River, Colorado and Utah. *Geological Society of America Bulletin*, *97*(8), 1012-1023. https://doi.org/10.1130/0016-7606(1986)97<1012:DEOFGR>2.0.CO;2

Ashmore, P. E. (1991). Channel morphology and bed load pulses in braided, gravel-bed streams. *Geografiska Annaler: Series A, Physical Geography*, *73*(1), 37-52.

Ashmore, P. E. (2001). Braiding phenomena: statics and kinetics. In M. P. Mosley (Ed.), *Gravel Bed Rivers V* (pp. 95-121). Wellington, New Zealand: New Zealand Hydrological Society.

Ashmore, P. E. (2013). Morphology and dynamics of braided rivers. In J. F. Shroder (Ed.), *Treatise on Geomorphology*, *Vol. 9* (pp. 289-312). Amsterdam, Netherlands: Elsevier.

Ashmore, P. E., & Church, M. (1998). Sediment transport and river morphology: a paradigm for study. In P. C. Klingeman, R. L. Beschta, P. D. Komar, J. B. Bradley (Eds.), *Gravel-Bed Rivers in the Environment* (pp. 115-148). Highlands Ranch, CO: Water Resources Publications LLC

Ashmore, P., Bertoldi, W., & Tobias Gardner, J. (2011). Active width of gravel-bed braided rivers. *Earth Surface Processes and Landforms*, *36*(11), 1510-1521. https://doi.org/10.1002/esp.2182

Bertoldi, W., Zanoni, L., & Tubino, M. (2009). Planform dynamics of braided streams. *Earth Surface Processes and Landforms*, *34*(4), 547-557. https://doi.org/10.1002/esp.1755

Bertrand, M., & Liébault, F. (2018). Active channel width as a proxy of sediment supply from mining sites in New Caledonia. Earth Surface Processes and Landforms. https://doi.org/10.1002/esp.4478

Blum, M. D., & Törnqvist, T. E. (2000). Fluvial responses to climate and sea level change: a review and look forward. *Sedimentology*, *47*(s1), 2-48. https://doi.org/10.1046/j.1365-3091.2000.00008.x

Bollati, I. M., Pellegrini, L., Rinaldi, M., Duci, G., & Pelfini, M. (2014). Reach-scale morphological adjustments and stages of channel evolution: the case of the Trebbia River (northern Italy). *Geomorphology*, *221*, 176-186. https://doi.org/10.1016/j.geomorph.2014.06.007

Brandt, S. A. (2000). Classification of geomorphological effects downstream of dams. *Catena*, *40*(4), 375-401. https://doi.org/10.1016/S0341-8162(00)00093-X

Brasington, J., Rumsby, B. T., & McVey, R. A. (2000). Monitoring and modelling morphological change in a braided gravel-bed river using high resolution GPS-based survey. *Earth Surface Processes and Landforms*, *25*(9), 973-990. https://doi.org/10.1002/1096-9837(200008)25:9<973::AID-ESP111>3.0.CO;2-Y

Brasington, J., Langham, J., & Rumsby, B. (2003). Methodological sensitivity of morphometric estimates of coarse fluvial sediment transport. *Geomorphology*, *53*(3), 299-316. https://doi.org/10.1016/S0169-555X(02)00320-3

Bridge, J. S. (1993). The interaction between channel geometry, water flow, sediment transport and deposition in braided rivers. *Geological Society, London, Special Publications*, *75*(1), 13-71. https://doi.org/10.1144/GSL.SP.1993.075.01.02

Bridge, J. S. (2009). *Rivers and floodplains: forms, processes, and sedimentary record*. Hoboken, NJ: John Wiley & Sons

Brierley, G. J., & Fryirs, K. A. (2013). *Geomorphology and river management: applications of the river styles framework*. Hoboken, NJ: John Wiley & Sons

Carley, J. K., Pasternack, G. B., Wyrick, J. R., Barker, J. R., Bratovich, P. M., Massa, D. A., ... & Johnson, T. R. (2012). Significant decadal channel change 58–67 years post-dam accounting for uncertainty in topographic change detection between contour maps and point cloud models. *Geomorphology*, *179*, 71-88. https://doi.org/10.1016/j.geomorph.2012.08.001

Carling, P. A., & Reader, N. A. (1982). Structure, composition and bulk properties of upland stream gravels. *Earth Surface Processes and Landforms*, *7*(4), 349-365. https://doi.org/10.1002/esp.3290070407

Church, M. (2006). Bed material transport and the morphology of alluvial river channels. *Annu. Rev. Earth Planet. Sci.*, *34*, 325-354. https://doi.org/10.1146/annurev.earth.33.092203.122721

Church, M., & Ferguson, R. I. (2015). Morphodynamics: Rivers beyond steady state. *Water Resources Research*, *51*(4), 1883-1897. https://doi.org/10.1002/2014WR016862

Clerici, A., Perego, S., Chelli, A., & Tellini, C. (2015). Morphological changes of the floodplain reach of the Taro River (Northern Italy) in the last two centuries. *Journal of hydrology*, *527*, 1106-1122. https://doi.org/10.1016/j.jhydrol.2015.05.063

Curtis, K. E., Renshaw, C. E., Magilligan, F. J., & Dade, W. B. (2010). Temporal and spatial scales of geomorphic adjustments to reduced competency following flow regulation in bedload-dominated systems. *Geomorphology*, *118*(1-2), 105-117. https://doi.org/10.1016/j.geomorph.2009.12.012

Dietrich, W. E., Kirchner, J. W., Ikeda, H., & Iseya, F. (1989). Sediment supply and the development of the coarse surface layer in gravel-bedded rivers. *Nature*, *340*(6230), 215. https://doi.org/10.1038/340215a0

Duci, G., (2011). Variazioni morfologiche recenti ed attuali di alvei fluviali dell'Appennino Settentrionale, (Doctoral dissertation). Pavia, Italy: Scuola di Dottorato in Scienze e Tecnologie, University of Pavia

Egozi, R., & Ashmore, P. (2008). Defining and measuring braiding intensity. *Earth Surface Processes and Landforms*, *33*(14), 2121-2138. https://doi.org/10.1002/esp.1658

Falcucci, A., Maiorano, L., & Boitani, L. (2007). Changes in land-use/land-cover patterns in Italy and their implications for biodiversity conservation. *Landscape ecology*, *22*(4), 617-631. https://doi.org/10.1007/s10980-006-9056-4

Ferguson, R. (2007). Gravel-bed rivers at the reach scale. In H. Habersack, H. Piégay, M. Rinaldi (Eds.), *Gravel-bed Rivers VI: from process understanding to river restoration* (pp. 33-60). Amsterdam, Netherlands: Elsevier.

Fuchs, R., Herold, M., Verburg, P. H., Clevers, J. G., & Eberle, J. (2015). Gross changes in reconstructions of historic land cover/use for Europe between 1900 and 2010. *Global change biology*, *21*(1), 299-313. https://doi.org/10.1111/gcb.12714

Grabowski, R. C., & Gurnell, A. M. (2016). Using historical data in fluvial geomorphology. In G.M. Kondolf, H. Piégay (Eds.), Tools in fluvial geomorphology (pp. 56-76). Hoboken, NJ: John Wiley & Sons. https://doi.org/10.1002/9781118648551.ch4

Graf, W. L. (2006). Downstream hydrologic and geomorphic effects of large dams on American rivers. *Geomorphology*, *79*(3-4), 336-360. https://doi.org/10.1016/j.geomorph.2006.06.022

Graham, D. J., Reid, I., & Rice, S. P. (2005a). Automated sizing of coarse-grained sediments: image-processing procedures. *Mathematical Geology*, *37*(1), 1-28. https://doi.org/10.1007/s11004-005-8745-x

Graham, D. J., Rice, S. P., & Reid, I. (2005b). A transferable method for the automated grain sizing of river gravels. *Water Resources Research*, *41*(7). https://doi.org/10.1029/2004WR003868

Graham, D. J., Rollet, A. J., Piégay, H., & Rice, S. P. (2010). Maximizing the accuracy of image-based surface sediment sampling techniques. *Water Resources Research*, *46*(2). https://doi.org/10.1029/2008WR006940

Grant, G. E. (2012). The geomorphic response of gravel-bed rivers to dams: perspectives and prospects. In M. Church, P. M. Biron, A. G. Roy (Eds.), *Gravel-bed Rivers: Processes, Tools, Environments* (pp. 165-181). Hoboken, NJ: John Wiley & Sons

Grant, G. E., O'Connor, J. E., & Wolman, M. G. (2013). A river runs through it: conceptual models in fluvial geomorphology. In J. F. Shroder (Ed.), *Treatise on Geomorphology*, *Vol. 9* (pp. 289-312). Amsterdam, Netherlands: Elsevier.

Grant, G. E., Schmidt, J. C., & Lewis, S. L. (2003). A geological framework for interpreting downstream effects of dams on rivers. In J. E. O'Connor, G. E. Grant (Eds.), *A peculiar river* (pp. 203-219). Washington, DC: American Geophysical Union.

Gregory, K. J. (2006). The human role in changing river channels. *Geomorphology*, *79*(3-4), 172-191. https://doi.org/10.1016/j.geomorph.2006.06.018

Griffiths, G. A. (1979). Recent sedimentation history of the Waimakariri River, New Zealand. *Journal of Hydrology (New Zealand), 18*(1), 6-28. http://www.jstor.org/stable/43944437

Griffiths, G. A. (1993). Sediment translation waves in braided gravel-bed rivers. *Journal of Hydraulic Engineering*, *119*(8), 924-937. https://doi.org/10.1061/(ASCE)0733-9429(1993)119:8(924)

Gumiero, B., Rinaldi, M., Belletti, B., Lenzi, D., & Puppi, G. (2015). Riparian vegetation as indicator of channel adjustments and environmental conditions: the case of the Panaro River (Northern Italy). *Aquatic sciences*, *77*(4), 563-582. https://doi.org/10.1007/s00027-015-0403-x

Ham, D. G., & Church, M. (2000). Bed-material transport estimated from channel morphodynamics: Chilliwack River, British Columbia. *Earth Surface Processes and Landforms*, *25*(10), 1123-1142. https://doi.org/10.1002/1096-9837(200009)25:10<1123::AID-ESP122>3.0.CO;2-9

Haschenburger, J. K. (2013). Bedload kinematics and fluxes. In J. F. Shroder (Ed.), *Treatise on Geomorphology*, *Vol. 9* (pp. 103-123). Amsterdam, Netherlands: Elsevier.

Hassan, M. A., Egozi, R., & Parker, G. (2006). Experiments on the effect of hydrograph characteristics on vertical grain sorting in gravel bed rivers. *Water Resources Research*, *42*(9). https://doi.org/10.1029/2005WR004707

Heckmann, T., Haas, F., Abel, J., Rimböck, A., & Becht, M. (2017). Feeding the hungry river: Fluvial morphodynamics and the entrainment of artificially inserted sediment at the dammed river Isar, Eastern Alps, Germany. *Geomorphology*, *291*, 128-142. https://doi.org/10.1016/j.geomorph.2017.01.025

Hoffmann, T., Thorndycraft, V. R., Brown, A. G., Coulthard, T. J., Damnati, B., Kale, V. S., ... & Walling, D. E. (2010). Human impact on fluvial regimes and sediment flux during the Holocene: Review and future research agenda. *Global and Planetary Change*, *72*(3), 87-98. https://doi.org/10.1016/j.gloplacha.2010.04.008

James, L. A., Watson, D. G., & Hansen, W. F. (2007). Using LiDAR data to map gullies and headwater streams under forest canopy: South Carolina, USA. *Catena*, *71*(1), 132-144. https://doi.org/10.1016/j.catena.2006.10.010

Kondolf, G. M. (1997). Hungry water: effects of dams and gravel mining on river channels. *Environmental management, 21*(4), 533-551. https://doi.org/10.1007/s002679900048

Kondolf, G. M., Gao, Y., Annandale, G. W., Morris, G. L., Jiang, E., Zhang, J., ... & Hotchkiss, R. (2014). Sustainable sediment management in reservoirs and regulated rivers: Experiences from five continents. *Earth's Future*, *2*(5), 256-280. https://doi.org/10.1002/2013EF000184

Lallias-Tacon, S., Liébault, F., & Piégay, H. (2014). Step by step error assessment in braided river sediment budget using airborne LiDAR data. *Geomorphology*, *214*, 307-323. https://doi.org/10.1016/j.geomorph.2014.02.014

Lane, E. W. (1955). Importance of fluvial morphology in hydraulic engineering. *Proceedings (American Society of Civil Engineers); v. 81, paper no. 745*.

Lane, S. N., Richards, K. S., & Chandler, J. H. (1995). Morphological Estimation of the Time-Integrated Bed Load Transport Rate. *Water Resources Research*, *31*(3), 761-772. https://doi.org/10.1029/94WR01726

Lane, S. N., Westaway, R. M., & Murray Hicks, D. (2003). Estimation of erosion and deposition volumes in a large, gravel-bed, braided river using synoptic remote sensing. *Earth Surface Processes and Landforms*, *28*(3), 249-271. https://doi.org/10.1002/esp.483

Liébault, F., & Piégay, H. (2001). Assessment of channel changes due to long-term bedload supply decrease, Roubion River, France. *Geomorphology*, *36*(3-4), 167-186. https://doi.org/10.1016/S0169-555X(00)00044-1

Little, W. C., & Mayer, P. G. (1976). Stability of channel beds by armoring. *Journal of the Hydraulics Division*, *102* (ASCE# 12519).

Lobera, G., Andrés-Domenech, I., López-Tarazón, J. A., Millán-Romero, P., Vallés, F., Vericat, D., & Batalla, R. J. (2017). Bed disturbance below dams: observations from two Mediterranean rivers. *Land Degradation & Development*, *28*(8), 2493-2512. https://doi.org/10.1002/ldr.2785

Macklin, M. G., & Lewin, J. (1989). Sediment transfer and transformation of an alluvial valley floor: the River South Tyne, Northumbria, UK. *Earth surface processes and landforms*, *14*(3), 233-246. https://doi.org/10.1002/esp.3290140305

Macklin, M. G., & Lewin, J. (2003). River sediments, great floods and centennial-scale holocene climate change. *Journal of Quaternary Science*, *18*(2), 101-105. https://doi.org/10.1002/jqs.751

Madej, M. A., & Ozaki, V. (1996). Channel response to sediment wave propagation and movement, Redwood Creek, California, USA. *Earth Surface Processes and Landforms*, *21*(10), 911-927. https://doi.org/10.1002/(SICI)1096-9837(199610)21:10<911::AID-ESP621>3.0.CO;2-1

Malhotra, S. L. (1951). Effects of barrages and weirs on the regime of rivers. In *Proceedings of the International Association of Hydrological Sciences, 4th Meeting* (pp. 335-347).

Marchetti, M. (2002). Environmental changes in the central Po Plain (northern Italy) due to fluvial modifications and anthropogenic activities. *Geomorphology*, *44*(3-4), 361-373. https://doi.org/10.1016/S0169-555X(01)00183-0

Martin, Y., & Church, M. (1995). Bed-material transport estimated from channel surveys: Vedder River, British Columbia. *Earth Surface Processes and Landforms*, *20*(4), 347-361. https://doi.org/10.1002/esp.3290200405

McLean, D. G., & Church, M. (1999). Sediment transport along lower Fraser River: 2. Estimates based on the long-term gravel budget. *Water Resources Research*, *35*(8), 2549-2559. https://doi.org/10.1029/1999WR900102

Merz, J. E., Pasternack, G. B., & Wheaton, J. M. (2006). Sediment budget for salmonid spawning habitat rehabilitation in a regulated river. *Geomorphology*, *76*(1), 207-228. https://doi.org/10.1016/j.geomorph.2005.11.004

Milan, D. J., Heritage, G. L., Large, A. R., & Fuller, I. C. (2011). Filtering spatial error from DEMs: Implications for morphological change estimation. *Geomorphology*, *125*(1), 160-171. https://doi.org/10.1016/j.geomorph.2010.09.012

Murphy, P. N., Ogilvie, J., Meng, F. R., & Arp, P. (2008). Stream network modelling using lidar and photogrammetric digital elevation models: a comparison and field verification. *Hydrological Processes*, *22*(12), 1747-1754. https://doi.org/10.1002/hyp.6770

Nicholas, A. P. (2000). Modelling bedload yield in braided gravel bed rivers. *Geomorphology*, *36*(1-2), 89-106. https://doi.org/10.1016/S0169-555X(00)00050-7

Nicholas, A. P., Ashworth, P. J., Kirkby, M. J., Macklin, M. G., & Murray, T. (1995). Sediment slugs: large-scale fluctuations in fluvial sediment transport rates and storage volumes. *Progress in physical geography*, *19*(4), 500-519. https://doi.org/10.1177/030913339501900404

Parker, G., & Sutherland, A. J. (1990). Fluvial armor. *Journal of Hydraulic Research*, *28*(5), 529-544. https://doi.org/10.1080/00221689009499044

Passalacqua, P., Belmont, P., Staley, D. M., Simley, J. D., Arrowsmith, J. R., Bode, C. A., ... & Wheaton, J. M. (2015). Analyzing high resolution topography for advancing the understanding of mass and energy transfer through landscapes: A review. *Earth-Science Reviews*, *148*, 174-193. https://doi.org/10.1016/j.earscirev.2015.05.012

Peirce, S., Ashmore, P., & Leduc, P. (2018). The variability in the morphological active width: Results from physical models of gravel-bed braided rivers. Earth Surface Processes and Landforms. https://doi.org/10.1002/esp.4400

Pellegrini, L., Maraga, F., Turitto, O., Audisio, C., Duci, G., Pavia, U., & Ferrata, V. (2008). Evoluzione morfologica di alvei fluviali mobili nel settore occidentale del bacino padano. *Il Quaternario*, *21*(1B), 251-266.

Petts, G. E. (1979). Complex response of river channel morphology subsequent to reservoir construction. *Progress in Physical Geography*, *3*(3), 329-362.

Petts, G. E. (1984). *Impounded rivers: perspectives for ecological management*. Hoboken, NJ: John Wiley & Sons

Petts, G. E., & Greenwood, M. (1985). Channel changes and invertebrate faunas below Nant-Y-Moch dam, River Rheidol, Wales, UK. *Hydrobiologia*, *122*(1), 65-80.

Petts, G. E., & Gurnell, A. M. (2005). Dams and geomorphology: research progress and future directions. *Geomorphology*, *71*(1-2), 27-47. https://doi.org/10.1016/j.geomorph.2004.02.015

Phillips, J. D., Slattery, M. C., & Musselman, Z. A. (2005). Channel adjustments of the lower Trinity River, Texas, downstream of Livingston Dam. *Earth Surface Processes and Landforms*, *30*(11), 1419-1439. https://doi.org/10.1002/esp.1203

Pitlick, J., & Wilcock, P. R. (2001). Relations between streamflow, sediment transport, and aquatic habitat in regulated rivers. *Geomorphic processes and riverine habitat*, 185-198. https://doi.org/10.1029/WS004p0185

Pohl, M. (2004). Channel bed mobility downstream from the Elwha dams, Washington. *The Professional Geographer*, *56*(3), 422-431. https://doi.org/10.1111/j.0033-0124.2004.05603010.x

Preciso, E., Salemi, E., & Billi, P. (2012). Land use changes, torrent control works and sediment mining: effects on channel morphology and sediment flux, case study of the Reno River (Northern Italy). *Hydrological Processes*, *26*(8), 1134-1148. https://doi.org/10.1002/hyp.8202

Schmidt, J. C., & Wilcock, P. R. (2008). Metrics for assessing the downstream effects of dams. *Water Resources Research*, *44*(4). https://doi.org/10.1029/2006WR005092

Rinaldi, M., Gurnell, A. M., Del Tánago, M. G., Bussettini, M., & Hendriks, D. (2016). Classification of river morphology and hydrology to support management and restoration. *Aquatic sciences*, *78*(1), 17-33. https://doi.org/10.1007/s00027-015-0438-z

Rinaldi, M., Simoncini, C., & Sogni, D. (2005a). Variazioni morfologiche recenti di due alvei ghiaiosi appenninici: il F. *il F. Vara. Geografia Fisica e Dinamica Quaternaria Suppl*, *7*, 313-319.

Rinaldi, M., Surian, N., Comiti, F., & Bussettini, M. (2013). A method for the assessment and analysis of the hydromorphological condition of Italian streams: the Morphological Quality Index (MQI). *Geomorphology*, *180*, 96-108. https://doi.org/10.1016/j.geomorph.2012.09.009

Rinaldi, M., Surian, N., Comiti, F., & Bussettini, M. (2015). A methodological framework for hydromorphological assessment, analysis and monitoring (IDRAIM) aimed at promoting integrated river management. *Geomorphology*, *251*, 122-136. https://doi.org/10.1016/j.geomorph.2015.05.010

Rinaldi, M., Surian, N., Comiti, F., Bussettini, M., Belletti, B., Nardi, L., ... & Golfieri, B. (2012). Guidebook for the evaluation of stream morphological conditions by the morphological quality index (MQI). *Version*, *1*, 85. Roma, Italy: Istituto Superiore per la Protezione e la Ricerca Ambientale

Rinaldi, M., Teruggi, L. B., Simoncini, C., & Nardi, L. (2008). Dinamica recente ed attuale di alvei fluviali: alcuni casi di studio appenninici (Italia Centro-Settentrionale). *Il Quaternario*, *21*(1B), 291-302.

Scorpio, V., Aucelli, P. P., Giano, S. I., Pisano, L., Robustelli, G., Rosskopf, C. M., & Schiattarella, M. (2015). River channel adjustments in Southern Italy over the past 150 years and implications for channel recovery. *Geomorphology*, *251*, 77-90. https://doi.org/10.1016/j.geomorph.2015.07.008

Scorpio, V., & Rosskopf, C. M. (2016). Channel adjustments in a Mediterranean river over the last 150 years in the context of anthropic and natural controls. *Geomorphology*, *275*, 90-104. https://doi.org/10.1016/j.geomorph.2016.09.017

Sear, D. A. (1995). Morphological and sedimentological changes in a gravel-bed river following 12 years of flow regulation for hydropower. *River Research and Applications*, *10*(2-4), https://doi.org/247-264. 10.1002/rrr.3450100219

Słowik, M., Dezső, J., Marciniak, A., Tóth, G., & Kovács, J. (2018). Evolution of river planforms downstream of dams: Effect of dam construction or earlier human-induced changes?. *Earth Surface Processes and Landforms*. https://doi.org/10.1002/esp.4371

Storz-Peretz, Y., & Laronne, J. B. (2013). Automatic grain sizing of vertical exposures of gravelly deposits. *Sedimentary Geology*, *294*, 13-26. https://doi.org/10.1016/j.sedgeo.2013.05.004

Surian, N. (2006). Effects of human impact on braided river morphology: examples from Northern Italy. In G.H. Sambrook Smith, J.L. Best, C.S. Bristow, G.E. Petts (Eds.), *Braided rivers: Processes, Deposits, Ecology and Management* (pp. 233-256). Oxford, UK: Blackwell Publishing Ltd

Surian, N., & Cisotto, A. (2007). Channel adjustments, bedload transport and sediment sources in a gravel-bed river, Brenta River, Italy. *Earth Surface Processes and Landforms*, *32*(11), 1641-1656. https://doi.org/10.1002/esp.1591

Surian, N., & Rinaldi, M. (2003). Morphological response to river engineering and management in alluvial channels in Italy. *Geomorphology*, *50*(4), 307-326. https://doi.org/10.1016/S0169-555X(02)00219-2

Surian, N., & Rinaldi, M. (2004). Channel adjustments in response to human alteration of sediment fluxes: examples from Italian rivers. In V. Golosov, V. Belyaev, D. E. Walling (Eds.), *Sediment Transfer Through the Fluvial System: Proceedings of the International Symposium Held at Moscow, Russia, from 2 to 6 August, 2004 (No. 288).* (pp. 276-282). Oxfordshire, UK: IAHS publications

Surian, N., Rinaldi, M., & Pellegrini, L. (2009b). Linee guida per l'analisi geomorfologica degli alvei fluviali e delle loro tendenze evolutive. Padova, Italy: Coop. Libraria Editrice Università di Padova

Surian, N., Rinaldi, M., Pellegrini, L., Audisio, C., Maraga, F., Teruggi, L., ... & Ziliani, L. (2009a). Channel adjustments in northern and central Italy over the last 200 years. In L. A. James, S. L. Rathburn, G. R. Whittecar (Eds.), *Management and restoration of fluvial systems with broad historical changes and human impacts: geological society of America Special Paper (Vol. 451)* (pp. 83-95). Boulder, CO: Geological Society of America

Surian, N., Ziliani, L., Comiti, F., Lenzi, M. A., & Mao, L. (2009c). Channel adjustments and alteration of sediment fluxes in gravel-bed rivers of North-Eastern Italy: potentials and limitations for channel recovery. *River Research and Applications*, *25*(5), 551-567. https://doi.org/10.1002/rra.1231

Vericat, D., & Batalla, R. J. (2005). Sediment transport in a highly regulated fluvial system during two consecutive floods (lower Ebro River, NE Iberian Peninsula). *Earth Surface Processes and Landforms*, *30*(4), 385-402. https://doi.org/10.1002/esp.1145

Vericat, D., & Batalla, R. J. (2006). Sediment transport in a large impounded river: The lower Ebro, NE Iberian Peninsula. *Geomorphology*, *79*(1-2), 72-92. https://doi.org/10.1016/j.geomorph.2005.09.017

Vericat, D., Batalla, R. J., & Garcia, C. (2006). Breakup and reestablishment of the armour layer in a large gravel-bed river below dams: The lower Ebro. *Geomorphology*, *76*(1-2), 122-136. https://doi.org/10.1016/j.geomorph.2005.10.005

Vericat, D., Batalla, R. J., & Garcia, C. (2008). Bed-material mobility in a large river below dams. *Geodinamica Acta*, *21*(1-2), 3-10. https://doi.org/10.3166/ga.21.3-10

Vericat, D., Wheaton, J. M., & Brasington, J. (2017). Revisiting the Morphological Approach: Opportunities and Challenges with Repeat High-Resolution Topography. In D. Tsutsumi, J. B.

Laronne (Eds.), *Gravel-Bed Rivers: Processes and Disasters* (pp. 121-158). Hoboken, NJ: John Wiley & Sons

Wheaton, J. M. (2008). Uncertainty in morphological sediment budgeting of rivers, (Doctoral dissertation). Retrieved from http://www.joewheaton.org/. Southampton, UK: University of Southampton

Wheaton, J. M., Brasington, J., Darby, S. E., & Sear, D. A. (2010). Accounting for uncertainty in DEMs from repeat topographic surveys: improved sediment budgets. *Earth Surface Processes and Landforms*, *35*(2), 136-156. https://doi.org/10.1002/esp.1886

Williams, R. (2012). DEMs of difference. *Geomorphological Techniques*, *2*(3.2).

Williams, G. P., & Wolman, M. G. (1984). Downstream effects of dams on alluvial rivers. Geological Survey Professional Paper 1286. Washington, DC: US Government Printing Office

Wohl, E., Bledsoe, B. P., Jacobson, R. B., Poff, N. L., Rathburn, S. L., Walters, D. M., & Wilcox, A. C. (2015). The natural sediment regime in rivers: Broadening the foundation for ecosystem management. *BioScience*, 65(4), 358-371. https://doi.org/10.1093/biosci/biv002

5. ARE RELIABLE METHODS AVAILABLE TO ESTIMATE BED MATERIAL TRANSPORT IN LARGE GRAVEL-BED RIVERS? A FIRST COMPARISON BETWEEN VIRTUAL VELOCITY APPROACH AND MORPHOLOGICAL METHOD

Andrea Brenna[1], Nicola Surian[1], and Luca Mao[2]

[1] *Department of Geosciences, University of Padova, Padova, Italy.*

[2] *School of Geography, University of Lincoln, Lincoln, UK.*

In preparation.

Abstract

The bed material transport represents one of the key factors controlling the morphodynamics of the large gravel-bed rivers although its estimation is a challenging task. One promising alternative to achieve transport estimates in those fluvial contexts is the virtual velocity approach, a hybrid solution based on a theoretical framework and use of tracers, potentially suitable in a wide range of gravel-bed rivers. Despite some approach applications and methodological improvements have been recently addressed, the reliability of the obtained transport estimates remains unverified since no comparisons with results of independent methods have been already performed. This work aims to validate the bed material load estimates obtained by the virtual velocity approach in a study sector of the Parma River (Italy) for the period April 2016 - April 2017, comparing such estimates with the results provided by the morphological method. Furthermore, we employed three classical transport formulas to add another independent comparison term. The results, referring to the coarse component of the bed material transport, point out that the virtual velocity approach estimates are remarkably similar with those provided by the sediment budgeting procedure. On the other hand, it is confirmed that transport formulas provide significantly different transport values at the same comparison sections. Under the study conditions, the virtual velocity approach, being based on data collected in the field and reach-specific calculation relations, results to be sensitive at the local bed material features which control the sediments dynamics and it is able to provide reliable transport estimates under different channel settings and mobility conditions.

1. Introduction

Gravel-bed rivers are alluvial channels where the coarse material (i.e. from fine gravel to small boulders) dominates the character of the bed deposits (Church, 2010). One of the key factors controlling the evolution and morphodynamics of gravel-bed rivers is the bed material load, defined by Church (2006) as the mobilization of the coarse sediment that

forms the bed and lower banks often transported as bedload (Church, 2006; Church and Ferguson, 2015). Moving from mountain to lowland areas, gravel-bed rivers typically shift from steep and narrow streams with cascade or riffle-pool morphologies to large systems characterized by active channels wider than some tens of meters and morphologies varying from single thread to braided configuration (Church, 2006, 2010). Especially in "large gravel-bed rivers" (i.e. rivers with channel larger than 20-30 m, as stated by Church (1992)), the high spatial and temporal variability of bed material transport (e.g. Hoey, 1992; Lisle et al., 2000; Clayton and Pitlick, 2007; Ryan and Dixon, 2007) makes the quantification of that process extremely challenging (Ferguson, 2007; Haschenburger, 2013; Wohl et al., 2015). Point measurements using direct sampling (e.g. Bunte at al., 2004) or indirect field techniques (e.g. passive acoustic methods as in Rickenmann et al., 2014) are available but more suitable for small streams (Ferguson, 2007). Besides, the use of theoretically-based transport formulas often provides incongruent results (Martin and Ham, 2005). Among the possible alternatives to achieve reliable estimates of such key process, Ferguson (2007) suggested (i) the inverse solution (or "morphological method", after Ashmore and Church, 1998) based on the erosion and deposition volumes evaluation and (ii) the use of data provided by tracers monitoring to estimate the flux starting from the virtual velocity of moved grains.

The morphological method has a long application history (e.g. Goff and Ashmore, 1994; Martin and Church, 1995; McLean and Church, 1999), is based on a solid theoretical paradigm (Ashmore and Church, 1998) and has been progressively improved by the increased quality of the topographical data (e.g. Legleiter, 2012; Passalacqua et al., 2015) and uncertainties estimation procedures (e.g. Brasington et al., 2003; Wheaton et al., 2010). The morphological method allows to calculate the transport rate using the diffused sediment budgeting procedure, which assumes that the volumetric variation of sediment stored in a river reach is equal to the difference between the sediment entering and leaving from the reach. As such, the method represents a sound way to obtain reliable average bed material transport estimates over defined time periods, but it is not ubiquitously applicable at all rivers contexts as it requires to define a river-section included in the study sector where the transport is known, estimable or negligible (Vericat et al., 2017). This condition is typically satisfied when one can identify a zero-flux sediment boundary such as the distal gravel-sand transition, a dam or a lake as done by Ham and Church (2000), Merz et al. (2006) and Surian and Cisotto (2007).

Even if the use of tracers represents a technique employed from long time for monitoring the sediment dynamics in fluvial geomorphology (see Hassan and Roy (2016) for a review), the virtual velocity approaches to address the transport estimation in gravel-bed rivers have been rarely used. Some theoretical frameworks and applications were proposed by Wilcock (1997), Haschenburger and Church (1998), Liébault and Laronne (2008) and Mao et al. (2017) to determine the bed material load at a river cross-section during a competent event, starting from tracers data and involving the calculation of the tractive forces induced by the water flow on the streambed. One fundamental strength of the virtual velocity approach is the possibility to apply the method in a wide range of large gravel-bed rivers without specific boundary conditions, as it requires only an adequate field monitoring activities and data processing (i.e. there is no need of a zero-flux sediment boundary). Because it is a hybrid method (i.e. a method based on theoretical frameworks but requiring several field data) rather than a direct measurement procedure, the virtual velocity approach is subject to some simplifications and assumptions imposed by the adopted theoretical framework and to field-monitoring data uncertainties. Mao et al. (2017) observed significant differences between outputs obtained adopting their virtual velocity estimation procedure and results provided by two classical transport formulas. Nevertheless, direct comparison between transport estimates carried out at the same study site by a virtual velocity approach and another independent estimation technique reliable for the considered river-type (i.e. large gravel-bed rivers) still does not exist. For this reason, it is not possible to validate the estimates provided by the virtual velocity approaches and to define if such method provides reliable volume of mobilized coarse bed material.

In this work we compare the results obtained by Brenna et al. (2018a) and Brenna et al. (2018b) who estimated the bed material transport regime along the same sector of the Parma River (Italy) using a virtual velocity approach and a morphological method, respectively. The aim of this work is to validate, for the first time, the transport estimates obtained via virtual velocity approach comparing such estimates with those provided by an independent and reliable method as the morphological budgeting procedure. Specifically we (i) addressed a comparison of the transport estimates obtained for the same period at four different locations using the two methods, (ii) introduced three theoretically-based transport formulas to extend the estimates comparison and (iii) analyzed the result matches or discrepancies in function of the local characteristics of the reaches defined in the study sector.

2. Materials and Methods

2.1 Study sector

Data and results employed in this work have been collected in a sector of the Parma River (Italy) (Figure 1). River catchment has an extension of 815 km^2 and the total river length is about 92 km, flowing from the North-Apennine to the Po River.

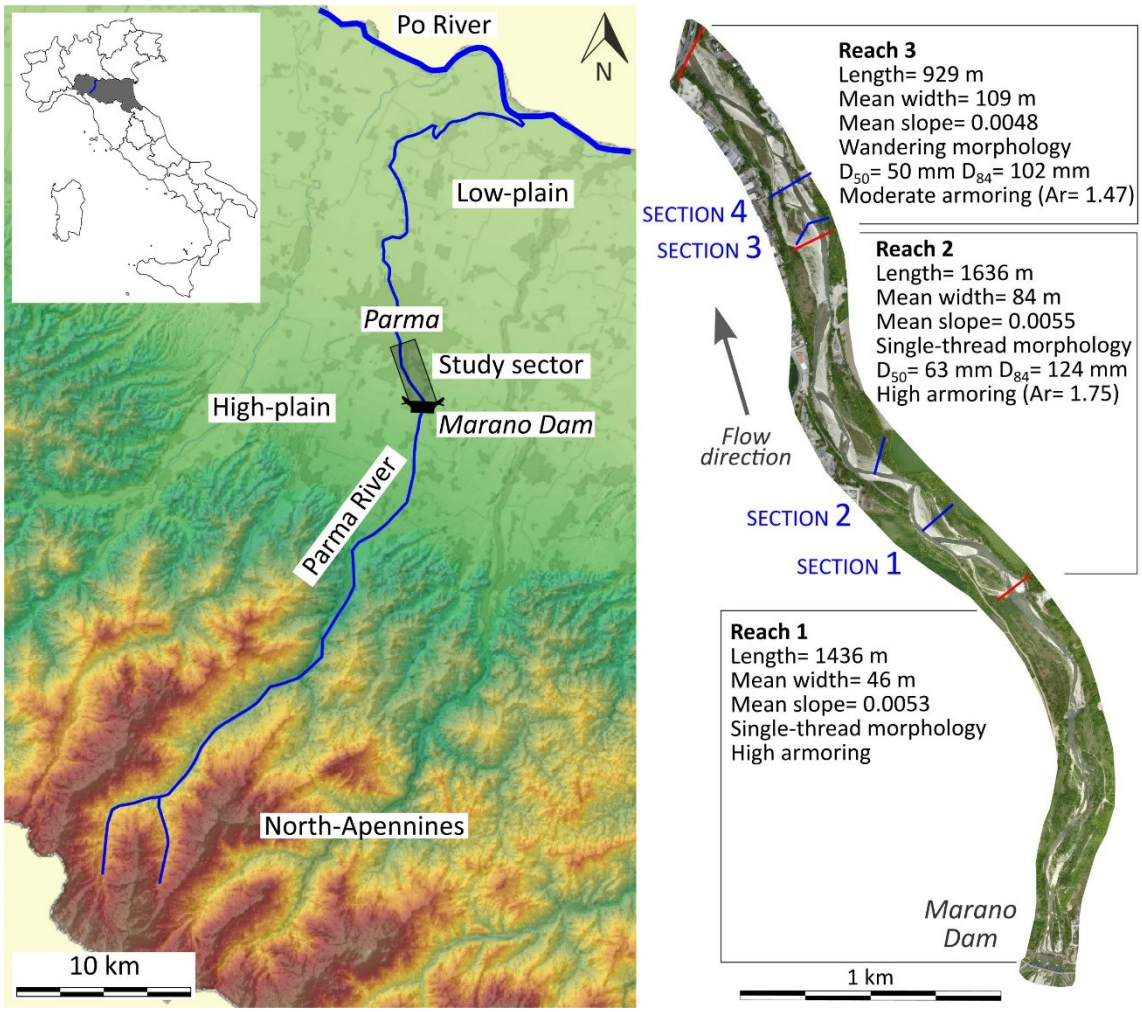

Figure 1. General setting of the Parma River catchment and the study area. For each of the three reaches identified within the study sector the main morphological and streambed sediments characteristics are reported as well.

The river hydrological regime is characterized by torrential behavior with precipitations and floods typically occurring during winter and spring while a long dry period leads to water discharge close to zero during summer. The high-plain part of the river course represents a typical example of large gravel bed river with braided morphology (braiding index = 2.5-3) and mean channel width of 300-350 m. The 4-km long study sector is located

immediately downstream from the Marano dam which represents a zero bed-material flux boundary (dam closure occurred in 2005). The deficit of sediment input from the upstream has led to notable changes in channel pattern downstream from the dam (Brenna et al., 2018b), the channel has become narrower (width between 60 and 160 m) and characterized by single-thread or wandering configurations. Along the study sector three different reaches (sensu Brierley and Fryirs, 2013) with peculiar features were recognized by Brenna et al. (2018b) based on morphological and streambed sediments characteristics as summarized in Figure 1.

The study sector is suitable for independent calculations of the bed material load employing the morphological method (Brenna et al., 2018b) and the virtual velocity approach (Brenna et al., 2018a) for three reasons: (i) it includes a zero-flux coarse sediment section it allows the application of the morphological method by the independent sediment budgeting procedure; (ii) it shows a marked longitudinal gradient of channel characteristics along a relatively short distance (i.e. 3 reaches in 4 km) allowing to compare the performance of the two estimation methods under different boundary conditions (i.e. channel morphology and streambed features); (iii) it features the presence of a dam equipped with a gauging station makes easier the hydrological monitoring.

2.2 Bed material load estimation through the virtual velocity approach

Brenna et al. (2018a) used data collected during a monitoring activities based on tracers carried out in the Parma River, to analyze the coarse sediment transport (for clasts larger than 6 mm) through a virtual velocity approach based on the Wilcock's framework (1997). They estimated the bed material load at four cross-sections located along two reaches of the Parma River (sections 1, 2, 3, 4; see Figure 1) during nine competent events that occurred between January 2016 and May 2017 (Figure 2). Collecting data in the field from tracers, scour chains, hydrometers, and grain size analysis, they developed empirical relations between the tractive forces induced by the water flow on the streambed and the transport activation thresholds, the thickness of the active layer and the virtual velocity of the moved grains (Brenna et al., 2018c). Those data, combined with equations for the fractional transport calculation (Wilcock, 1997), allowed to relate the dimensionless shear stress (τ^*) induced by the water flow on the streambed with the instantaneous-local bed material flux. Finally, the bed material load at a river section during a competent event was estimated integrating the instantaneous-local flux over the time (i.e. competent event hydrograph) and space (i.e. section topography) (as described in Brenna et al., 2018c).

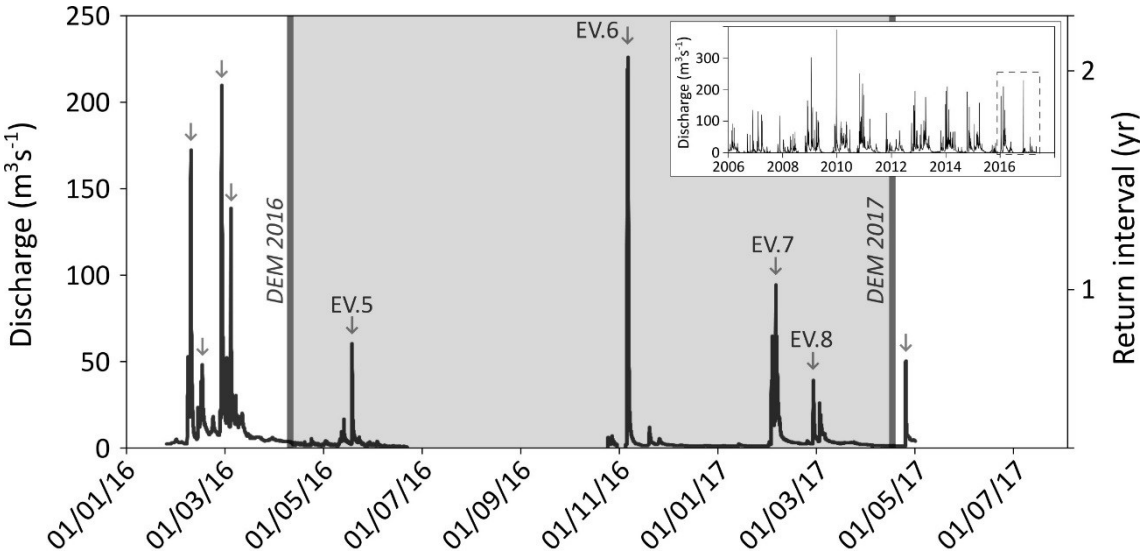

Figure 2. Study sector hydrograph during the comparison period (April 2016 – April 2017, highlighted by the grey box). The vertical arrows point out the occurred competent events. Four formative floods occurred during the considered year, which are identified as events 5, 6, 7 and 8, following Brenna et al. (2018a).

2.3 Sediment regime analysis using the morphological method

Brenna et al. (2018b) calculated the volumetric variations in sediment stored along the same study sector employing LiDAR and photogrammetric Digital Elevation Models (DEM). Calculations were carried out for three periods after dam closure (i.e. 2006-2008, 2008-2016, and April 2016 - April 2017). Errors have been considered in different ways depending from the employed data features as described by Vericat et al. (2017) and using the Geomorphic Change Detection Software (Wheaton et al., 2010) to derive the three study-sector DEMs of Difference (DoD: see Williams (2012) for a complete definition). Exploiting the zero-flux coarse sediment boundary represented by the Marano dam, they adopted the sediment budgeting procedure to convert the volumetric changes into coarse sediment transport at seven sections (the 3 reaches limits and the four sections adopted for the virtual velocity estimation by Brenna et al. (2018a). For addressing the conversion from volumetric data to sediment transport estimates, they considered both the bed material porosity and the percentage of bed material finer than 6 mm (excluded from the calculation).

2.4 Comparison of results from the virtual velocity approach and morphological method

A comparison between the virtual velocity approach (Brenna et al., 2018a) and the morphological method (Brenna et al., 2018b) transport estimates was feasible for the

period from April 2016 to April 2017. Specifically, the sediment budgeting procedure considered the more recent DEMs and the relative DoD (2016-2017), while the virtual velocity approach focused on the four competent events that occurred during that period (Figure 2). The discharges that occurred during the considered time interval (i.e. floods with recurrence interval between <1 yr and 2.1 yr) are conform with the typical hydrological behavior characterizing the annual regime of the Parma River (see the box in Figure 2). To compare the results provided by the two methods, we summed the event transport estimates obtained for the four events occurred between April 2016 and April 2017 (Figure 2) by Brenna et al. (2018a) at each of the four cross-sections (Figure 1) and compared those results with the bed material load provided by the morphological method. Both the considered calculations provide estimates about the bed material load transited though some sections located along the study sector considering only the fraction of the flux coarser than 6 millimeters. Estimates obtained through the two approaches refer to the coarser part of the bed material load (lower grain size limit of 6 mm, falling into the fine gravel class) from which are excluded the very fine gravel and the sand representing about 20% of the bed material in the considered river sector (Brenna et al., 2018c).

2.5 Theoretically-based transport formulas

In order to add another term of comparison, we considered three transport formulas based on surface grain-size data for calculating the transport at the same locations considered by the virtual velocity and morphological approaches. Specifically we used:

The Wong and Parker (W&P) relation (2006)

It represents a revisited version of the classical Meyer-Peter and Mueller equation (1948) (i.e. one of the most frequently used relation for the calculation of the coarse sediment transport, e.g. Gomez and Church, 1989; Nicholas, 2000; Martin and Ham, 2005; Lopez et al., 2014) amending some critical points of the original formulation. To calculate the unit-instantaneous bed material load, the equation reads as:

$$q_v^u[m^3 s^{-1} m^{-1}] = 3.97\sqrt{g\left(\frac{\rho_s}{\rho_w} - 1\right) D_{50}^3}\,[\tau^* - 0.00495]^{\frac{3}{2}} \quad (1)$$

where g is the gravity acceleration (in ms^{-2}), ρ_s and ρ_w are the sediment and water densities (in kgm^{-3}) and D_{50} is the median surface grain size (in m).

The dimensionless shear stress induced by the water flow on the streambed (τ^*) has been calculated through the depth-slope approach (e.g. Mueller et al., 2005; Wilcock, 1993) as:

$$\tau^* = \frac{\rho_w g h_w S}{(\rho_s - \rho_w) g D_{50}} \quad (2)$$

where h_w is the local water depth (in m), and S is the local streambed slope (in m m^{-1}). To initiate the transport, the W&P equation considers a fixed threshold for τ^* of 0.00495.

The Recking formula (2010)

It has been developed based on flume and river data for addressing transport estimations in a broad spectrum of gravel-bed river contexts, also similar to the one considered in this work in terms of grain size and slope. Due to the simplicity of use and limited input data required, the Recking's equation (2010) has been adopted in this work for our calculations. As reported in Recking et al. (2012) the non-threshold equation can be written as:

$$q_v^u[m^3 s^{-1} m^{-1}] = \frac{14\sqrt{g\left(\frac{\rho_S}{\rho_w}-1\right)D_{84}^3}(\tau_{84}^*)^{2.5}}{1+\left[\frac{(5S+0.06)\left(\frac{D_{50}}{D_{84}}\right)^{4.4\sqrt{S}-1.5}}{\tau_{84}^*}\right]^4} \quad (3)$$

where, differently from equation (1), are considered also the D_{84} of surface sediments (in m) (giving more importance to the coarse fraction of the bed material) and the dimensionless shear stress calculated depending from this gran size parameter as:

$$\tau_{84}^* = \frac{\rho_w g h_w S}{(\rho_s - \rho_w) g D_{84}} \quad (4)$$

The Wilcock and Crowe (W&C) model (2003)

The transport model has been developed from flume experiments specifically in order to include the sand and its effects on the bed material load. The considered study sector sediments are characterized by 20% in volume of material finer than 6 mm (Brenna et al,) and by a mean presence of sand equal to 6-10% making the Wilcock and Crowe model (2003) suitable for the application in this context. We applied the calculation not considering the fractional transport but using the surface D_{50} through the formula:

$$q_v^u[m^3s^{-1}m^{-1}] = \frac{W^*\left(\frac{\tau}{\rho_w}\right)^{\frac{3}{2}}}{\left(\frac{\rho_S}{\rho_w}-1\right)g} \quad (5)$$

where τ is the shear stress induced by the water flow on the streambed ($\tau = \rho_w g h_w S$, in $kgm^{-1}s^{-2}$). W^* is the dimensionless transport rate and is calculated through the equations:

$$W^* = 0.002\Phi^{7.5} \quad \text{for } \Phi < 1.35 \quad (6)$$

$$W^* = 14\left(1 - \frac{0.894}{\Phi^{\frac{1}{2}}}\right)^{4.5} \quad \text{for } \Phi \geq 1.35 \quad (7)$$

where Φ is equal to ($\tau/\ \tau_{rm}$) with τ_{rm} equal to the reference shear stress of median size of bed surface taking into account for the proportion of sand in surface size distribution (F_s) and calculated as:

$$\tau_{rm} = (0.021 + 0.015exp[-20F_s])\left[\left(\frac{\rho_s}{\rho_w} - 1\right)\rho_w g D_{50}\right] \quad (8)$$

The three selected equations allow to calculate the instantaneous-unit bed material transport ($m^3s^{-1}m^{-1}$) in function of the dimensionless shear stress locally induced by the water flow on the river bed over the time with limited knowledge of surface sediments data and channel geometry. The employed formulas have been applied considering the data collected during the monitoring addressed for the virtual velocity approach application by Brenna et al. (2018c) and the adopted calculation procedure is similar to that used by Brenna et al. (2018a). Considering the cross-sections geometry, the local streambed slope (S), the mean values of grain sizes (D_{50} and D_{84}) for each morphological unit and the sediment characteristics (e.g. density of the grains, ρ_s= 2600 kgm^{-3}) defined for each reach (reach 2 and reach 3 features respectively applied to sections 1-2 and 3-4 calculations; see Figure 1), we calculated the instantaneous unit-bed material transport (q_v^u) through the transport relations (Equations (1), (3), (5)). Finally, the event-section bed material fluxes were estimated integrating the instantaneous-local estimates over the time (i.e. competent event hydrograph) and space (i.e. cross-section topography). The described procedure was applied at the same events and sections considered by the virtual velocity approach. Due to the similarity of calculation procedures and since the formulas focus on the bedload mechanism for the coarse fraction of the particles (except for W&C model that considers also the sand), the data obtained by the equations are directly comparable to the virtual velocity approach estimates of the coarse fraction of the bed material load.

3. Results

3.1 Estimates of bed material transport by the virtual velocity and the morphological methods

The morphological method provides an estimation of the bed material load along the study sector over the period between the two considered DEMs (April 2016 - April 2017) while the virtual velocity approach estimates refer to volumes of material mobilized at the sections under consideration during a single competent event. Having two different time scale (i.e. one year vs single event), we added the single estimates provided by the virtual velocity approach at each section during the competent events obtaining transport values for the whole period of comparison (Table 1).

Reach	Section	Event 5	Event 6	Event 7	Event 8	Total period
R2	S1	3 ± 3	158 ± 74	29 ± 24	5 ± 5	195 ± 78
	S2	20 ± 20	238 ± 108	46 ± 42	11 ± 11	315 ± 118
R3	S3	107 ± 54	746 ± 230	456 ± 203	210 ± 107	1519 ± 329
	S4	167 ± 87	601 ± 171	397 ± 152	191 ± 79	1356 ± 257

Table 1. Bed material transport estimates obtained by the virtual velocity approach for the four competent events that occurred between April 2016 and April 2017. Results are expressed as volume (m^3) of bed material coarser than 6 mm transported at a specific section during an entire competent event (modified from Brenna et al. (2018a)).

Sections 1 and 2 are located within reach 2, which is characterized by strong alterations due to human impacts (see Figure 1). The sediment starvation due to the dam led to alterations of transport processes with a decrease of the natural sediment mobility and flux (Brenna et al., 2018a). Subsequently, a general channel re-arrangement occurred through narrowing, incision and bed armoring (Brenna et al., 2018b) conforming with the degradation adjustment style (Petts, 1984). At section 1 the estimates provided by virtual velocity and morphological methods are extremely low (Figure 3). Indeed, during the entire period a total of 195 ± 78 m^3 and of 122 ± 588 m^3 are respectively provided by the two methods (Table 2). Considering the uncertainty bands, there is a good overlapping between the two estimates. A slight increase of bed material transport was obtained at section 2 by the virtual velocity calculation (315 ± 118 m^3) while the morphological method gave a value of 125 ± 681 m^3, very similar to the estimate obtained at section 1. The morphological method estimate was lower than the virtual velocity one, also considering the uncertainty bands.

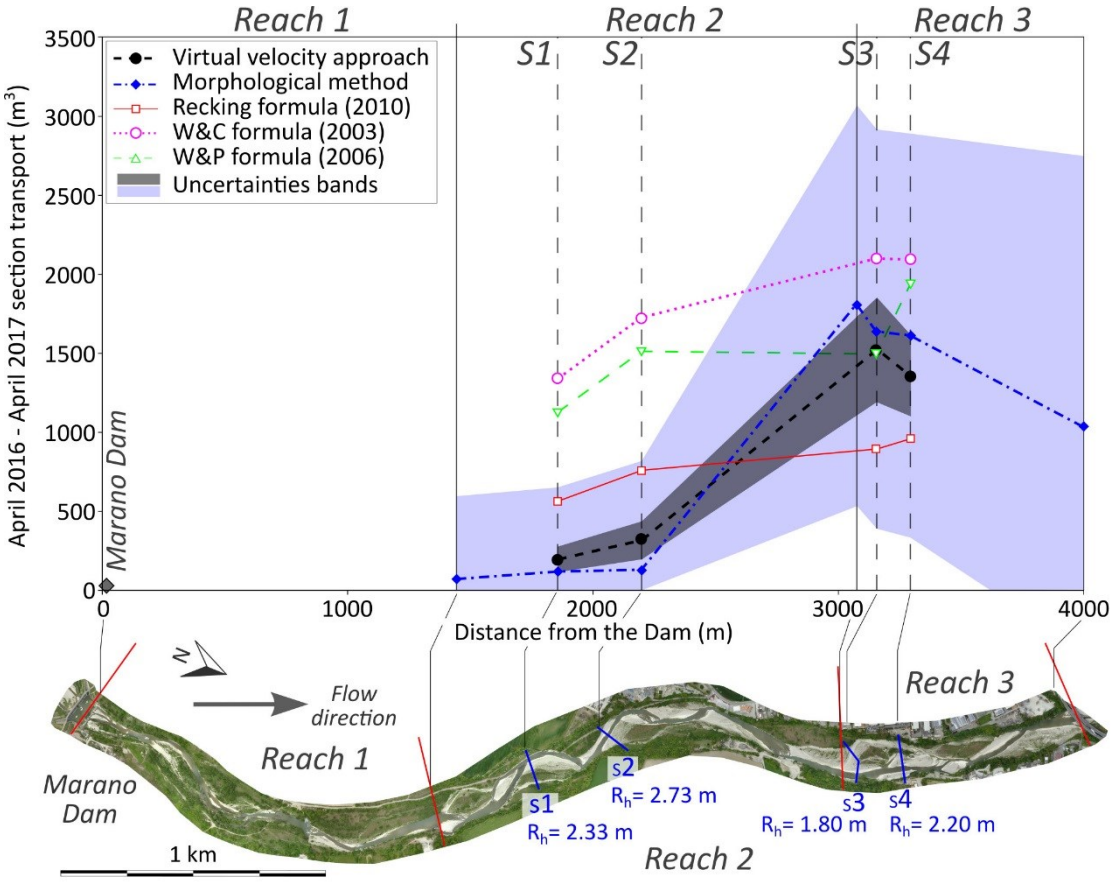

Figure 3. Coarse bed material transport estimated using the two analyzed methods and three transport formulas along the study sector (four comparison sections and the reaches limits) during the entire comparison period (April 2016 - April 2017). On the bottom is plotted a drone-photo of the study reach with the position of the considered cross-sections and their hydraulic radius (R_h).

Moving downstream along the study sector the bed alteration due to the dam progressively decreases. Considering the increase in channel width and morphological complexity and the decrease of bed armoring (see Figure 1), the limit between reach 2 and reach 3 has been identified approximately 3 km downstream from the zero-flux dam boundary (Brenna et al., 2018b). At that section, the morphological method highlights a remarkable increase of sediment flux which is 1811 ± 1280 m^3. Results provided by two estimation methods at sections 3 and 4 (Figure 3) confirm the occurrence of higher bed material transport along reach 3 in comparison to that obtained at reach 2. At section 3 estimates derived by both methods are very close: 1519 ± 329 m^3 of bed material load are calculated by the virtual velocity approach while 1645 ± 1284 m^3 by the sediment budgeting procedure. Similar values characterize section 4 where the virtual velocity approach gives sediment flux equal to 1356 ± 257 m^3 (slightly lower than one obtained at section 3) and the morphological method estimate is of 1618 ± 1294 m^3 (Table 2). Transport value

provided by the morphological method is placed on the upper limit of the virtual velocity result variability range.

Moving towards the downstream limit of the study sector (4 km downstream from the dam), the morphological method provides a value of 1086 ± 1739 m^3. It is worth noting that both methods show a remarkable longitudinal increase of sediment transport moving away from the dam zero-flux boundary (Figure 3).

	Section 1	Section 2	Section 3	Section 4
Morphological Method	122±588	125±681	1645±1284	1618±1294
Virtual Velocity Approach	195±78	315±118	1519±329	1356±257
Recking formula (2010)	562	757	896	959
W&C formula (2003)	1337	1723	2098	2095
W&P formula (2006)	1125	1515	1500	1938

Table 2. Summary of the bed-material transport estimates (expressed as volume of sediments in m^3) obtained using the two tested approaches and the three considered transport-formulas at the four cross-section for the entire comparison period (April 2016 - April 2017).

3.2 Transport formulas estimates and comparison with virtual velocity and morphological method results

The transport estimates obtained for the period April 2016 - April 2017 at the four cross-sections using the three adopted formulas are significantly different (Figure 3 and Table 2). At sections 1 and 2, W&C (2003) and W&P (2006) relations provide similar results (section 1: W&C= 1337 m^3, W&P= 1125 m^3; section 2: W&C= 1723 m^3, W&P= 1513 m^3) which are between 5 times and one order of magnitude higher than those provided by the virtual velocity and morphological methods. The Recking formula results (562 m^3 and 757 m^3 respectively at sections 1 and 2) are relatively closer (between 2 and 6 times higher) to the estimates carried out by the two methods tested in this work. Along the high transport-altered reach 2, the three formulas provided results significantly different (i.e. higher) from those of the virtual velocity approach and morphological method.

Estimates obtained at sections 3 and 4 by the two independent approaches and the three theoretically-based transport formulas are more similar. At section 3, W&P (2006) relation estimates a bed material transport during the whole comparison period of 1500 m^3 which is equal to the virtual velocity approach estimate and similar to the morphological method one. The Recking formula (2010) result is about 40% lower (896 m^3) while the W&C model (2003) provides a transport estimate about 40% higher than the virtual velocity and W&P

ones (2098 m^3). The estimate comparison remains similar at section 4, where Recking (2010) and W&C (2003) formulas provide transport values equal to 959 m^3 (Recking) and 2095 m^3 (W&C), respectively lower (about 30-40%) and higher (about 35-50%) than those obtained by the virtual velocity and morphological methods. The W&P formula (2006) estimates a transport of 1938 m^3 deviating from the virtual velocity result (i.e. about 40% higher).

The three considered equations show variations in longitudinal transport estimates less marked in comparison with the virtual velocity and morphological methods. W&C formula (2003) provides the highest transport estimates while the Recking equation (2010) estimates are the lowest. As shown in Figure 3, the W&C (2003) and W&P (2006) formulas give results higher than the virtual velocity and morphological methods along the entire study sector, while Recking approach (2010) estimates are higher at the human-impacted reach 2 and lower at the more natural and dynamic reach 3 in comparison with the two tested approaches.

4. Discussion

4.1 How similar are the sediment transport estimates?

Transport estimates carried out by the virtual velocity approach (Brenna et al., 2018a) and derived from a morphological method (Brenna et al, 2018b) are significantly similar at least at three of the four comparison sections along the study sector (Table 2). Only at section 2, located into reach 2 that is high impacted from a sediment dynamics point of view (Brenna et al., 2018a), the two methods provide slightly different results since the morphological method estimate is out from the variability band of the virtual velocity approach estimation (Figure 3). The estimates highlight also very similar trends in longitudinal variation of sediment flux even if the morphological method downstream-increasing trend is slightly more pronounced than the virtual velocity one (Figure 3).

The comparison is more complex to interpret when introducing the results of the three transport formulas as well (see Table 2). At sections located in reach 2 (i.e. sections 1 and 2) the formulas estimates are always much higher than the values obtained by the two considered approaches, with the Recking equation (2010) providing the relatively most comparable values (Figure 3). At reach 3 (i.e. sections 3 and 4) the formulas and the two tested methods are more similar (in particular considering the W&P equation (2006)) but

in general the formulas estimates are out from the variability band of the virtual velocity approach estimations (Figure 3).

4.2 What are we really estimating using the different approaches?

As highlighted by Church (2006) it is important to distinguish the meaning of "bedload transport" and "bed material transport" since the two terms belong to different categorization of fluvial sediment transport (see Hicks and Gomez, 2016) and refer to different concepts despite, often, the bed material load is mainly transported as bedload. Bedload transport refers to the mobilization and transport of coarse material in the close proximity of the riverbed by rolling, sliding and saltating (Gomez, 1991). Sediments transported as bedload can be sourced by either the bed and banks of a certain reach, and from upstream reaches. The bed material transport is the fraction of transport for which sediments are provided by the alluvial channel (i.e. bed and lower banks; Church, 2006). Due to the conceptual differences behind the two terms, the bed material transport and the bedload can also differ from a quantitative point of view at least for two reasons: (i) the sediment grain size: considering a river reach and a single competent event, the bed material load passing through a reference-section can include also fine material (e.g. sand) which is mobilized from the channel bed into suspension; (ii) the origin of the material: during a flood several processes (e.g. bank erosion) can import coarse material originally stored out from the channel which is then mobilized as bedload but was not strictly part of the bed material load referring to the specific transport event.

Both direct (e.g. traps) and indirect (e.g. geophones) field techniques typically measure the bedload (e.g. Bunte et al., 2007; Rickenmann, 2017), as the surveys capture all sediments passing through a cross-sections, irrespective of their provenance. However, the estimates carried out by the approaches considered in this work (morphological method and virtual velocity) are more difficult to be classified. For instance, the morphological method would account for fine sediments moved in suspension, and the virtual velocity approach would not account for fine gravel transport that can be transported as a bedload. In order to make equal the two transport values from a quantitative point of view (but maintaining the conceptual differences) it is possible to shrink the range of the considered grain size and to use an adequate time scale of analysis. The virtual velocity approach, based on field data collected in the bed and focusing only on the in-channel dynamics (e.g. it does not consider bank erosion), potentially provides bed material transport estimates but, for practical reasons affecting tracers monitoring (e.g. grain size that can be recovered), limits its

estimates to the coarse fraction (i.e. 6 mm in our case) of the bed material load. The morphological method applied over a time scale larger than one event (in this work one year with four formative floods) is potentially able to give an estimate of the total bed material flux except for the very fine material component moved out from the considered river sector (e.g. fine sand entrained from the bed but mobilized in suspension over long distances). Nevertheless, by considering the fraction of bed material coarser than 6 mm to convert the volume changes in sediment transport, Brenna et al. (2018b) obtained also in this case the coarse fraction of the bed material transport. W&P (2006) and Recking (2010) equations, focusing on the coarse part of the transport, provide bedload estimates but actually, if applied analogously to the virtual velocity approach as we did in this study, the results can be mutually compared. W&C model (2003), as stated by the authors, estimates the transport involving the whole spectrum of grain size (i.e. including sand) providing values that approaches the concept of total bed material load.

From the reported overview of the transport concepts, and considering the application procedures adopted for the estimation approaches, it seems reasonable to accept that all the obtained values, excluding the W&C model (2003) results, refer to the coarse fraction of the bed material transport ("coarse bed material transport" or "gravel-bed material transport") and so they are comparable. It is also possible to speculate that, in the study sector, the obtained coarse bed material flux estimates could be similar to the total bed material load due to the relatively poor presence of fine material, while marked differences could occur in different contexts such as in mixed sandy-gravel channels.

4.3 How reliable are the obtained coarse bed material transport estimates?

Results obtained using the independent virtual velocity and morphological methods are remarkably similar along the whole study sector, considering both the numerical values obtained for the analyzed period and the longitudinal transport trends. Several previous works (see Vericat et al. (2017) for a complete review) highlight the reliability of the transport estimates provided by the morphological method, in particular if based on the sediment budgeting procedure. Because the two independent methods provided similar bed material load estimates at the four sections, it is reasonable to state that the virtual velocity approach applied by Brenna et al. (2018a) following the procedure described by Brenna et al. (2018c) and based on the Wilcock's framework (1997), provided a comparable and reliable estimates along the entire considered study sector.

The adopted transport formulas have variable performance when compared to the virtual velocity approach and the morphological method. Where the river conditions are more impacted (i.e. reach 2, with diffused bed armoring and altered sediment dynamics) the general reliability of the tested formulas becomes lower while in less altered reaches (i.e. reach 3, characterized by more natural sediment mobility) the equations provides results that are more similar to those obtained by the virtual velocity and morphological methods. Selecting for each section the estimate obtained through transport formula that is closer to the reliable transport values, an acceptable concordance between the formulas and the analyzed approaches results is obtained, but at different sections different formulas achieve this goal (Figure 4).

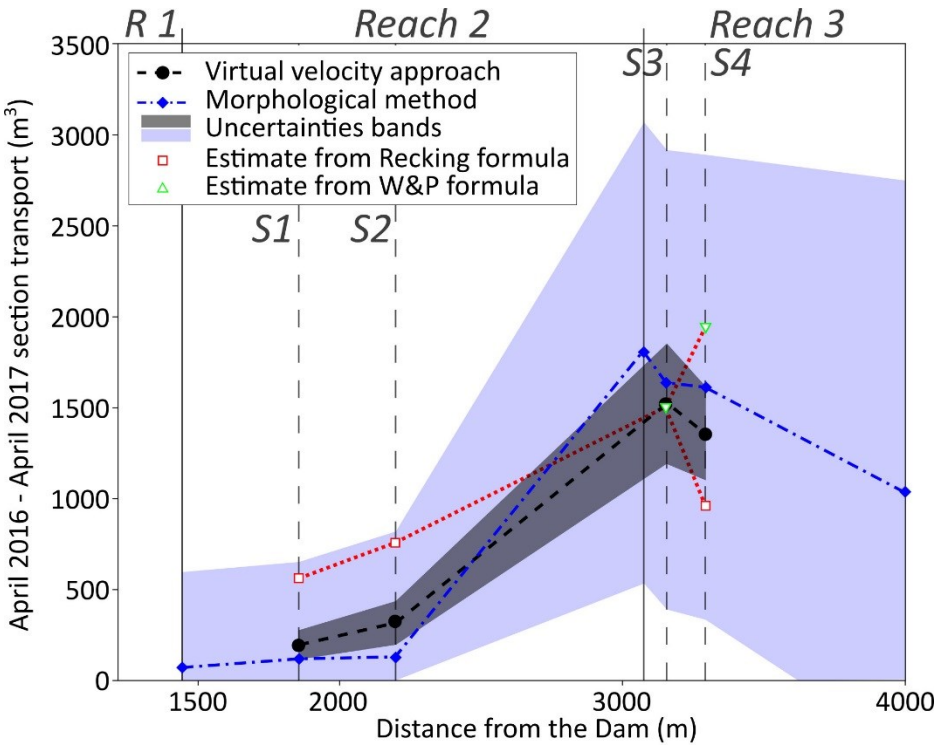

Figure 4. Coarse bed material transport estimated at the comparison locations using the two analyzed methods and considering the transport formulas estimations which are closer to the reliable flux values (i.e. virtual velocity or morphological results).

Recking formula (2010), conforming with its develop characteristics, provided relatively better results in comparison with the other equations along the high armored reach 2 (where the transport is largely inhibited) while the best transport estimates along reach 3 (characterized by finer and more mobile streambed material) have been achieved by the W&P relation (2006) (Figure 4). The W&C model (2003) outputs were constantly the highest probably because the method considers the entire grain size spectrum of the

mobilized material (including sand and very fine gravel, not considered by the other approaches). The results confirm that it is difficult to select *a priori* the best equation for estimating the coarse sediment transport at a specific river location and suggest that, also for a single river segment or reach, it is necessary to adopt different formulas at different sections for achieving reliable estimations about the coarse flux occurring during one or more competent events.

Brenna et al. (2018a) highlighted the different mobile-sediment availability along the Parma River study sector due to the impact induced on the channel dynamics by the dam zero-flux coarse sediment boundary. The virtual velocity approach, as hybrid solution based on a theoretical framework and reach-specific empirical equations developed from field data (Brenna et al., 2018c), is able to take into account for local variations in streambed-mobility conditions. This conclusion is supported by the marked longitudinal increasing trend characterizing the transport estimates obtained using the virtual velocity approach along the 4-km human-impacted study sector, conforming to the morphological method evidences (Figure 3). Differently from the transport formulas, the virtual velocity approach is sensitive to the local channel-sediments features (not only the grain size distribution but also the structure, armoring and fabric) controlling the transport processes. The virtual velocity approach, if based on an adequate field data monitoring and calculation procedures (e.g. develop of reach-specific empirical relations and adoption of realistic data input configurations as in the considered works), is potentially able to provide reliable bed material load estimates in several contexts and under different transport conditions. On the contrary, the almost flat longitudinal trends characterizing the transport formula estimates (Figure 3) suggest that those methods are poorly sensitive to sediment mobility parameters affecting a river channel at a local scale (e.g. reach or morphological unit).

4.4 Limitations and future perspectives for the virtual velocity approach

The adopted virtual velocity approach allowed us to focus only about the coarse component of the bed material transport due to the caliber limitations affecting the passive tracers employed by Brenna et al. (2018c) and since the adopted framework (Wilcock, 1997) was specifically developed for the gravel entrainment, displacement and transport evaluation. In order to move from the "coarse bed material load" to the "bed material load", considering that the two values can be remarkably different in some gravel-bed rivers with a significant presence of fine material in the bed, it is necessary to include the estimation of the sand and very fine gravel into the calculation. To employ tracers revealing sand

dynamics is a challenge activity that however has been addressed using radioactive or fluorescent tracers in some rivers (e.g. Hubbell and Sayre, 1964; Crickmore, 1967) or, more commonly, in coastal environments (e.g. Komar and Inman, 1970; Badr and Lofty, 1999; Klein et al., 2007). To use those techniques and dispersion models based on tracers data (e.g. Bradley et al., 2010) or simply integrating the virtual velocity approach with transport equations able to estimate also the finer transport component (e.g. Wilcock, 2001; Wilcock and Crowe, 2003) could represent valid alternatives for achieving a complete quantification of the bed material load by hybrid approaches.

The morphological method transport estimates, despite being robust, are characterized by wide error-bands associated with the volume of mobilized coarse material at the considered sections (Figure 3). Those uncertainties are due to the quality of the spatial data used for deriving the volumetric changes by Brenna et al. (2018b) which employed Digital Elevation Models of the study sector obtained by photogrammetric technique. The presence of areas within the channel covered by vegetation or water increases the errors in the DEM of Difference derived between 2016 and 2017 and, in turn, the uncertainties of the transport estimates. In particular, the lack of spatial information in the wet part of the channel could represent an impacting source of uncertainties because, even if this area generally represents a small portion of the active channel it may account for a significant part of erosion and deposition volumes since it is exposed to the highest hydraulic forces (e.g. Lallias-Tacon et al., 2014). The errors could be reduced employing terrain models acquired by LiDAR, bathymetric-LiDAR which allows to map the channel bottom also in presence of water (e.g. Mandlburgere et al., 2015) or including a reconstruction of the channel bathymetry from image processing (e.g. Legleiter, 2012, 2016). Obtaining more accurate estimates from morphological method could improve the quality and the meaningfulness of the comparison with the virtual velocity approach.

The estimates analyzed in this work refer to the coarse bed material load occurred during one hydrological year at four river cross-sections. Future methods-results comparisons could consider the transport over different time scales (e.g. a single competent event or a longer study period) and flood magnitudes or in other gravel-bed river contexts (e.g. channel with, slope, sediments type etc.) in order to verify the performance of the virtual velocity approach for estimating the bed material load in a wider range of conditions.

Thanks to the tested reliability of the estimates provided by the virtual velocity approach (Wilcock, 1997) after the improvements achieved by Brenna et al. (2018c), the virtual

velocity approach seems to represent a viable alternative for obtaining local quantification of the bed material load (e.g. at the monitored river sections). This means that the morphological method, which provides estimates at larger spatial scale, could be applied in a wider spectrum of situations using the virtual velocity approach estimates as input (i.e. having a section where the sediment transport is known).

5. Conclusions

In this work we compared the results obtained about the coarse fraction of the bed material load mobilized along the same 4-km study sector of a large gravel-bed river using the virtual velocity and the morphological methods. The comparison was expanded performing the same calculation by three classical transport formulas applied at the same river locations (i.e. four cross-sections) and study period (i.e. April 2016 - April 2017). Comparing the results obtained through the adopted independent approaches, the derived conclusions are:

(i) For the considered comparison period and study area, the estimates provided by the virtual velocity approach are remarkably similar with those obtained using a robust morphological method. Under the research comparison-conditions (i.e. time scale of analysis and selected case study), considering the values obtained from the morphological approach as very close to the "real transport", the virtual velocity approach provides reliable estimates of the annual coarse bed material transport.

(ii) In accordance with results provided by previous works, different transport formulas provide significantly different estimates. Some of the tested equations provide sediment flux values sufficiently similar with those estimated by the virtual velocity approach but no equation achieved this goal along the whole study sector since the formulas are not sensitive to the local bed material structure (e.g. armoring) and sediment availability.

(iii) Being strictly based on field monitoring data capturing the local channel and sediments characteristics which control transport processes, the virtual velocity approach provided reliable transport estimates (i.e. similar to the morphological method ones) along the two remarkably different reaches characterizing the study sector. Considering the results provided by this first comparison and validation, the

method should be able to provide reliable estimates in different gravel-bed rivers contexts and under different transport conditions.

(iv) The virtual velocity approach represents one the few alternatives adequate to calculate reliable estimates of the coarse component of the bed material load in large gravel-bed rivers. For making the method suitable also for gravel-bed channels characterized by significant percentages of fine material (i.e. sand and very fine gravel) in the streambed, it is still necessary to develop the calculation procedure in order to include that component in the estimation, obtaining as result the "total bed material transport".

References

Ashmore, P. E., & Church, M. (1998). Sediment transport and river morphology: a paradigm for study. In P. C. Klingeman, R. L. Beschta, P. D. Komar, J. B. Bradley (Eds.), *Gravel-Bed Rivers in the Environment* (pp. 115-148). Highlands Ranch, CO: Water Resources Publications LLC

Badr, A. A., & Lotfy, M. F. (1999). Tracing beach sand movement using fluorescent quartz along the Nile Delta promontories, Egypt. *Journal of Coastal Research*, 261-265.

Bradley, D. N., Tucker, G. E., & Benson, D. A. (2010). Fractional dispersion in a sand bed river. *Journal of Geophysical Research: Earth Surface*, *115*(F1). https://doi.org/10.1029/2009JF001268

Brasington, J., Langham, J., & Rumsby, B. (2003). Methodological sensitivity of morphometric estimates of coarse fluvial sediment transport. *Geomorphology*, *53*(3), 299-316. https://doi.org/10.1016/S0169-555X(02)00320-3

Brenna, A., Surian, N., & Mao, L. (2018a). Sediment Mobility and Bed Material Transport Estimation in a Gravel-bed River Downstream of a Dam. *Earth Surface Processes and Landforms* (submitted)

Brenna, A., Surian, N., & Mao, L. (2018b). Alteration of Sediment Transport and Channel Morphology in a Gravel-bed River Downstream of a Dam. To be submitted to *Geomorphology*

Brenna, A., Surian, N., & Mao, L. (2018c). Virtual Velocity Approach for Estimating Bed Material Transport in Gravel-Bed Rivers: Key Factors and Significance. *Water Resources Research* (under review)

Brierley, G. J., & Fryirs, K. A. (2013). Geomorphology and river management: applications of the river styles framework. Hoboken, NJ: John Wiley & Sons

Bunte, K., Abt, S. R., Potyondy, J. P., & Ryan, S. E. (2004). Measurement of coarse gravel and cobble transport using portable bedload traps. *Journal of Hydraulic Engineering*, *130*(9), 879-893. https://doi.org/10.1061/(ASCE)0733-9429(2004)130:9(879)

Bunte, K., Swingle, K. W., & Abt, S. R. (2007). Guidelines for using bedload traps in coarse-bedded mountain streams: construction, installation, operation, and sample processing. Gen. Tech. Rep. RMRS-GTR-191. Fort Collins, CO: U.S. Department of Agriculture, Forest Service, Rocky Mountain Research Station. https://doi.org/10.2737/RMRS-GTR-191

Church M. (1992). Channel Morphology and Typology. In: P. Callow, G.E. Petts (Eds.), *The Rivers Handbook* (pp. 126-143). Oxford, UK: Blackwell Publishing Ltd

Church, M. (2006). Bed material transport and the morphology of alluvial river channels. *Annu. Rev. Earth Planet. Sci*., 34, 325-354. https://doi.org/10.1146/annurev.earth.33.092203.122721

Church, M. (2010). Gravel-Bed Rivers. In T. P. Burt, R. J. Allison (Eds.), *Sediment Cascades: An Integrated Approach* (pp. 241-269). Hoboken, NJ: John Wiley & Sons

Church, M., & Ferguson, R. I. (2015). Morphodynamics: Rivers beyond steady state. *Water Resources Research*, 51(4), 1883-1897. https://doi.org/10.1002/2014WR016862

Clayton, J. A., & Pitlick, J. (2007). Spatial and temporal variations in bed load transport intensity in a gravel bed river bend. *Water Resources Research*, 43(2). https://doi.org/10.1029/2006WR005253

Crickmore, M. J. (1967). Measurement of sand transport in rivers with special reference to tracer methods. *Sedimentology*, *8*(3), 175-228. https://doi.org/10.1111/j.1365-3091.1967.tb01321.x

Ferguson, R. (2007). Gravel-bed rivers at the reach scale. In H. Habersack, H. Piégay, M. Rinaldi (Eds.), *Gravel-bed Rivers VI: from process understanding to river restoration* (pp. 33-60). Amsterdam, Netherlands: Elsevier.

Goff, J. R., & Ashmore, P. (1994). Gravel transport and morphological change in braided Sunwapta River, Alberta, Canada. *Earth Surface Processes and Landforms*, *19*(3), 195-212. https://doi.org/10.1002/esp.3290190302

Gomez, B. (1991). Bedload transport. *Earth-Science Reviews*, *31*(2), 89-132. https://doi.org/10.1016/0012-8252(91)90017-A

Gomez, B., & Church, M. (1989). An assessment of bed load sediment transport formulae for gravel bed rivers. *Water Resources Research*, *25*(6), 1161-1186. https://doi.org/10.1029/WR025i006p01161

Ham, D. G., & Church, M. (2000). Bed-material transport estimated from channel morphodynamics: Chilliwack River, British Columbia. *Earth Surface Processes and Landforms*, *25*(10), 1123-1142. https://doi.org/10.1002/1096-9837(200009)25:10<1123::AID-ESP122>3.0.CO;2-9

Haschenburger, J. K. (2013). Bedload kinematics and fluxes. In J. F. Shroder (Ed.), *Treatise on Geomorphology*, Vol. 9 (pp. 103-123). Amsterdam, Netherlands: Elsevier.

Haschenburger, J. K., & Church, M. (1998). Bed material transport estimated from the virtual velocity of sediment. *Earth Surface Processes and Landforms*, *23*(9), 791-808. https://doi.org/10.1002/(SICI)1096-9837(199809)23:9<791::AID-ESP888>3.0.CO;2-X

Hassan, M. A., & Roy, A. G. (2016). Coarse particle tracing in fluvial geomorphology. In G.M. Kondolf, H. Piégay (Eds.), *Tools in fluvial geomorphology* (pp. 306-323). Hoboken, NJ: John Wiley & Sons. https://doi.org/10.1002/9781118648551.ch14

Hicks, D. M., & Gomez, B. (2016). Sediment transport. In G.M. Kondolf, H. Piégay (Eds.), *Tools in fluvial geomorphology* (pp. 324-356). Hoboken, NJ: John Wiley & Sons. https://doi.org/10.1002/9781118648551.ch15

Hoey, T. (1992). Temporal variations in bedload transport rates and sediment storage in gravel-bed rivers. *Progress in physical geography*, 16(3), 319-338. https://doi.org/10.1177/030913339201600303

Hubbell, D. W., & Sayre, W. W. (1964). Sand transport studies with radioactive tracers. *Journal of the Hydraulics Division*, *90*(3), 39-68.

Klein, M., Zviely, D., Kit, E., & Shteinman, B. (2007). Sediment transport along the coast of Israel: Examination of fluorescent sand tracers. *Journal of Coastal Research*, 1462-1470.

Komar, P. D., & Inman, D. L. (1970). Longshore sand transport on beaches. *Journal of geophysical research*, *75*(30), 5914-5927. https://doi.org/10.1029/JC075i030p05914

Lallias-Tacon, S., Liébault, F., & Piégay, H. (2014). Step by step error assessment in braided river sediment budget using airborne LiDAR data. *Geomorphology*, *214*, 307-323. https://doi.org/10.1016/j.geomorph.2014.02.014

Legleiter, C. J. (2012). Remote measurement of river morphology via fusion of LiDAR topography and spectrally based bathymetry. *Earth Surface Processes and Landforms*, *37*(5), 499-518. https://doi.org/10.1002/esp.2262

Legleiter, C. J. (2016). Inferring river bathymetry via image-to-depth quantile transformation (IDQT). *Water Resources Research*, *52*(5), 3722-3741. https://doi.org/10.1002/2016WR018730

Liébault, F., & Laronne, J. B. (2008). Evaluation of bedload yield in gravel-bed rivers using scour chains and painted tracers: the case of the Esconavette Torrent (Southern French Prealps). *Geodinamica Acta*, *21*(1-2), 23-34. https://doi.org/10.3166/ga.21.23-34

Lisle, T. E., Nelson, J. M., Pitlick, J., Madej, M. A., & Barkett, B. L. (2000). Variability of bed mobility in natural, gravel-bed channels and adjustments to sediment load at local and reach scales. *Water Resources Research*, 36(12), 3743-3755. https://doi.org/10.1029/2000WR900238

López, R., Vericat, D., & Batalla, R. J. (2014). Evaluation of bed load transport formulae in a large regulated gravel bed river: The lower Ebro (NE Iberian Peninsula). *Journal of hydrology*, *510*, 164-181. https://doi.org/10.1016/j.jhydrol.2013.12.014

Mandlburger, G., Hauer, C., Wieser, M., & Pfeifer, N. (2015). Topo-bathymetric LiDAR for monitoring river morphodynamics and instream habitats—A case study at the Pielach River. *Remote Sensing*, *7*(5), 6160-6195. https://doi.org/10.3390/rs70506160

Mao, L., Picco, L., Lenzi, M. A., & Surian, N. (2017). Bed material transport estimate in large gravel-bed rivers using the virtual velocity approach. *Earth Surface Processes and Landforms*, *42*(4), 595-611. https://doi.org/10.1002/esp.4000

Martin, Y., & Ham, D. (2005). Testing bedload transport formulae using morphologic transport estimates and field data: lower Fraser River, British Columbia. *Earth Surface Processes and Landforms*, *30*(10), 1265-1282. https://doi.org/10.1002/esp.1200

Martin, Y., & Church, M. (1995). Bed-material transport estimated from channel surveys: Vedder River, British Columbia. *Earth Surface Processes and Landforms*, *20*(4), 347-361. https://doi.org/10.1002/esp.3290200405

McLean, D. G., & Church, M. (1999). Sediment transport along lower Fraser River: 2. Estimates based on the long-term gravel budget. *Water Resources Research*, *35*(8), 2549-2559. https://doi.org/10.1029/1999WR900102

Merz, J. E., Pasternack, G. B., & Wheaton, J. M. (2006). Sediment budget for salmonid spawning habitat rehabilitation in a regulated river. *Geomorphology*, *76*(1), 207-228. https://doi.org/10.1016/j.geomorph.2005.11.004

Meyer-Peter, E., & Müller, R. (1948). Formulas for bed-load transport. In *IAHSR 2nd meeting, Stockholm, appendix 2*. IAHR.

Mueller, E. R., Pitlick, J., & Nelson, J. M. (2005). Variation in the reference Shields stress for bed load transport in gravel-bed streams and rivers. *Water Resources Research*, *41*(4). https://doi.org/10.1029/2004WR003692

Nicholas, A. P. (2000). Modelling bedload yield in braided gravel bed rivers. *Geomorphology*, *36*(1-2), 89-106. https://doi.org/10.1016/S0169-555X(00)00050-7

Passalacqua, P., Belmont, P., Staley, D. M., Simley, J. D., Arrowsmith, J. R., Bode, C. A., ... & Wheaton, J. M. (2015). Analyzing high resolution topography for advancing the understanding of mass and energy transfer through landscapes: A review. *Earth-Science Reviews*, *148*, 174-193. https://doi.org/10.1016/j.earscirev.2015.05.012

Petts, G. E. (1984). *Impounded rivers: perspectives for ecological management*. Hoboken, NJ: John Wiley & Sons

Recking, A. (2010). A comparison between flume and field bed load transport data and consequences for surface-based bed load transport prediction. *Water Resources Research*, *46*(3). https://doi.org/10.1029/2009WR008007

Recking, A., Liébault, F., Peteuil, C., & Jolimet, T. (2012). Testing bedload transport equations with consideration of time scales. *Earth Surface Processes and Landforms*, *37*(7), 774-789. https://doi.org/10.1002/esp.3213

Rickenmann, D. (2017). Bedload transport measurements with geophones, hydrophones, and underwater microphones (passive acoustic methods). In D. Tsutsumi, J. B. Laronne (Eds.), *Gravel-Bed Rivers: Processes and Disasters* (pp. 185-208). Hoboken, NJ: John Wiley & Sons

Rickenmann, D., Turowski, J. M., Fritschi, B., Wyss, C., Laronne, J., Barzilai, R., ... & Habersack, H. (2014). Bedload transport measurements with impact plate geophones: comparison of sensor calibration in different gravel-bed streams. *Earth Surface Processes and Landforms*, *39*(7), 928-942. https://doi.org/10.1002/esp.3499

Ryan, S. E., & Dixon, M. K. (2007). 15 Spatial and temporal variability in stream sediment loads using examples from the Gros Ventre Range, Wyoming, USA. In H. Habersack, H. Piégay, M. Rinaldi (Eds.), *Gravel-Bed Rivers VI: From Process Understanding to River Restoration* (pp. 387-407). Amsterdam, Netherlands: Elsevier.

Surian, N., & Cisotto, A. (2007). Channel adjustments, bedload transport and sediment sources in a gravel-bed river, Brenta River, Italy. *Earth Surface Processes and Landforms*, *32*(11), 1641-1656. https://doi.org/10.1002/esp.1591

Vericat, D., Wheaton, J. M., & Brasington, J. (2017). Revisiting the Morphological Approach: Opportunities and Challenges with Repeat High-Resolution Topography. In D. Tsutsumi, J. B. Laronne (Eds.), *Gravel-Bed Rivers: Processes and Disasters* (pp. 121-158). Hoboken, NJ: John Wiley & Sons

Wheaton, J. M., Brasington, J., Darby, S. E., & Sear, D. A. (2010). Accounting for uncertainty in DEMs from repeat topographic surveys: improved sediment budgets. *Earth Surface Processes and Landforms*, *35*(2), 136-156. https://doi.org/10.1002/esp.1886

Wilcock, P. R. (1993). Critical shear stress of natural sediments. *Journal of Hydraulic Engineering*, *119*(4), 491-505. https://doi.org/10.1061/(ASCE)0733-9429(1993)119:4(491)

Wilcock, P. R. (1997). Entrainment, displacement and transport of tracer gravels. *Earth Surface Processes and Landforms*, *22*(12), 1125-1138. https://doi.org/10.1002/(SICI)1096-9837(199712)22:12<1125::AID-ESP811>3.0.CO;2-V

Wilcock, P. R. (2001). Toward a practical method for estimating sediment-transport rates in gravel-bed rivers. *Earth Surface Processes and Landforms*, *26*(13), 1395-1408. https://doi.org/10.1002/esp.301

Wilcock, P. R., & Crowe, J. C. (2003). Surface-based transport model for mixed-size sediment. *Journal of Hydraulic Engineering*, *129*(2), 120-128. https://doi.org/10.1061/(ASCE)0733-9429(2003)129:2(120)

Williams, R. (2012). DEMs of difference. *Geomorphological Techniques*, 2(3.2).

Wohl, E., Bledsoe, B. P., Jacobson, R. B., Poff, N. L., Rathburn, S. L., Walters, D. M., & Wilcox, A. C. (2015). The natural sediment regime in rivers: Broadening the foundation for ecosystem management. *BioScience*, 65(4), 358-371. https://doi.org/10.1093/biosci/biv002

Wong, M., & Parker, G. (2006). Reanalysis and correction of bed-load relation of Meyer-Peter and Müller using their own database. *Journal of Hydraulic Engineering*, *132*(11), 1159-1168. https://doi.org/10.1061/(ASCE)0733-9429(2006)132:11(1159)

6. DISCUSSION AND CONCLUSIONS

The research conducted in this work focused on the estimate of the bed material transport along a study-sector of a gravel-bed river (Parma River, Italy) affected by a dam. The transport estimates have been addressed employing the two independent methods identified by Ferguson (2007) as the viable alternatives for quantifying the bed material load in the context of large gravel-bed rivers, where the estimation of this process represents still a challenging task (Ferguson, 2007; Haschenburger, 2013; Wohl et al., 2015). The two adopted estimation approaches are (i) the morphological method (Ashmore and Church, 1998) based on the erosion and deposition volumes evaluation along a river sector and (ii) the use of tracers to estimate the flux starting from the virtual velocity of the particles entrained from the streambed.

1. Estimate of bed material load in large gravel-bed rivers: methodological outcomes

Main results of the research

The morphological method provides robust transport estimates but, for calculating the sediment transport by the sediment budgeting procedure, it requires to include a section within the study sector where the coarse sediment transport is known (Vericat et al., 2017). The virtual velocity approach is potentially applicable in a wide spectrum of gravel-bed rivers without specific application constrains but it has been rarely applied in real case studies, leading to a poor methodological development and evaluation of its performance in terms of estimates reliability. Due to the need of developing reliable estimation methods adoptable in different large gravel-bed river contexts, we focused our research on some methodological issues related with the performance evaluation and improvement of the virtual velocity approach. With this in mind, the following points (i) and (ii) respectively respond to the research questions (a) (*how is it possible to improve the virtual velocity approach application and which factors have to be considered for obtaining reliable bed material transport estimates in different large gravel-bed river contexts?*) and (b) (*How reliable and accurate are the transport estimates provided by the virtual velocity approach, considering different gravel-bed river contexts and time scales of analysis?*) stated in the introduction.

The most important methodological outcomes of this work are:

(i) Some crucial improvements of the virtual velocity approach have been achieved in particular regarding: (i) the adoption of appropriate spatial scales for

data collection and processing (i.e. reaches for empirical relationships between dimensionless shear stress, calculation parameters and transport rating curves and morphological units for grain size definition); (ii) the jointly use of painted particles and PIT tagged clasts for achieving reliable estimates of the sediment displacement lengths; (iii) the development of different data-input configurations for taking into account some aspects related to the natural complexity of river morphodynamics and sediment transport. The achieved improvements make the hybrid virtual velocity approach based on the theoretical framework developed by Wilcock (1997) a suitable tool for estimating the bed material load in large gravel-bed rivers. A protocol adaptable to different types of large-gravel bed rivers in function of their morphological configuration, streambed sediments characteristics and topographical stability of the section (which depends both by sediment availability and magnitude of the transport event) was developed.

(ii) We compared the estimates of the bed material load mobilized along the same 4-km long study sector provided by the virtual velocity approach and by a robust morphological method involving the sediment budgeting procedure during a 12-months comparison period (April 2016 - April 2017). The yearly estimates provided by the two independent approaches are remarkably similar at the four considered cross-sections. Starting from this comparison results, was possible to conclude that, under the research conditions, the virtual velocity approach provides reliable estimates of the annual coarse bed material transport.

(iii) Considering (1) the difficulties for obtaining reliable bed material load estimates in the context of large gravel-bed rivers, (2) the limited applicability of the sediment budgeting approach and (3) the crucial importance in the quantification of this fluvial process for several scientific and practical (e.g. sediment and infrastructures management) issues, the virtual velocity approach represents a viable alternative for achieving the estimation of the bed material flux, since it is sensitive to the local streambed characteristics which, superimposing the hydraulic forcing (Vázquez-Tarrío et al., 2018), determine the mobility of the channel sediments and finally the coarse sediment transport.

Application, wider implications and future perspectives of the tested approaches

The bed material transport in gravel-bed rivers is affected by high spatial and temporal variability at several scales (e.g. Clayton and Pitlick, 2007; Ryan and Dixon, 2007). The

morphological method is able to provide time-integrated transport values at different channel sections depending by the time resolution of the employed channel-topography data (e.g. digital elevation models) and their spatial extension (Lane et al., 1995). In particular, the time interval between two successive employed topographic surveys determines the time-resolution of the estimates while the total period covered by all available spatial data represents the temporal extension for which it is possible to address the transport calculation.

The virtual velocity approach developed in this work, based on the Wilcock's theoretical framework (1997), relates the tractive forces locally and instantaneously induced by the water flow on the streambed with the bed material load, potentially providing the local and instantaneous value of the transport based on the defined transport-rating curves. The “actual instantaneous-local transport” and the "actual instantaneous-section transport" are high variable considering a fixed dimensionless shear stress (Hoey, 1992; Cudden and Hoey, 2003; Bunte and Abt, 2005) and a given water discharge (Ashmore, 2013), respectively. The transport estimates carried out by the virtual velocity approach, taking in account for this variability based on several field observations, can be considered reliable only at the competent-event time scale for the cross-section spatial scale.

Having in mind the reported clarifications about the transport estimates provided by the two considered methods, we summarize some points about the adoption of these techniques for the quantitative analysis of the coarse bed material flux in large gravel-bed rivers under different application conditions (i.e. event magnitude, time and spatial analysis scales):

(i) The empirical relations leading the transport estimate using the virtual velocity approach derive from data collected during field monitoring. The adopted field techniques are effective under a specific range of tractive forces, in fact, if the dimensionless shear stress is very high, the passive tracers recovery rate is drastically reduced and the scour chains are likely removed from the bed. For this reason, the field monitoring can be carried out for ordinary transport events but not for large floods (e.g. floods with RI = 50-100 yr). In this work we monitored events with a recurrence interval up to 2 yr, collecting data under a range of dimensionless shear stress up to 0.12. The empirical relations between dimensionless shear stress and calculation parameters are high reliable for that tractive forces interval (conforming to the higher values calculated for the nine calculation events that

occurred during the study period) while for higher τ^* they are based only on extrapolation procedures. Applying the empirical relations and the transport rating curves at events characterized by higher tractive forces active on the bed could reduce the reliability of the transport estimation. Due (1) to the technical limitations of the employed field techniques and (2) to the relation between monitored dimensionless shear stress range and reliability of the calculation relations, the virtual velocity approach seems more suitable for estimating the sediment load in response to more frequent competent events (i.e. from low magnitude and very frequent events up to 5-10 yr floods) which are the most effective in terms of sediment transport and river morphodynamic control (Wolman and Miller, 1960; Andrews, 1980) also for bedload-dominated streams (i.e. gravel-bed rivers; see Emmet and Wolman (2001)). The morphological method is not affected by such kind of event-magnitude limitation, in fact it is affected by minor uncertainties when the channel changes could be very intense (e.g. considering longer time intervals or including a high magnitude event in the study period), especially if the topographical data are characterized by relatively small errors (McLean and Church, 1999).

(ii) In this study, we calculated the bed material load using the virtual velocity approach at the four cross-sections adopted also for the field monitoring. The method requires as input factors for addressing the transport estimation the cross-section topography, the water level over the time, the local grain sizes and the rating curves between dimensionless shear stress and unit bed-material load. The rating-curves are reach-specific, since they derive from the empirical relations describing the calculation parameter trends (e.g. d_s, Y) which must be define for specific reaches (sensu Brierley and Fryirs, 2013). To extend spatially the estimates, it is possible to address the calculation of the transport in correspondence of river sections different from those used for the field-data collection. To do this it is necessary to (1) define the topography of the new calculation section and the local water level over the time and (2) to select sections located within the same reach where the empirical relations were developed or to identify sections within a reach with morphological and channel sediments characteristics similar to those of the monitoring reach. Due to the remarkable site-specificity, affecting the transport rating curves (Schneider et al., 2015) additional studies are required for understanding how the calculation relations defined for the transport estimate by virtual velocity approach can be exported in context different from the development site.

(iii) Due to the high longitudinal variability of the sediment transport along a single river course (e.g. McLean and Church, 1999; Surian and Cisotto, 2007), it is often required, depending by the study aims, to define the bed material load at several river sections. The field efforts required for applying the virtual velocity approach addressing a detailed monitoring and the open questions about the spatial extensibility of its calculation relations, suggest that the virtual velocity approach seems more suitable for calculating the sediment transport in correspondence of a limited number of cross-sections. On the contrary, the morphological method is adequate for defining the sediment regime along extended river sectors but it is not independently applicable everywhere. Proved that the virtual velocity approach represents a reliable alternative for estimating the coarse bed material transport at the adequate spatial (i.e. cross-section) and time (i.e. event or multiple events) scale, an effective strategy could be to couple the two approaches. In this way the virtual velocity approach would provide reliable transport estimates at one cross-section, solving the limiting condition affecting the morphological method about the necessity of knowing the sediment flux at a section located within the study sector, while the sediment budgeting procedure would allow to spatially extend the calculation over a longitudinal area determined by available topographical data.

(iv) Since (1) the channel material characteristics are a key factor controlling the sediment transport and (2) the rating-curves developed for the estimation of the bed material flux using the virtual velocity approach are directly derived from field data, their temporal validity is strictly determined by the persistence over the time of the streambed conditions for which they have been developed. In other words, the empirical relations between the calculation parameters and the dimensionless shear stress and, in turn, the transport rating-curves, can be applied for the sediment load estimate until the channel-material conditions (e.g. grain size, fabric, armoring) remain similar with those characterizing the streambed during the field data collection. For instance, the Parma River sector considered in this work experienced a strong alteration during the last decades due to the closure of a dam inducing remarkable variations in surface sediments characteristics and channel geometry. The transport rating curves have been developed after a monitoring addressed in the period 2016 - 2017. Since the present conditions of the river are different from those characterizing the river in the past (i.e. before and immediately after the construction of the dam) and the study sector is still experiencing an

unstable condition, the derived virtual velocity relations cannot be applied for estimating the transport in the past and they will probably become obsolete in the near future requiring new field monitoring and adjustment of the empirical relations. For this reason, it was not possible to apply the virtual velocity approach for estimating the transport during the periods 2006-2008 and 2008-2016 for which are available morphological estimates of the bed material load, limiting the comparison period of our research at the April 2016 - April 2017 time interval. In more stable river contexts, the channel conditions can remain unchanged for long time interval allowing the employment of the derived empirical transport curves for longer periods, back and forth over time. Additional studies are required for quantitatively evaluating the impact of the variations of the streambed sediment characteristics (over the time for unstable rivers, but also in the space for applying the calculation at different locations from those considered in the field monitoring) on the empirical calculation-parameters relations and transport rating-curves.

2. Sediment dynamics and channel evolution in a gravel-bed river impacted by human interventions

The Parma River study sector is remarkably affected by human activities, mainly due to the river regulation operated through the construction of a retention basin between 1988 and 1993 and the closure of the basin dam in 2004 - 2005. This particular condition allowed us to focus a part of our research on the effects induced by the closure of a dam representing a zero-flux sediment boundary in relation to the coarse component of the bed material on a gravel-bed river sector in terms of sediment dynamics, transport regimes, morphological evolution and the morphodynamic relations existing between these factors.

Answering to the research question (c) reported in the introduction (*To what extent is a dam able to impact on sediment mobility and transport regime of a large gravel-bed river and which relations exist between sediment transport and other key factors of river morphodynamics?*), the main results obtained about the sediment dynamics and channel evolution in a typical example of gravel-bed river impacted by human regulation are:

(i) The considered study sector has been highly altered by the dam which, interrupting the longitudinal continuity of the coarse sediment transfer, influenced its evolution in terms of morphology, bed material characteristics and bed material transport rates. Since the basin construction and dam closure, the study sector experienced incision, morphological complexity reduction, streambed surface

coarsening, armoring and decrease in the sediment mobility and transport. The observed trend is conform to the typical degradation evolution described by Petts (1984).

(ii) The sediment regime estimates carried out by the two adopted approaches indicate that the sediment transport increases moving away from the dam zero-flux sediment boundary, but a general decreasing trend of the bed material load has been observed over the time since dam closure in 2005, with a reduction of about 85% of the transport 4-km downstream from the dam (decreasing from 14.000 $m^3 yr^{-1}$ to 2000 $m^3 yr^{-1}$) over 12 years. This reduction could have started even before, starting from the basin construction works in the 1990s and it has been interpreted as due to the flowing of a "mobile sediment-wave tail" under-supplied from upstream sediment contribution which progressively depleted the impacted sector of all the transportable material. The induced evolution from a pre-dam to a post-dam quasi-equilibrium state (Petts and Gurnell, 2005) has been likely completed along reaches 1 and 2 while is still ongoing at reach 3.

We were able to study both the morphological and the sediment transport responses due to the dam closure and to find relations between these two aspects of the morphodynamics. From a practical point of view, the quantitative relationships obtained for the case study between the sediment regime alteration and the morphological responses can be useful for the river management. For instance, due to the high number of dams regulating gravel-bed rivers worldwide (Grant, 2012), river managers are interested in understanding how the interventions aimed at recovering more natural river conditions (river restoration strategy, e.g. gravel augmentation analyzed by flume experiments by Sklar et al. (2009)) can be successful. Real data relating sediment transport variations and morphological changes can improve our knowledge about this and other rivers-managing issues.

References

Andrews, E. D. (1980). Effective and bankfull discharges of streams in the Yampa River basin, Colorado and Wyoming. *Journal of Hydrology*, *46*(3-4), 311-330. https://doi.org/10.1016/0022-1694(80)90084-0

Ashmore, P. E. (2013). Morphology and dynamics of braided rivers. In J. F. Shroder (Ed.), *Treatise on Geomorphology*, *Vol. 9* (pp. 289-312). Amsterdam, Netherlands: Elsevier.

Ashmore, P. E., & Church, M. (1998). Sediment transport and river morphology: a paradigm for study. In P. C. Klingeman, R. L. Beschta, P. D. Komar, J. B. Bradley (Eds.), *Gravel-Bed Rivers in the Environment* (pp. 115-148). Highlands Ranch, CO: Water Resources Publications LLC

Brierley, G. J., & Fryirs, K. A. (2013). Geomorphology and river management: applications of the river styles framework. Hoboken, NJ: John Wiley & Sons

Bunte, K., & Abt, S. R. (2005). Effect of sampling time on measured gravel bed load transport rates in a coarse-bedded stream. *Water Resources Research*, *41*(11). https://doi.org/10.1029/2004WR003880

Clayton, J. A., & Pitlick, J. (2007). Spatial and temporal variations in bed load transport intensity in a gravel bed river bend. *Water Resources Research*, *43*(2). https://doi.org/10.1029/2006WR005253

Cudden, J. R., & Hoey, T. B. (2003). The causes of bedload pulses in a gravel channel: The implications of bedload grain-size distributions. *Earth Surface Processes and Landforms*, *28*(13), 1411-1428. https://doi.org/10.1002/esp.521

Emmett, W. W., & Wolman, M. G. (2001). Effective discharge and gravel-bed rivers. *Earth Surface Processes and Landforms*, *26*(13), 1369-1380. https://doi.org/10.1002/esp.303

Ferguson, R. I. (2007). Gravel-bed rivers at the reach scale. In H. Habersack, H. Piégay, M. Rinaldi (Eds.), *Gravel-bed Rivers VI: from process understanding to river restoration* (pp. 33-60). Amsterdam, Netherlands: Elsevier.

Haschenburger, J. K. (2013). Bedload kinematics and fluxes. In J. F. Shroder (Ed.), *Treatise on Geomorphology*, *Vol. 9* (pp. 103-123). Amsterdam, Netherlands: Elsevier.

Hoey, T. (1992). Temporal variations in bedload transport rates and sediment storage in gravel-bed rivers. *Progress in physical geography*, *16*(3), 319-338. https://doi.org/10.1177/030913339201600303

Lane, S. N., Richards, K. S., & Chandler, J. H. (1995). Morphological Estimation of the Time-Integrated Bed Load Transport Rate. *Water Resources Research*, *31*(3), 761-772. https://doi.org/10.1029/94WR01726

McLean, D. G., & Church, M. (1999). Sediment transport along lower Fraser River: 2. Estimates based on the long-term gravel budget. *Water Resources Research*, *35*(8), 2549-2559. https://doi.org/10.1029/1999WR900102

Petts, G. E. (1984). *Impounded rivers: perspectives for ecological management*. Hoboken, NJ: John Wiley & Sons

Petts, G. E., & Gurnell, A. M. (2005). Dams and geomorphology: research progress and future directions. *Geomorphology*, *71*(1-2), 27-47. https://doi.org/10.1016/j.geomorph.2004.02.015

Ryan, S. E., & Dixon, M. K. (2007). 15 Spatial and temporal variability in stream sediment loads using examples from the Gros Ventre Range, Wyoming, USA. In H. Habersack, H. Piégay, M. Rinaldi (Eds.), *Gravel-Bed Rivers VI: From Process Understanding to River Restoration* (pp. 387-407). Amsterdam, Netherlands: Elsevier.

Schneider, J. M., Rickenmann, D., Turowski, J. M., Bunte, K., & Kirchner, J. W. (2015). Applicability of bed load transport models for mixed-size sediments in steep streams considering macro-roughness. *Water Resources Research*, *51*(7), 5260-5283. https://doi.org/10.1002/2014WR016417

Sklar, L. S., Fadde, J., Venditti, J. G., Nelson, P., Wydzga, M. A., Cui, Y., & Dietrich, W. E. (2009). Translation and dispersion of sediment pulses in flume experiments simulating gravel augmentation below dams. *Water resources research*, *45*(8). https://doi.org/10.1029/2008WR007346

Surian, N., & Cisotto, A. (2007). Channel adjustments, bedload transport and sediment sources in a gravel-bed river, Brenta River, Italy. *Earth Surface Processes and Landforms*, *32*(11), 1641-1656. https://doi.org/10.1002/esp.1591

Vázquez-Tarrío, D., Recking, A., Liébault, F., Tal, M., & Menéndez-Duarte, R (2018). Particle transport in gravel-bed rivers: revisiting passive tracer data. *Earth Surface Processes and Landforms*. https://doi.org/10.1002/esp.4484

Vericat, D., Wheaton, J. M., & Brasington, J. (2017). Revisiting the Morphological Approach: Opportunities and Challenges with Repeat High-Resolution Topography. In D. Tsutsumi, J. B. Laronne (Eds.), *Gravel-Bed Rivers: Processes and Disasters* (pp. 121-158). Hoboken, NJ: John Wiley & Sons

Wilcock, P. R. (1997). Entrainment, displacement and transport of tracer gravels. *Earth Surface Processes and Landforms*, *22*(12), 1125-1138. https://doi.org/10.1002/(SICI)1096-9837(199712)22:12<1125::AID-ESP811>3.0.CO;2-V

Wohl, E., Bledsoe, B. P., Jacobson, R. B., Poff, N. L., Rathburn, S. L., Walters, D. M., & Wilcox, A. C. (2015). The natural sediment regime in rivers: Broadening the foundation for ecosystem management. *BioScience*, 65(4), 358-371. https://doi.org/10.1093/biosci/biv002

Wolman, M. G., & Miller, J. P. (1960). Magnitude and frequency of forces in geomorphic processes. *The Journal of Geology*, *68*(1), 54-74. https://doi.org/10.1086/626637

APPENDIX 1. SUPPORTING INFORMATION FOR "VIRTUAL VELOCITY APPROACH FOR ESTIMATING BED MATERIAL TRANSPORT IN GRAVEL-BED RIVERS: KEY FACTORS AND SIGNIFICANCE"

Andrea Brenna[1], Nicola Surian[1], and Luca Mao[2]

[1] *Department of Geosciences, University of Padova, Padova, Italy.*

[2] *School of Geography, University of Lincoln, Lincoln, UK.*

Water Resources Research, in revision.

Introduction

Several data were collected in the field in order to obtain the necessary inputs required for the virtual velocity approach. First, a detailed summary of grain size classes distribution is reported, associated to the classification of morphological units (streambed sediments were divided in function of section location and morphological unit) (Tables S1 and S2). Then, we provide additional details about original data used to derive the relations reported in the paper. The dataset, divided according to mobility conditions associated with each monitored area, allows to derive the transport processes thresholds and the relationships between dimensionless shear stress (τ^*), percentage of mobilized streambed material (Y) for partial transport conditions, and active layer thickness (d_s) for full mobility (Table S3, S4, S5 and S6). For each monitored area the installation location is reported in order to distinguish between sections 1-2 and sections 3-4 sub-sets. We reported also two additional figures to show the field installation of the study sites (painted areas and PIT tags) (Figure S1) and the workflow adopted during this study in order to apply the virtual velocity approach (Figure S2). Finally, the dataset used to analyze the tracer travel distances and the virtual velocity is presented (Table S7) with the relations derived in this work between the virtual velocity of moved grains, grain size and dimensionless shear stress compared with those obtained by Mao et al. (2017) (Figure S3).

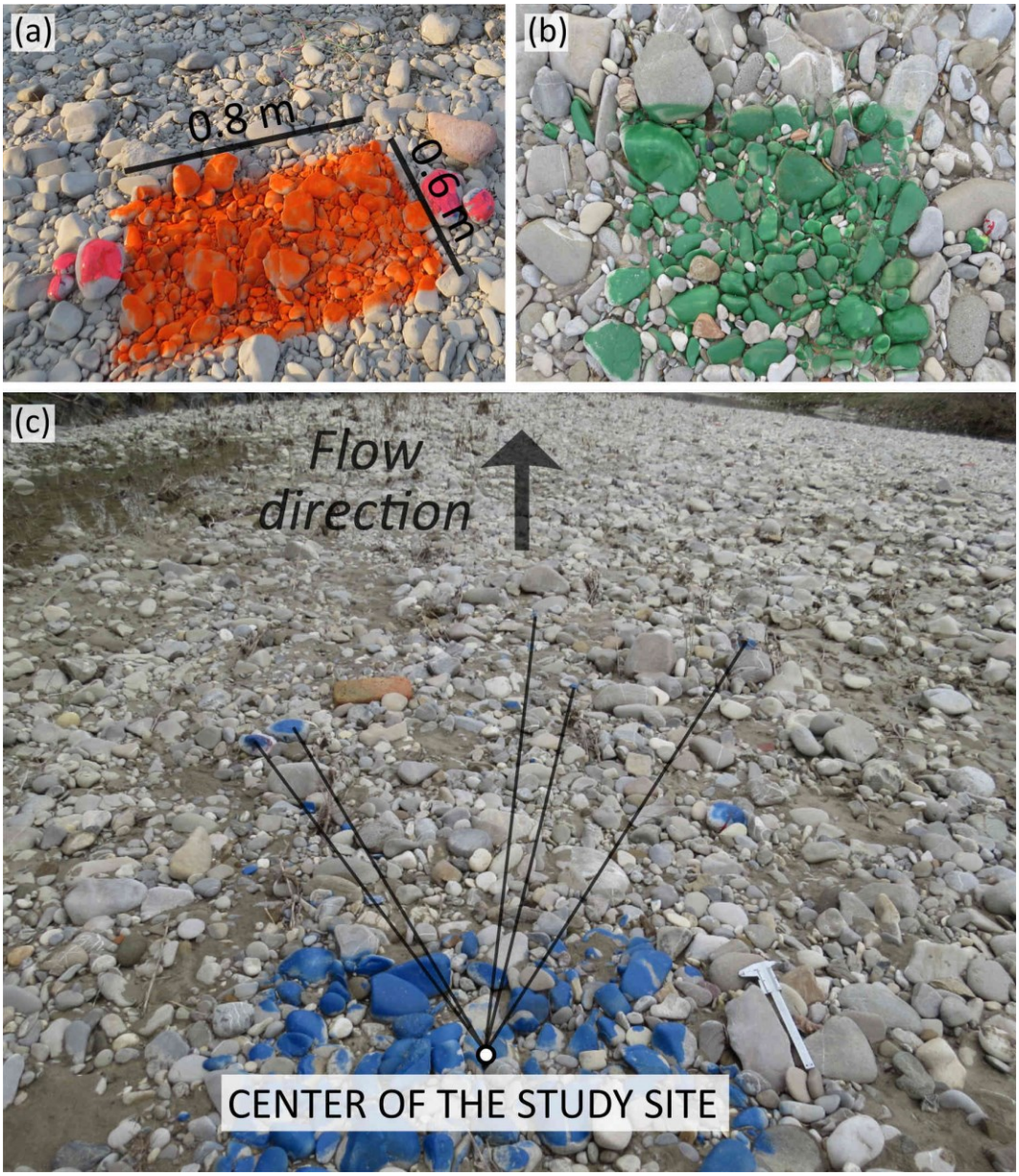

Figure S1. Pictures of the study sites: pre-event installation of a painted patch and PIT tagged clasts (colored in pink) (a); vertical post-event photo of a study site experienced slight partial mobility during a competent flood with residual painted clasts and PIT tags not mobilized by the water flow (b); perspective post-event photo of a study site experienced partial mobility during a competent event: the center of the original painted area and the single displacement lengths of some mobilized and surveyed tracer clasts are highlighted (c). The adopted painting procedure (i.e. painting of the streambed surface using a fluorescent spray paint) has the advantages of avoiding to disturb the surface bed material and easily marking a large number of clasts without grain size limitations but, painting only the surface of the material, only the "half-part" exposed of the clasts is colored. This can cause difficult in detection if the clasts have rolled over exposing the unpainted site, lowering the recovery-rate.

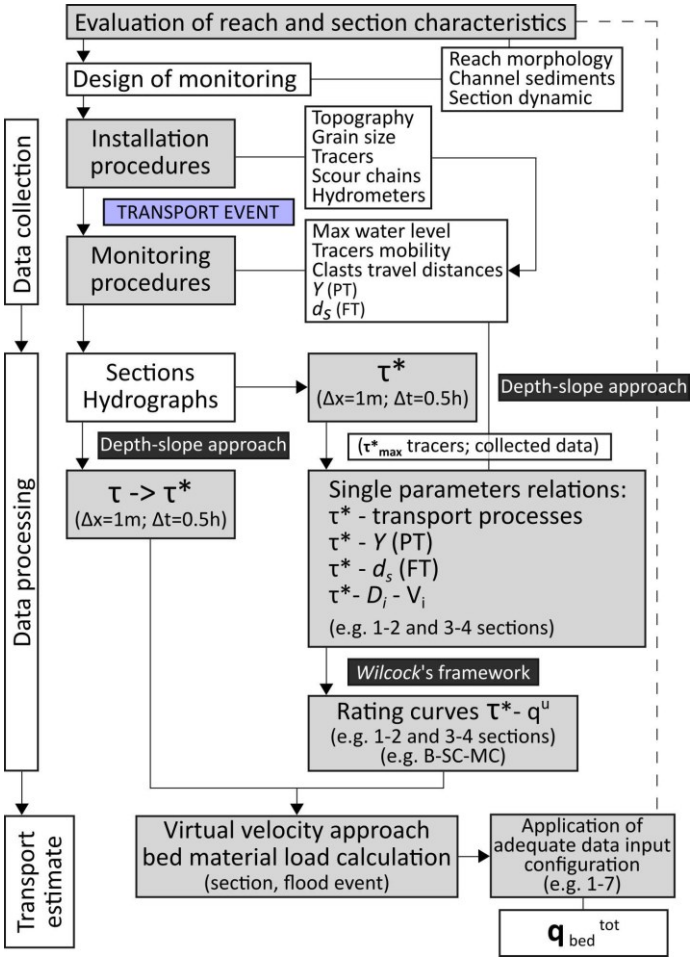

Figure S2. Virtual velocity approach workflow. Starting from the upper part, the entire process finalized to calculate the bed material load can be divided in data collection, data processing and transport estimate. In order to accurately design the entire estimation process it is important to consider the local study area characteristics.

		Upstream Reach (Sections 1-2)			***Downstream Reach (Sections 3-4)***		
		SC	***B***	***MC***	***SC***	***B***	***MC***
Grain size and sediment structure	***D_{50} (D_{84}) Surface (mm)***	58 (110)	63 (118)	106 (192)	42 (79)	53 (104)	86 (161)
		Sect.1: 65 (125)		Sect. 2: 61 (120)	Sect.3: 53 (102)		Sect.4: 50 (109)
		---------- 63 (124) ----------			---------- 50 (102) ----------		
	D_{50} (D_{84}) sub-surface (mm)	---------- 37 (83) ----------			---------- 35 (75) ----------		
		---------- 36 (79) ----------					
	Armoring ratio	1.56	1.70	2.86	1.20	1.51	2.46
	Imbrication and grain sorting	Yes	Yes	Yes	No	No	Yes
	Armoring	++	++	+++	+	+	+++

Table S1. Summary of channel surface and subsurface material characteristic parameters. Grain size D_{50} and D_{84} are grouped in function of different criteria. Armor ratios are calculated as $D_{50}^{surface}/D_{50}^{sub\text{-}surface}$ using data from the same study sector location (sections 1-2 and sections 3-4).

Considering both the armor ratios and field evidences, we identify different armoring classes for each morpho-unit at different locations: very high (+++), high (++), moderate (+).

Grain size class (mm)	*Sections 1-2*			*Sections 3-4*		
	SC	*B*	*MC*	*SC*	*B*	*MC*
6-8	1,3%	1,2%	1,0%	1,9%	1,6%	0,9%
8-11,2	2,6%	2,6%	1,5%	4,2%	2,8%	1,6%
11,2-16	4,2%	4,0%	2,4%	6,6%	4,6%	2,6%
16-22,6	6,0%	6,2%	2,5%	10,7%	7,8%	3,6%
22,6-32	12,0%	10,0%	4,4%	15,8%	11,0%	5,1%
32-45,2	13,4%	13,3%	4,6%	17,5%	15,8%	7,2%
45,2-64	14,2%	16,2%	10,6%	18,3%	18,4%	15,3%
64-90,5	18,1%	17,4%	18,5%	15,1%	18,3%	16,1%
90,5-124	22,7%	15,9%	19,6%	6,4%	11,8%	25,1%
124-181	5,6%	10,3%	12,5%	2,4%	5,2%	12,9%
>181	0,0%	2,8%	22,4%	1,0%	2,7%	9,5%

Table S2. Surface sediment grain size distributions expressed as percentage of material falling in each grain size class, according to location (sections 1-2 and 3-4) and morphological unit (MC: main channel; SC: secondary channel; B: bar). Clasts finer than 6 mm are excluded from this analysis. The mean reported percentages derives from image grain size analysis carried out for an adequate number of sites: 5 photos for the main channel at sections 1-2; 7 photos for the secondary channel at sections 1-2; 32 photos for bar at sections 1-2; 6 photos for the main channel at sections 3-4; 16 photos for the secondary channel at sections 3-4; and 39 photos for bars at sections 3-4.

Study site ID	*Mobility condition*	*Study area location (sect.)*	τ^*_{max}	*Y [0-1]*	d_s *(m)*
114	AWS	1-2	0,000	0,00	0,00
115	AWS	1-2	0,000	0,00	0,00
124	AWS	1-2	0,000	0,00	0,00
223	AWS	1-2	0,000	0,00	0,00
312	AWS	1-2	0,000	0,00	0,00
321	AWS	1-2	0,000	0,00	0,00
322	AWS	1-2	0,000	0,00	0,00
415	AWS	1-2	0,000	0,00	0,00
514	AWS	1-2	0,000	0,00	0,00
147	AWS	3-4	0,000	0,00	0,00
148	AWS	3-4	0,000	0,00	0,00
234	AWS	3-4	0,000	0,00	0,00
332	AWS	3-4	0,000	0,00	0,00
334	AWS	3-4	0,000	0,00	0,00
545	AWS	3-4	0,000	0,00	0,00
634	AWS	3-4	0,000	0,00	0,00
637	AWS	3-4	0,000	0,00	0,00
645	AWS	3-4	0,000	0,00	0,00

Table S3. Complete data set regarding monitored study areas in above water stage conditions (AWS). Location of study site (divided in sections 1-2 and 3-4), maximum dimensionless shear stress experienced by the area during the flood (τ^*_{max}), measured percentage of mobilized streambed (Y) and exchange depth thickness (d_s) are reported.

Study site ID	*Mobility condition*	*Study area location (sect.)*	τ^*_{max}	*Y [0-1]*	d_s *(m)*
523	NM	1-2	0,001	0,00	0,00
314	NM	1-2	0,003	0,00	0,00
625	NM	1-2	0,006	0,00	0,00
313	NM	1-2	0,011	0,00	0,00
615	NM	1-2	0,012	0,00	0,00
624	NM	1-2	0,013	0,00	0,00
512	NM	1-2	0,020	0,00	0,00
221	NM	1-2	0,030	0,00	0,00
333	NM	3-4	0,002	0,00	0,00
232	NM	3-4	0,006	0,00	0,00
642	NM	3-4	0,008	0,00	0,00
533	NM	3-4	0,009	0,00	0,00
636	NM	3-4	0,011	0,00	0,00
532	NM	3-4	0,011	0,00	0,00
646	NM	3-4	0,013	0,00	0,00
641	NM	3-4	0,013	0,00	0,00
233	NM	3-4	0,014	0,00	0,00
342	NM	3-4	0,015	0,00	0,00
241	NM	3-4	0,016	0,00	0,00
631	NM	3-4	0,017	0,00	0,00
643	NM	3-4	0,021	0,00	0,00
343	NM	3-4	0,023	0,00	0,00

Table S4. Complete data set regarding monitored study areas in no-motion conditions (NM). Location of study site (divided in sections 1-2 and 3-4), maximum dimensionless shear stress experienced by the area during the flood (τ^*_{max}), measured percentage of mobilized streambed (Y) and active layer thickness (d_s) are reported. Data reported in this table were used to derive the mobility conditions thresholds concerning the no-motion ranges (Figure 7).

Study site ID	*Mobility condition*	*Study area location (sect.)*	τ^*_{max}	*Y [0-1]*	d_s *(m)*
612	PT	1-2	0,006	0,01	0,00
613	PT	1-2	0,013	0,01	0,00
513	PT	1-2	0,016	0,05	0,00
623	PT	1-2	0,020	0,01	0,00
213	PT	1-2	0,020	0,05	0,00
113	PT	1-2	0,021	0,05	0,00
621	PT	1-2	0,021	0,13	0,00
311	PT	1-2	0,022	0,06	0,00
611	PT	1-2	0,026	0,23	0,00
323	PT	1-2	0,028	0,40	0,00
324	PT	1-2	0,029	0,50	0,00
123	PT	1-2	0,031	0,62	0,00
212	PT	1-2	0,033	0,66	0,00
222	PT	1-2	0,038	0,60	0,00
413	PT	1-2	0,040	0,82	0,00
211	PT	1-2	0,042	0,79	0,00
414	PT	1-2	0,044	0,95	0,00
122	PT	1-2	0,045	0,64	0,00
521	PT	1-2	0,045	0,92	0,00
422	PT	1-2	0,047	0,90	0,00
622	PT	1-2	0,048	0,99	0,00
614	PT	1-2	0,059	0,89	0,00
526	PT	1-2	0,063	0,99	0,00
214	PT	1-2	0,071	0,99	0,00
535	PT	3-4	0,008	0,05	0,00
644	PT	3-4	0,012	0,01	0,00
632	PT	3-4	0,015	0,01	0,00
242	PT	3-4	0,016	0,20	0,00
331	PT	3-4	0,016	0,06	0,00
231	PT	3-4	0,018	0,25	0,00
341	PT	3-4	0,019	0,29	0,00
243	PT	3-4	0,022	0,57	0,00
434	PT	3-4	0,023	0,86	0,00
133	PT	3-4	0,024	0,66	0,00
541	PT	3-4	0,025	0,41	0,00
145	PT	3-4	0,025	0,50	0,00
144	PT	3-4	0,029	0,97	0,00
335	PT	3-4	0,029	0,59	0,00
531	PT	3-4	0,030	0,57	0,00
142	PT	3-4	0,031	0,92	0,00
542	PT	3-4	0,031	0,82	0,00
442	PT	3-4	0,034	0,95	0,00
432	PT	3-4	0,035	0,94	0,00
543	PT	3-4	0,035	0,88	0,00
134	PT	3-4	0,036	0,80	0,00
433	PT	3-4	0,037	0,92	0,00
633	PT	3-4	0,037	0,99	0,00
536	PT	3-4	0,048	0,90	0,00
544	PT	3-4	0,051	0,98	0,00
635	PT	3-4	0,084	0,99	0,00

Table S5. Complete data set regarding monitored study areas in partial transport conditions (PT). Location of study site (divided in sections 1-2 and 3-4), maximum dimensionless shear stress experienced by the area during the flood (τ^*_{max}), measured percentage of mobilized streambed (Y)

and active layer thickness (d_s) are reported. Data reported in this table were used to derive the mobility conditions thresholds concerning the partial transport ranges (Figure 7) and to obtain the relations between τ^* and the percentage of mobilized streambed (Figure S1; equations (8) and (9)).

Study site ID	*Mobility condition*	*Study area location (sect.)*	τ^*_{max}	*Y [0-1]*	d_s *(m)*
524	FT	1-2	0,027	1,00	0,05
525	FT	1-2	0,048	1,00	0,07
112	FT	1-2	0,051	1,00	0,10
511	FT	1-2	0,054	1,00	0,12
522	FT	1-2	0,057	1,00	0,20
423	FT	1-2	0,061	1,00	0,30
412	FT	1-2	0,062	1,00	0,11
121	FT	1-2	0,071	1,00	0,13
411	FT	1-2	0,088	1,00	0,22
111	FT	1-2	0,092	1,00	0,41
424	FT	1-2	0,095	1,00	0,37
421	FT	1-2	0,102	1,00	0,46
135	FT	3-4	0,024	1,00	0,06
136	FT	3-4	0,028	1,00	0,05
141	FT	3-4	0,037	1,00	0,10
146	FT	3-4	0,037	1,00	0,06
132	FT	3-4	0,041	1,00	0,12
431	FT	3-4	0,055	1,00	0,14
534	FT	3-4	0,068	1,00	0,18
435	FT	3-4	0,070	1,00	0,15
131	FT	3-4	0,070	1,00	0,10
443	FT	3-4	0,076	1,00	0,20
143	FT	3-4	0,078	1,00	0,28
444	FT	3-4	0,091	1,00	0,38
441	FT	3-4	0,101	1,00	0,38
436	FT	3-4	0,111	1,00	0,42
445	FT	3-4	0,121	1,00	0,56

Table S6. Complete data set regarding monitored study areas in full mobility conditions (FT). Location of study site (divided in sections 1-2 and 3-4), maximum dimensionless shear stress experienced by the area during the flood (τ^*_{max}), measured percentage of mobilized streambed (Y) and active layer thickness (d_s) are reported. Data reported in this table were used to derive the mobility conditions thresholds concerning the full transport ranges (Figure 7) and to obtain the relations between τ^* and the exchange depth thickness (Figure 8; equations (10) and (11)).

Study site ID	τ^*_{max}	*Mobility time interval (h)* ($\tau^* > \tau^*_c$)	*Grain size class (mm)*	*Number of found tracers*	L_i *mean (m)*	V_i (mh^{-1})
242	0,016 (PT)	0,5	6-8	12	1,31	2,62
			8-11,2	5	1,26	2,52
			11,2-16	12	1,22	2,44
			16-22,6	25	1,24	2,48
			22,6-32	8	1,11	2,22
			32-45,2	21 (1 PIT)	1,13	2,26
			45,2-64	3 (1 PIT)	0,74	1,48
			64-90,5	3 PITs	0,00	0,00
			90,5-124	3 PITs	0,00	0,00
			124-181	0	-	-
222	0,038 (PT)	1	6-8	34	1,88	1,88
			8-11,2	29	3,53	3,53
			11,2-16	50	3,51	3,51
			16-22,6	21	3,48	3,48
			22,6-32	69 (1 PIT)	3,50	3,50
			32-45,2	75 (2 PITs)	3,09	3,09
			45,2-64	32 (2 PITs)	1,92	1,92
			64-90,5	12 (1 PIT)	1,10	1,10
			90,5-124	2 PITs	0,00	0,00
			124-181	0	-	-
442	0,34 (PT)	13,5	6-8	7	-	-
			8-11,2	39	36,12	2,68
			11,2-16	9	21,80	1,61
			16-22,6	59	34,40	2,55
			22,6-32	88	19,05	1,41
			32-45,2	98 (2 PITs)	18,91	1,40
			45,2-64	12 (3 PITs)	20,22	1,50
			64-90,5	6 (1 PIT)	11,80	0,87
			90,5-124	2 PITs	0,00	0,00
			124-181	0	-	-
423	0,061 (FT)	29,5	8-11,2	0	-	-
			11,2-16	0	-	-
			16-22,6	0	-	-
			22,6-32	7	78,11	2,65
			32-45,2	7 (1 PIT)	64,30	2,18
			45,2-64	8 (2 PITs)	84,86	2,88
			64-90,5	11 (2 PITs)	80,23	2,72
			90,5-124	6 (1 PIT)	71,02	2,41
			124-181	1 PIT	65,19	2,21
			>181	0	-	-
111	0,092 (FT)	22	8-11,2	0	-	-
			11,2-16	0	-	-
			16-22,6	0	-	-
			22,6-32	1	94,98	4,32
			32-45,2	3 (1 PIT)	82,52	3,75
			45,2-64	2 (1 PIT)	104,89	4,77
			64-90,5	3 (1 PIT)	78,90	3,59
			90,5-124	4 (2 PITs)	75,95	3,45
			124-181	0	-	-
			>181	0	-	-
441	0,101 (FT)	29	8-11,2	0	-	-
			11,2-16	0	-	-
			16-22,6	0	-	-
			22,6-32	0	-	-
			32-45,2	0	-	-
			45,2-64	2 (1 PIT)	116,84	4,03
			64-90,5	3 PITs	106,67	3,68
			90,5-124	0	-	-
			124-181	1 PIT	112,39	3,88
			>181	0	-	-

Table S7. Summary of data employed to analyze the tracer travel distance (Figure 9). For six study areas, the calculated transport process duration, the number of moved painted clasts found of each

grain size class, the measured mean travel distances of each grain size class, and the relative derived virtual velocity (used for obtaining equations (12) and (13)) have been reported.

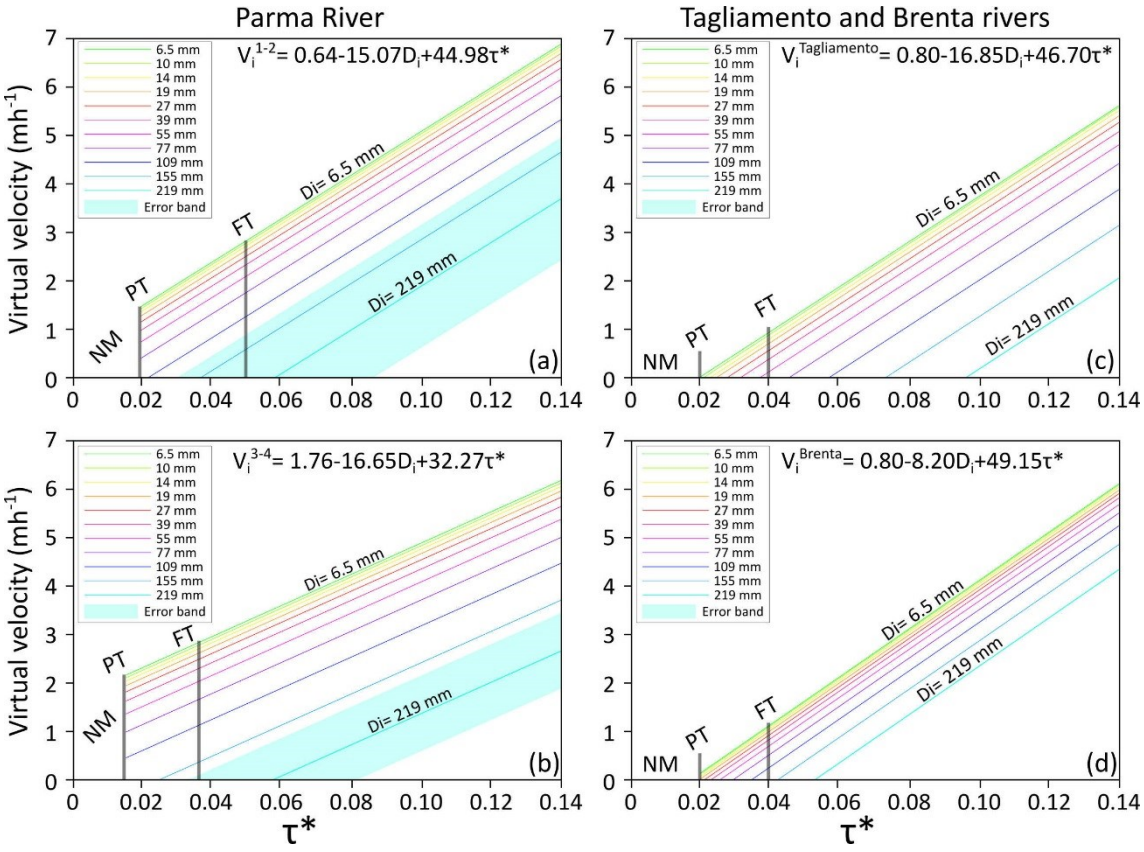

Figure S3. Plots of the empirical relations derived between the virtual velocity of the moved grains, the particle grain size and the dimensionless shear stress. Each colored line refers to a specific grain size (included in one of the 11 grain size classes adopted in the work) and the vertical grey lines identify the thresholds necessary for inducing partial and full mobility at the study sites. In (a) and (b) are presented the relations obtained for the two reaches of the Parma River investigated in this work while in (c) and (d) are reported the relations derived by Mao et al. (2017) for the Tagliamento River and Brenta River, respectively. Relationships derived at the four study sites in the two works are quite similar: in all cases virtual velocity has direct and inverse relations with τ^* and grains size (D_i) respectively, but the equation coefficients are different leading to different impactful of the two parameters on the control of the grains virtual velocity. For instance, the grain size plays a marginal role in the Brenta River relation where the τ^* is more impactful than in all other sites (d). The grain size is instead very important in controlling the particles virtual velocity at the downstream reach of the Parma River (b) and in Tagliamento River relations (c).

APPENDIX 2. SUPPORTING INFORMATION FOR "SEDIMENT MOBILITY AND BED MATERIAL TRANSPORT ESTIMATION IN A GRAVEL-BED RIVER DOWNSTREAM OF A DAM"

Andrea Brenna[1], Nicola Surian[1], and Luca Mao[2]

[1] *Department of Geosciences, University of Padova, Padova, Italy.*

[2] *School of Geography, University of Lincoln, Lincoln, UK.*

Submitted to *Earth Surface Processes and Landforms*.

	Sections 1-2 (Reach 2)	Sections 3-4 (Reach 3)
τ^* mobility thresholds	NM-PT: 0.020 PT-FT: 0.048	NM-PT: 0.015 PT-FT: 0.037
Y (%)	$Y^{1\text{-}2} = 4.10+1.04\log(\tau^*)$ (R^2= 0.93, Conf. Limit= 0.08)	$Y^{3\text{-}4} = 4.16+0.97\log(\tau^*)$ (R^2= 0.82, Conf. Limit= 0.11)
d_s (m)	$d_s^{1\text{-}2} = -0.021+40.258(\tau^*)^2$ (R^2= 0.74, Conf. Limit= 0.09 m)	$d_s^{3\text{-}4} = 0.011+35.647(\tau^*)^2$ (R^2= 0.83, Conf. Limit= 0.06 m)
V_i (mh^{-1})	$V_i^{1\text{-}2}= 0.64-15.07D_i+44.98\tau^*$ (R^2= 0.49, estimate SE= 1.27 mh^{-1}, p-value < 0.05)	$V_i^{3\text{-}4}= 1.76-16.65D_i+32.23\tau^*$ (R^2= 0.48, estimate SE= 0.78 mh^{-1}, p-value < 0.05)

Table S1. Empirical relations derived by Brenna et al. (2018) between the calculation parameters and the dimensionless shear stress active on the streambed (τ^*) using the data collected in the field during the monitoring activities (Y: percentage of mobilized streambed surface under partial transport conditions; d_s: the thickness of the bed mobile surface layer under full transport conditions; V_i: the virtual velocity characterizing the i-size particles movement). Such relations have been employed for calculating the instantaneous and local mass of entrained sediment, which is the first data required to determine the total volume of bed material load mobilized during a competent event and passing through a specific cross-section.

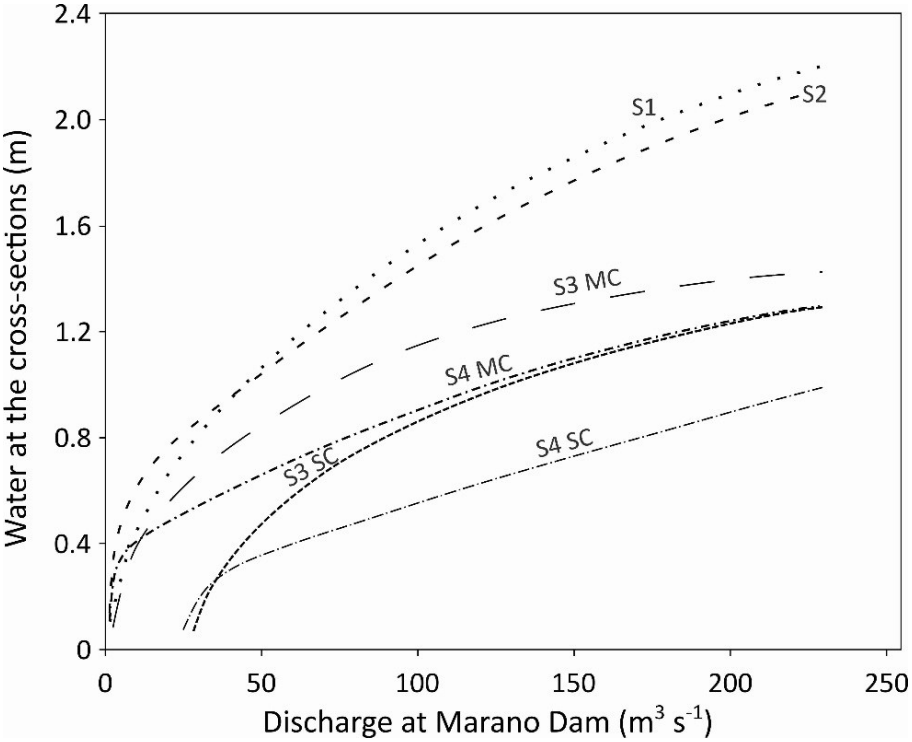

Figure S1. The local water stages as a function of water discharge at the four cross-sections. For sections 3 and 4, characterized by a multi-threads geometry, two different relation have been derived for the main and secondary channels, based on field data (i.e. trash-lines) and local hydrometers data.

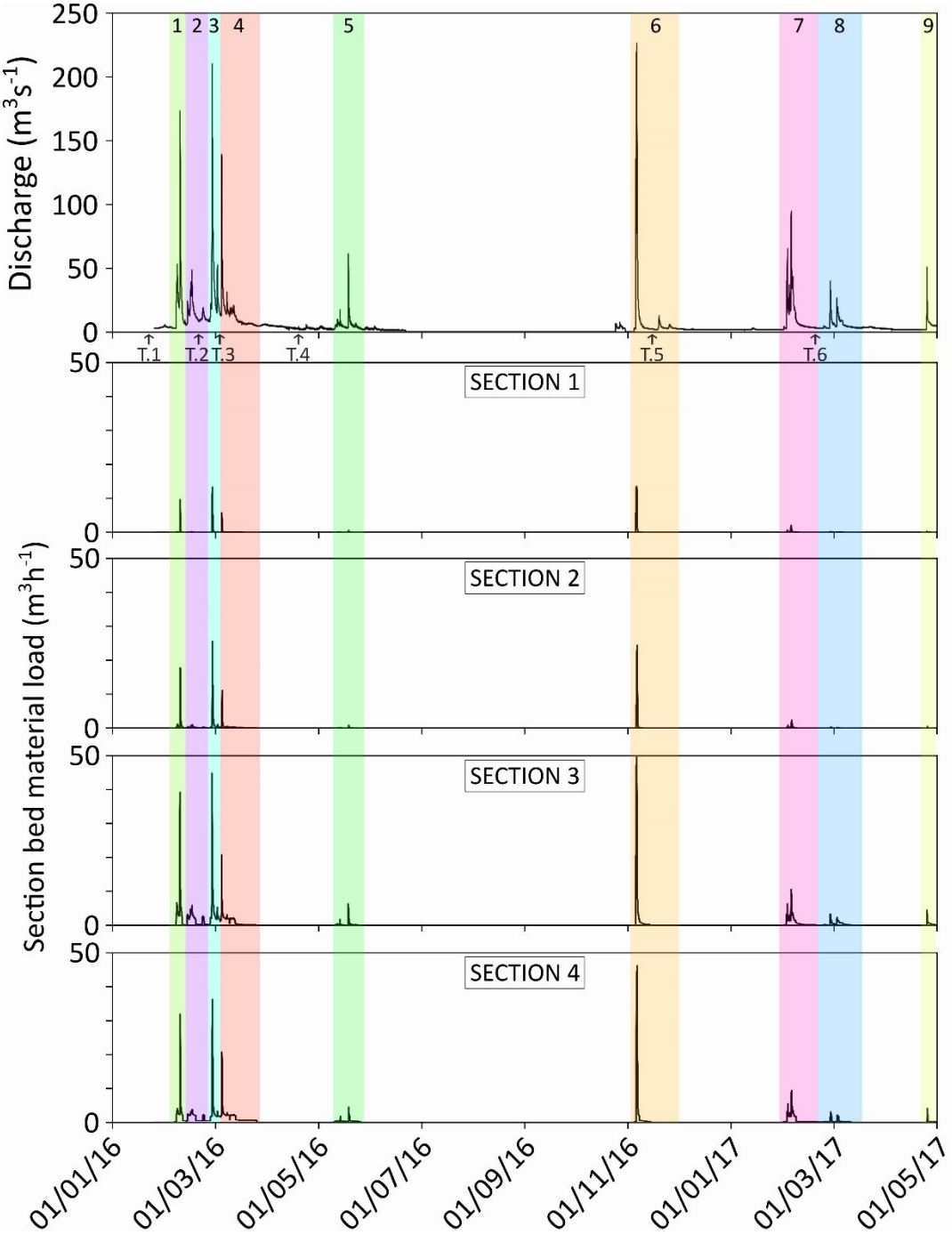

Figure S2. Instantaneous section bed material load estimated for the entire calculation period at the four cross-sections. During the same competent event (identified by the vertical bands and numbers from 1 to 9), the duration of active transport is different at each section (i.e. shorter at sections 1 and 2, longer at sections 3 and 4) as the calculated instantaneous-section transport (for a proper comparison it should be paid attention at the transport occurring during the events peaks). For such reasons the total bed material loads estimated during the same flood (with the same water discharge at the four considered sections in terms of discharge at the event peak and effective runoff) are different at the four cross-sections.

	SECTION	Q total event (m^3)	% PT
EVENT 1	Section 1	53 ± 29	24
	Section 2	155 ± 87	40
	Section 3	587 ± 200	33
	Section 4	443 ± 140	23
EVENT 2	Section 1	1 ± 1	100
	Section 2	81 ± 78	100
	Section 3	460 ± 187	68
	Section 4	424 ± 157	30
EVENT 3	Section 1	110 ± 55	17
	Section 2	269 ± 132	29
	Section 3	771 ± 252	32
	Section 4	597 ± 199	17
EVENT 4	Section 1	36 ± 30	57
	Section 2	168 ± 141	77
	Section 3	611 ± 257	57
	Section 4	745 ± 276	56
EVENT 5	Section 1	3 ± 3	100
	Section 2	20 ± 20	100
	Section 3	107 ± 54	84
	Section 4	167 ± 87	83
EVENT 6	Section 1	158 ± 74	13
	Section 2	238 ± 108	15
	Section 3	746 ± 230	19
	Section 4	601 ± 171	20
EVENT 7	Section 1	29 ± 24	73
	Section 2	46 ± 42	88
	Section 3	456 ± 203	63
	Section 4	397 ± 152	49
EVENT 8	Section 1	5 ± 5	100
	Section 2	11 ± 11	100
	Section 3	210 ± 107	93
	Section 4	191 ± 79	66
EVENT 9	Section 1	3 ± 3	100
	Section 2	5 ± 5	100
	Section 3	82 ± 41	81
	Section 4	61 ± 26	67

Table S2. Bed material transport obtained for each event during the study period at the four considered cross-sections. For each estimate the total bed material load occurred at a specific section during the entire competent event and the percentage of that sediment volume mobilized under partial transport condition (i.e. partial transport contribution) are reported.

		Section 1		Section 2		Section 3		Section 4	
		C	B	C	B	C	B	C	B
Ev. 1	TT (m^3)	**21,8**	**30,8**	**55,5**	**99,2**	**536,2**	**50,5**	**417,9**	**25,3**
	FT (m^3)	7,9	4,9	24,4	68,4	371,0	31,7	328,8	11,6
	PT (m^3)	13,9	25,9	31,1	30,8	167,5	23,2	89,1	13,7
Ev. 2	TT (m^3)	**1,2**	**0,1**	**49,0**	**32,4**	**448,8**	**11,0**	**422,5**	**1,4**
	FT (m^3)	0,0	0,0	0,00	0,0	145,4	0,0	294,8	0,0
	PT (m^3)	1,2	0,1	49,0	32,4	303,4	11,0	127,7	1,4
Ev. 3	TT (m^3)	**43,7**	**65,9**	**91,0**	**178,0**	**539,1**	**232,0**	**563,6**	**33,0**
	FT (m^3)	31,9	58,7	52,8	138,2	365,4	159,2	478,6	14,1
	PT (m^3)	11,8	7,2	38,2	39,8	173,7	72,8	85,0	18,9
Ev. 4	TT (m^3)	**30,1**	**6,4**	**126,4**	**41,9**	**577,7**	**33,4**	**691,5**	**53,3**
	FT (m^3)	11,3	4,5	16,7	22,8	246,3	14,23	315,7	12,7
	PT (m^3)	18,8	1,9	109,7	19,1	331,4	19,1	375,8	40,6
Ev. 5	TT (m^3)	**3,3**	**0,1**	**18,7**	**1,2**	**105,4**	**1,2**	**158,2**	**1,6**
	FT (m^3)	0,00	0,0	0,00	0,0	17,1	0,0	28,2	0,0
	PT (m^3)	3,3	0,1	18,7	1,2	88,3	1,2	130	1,6
Ev. 6	TT (m^3)	**92,2**	**65,4**	**90,3**	**147,9**	**662,8**	**83,7**	**531,2**	**69,6**
	FT (m^3)	79,8	57,6	71,6	130,1	545,5	61,3	435,6	44,1
	PT (m^3)	12,4	7,8	18,7	17,8	117,3	22,3	95,6	25,45
Ev. 7	TT (m^3)	**25,8**	**3,1**	**28,6**	**17,8**	**346,8**	**109,6**	**324,9**	**58,1**
	FT (m^3)	7,5	0,2	0,0	5,7	110,4	57,0	181,3	12,2
	PT (m^3)	18,3	2,9	28,6	12,1	236,3	52,6	143,6	45,9
Ev. 8	TT (m^3)	**5,3**	**0,00**	**9,4**	**1,7**	**178,6**	**31,5**	**173,1**	**7,8**
	FT (m^3)	0,00	0,00	0,0	0,0	9,7	5,2	61,5	0,0
	PT (m^3)	5,3	0,00	9,4	1,7	169,0	26,3	111,6	7,8
Ev. 9	TT (m^3)	**2,5**	**0,0**	**0,7**	**4,5**	**67,9**	**13,8**	**55,6**	**5,8**
	FT (m^3)	0,00	0,00	0,0	0,0	10,6	4,7	20,3	0,0
	PT (m^3)	2,5	0,00	0,7	4,5	57,3	9,1	35,3	5,8
Total period	TT (m^3)	**225,9**	**171,8**	**469,5**	**524,6**	**3463,3**	**566,5**	**3360,1**	**265,9**
	FT (m^3)	138,4	125,9	165,5	365,3	1821,4	333,3	2247,4	104,2
	PT (m^3)	89,8	43,6	304,0	159,3	1644,1	233,2	1213,5	161,7

Table S3. Volume of sediment moved as bed material transport during each competent event at the four cross-sections classified in function of the transport mechanism (partial or full mobility) and of the morphological unit where the material has been entrained and mobilized. C= channels, B= bars.

ACKNOWLEDGMENTS

This Ph.D. research project and my fellowship were supported by funds from the University of Padova.

I would like to thank all the people that contributed to my Ph.D. thesis starting from my supervisor Prof. Nicola Surian (University of Padova) and co-supervisor Prof. Luca Mao (University of Lincoln, UK) who introduced me to the fields of fluvial geomorphology and sediment transport. They taught me the basis of the scientific research and steadily improved my work.

The field data collection carried out in this work has been a complex and time-consuming activity. I would like to thank Dr. Silvano Pecora, Dr. Mauro Del Longo, Dr. Monica Branchi and Dr. Paolo Leoni from "Servizio Idro-Meteo-Clima" of Arpae Emilia-Romagna for providing hydrological and meteorological data and for their very helpful support throughout the whole field monitoring in the Parma River; Dr. Maria Laura Trento and Pietro Brenna for field assistance.

Many thanks also to Prof. Joseph M. Wheaton who hosted me at the "Ecogeomorphology and Topographic Analysis Laboratory", Department of Watershed Sciences of the Utah State University in Logan (USA). Joe greatly improved my work, in particular regarding the application of the morphological method.

Thanks also to Prof. Peter R. Wilcock, Watershed Sciences Department Head during my visiting period in Logan, for his hospitality and the useful scientific research advices.

My gratitude is extended to Dr. Marco Cavalli from CNR Irpi Padova for his precious suggests about the acquisition and elaboration of remote sensing data.

This thesis has been reviewed and evaluated by Dr. Frèdèric Lièbault (University of Grenoble Alpes - Irstea, France) and Prof. Damià Vericat (University of Lleida, Spain). They provided me constructive comments and useful advices for improving the quality of my work.

Finally, I would like to express my gratitude to the people which, with their affection, supported and encouraged me during this wonderful period in Padova.